

Environmental fatigue models and evidence for LWR water

Authors: Tommi Seppänen, Jussi Solin

Confidentiality: VTT Public

Report's title	
Environmental fatigue models and evidence for LWR water	
Customer, contact person, address	Order reference
SAFER2028	
Project name	Project number/Short name
Total Fatigue Life in Plant Environment	136062 - SAFER2028_TOFFEE 2023
Author(s)	Pages
Tommi Seppänen, Jussi Solin	201/
Keywords	Report identification code
fatigue, environmental effects, stainless steel	VTT-R-00228-24
Summary	
<p>This report completes the task and goal of the SAFER2028 / TOFFEE 2023 project:</p> <p>“In 2023, the task will focus on assessment of current best practices for taking the environmental effect into account in fatigue design by surveying existing EAF models. This work will provide a baseline against which the currently developed model is compared later in the project, aimed for 2024. A VTT research report will be written on this work in 2023.”</p> <p>An extensive and detailed summary on the evolution of Codes and Standards from the perspective of fatigue and EAF is provided. A particular emphasis is placed on the ASME Code and comparisons with the RCC-M and other Codes. Analysis of the fundamental principles originally adopted and along the years supplemented to the ASME Code, Section III serves as background information on roots also for the other codes.</p> <p>Endorsement by the U.S. NRC raised the NUREG/CR-6909 report and as a major milestone for EAF, but many European stakeholders sought for alternative approaches. Research was directed in determining fatigue curves for restricted groups of stainless steels and in developing less conservative approaches for application of F_{en} factors in fatigue assessment. New solutions have been proposed and adopted in Codes and Standards, such as ASME, RCC-M, JSME and KTA. Future reharmonization of the international activities and regulation has become increasingly complex due to this divergence.</p> <p>A wealth of experimental evidence exists to support arguments for or against a particular methodology. A selection of international research and laboratory evidence of environmental effects is introduced and discussed. An overview of experimental research at VTT under the current and previous research programmes is presented, including an improved EAF approach proposed.</p>	
Confidentiality	VTT Public
Espoo 5.4.2024	
Written by	Reviewed by
Tommi Seppänen Research Team Leader	Juha Kuutti Research Team Leader
VTT's contact address	
Kivimiehentie 3, 02150 Espoo	
Distribution (customer and VTT)	
SAFER TAG4.1, VTT archive	
<p><i>The use of the name of “VTT” in advertising or publishing of a part of this report is only permissible with written authorisation from VTT Technical Research Centre of Finland Ltd.</i></p>	



Approval

VTT TECHNICAL RESEARCH CENTRE OF FINLAND LTD

Date:

5.4.2024

Signature:

Name:

Jani Halinen

Title:

Vice President, Nuclear Energy

Contents

1.	Introduction.....	5
2.	Codified design curves and margins	7
2.1	Design by analysis in brief	7
2.2	ASME 1963 & 1983 design fatigue curves.....	9
2.3	ASME 2010 design fatigue curve.....	14
2.4	Alternative design fatigue curves as evolutions of ASME III.....	20
2.4.1	RCC-M (France)	20
2.4.2	JSME (Japan).....	23
2.4.3	KTA (Germany)	29
2.4.4	PNAE-G-7 (Russia)	32
3.	Explicit methods to account for EAF	34
3.1	Introduction to existing methodologies.....	34
3.1.1	EAF design curves	34
3.1.2	F_{en} models	35
3.2	Overview of EAF approaches in codes, standards and regulations	39
3.2.1	ASME (USA)	39
3.2.2	JSME (Japan).....	50
3.2.3	RCC-M (France)	61
3.2.4	KTA (Germany)	67
3.3	Recent and emerging approaches.....	68
3.3.1	Recent ASME Code Cases.....	72
3.3.2	ASME Working Group ongoing activities	74
3.3.3	VTT plastic strain-based approach	79
4.	Laboratory evidence of environmental effects.....	84
4.1	USA.....	84
4.2	Japan	93
4.3	France	112
4.4	UK	123
4.5	Finland	130
4.5.1	Research of environmental fatigue in Finland – 50 years of experience.....	130
4.5.2	Niobium stabilized alloy 1.4550 (comparable to AISI 347)	131
4.5.3	Material response – effect of strain rate and environment.....	137
4.5.4	Alloy 304L and simulation on transients in plant	140
4.5.5	Transferability of F_{en} factors for fatigue transients in plant.....	142
4.5.6	Alloy 316L – an EPR relevant Z2CND1812N2 pipe.....	146
4.5.7	Discussion on transferability of EAF data.....	152
5.	Practical application in stress analysis.....	154
5.1	Alternative procedures for determining F_{en}	154
5.2	Three levels of detail for determining F_{en}	155
5.2.1	The Factor Multiplication Method	155
5.2.2	The Simplified Method	156

5.2.3	The Detailed Method	158
5.2.4	Usage factor for environmental fatigue	158
5.3	Threshold strain for determining F_{en}	158
5.4	Calculation example	159
6.	Summary	165
	References.....	167
7.	Appendices.....	188
7.1	Evolution of F_{en} models in NUREG reports for US NRC.....	188
7.1.1	F_{en} models before NUREG/CR-6909	188
7.1.2	F_{en} model in NUREG/CR-5704 (stainless steels)	190
7.1.3	F_{en} models in NUREG/CR-6909.....	195
7.2	Japanese F_{en} models in JSME S NF1-2009.....	198
7.2.1	F_{en} models in JSME S NF1-2006 and JSME S NF1-2009.....	198
7.2.2	Comparison of F_{en} models in JSME S NF1-2009 and NUREG/CR-6909	200

1. Introduction

Metal fatigue is recognized as a degradation mechanism related to cyclic straining, potentially leading to initiation of crack(s) followed by growth of a leading crack until end of service life, detection or 'failure'. Crack growth until failure in a brittle reactor pressure vessel might potentially result to a 'loss of coolant accident', but less dramatic failure conditions are anticipated in primary piping components made of ductile steels. Leaks of primary coolant due to fatigue have been rare and mitigation of 'fatigue damage' in the meaning applied in reactor design calculations (ASME III) is often motivated by aims of extending the plant life or reducing the need of excessive inspection for safe operation. Crack growth due to unknown factors is addressed by in-service inspection (ASME XI). Environmental effects enhancing rates of crack growth have long been part of the unknowns and in focus of research, but acceleration of crack initiation due to environmental fatigue (EAF) has attracted much interest during recent twenty years. Uniting of these two phases of environmental fatigue and points of view (ASME III & XI) together under emerging concepts of 'total life approaches' will be a challenge for next decade(s). However, notable unknowns and obscurities remain to be solved to ensure unbiased EAF results in laboratory and in fatigue assessments of reactor components.

Environmental effects have become a commonly disputed item within the several interlinked effects and assumptions embedded in the codified fatigue assessments. The fatigue design curves and allowed numbers of transients in plant are based on cycles applied to meet the failure criterion set for standard axial fatigue tests (ASTM E606) in laboratory. The design criterion in the ASME Code, Section III was originally based on cycles up to fracture of the specimens tested at an operation temperature in air. The current fatigue criteria are tuned to represent 25 % drop in load carrying capacity of specimens tested at room temperature. In lack of standard tests in hot water, non-standard methods have been applied to demonstrate potentially significant effects of reactor coolant on the fatigue crack initiation lifetimes. Fatigue design curves adjusted to shorter endurance were proposed, but the current state of the art is based on fatigue curves in air and a parametrised factor for environmental effects.

A common scenario of environmental fatigue in reactor primary circuit is 'thermal fatigue' at locations where changes of water temperature cause thermal gradients and out-of-phase elongations within the wall thickness. Local plastic yielding and initiation of cracks occurs at the inner surface which is in contact with the coolant water and thus also subject for environmental effects. Surface cracking may be followed by growth of a leading crack in depth and length until arrest, detection by NDT or leak. However, without significant contribution of bending or other mechanical loads, the probability of a leak remains typically low because the cyclic thermal strains and driving force for crack growth decrease in depth. It is possible that a fatigue assessment is simultaneously unconservative against initiation of a crack and overly conservative in predicting the depth of the crack.

Inconsistency between laboratory and plant operating experience delayed the establishment of Codified consensus approaches to environmentally assisted fatigue (EAF). The methods and models applied in laboratory to determine environmental fatigue correction factors (F_{en}) are not identical and fully compatible with the models and assumptions applied for assessment of fatigue in reactor components. Furthermore, typically inverse correlation between accumulation of fatigue usage and significance of environmental effects during various fatigue transients makes the reduction in safe life easily overpredicted when applying conservative design approaches. Concerns on transferability of laboratory results and EAF models to component performance are unavoidable, but progress in experimental and analysis models together with better understanding of the design criteria and divergent evolution of international Codes and Standards may reduce the gaps and uncertainties in transferability.

The scope of EAF extends beyond the correction factors, which are inseparable from specific reference and/or design fatigue curves. The recent divergence has made assessment of transferability and future reharmonization of the international regulation increasingly complex. To maintain consistency, it becomes important to know the background of differences between the Codes and various approaches. This is of particular interest in Finland where reactors and components designed according to different Codes are

operated. Insufficient or excessive safety margins against fatigue can result to misjudgement in plant life management or bias in developing balanced programs of risk informed in-service inspection (RI-ISI).

This report describes the background to the existing F_{en} models, primarily for austenitic stainless steels, and discusses some of the publicly available experimental data used as the technical basis to support the methodologies. It is assumed that the reader understands the design by analysis principles of ASME III and similar Codes and therefore these topics will not be exhaustively covered. Some differences between the international Codes and Standards will be addressed and the need of consistency between models for EAF and design assessment is emphasized.

2. Codified design curves and margins

The most important nuclear design Codes have their roots in ASME Section III. When the Codes were developed, the effects of reactor coolant water on fatigue life were not considered explicitly in the design. However, the environmental effects were not ignored. Estimation of potential effects and consequences was addressed as responsibility of the designer and operator.

2.1 Design by analysis in brief

The American Society for Mechanical Engineers (ASME) Boiler and Pressure Vessel (B&PV) Code Section III was published in 1963 with the title “Rules for Construction of Nuclear Vessels”. The modern Section III “Rules for Construction of Nuclear Facility Components” covers a wide range of components including pressure vessels and piping. The design by analysis philosophy of subarticle NB-3200 has been a staple since 1963 (Hechmer & Hollinger, 2006), though the main body of text was transferred to Mandatory Appendix XIII “Design Based on Stress Analysis” in the 2017 Code edition. The given terminology originates from the integration of design and numerical stress analysis as opposed to the more straightforward but typically more conservative design by rule (or formula) principle.

The design by analysis procedure is based on applying the Tresca yield criterion with elastic stress analysis. The term equivalent intensity of combined stress (or stress intensity in short) S was introduced instead and by definition is twice the maximum shear stress. (ASME, 1969) For a mechanical designer to compare elastic stress analysis results with a design fatigue curve (DFC) constructed from strain-controlled results, the design curve strains are best represented by equivalent pseudo-stresses for convenience of using the same units. This simple transformation is done by multiplying the total strain amplitude ε_a with the elastic modulus E . The term S_a in the ASME B&PV Code is called the alternating stress intensity.

$$S_a = E \cdot \varepsilon_a \quad (1)$$

Stresses are categorized by their nature into primary, secondary and peak stresses. A designer must be familiar with stress categorization to fulfil Code limits. The prevention of fatigue crack initiation is based on limiting the magnitude and frequency of peak stresses, which are highly localized in nature. These stresses may originate from thermal fluctuation or mechanical loading, but their main characteristic is localized strain-controlled distortion, typically at a discontinuity such as a notch (see Figure 1) or at a surface subjected to thermal shock. Characteristically for peak stresses, no marked distortion occurs outside of a limited plastic zone. To evaluate the alternating component of stress intensity responsible for fatigue damage, the primary+secondary+peak principal stresses are calculated and stress differences defined as a function of time for a load cycle. The alternating stress intensity from stress analysis to be used in fatigue analysis, S_{alt} , is half of the absolute magnitude of the largest of these differences. (ASME, 1969, 2017). Before entering the fatigue design curve, S_{alt} may require modification for temperature, fatigue strength reduction factor or plasticity.

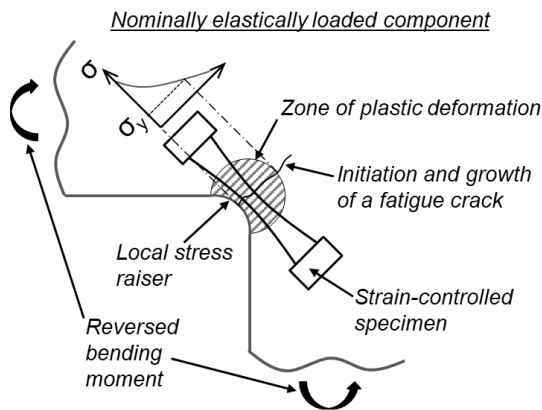


Figure 1. Schematic of strain-controlled condition at a notch root, constrained by surrounding elastic material. Modified from Coffin (1979).

Piping design rules in subarticle NB-3600 share similarities with the design by analysis principles in subarticle NB-3200 (e.g. stress categorization and limits). However, evaluation of allowable loadings itself is based on design by rule philosophy, meaning stress analysis is less tedious to perform with the trade-off of additional inherent conservatism.

From the perspective of fatigue, the design rules' major goal is obviously to design against leakage by through-wall cracks in pressure retaining components, and also in other less critical non-pressure boundary regions. In actual components, fatigue failures have most frequently been observed in piping components, nozzles, valves and pumps in descending order of documented cases (Iida, 1989, 1992). In pressurized water reactor (PWR) primary circuits, typical stainless steel components of importance from thermal transient perspective are the surge line, charging nozzles, safety injection nozzles, and the residual heat removal line. In boiling water reactors (BWR), typical stainless steel components of importance are recirculation system tees, safe end in the core spray line, and the residual heat removal line (Ware et al., 1995). High frequency vibration and thermal mixing can affect a number of different structural components other than the ones just listed (Iida, 1992).

The Design Specification is a mandatory document prepared by the owner/user of a nuclear power plant (NPP) for the manufacturer. It specifies the conditions for which a pressure vessel or component needs to be designed and fabricated. Furthermore, it contains information such as design pressure, temperature, environmental conditions and postulated cyclic information (design transients). Because this information is needed in advance, it is to an extent based on engineering judgement with the aim to envelope probable in-service loads. The Design Report includes the calculations and stress analysis, based on the Design Specification, which demonstrates that a component is within the allowable limits of stress and cyclic operation (Reedy, 2006). The fulfilment of Code design requirements validates a component for use but is not a valid indicator of a certain operational fatigue life. Indeed, the stress analyst has no control of how a plant is eventually operated (Cooper, 1992).

Accurate knowledge of loading information such as magnitudes, numbers of cycles and sequences is challenging to obtain prior to operation. Historical evidence of unforeseen loading types, at thermal mixing zones for example, demonstrates the difficulty of predetermining actual loading with confidence. On the other hand, in all reviewed cases of actual fatigue failures the ASME III design procedures would have successfully predicted failure if actual loading conditions had been known (EPRI, 1992).

It is necessary to emphasize that the intent of a Design Report is not to demonstrate a precise minimum value for cumulative usage factor (CUF) but rather to refine the analysis until $CUF < 1$ using the information made available in the Design Specification (Cooper, 1992). A high usage in the Design Report does not automatically mean that location is fatigue sensitive. Originally, the operating period was arbitrarily based on a life expectancy of 40 years (Reedy, 2006). The 40-year limit was also explicitly stated in the 1954 Atomic Energy Act.

The owner of a plant intends to demonstrate during operation that (Cooper, 1992):

- Design transients are much more severe than actual ones.
- Design transient budgets are much higher in number than actual cycle counts.
- Design transients represent the actual loading types and conditions.

Compliance with the above was believed to ensure no fatigue cracks would initiate as long as $CUF < 1$.

2.2 ASME 1963 & 1983 design fatigue curves

In the 1950's ASME appointed a committee with the task of writing a dedicated Nuclear Code section. As part of the process, a Sub-Task Group was set up to determine allowable fatigue stresses in design. In nuclear components, the number of stress cycles from quasi-static thermal transients was assumed to seldom exceed 10^5 and realistically be closer to 10^4 or even less for a 40-year design life (Langer, 1962). Fatigue analysis for ASME III also needed a different approach to the conventional design of rotating machinery, railway axles etc., where design cycles $>10^5$ or infinite life were often in focus.

Strain-life low cycle fatigue (LCF) principles of Coffin and Manson (Coffin, 1953, 1954; Manson, 1953, 1954), equation (2), were therefore well-suited for NPP components. It followed that ASME III DFCs were based on strain- rather than stress-controlled test results.

$$N^k \Delta \varepsilon_{pl} = C \quad (2)$$

In this equation, N is the number of cycles to fracture, $\Delta \varepsilon_{pl}$ is the plastic strain range and k and C are to be considered as material constants. According to Coffin, $k=0.5$. Considering that failure in uniaxial tension takes place in $\frac{1}{4}$ cycles, the constant C in equation (2) was theorized to be associated with the fracture ductility of a material ε_f , or more familiarly, to the reduction of area (RA) from a conventional tensile test according to equation (3) (Baldwin et al., 1957; Coffin, 1953).

$$C = \varepsilon_f / 2 = -1/2 \ln \frac{100 - \%RA}{100} \quad (3)$$

For compatibility with stress analysis i.e. equation (1), a suitable approach to LCF in nuclear applications was found by Langer (1962), who used the total strain amplitude ε_a , equation (4). This is simply the sum of both plastic and elastic strain amplitudes $\varepsilon_{a,pl}$ and $\varepsilon_{a,el}$, respectively. Note that amplitude is simply half of the range.

$$\varepsilon_a = \varepsilon_{a,el} + \varepsilon_{a,pl} \quad (4)$$

The elastic strain amplitude is calculated from its range $\Delta \varepsilon_{el}$, which is derived from stress range $\Delta \sigma$ through equation (5).

$$\varepsilon_a = \frac{\Delta \varepsilon_{el}}{2} = \frac{\Delta \sigma}{2E} \quad (5)$$

A practical design solution incorporating the Coffin-Manson relation in a total strain-based approach was described by Langer (1962). The plastic strain component was modelled using equation (2), whereas a fixed constant was chosen for the elastic part, representing the anticipated endurance limit at 10^7 cycles, ε_e (or S_e in stress intensity). Strain-controlled LCF test results could then easily be used to formulate material specific best-fit mean fatigue curves, which could again be expressed interchangeably in units of stress intensity by multiplying with the elastic modulus, equations (6) and (7).

$$\varepsilon_a = \frac{1}{4\sqrt{N}} \ln \frac{100}{100 - \%RA} + \varepsilon_e \quad (6)$$

$$S_a = \frac{E}{4\sqrt{N}} \ln \frac{100}{100 - \%RA} + S_e \quad (7)$$

Equations (6) and (7) are commonly referred to as Langer's equation.

The mean best-fit curve for austenitic stainless steels was obtained by minimizing (from experimental data in air) the sum of squares of the logarithms of stress intensity, which strictly speaking is the independent test variable. In strain amplitude form, the best-fit curve for austenitic stainless steels was expressed by equation (8) either as a function of fatigue life or strain amplitude.

$$\varepsilon_a = 32.36 \cdot N^{-0.5} + 0.167$$

$$\ln(N) = 6.954 - 2 \cdot \ln(\varepsilon_a - 0.167) \quad (8)$$

This best-fit curve (BFC) as well as the design fatigue curve (DFC) from the 1963 edition of ASME III are shown below in Figure 2 using the units of alternating stress intensity, as used in design.

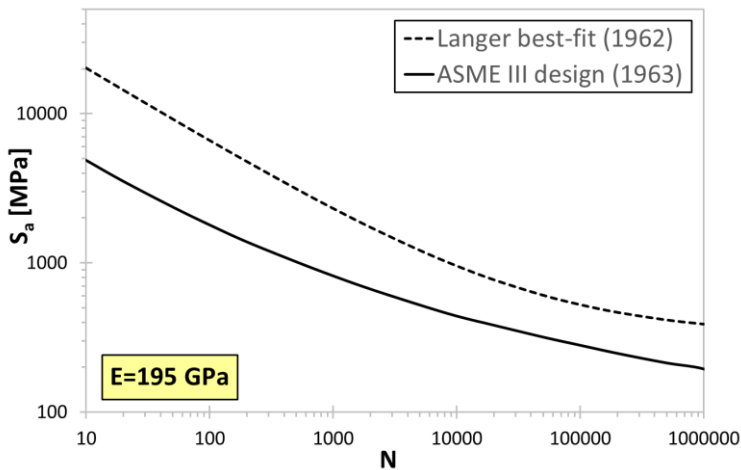


Figure 2. Stainless steel alloy best-fit and design fatigue curves for the first edition of ASME III in 1963, adjusted using $E=195$ GPa. (ASME, 1963; Langer, 1962)

The 1963 ASME III Code was not intended for HCF, and the design curves were provided up to 10^6 cycles only, but even this included extrapolation of the available strain-controlled experimental data. If the writers of ASME III had intended to develop procedures applicable for HCF, based on existing knowledge at the time, Coffin (1978), they could have very clearly expressed concern over applying LCF principles beyond one million cycles. As the ASME III stainless steel design curve now applies up to 10^{11} cycles, this has re-emerged as a discussion topic.

A further important determination in the fatigue curves is the value of elastic modulus in equation (7) because it is influenced by temperature. A mean or design curve expressed in stress intensity units shall be paired with a value of elastic modulus E_{curve} , so that the designer may shift the curve according to the case-specific modulus at the desired temperature, E_T . The modulus correction is shown in equation (9).

$$S_{a,design} = S_a \cdot \frac{E_{curve}}{E_T} \quad (9)$$

The correction means that for any paired modulus with the design curve, it is possible to adjust the curve accordingly to represent another temperature which the designer or stress analyst may be using. The 1963 edition of ASME III did not contain the modulus correction, equation (9), as this addition was made only in the 1968 Summer Addenda.

Whereas laboratory strain-controlled fatigue test results on polished specimens determine a best-fit mean curve for a specific material using Langer's equation, the curve used in design requires additional factors

beyond the obvious

to account for variables not covered by the best-fit curve. That is, for design of plant components the BFC shall never be used. Instead, the design fatigue curve shall be used. If the DFC, which in ASME III is aimed for air environments only, fails to capture certain influential factors on fatigue life (such as the effect of reactor coolant), then those effects would require further adjustment.

The transferability factors used on the BFC to obtain design values were set as 20 on cycles and two on stress/strain. The more bounding of the curves adjusted with transferability factors sets the DFC, as shown in Figure 3. The 1963 design fatigue curve was intentionally smoothened, rather than abruptly changing direction at the intersection where the curves with factors on life and stress intersect. Beyond the intersection the measured margin in fatigue life between BFC and DFC obviously grows to well beyond 20.

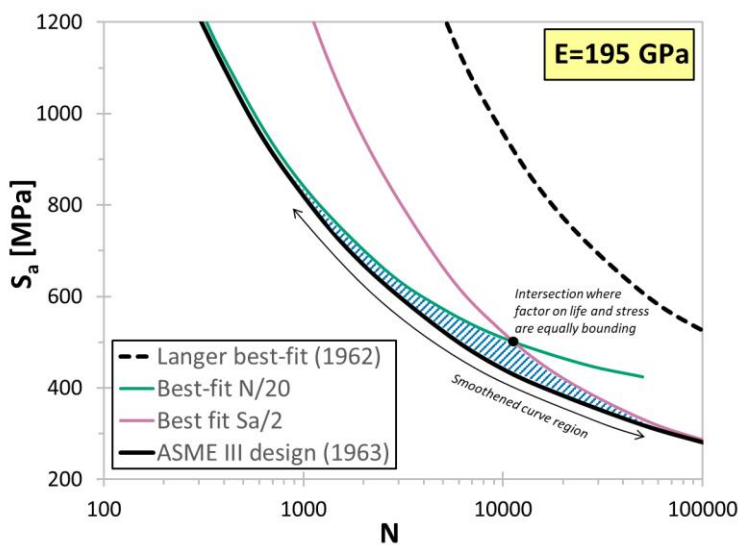


Figure 3. Design curve as the (smoothened) lower bound of the best-fit curve with transferability factors. Note that only the abscissa is in logarithmic scale.

The design basis closely followed that established by the United States Navy Bureau of Ships in the 1950's. The factor of 20 on cycles was divided as follows (U.S. DoC, 1958):

- Subfactor of 2 on material scatter, from minimum to mean.
- Subfactor of 2.5 for size effect.
- Subfactor of 4 on surface finish and atmosphere.

A precise description of the scatter subfactor was not given and with the available data only limited statistical analysis would have been possible. The factor has since been interpreted to represent a 95 % confidence level to the mean of experimental data (Van Der Sluys, 2003a). No evidence was explicitly given to justify the other subfactors, meaning they were intended by engineering judgement to cover effects which were either unknown or too difficult to quantify at the time. Therefore, better quantification of uncertainties could justify a re-evaluation of transferability factors without reducing safety (Reedy, 2006).

The meaning of "atmosphere" in the transferability factors is not explicitly written and has been debated multiple times, particularly after the potentially severe effects of the environment were first discovered. Recognized failure modes in the Code were both high-strain – low cycle fatigue and corrosion fatigue (ASME, 1969). Protection against environmental conditions was stated as the responsibility of the designer. The wording in the 1963 Code leaves room for interpretation, which may have led some readers to assume partial credit for a reactor coolant environment within the subfactor of four. Cooper (1992) has clarified that the wording was, however, intended to refer to provision in wall thickness for general corrosion. Nevertheless, O'Donnell (2014; 2005b, 2005a) states that in the 1950's and 1960's a factor of two was widely considered to bound detrimental environmental effects. O'Donnell et al. (1989) proposed

design S-N curves derived from crack growth rate data in light water reactor (LWR) coolant with a factor of 10 on life instead of 20 to acknowledge a moderate built-in environmental effect of two in the ASME III design curves. Because both “atmosphere” and surface finish were grouped as a single subfactor, an industry interpretation has also been that there is a synergistic influence of the two i.e. some effects of environment can be offset by less severe effects of a rough surface (EPRI, 2001b).

From 1974, the wording in ASME III NB-3121 read “*It should be noted that the tests on which the design fatigue curves are based did not include tests in the presence of corrosive environments which might accelerate fatigue failure*”. Van Der Sluys (1993) explains that to continue applying the ASME III design curves, the common practice in the nuclear industry was to simply assume the reactor coolant as non-corrosive. Meanwhile, the effect or non-effect of environment was not yet supported with experimental results. The reason may partly be explained by an underestimation of the potential effects, but a more limiting factor was unavailability of laboratory equipment to perform experiments with sufficient reliability. Laboratory practices were in fact not first developed until roughly 15 years after ASME III was published and continue to evolve to this day.

The design criteria documentation for ASME III (ASME, 1969) did not include a detailed discussion on the composition of the factor of two on stress/strain, which is not supportive of a safety factor interpretation. Manjoine and Tome (1983) have suggested the following subfactors, with each of the listed five having an average weight of 1.15 so that $1.15^5=2.01$:

- Surface finish to bound situations where a beneficial compressive residual stress (to prevent nucleation and to retard crack growth) is not induced at the surface following fabrication.
- Size effect to consider the difference in surface area under peak stress in a component and laboratory specimen.
- Material variability to bound heats of materials with varying yield and tensile strengths
- Environment to bound those heats of materials, where reduction in strength due to temperature exceeds that predicted by equation (9).
- Residual stress to cover retained effects at service temperature from either processing, fabrication or prior plastic strain history at areas other than welds.

No experimental evidence was provided to support the specific values for these subfactors. Thus, the average individual values of 1.15 are more engineering judgement rather than a scientific approach. The above proposal neglects interdependency of factors, which is an oversimplification (Manjoine & Tome, 1983). In terms of short fatigue crack initiation (<100 µm deep), the subfactor with the largest magnitude could also be argued to dominate over any cumulative effects (J. Keisler et al., 1995).

Cooper (1992) provided an alternative interpretation of the factor of two in the stress or strain direction. It may be more indicative of the original design criteria. The transition between LCF and HCF on the fatigue curve occurs close to 10^4 cycles, Figure 3. At this crossover point, a reduction factor of two on stress intensity/strain from the best-fit curve was approximately equally bounding as the transferability factor of twenty on cycles. No quantitative experimental data was used to support this approach, at least within the public literature.

Cumulative damage from a spectrum of varying strain amplitudes is considered by using the Palmgren-Miner linear damage rule (Miner, 1945; Palmgren, 1924). Although the linear damage rule is often criticized for its inability to physically account for sequence effects comprising both crack initiation and growth, literature results suggest that it is often reasonably accurate when the majority of fatigue life is spent in crack propagation (LCF). However, even then, it cannot account for effects such as crack closure (Frost et al., 1974; Pook, 2007). It can be difficult to justify highly accurate predictions of fatigue life through more complex cumulative damage methods than the linear damage rule, particularly when service histories are completely random.

The ASME B&PV Code uses the term usage factor (UF) for damage caused by a single level of alternating stress intensity. Cumulative UF (CUF) is a combination of usage factors from different levels of loading. Once CUF=1, crack initiation in a component is assumed. Originally the definition of CUF=1 in a smooth laboratory specimen was considered to be total separation of a specimen into two halves.

The effect of mean stress σ_m on fatigue curves is taken into account by use of the modified Goodman diagram. In the case of austenitic stainless steel, the endurance limit ($S_e = E \cdot \epsilon_e$) in equation (7) exceeded the cyclic yield stress. Thus, no mean stress correction was deemed necessary.

HCF had become an interesting topic in the nuclear community in the 1970's due to unanticipated high frequency vibrations encountered in specific piping applications. Developments in servohydraulic laboratory equipment allowed fatigue testing beyond 10^6 cycles more economically, leading to new results beyond the scope of the ASME III design curve technical basis. Thus, the ASME Code Subgroup on Fatigue Strength reviewed the Code design curves as summarized by Jaske and O'Donnell (1977). Data from multiple sources was collected and proposed a revision to the design curve was suggested, arguing that the 1963 DFC was nonconservative for HCF.

To consider fatigue lives in excess of 10^6 cycles, a solution was proposed and implemented into the Code in 1983. The criteria are described by Manjoine and Tome (1983). As it was recognized that mixing together LCF and HCF was problematic, and since Langer's curve was an adequate model for LCF, no changes were made to the 1963 stainless steel DFC, other than revising the paired elastic modulus to 195 GPa (room temperature value) in the Winter 1982 edition. This adjustment shifted the curve upwards, as required by equation (9).

Manjoine and Tome's proposal consisted of three different extension design curves covering the range from 10^6 – 10^{11} cycles (Figure 4). All three curves were bounded at a common point at 10^6 , corresponding to the ASME 1963 design curve. Curve A is a simple extrapolation of Langer's curve for strain-controlled conditions using equation (8) with transferability factor of two for stress/strain.

Curve B applies to strain-controlled conditions near welds and load-controlled conditions elsewhere. The mean stress correction is necessary for the load-controlled case. For strain-controlled loading, a high initial residual stress (e.g. due to welding) cannot be sustained due to plasticity and eventually relaxes. The B curve is bounded at three points: 10^6 (common for all curves), 10^8 based on experimental fatigue strength measurements and 10^{11} based on an extrapolation technique.

Curve C already includes the maximum effect of mean stress from the modified Goodman diagram and therefore no additional adjustment is needed. This curve is applied near welds for load-controlled cases. It may also be applied to base material for a conservative allowable S_a value.

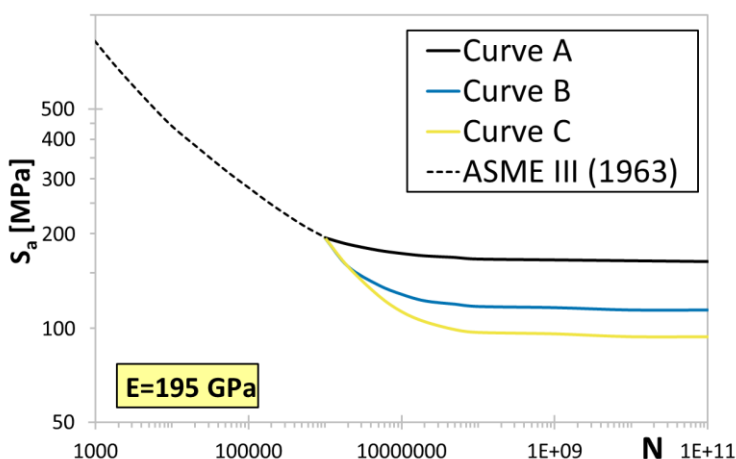


Figure 4. Design curve extension from 10^6 to 10^{11} cycles, as proposed by Manjoine and Tome (1983).

2.3 ASME 2010 design fatigue curve

The Code design curves from 1983 remained as such for several decades. Up until the mid-to-late 1990's there were no new serious efforts to question the applicability of the ASME III design curve. If not for concern over environmentally assisted fatigue (EAF), the design curves might still be as they were in 1983.

Starting in 1986 as part of the U.S. Nuclear Regulatory Commission (NRC) sponsored Environmentally Assisted Cracking in Light Water Reactors (EACLWR) program (O. K. Chopra, 2002; Kalinousky & Muscara, 2001), fatigue behaviour in air environment was considered in parallel with environmental effects to develop EAF models at Argonne National Laboratory (ANL). The following concerns primarily the update of the ASME III design fatigue curve, as EAF is discussed in chapter 3.

Like other laboratories performing EAF research, ANL started their experiments in air using a particular material heat of 316NG stainless steel, in form of 22 inch diameter pipe. As EACLWR continued to expand in magnitude and scope, the number of materials studied at ANL increased. In 1995 best-fit curves for existing fatigue data in air were provided in NUREG/CR-6335 (J. Keisler et al., 1995) with a slightly different functional form to Langer's equation, as given below:

$$\ln(N_{25}) = 7.072 - 1.98 \cdot \ln(\varepsilon_a - 0.12) \quad \text{for 316NG} \quad (10)$$

$$\ln(N_{25}) = 6.69 - 1.98 \cdot \ln(\varepsilon_a - 0.12) \quad \text{for 304 and 316} \quad (11)$$

The first constant essentially defines the LCF region, the constant 1.98 represents the slope and the constant 0.12 defines the endurance limit in units of strain amplitude (in %). In Langer's equation the slope term is fixed and equal to 2 [see equation (8)], whereas in the ANL model it is a fitted parameter. This kind of model was suggested already by Diercks (1979) in response to the design curve proposal by Jaske and O'Donnell (1977). Fatigue life N_{25} is defined as the number of cycles required for a 25 % peak tensile load drop rather than complete separation of specimen halves. Generally, the ANL equation is of the form

$$\ln(N_{25}) = A - B \cdot \ln(\varepsilon_a - C) \quad (12)$$

when expressed as a function of strain amplitude or

$$\varepsilon_a = A_1 \cdot N_{25}^{-n_1} + A_2 \quad (13)$$

when expressed as a function of fatigue life N_{25} .

Fitting of the constants was done by minimizing the sum of squares (SoS) of the Cartesian distance from experimental data to the best-fit curve, which was a new approach. The benefit of using this approach is that it is in principle not biased for either LCF or HCF. Minimizing the SoS for $\ln(N_{25})$ works well for LCF and is also correct in the sense that fatigue life is the dependent variable. However, this method becomes biased at low strain amplitude where the curve flattens near the endurance limit and most of the error is due to uncertainty in strain measurement (J. Keisler et al., 1995). Another disadvantage is the inability to use data potentially lying below the endurance limit. NUREG/CR-6335 (J. Keisler et al., 1995) gives more details about the method.

During The EACLWR project at ANL incorporation of other global research results, namely from Japan, meant larger databases could be collected and updated. Best-fit curves [equation (12)] were reiterated on multiple occasions and are provided below in chronological order. Note that equations (18)–(19) are identical to equations (14)–(15) but without the strain and temperature dependent terms. NUREG/CR-5704 (O. K. Chopra, 1999) is the only report in the EACLWR series in which the austenitic stainless steel best-fit curve in air contained terms for strain rate or temperature.

NUREG/CR-5704 (O. K. Chopra, 1999)

$$\ln(N_{25}) = 7.422 - 1.671 \cdot \ln(\varepsilon_a - 0.126) - T^* \varepsilon^* \quad \text{for 316NG} \quad (14)$$

$$\ln(N_{25}) = 6.703 - 2.030 \cdot \ln(\varepsilon_a - 0.126) - T^* \varepsilon^* \text{ for 304 and 316} \quad (15)$$

Effect of temperature through the transformed temperature term

$$T^* = 0 \quad (T < 250 \text{ }^\circ\text{C})$$

$$T^* = [(T - 250)/525]^{0.84} \text{ for } 250 \text{ }^\circ\text{C} \leq T < 400 \text{ }^\circ\text{C} \quad (16)$$

Effect of strain rate through the transformed temperature term

$$\varepsilon^* = 0 \text{ for } \dot{\varepsilon} > 0.4 \text{ \%}/\text{s}$$

$$\varepsilon^* = \ln(\dot{\varepsilon}/0.4) \text{ for } 0.0004 \text{ \%}/\text{s} \leq \dot{\varepsilon} \leq 0.4 \text{ \%}/\text{s}$$

$$\varepsilon^* = \ln(0.0004/0.4) \text{ for } \dot{\varepsilon} < 0.0004 \text{ \%}/\text{s} \quad (17)$$

NUREG/CR-6717 (O. K. Chopra & Shack, 2001)

$$\ln(N_{25}) = 7.422 - 1.671 \cdot \ln(\varepsilon_a - 0.126) \text{ for 316NG} \quad (18)$$

$$\ln(N_{25}) = 6.703 - 2.030 \cdot \ln(\varepsilon_a - 0.126) \text{ for 304 and 316} \quad (19)$$

NUREG/CR-6787 (O. K. Chopra, 2002)

$$\ln(N_{25}) = 7.433 - 1.782 \cdot \ln(\varepsilon_a - 0.126) \text{ for 316NG} \quad (20)$$

NUREG/CR-6909 Rev.0 (O. K. Chopra & Shack, 2007)

$$\ln(N_{25}) = 6.891 - 1.920 \cdot \ln(\varepsilon_a - 0.112) \text{ for 304, 304L, 316, 316L \& 316NG} \quad (21)$$

Figure 5 shows the evolution of these curves. Note that in the EACLWR final report NUREG/CR-6909 Rev.0 (O. K. Chopra & Shack, 2007):

1. A single regression (and design) curve was proposed using all (non-stabilized) stainless steel alloys. Until further notice, the derived design curve could be applied for stabilized stainless steels AISI 347 and 348 as well as cast alloys CF-3, CF-8 and CF-8M.
2. The range of applicability of the best-fit curve abruptly increased from 10^6 cycles to 10^{11} cycles.
3. A different kind of regression was done for constant A in equation (12) than in earlier reports in the EACLWR series.

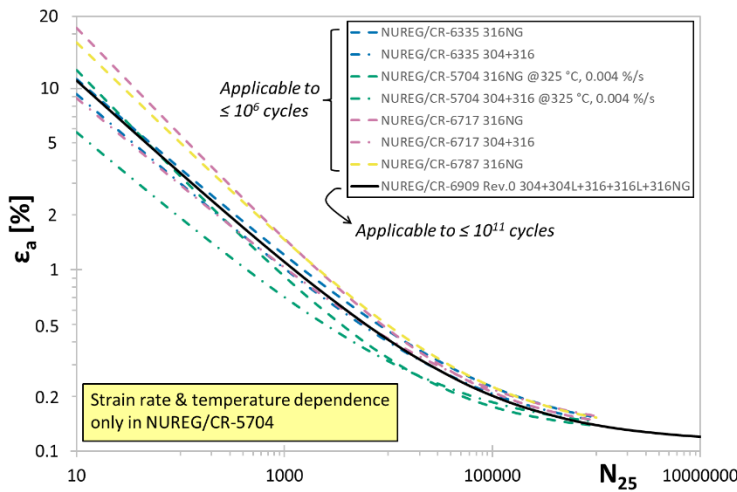


Figure 5. Evolution of best-fit curves defined in ANL reports.

For each material heat (or loading condition) with experimental results, the available data is considered a sample within a much larger population. Thus, each heat is characterized by the constant A in equation (12). Repeating this process for all heats enables construction of a rank-ordered cumulative probability distribution of A. The median value of the sample and normal distribution assumption are used to estimate the population behaviour for scatter. The desired percentiles can be read from the cumulative distribution plot as in Figure 6.

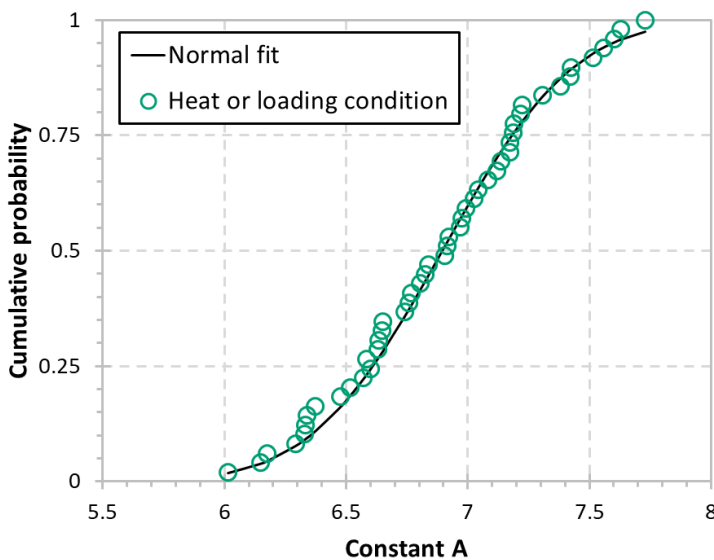


Figure 6. Cumulative distribution of constant A from NUREG/CR-6909 Rev. 0 stainless steel air data. (O. K. Chopra & Shack, 2007)

Fitting of constants B and C are not as clearly explained in NUREG/CR-6909, but some details were given at a 2006 Advisory Committee on Reactor Safeguards (ACRS) Subcommittee meeting prior to publication of Rev. 0 (U.S. NRC, 2006b). The constant C representing the endurance limit was assigned fixed value based on Japanese studies and the paper by Jaske and O'Donnell (1977). By conservatively fixing the endurance limit in this way, scatter increases.

Constant B representing the slope of the curve is determined from a best-fit, but it is not specified in ANL reports if a cumulative distribution of B was done or if it was based on regression of all data once constant A and C had already been fixed.

On the basis of equation (21) a single design curve was suggested in NUREG/CR-6909 Rev.0 (O. K. Chopra & Shack, 2007) to replace Langer's curve and the 1983 extension curves up to 10^{11} cycles. The proposed best-fit and design curves for stainless steel, in alternating stress intensity units, are shown in Figure 7, side by side with the old curves from Figure 2 and extension curve C from Figure 4. In NUREG/CR-6909 Rev. 1 (O. K. Chopra & Stevens, 2018) a re-evaluation of equation (21) was done using significantly more data points (622) than in Rev. 0 (357), but the result was essentially unchanged and no action was needed.

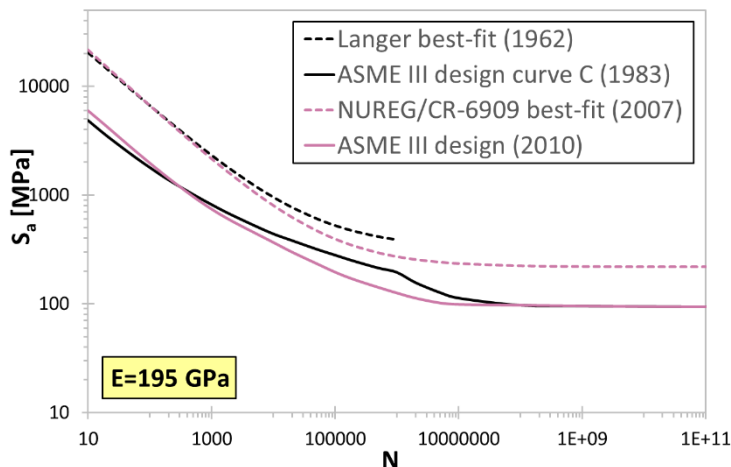


Figure 7. Stainless steel alloy proposed best-fit and design fatigue curves from NUREG/CR-6909, compared with old ASME curves. (ASME, 2010; O. K. Chopra & Shack, 2007)

Within the EACLWR project, the transferability factors used to obtain design curves in the 1960's were reassessed mainly based on literature studies for various material groups (carbon, low-alloy and stainless steels). The factors in air from these reports are summarized in Table 1. The shaded cells indicate a change in the range for a factor since the previous NUREG report in the EACLWR project.

There is close to an order of magnitude difference at the range extremes of total adjustment factors on fatigue life (bottom row of Table 1) if using simple multiplication of the NUREG/CR-6909 subfactor values. The maximum value 27.4 represents the unlikely combination of the poorest material heat with simultaneous maximum effects of size, surface finish etc. (O. K. Chopra & Shack, 2007; O. K. Chopra & Stevens, 2014, 2018).

ANL developed total adjustment factors on fatigue life by performing Monte Carlo simulations. All subfactors in Table 1 were considered to be independent, though it was acknowledged that some interactive effects likely exist. This was a conservative approach but necessary due to lack of better quantitative correlations. For subfactors other than material scatter and variability, the lower and upper ranges in Table 1 were assumed to represent the 5th and 95th percentiles of a lognormal distribution (O. K. Chopra & Shack, 2007).

For stainless steel, the overall transferability factor on life was quantified as 11.6 in NUREG/CR-6909 Rev. 0. The proposed design curve rounded this up to 12. Re-evaluation of the combined transferability factor was done in NUREG-6909 Rev.1 (draft and final version). The overall transferability factor for stainless steel reduced to 9.6 by using the same 5th percentile criteria as in Rev.0.

The transferability factor applied to stress or strain is equally important, as it is the more bounding of the two in the HCF end of the design curve. Subfactors affecting the transferability in the stress/strain direction were evaluated on several occasions as shown in Table 1. Essentially the same subfactors were identified for both fatigue life and stress/strain of the mean air curve. Most values listed in Table 1 were not evaluated based on direct experimental data but were instead transformed from the factor on fatigue life.

Basically the same mechanistic understanding of transferability subfactors applies to both fatigue life and stress/strain. One difference between transferability in horizontal or vertical direction is the notion of effects in the stress/strain direction not being cumulative but rather controlled by the single subfactor with the largest influence (J. Keisler et al., 1995). In the NUREG report series, the largest subfactor is suggested to come from material variability and scatter. For an unknown reason, quantification of the subfactors on strain were no longer included in any revisions of NUREG/CR-6909. Rather, a factor of two was selected as the margin in the design curve proposal.

The sequence of events eventually leading to the stainless steel design curve in Appendix I of ASME III being replaced with the ANL proposal is closely linked to evaluation of environmental effects and Regulatory Guide 1.207 Rev.0 (U.S. NRC, 2007a). Following its issuance, ASME also revised the design curve in the 2009b Addenda. In the 2010 Code edition (ASME, 2010), Langer's design curve and extension curves A, B and C were removed and replaced with the ANL design curve, applicable up to 10^{11} cycles. Although re-evaluation of the transferability factor on fatigue life in NUREG/CR-6909 Rev.1 (O. K. Chopra & Stevens, 2014, 2018) concluded that a value of 9.6 for stainless steel was sufficient, no further changes have been made to the ASME III design curve since 2009.

Table 1. Transferability factors for design curves in NUREG report series. Shaded cells indicate change of individual subfactors from the preceding reference.

Parameter	ASME III (1963)	NUREG/CR-6237 ³⁾	NUREG/CR-6335		NUREG/CR-5704	
	Factor on life	Factor on life	Factor on life	Factor on strain	Factor on life	Factor on strain
Material variability & scatter	2.0	–	2.5	1.7	2.5	1.4–1.7
Size effect	2.5	2	1.4	1.25	1.4	1.25
Surface finish & other factors ¹⁾	4	3.5	3	1.3	2.0–3.0	1.3
Loading history	–	–	–	–	1.5–2.5	1.5
Total adjustment	20.0	7.0 ²⁾	10.0	1.7	10.0–26.0	1.5–1.7

Parameter	NUREG/CR-6717 & 6787		NUREG/CR-6815		NUREG/CR-6909 Rev.0	NUREG/CR-6909 Rev.1
	Factor on life	Factor on strain	Factor on life	Factor on strain	Factor on life	Factor on life
Material variability & scatter	2.5	1.4–1.7	2.0	1.2–1.7	2.1–2.8	2.1–2.8
Size effect	1.4	1.25	1.4	1.25	1.2–1.4	1.0–1.4
Surface finish & other factors ¹⁾	2.0–3.0	1.6	3.0	1.6	2.0–3.5	1.5–3.5 ⁴⁾
Loading history	1.5–2.5	1.3–1.6	1.5–2.5	1.3–1.6	1.2–2.0	1.0–2.0
Total adjustment	10.0–26.0	1.6–1.7	12.5–21.0	1.6–1.7	6.0–27.4	3.15–27.4

¹⁾ includes effect of 'industrial' atmosphere in ASME III 1963

²⁾ before applying factor on material variability

³⁾ factors determined for ferritic steels only

⁴⁾ reduced lower limit is based on ferritic steel data, but also applied to austenitic stainless steels

2.4 Alternative design fatigue curves as evolutions of ASME III

2.4.1 RCC-M (France)

The French equivalent of ASME III is the RCC-M. The first edition of RCC-M was issued in 1980. Although the similarities between ASME III and RCC-M were evident from the beginning, they were not identical and have continued to diverge since.

Fatigue design curves for crack initiation (in an initially defect-free location) in RCC-M are located under the technical annexes in Section I, Subsection Z. The stainless steel DFC is paired with $E=179$ GPa and is identical with the ASME III design fatigue curve from 1963 i.e. Langer best-fit curve with transferability factors 20 and 2 on cycles and stress, respectively.

Similar to ASME III, RCC-M bases its fatigue design on either explicit or implicit consideration of the various factors that influence the fatigue “resistance” (of a material) and the “demand” placed upon it (severity of loading). DFCs are considered to implicitly contain several factors, including material manufacturing parameters such as ingot size, orientation, heat treatment, grain size, product shape, chemical composition, among others (Grandemange & Faidy, 2000).

The RCC-M criteria document assumes a global consensus regarding the validity of the old 20/2 transferability factors. In addition, it includes a table summarizing several sources, where different authors interpret the more detailed breakdown of the factors with differing emphasis (similarly to Table 1, but in greater detail). (AFCEN, 2014; Grandemange & Faidy, 2000).

The hand-in-hand evolution of DFCs between ASME III and RCC-M began to deviate in the 1980’s. The extension of ASME curves beyond 10^6 was not implemented in RCC-M. The RCC-M criteria document (AFCEN, 2014) acknowledges that the endurance limit may not be definite yet at 10^6 cycles, but rather than designing to accommodate these kinds of loadings (e.g. vibrations), the philosophy is to avoid such circumstances through improved design.

After NUREG/CR-6909 was published in the USA, a fatigue road map was drafted by Electricite de France (EDF) to introduce changes to the RCC-M code, Figure 8.

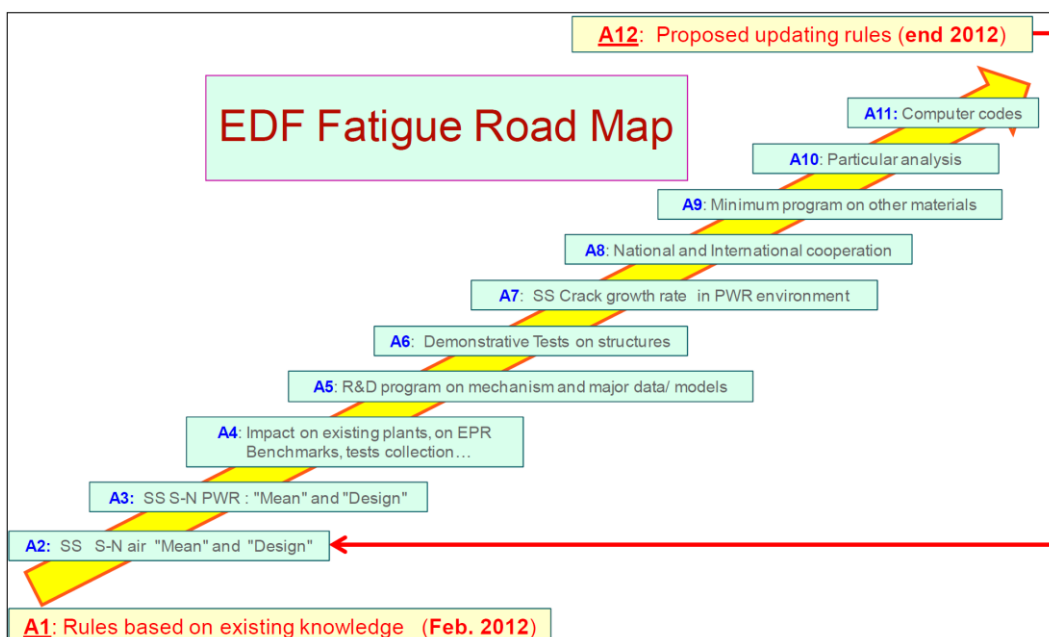


Figure 8. EDF fatigue road map. (Faidy, 2012)

Regarding fatigue crack initiation, concerns to address environmental effects and the potentially unconservative stainless steel DFC in HCF were written in the roadmap (Faidy, 2012). In principle, the planned modifications to RCC-M were no different in scope than the combined approach of ASME III + NUREG/CR-6909. Updates were planned to

- the best-fit fatigue curve for stainless steel,
- the design fatigue curve for stainless steel, and
- combination of the above with consideration of environmental effects.

The best-fit curve to French stainless steel data is given in equation (22) (Faidy, 2008). It is very similar to the NUREG/CR-6909 best-fit curve, equation (21), when expressed as a function of N_{25} .

$$\varepsilon_a = 32.093 \cdot N_{25}^{-0.5} + 0.112 \quad (22)$$

Statistical analysis suggested the NUREG mean curve to fit French 304L and 316L results with the same accuracy as NUREG/CR-6909 data itself (Métais et al., 2013). However, details of how the endurance limit parameter was derived are not known.

French research has aimed to better identify and quantify the subfactors for transferability in DFCs. The investigated subfactors were loosely similar in scope to those contained in the 2010 ASME DFC. Initially a global factor of 12 on fatigue life in air was derived, independently of those subfactors derived in NUREG/CR-6909 Rev. 0. When these numbers were derived, not all research programs had been completed yet. For example, roughness and transient shape studies in PWR environment were not concluded. A small provision for environmental effects is included in the total factor on life (Faidy, 2012). Subsequently, arguments were made by Faidy (2014) to reduce certain subfactors. If the fatigue usage of unity is defined as a 3 mm deep engineering crack, the size effect was proposed to reduce. Consequently, the overall factor on fatigue life reduces to 9. Secondly, for the strictly limited selection of RCC-M stainless steels the scatter factor may be reduced to as low as 2.0, further reducing to overall factor on life to 7.2.

Table 2. Transferability factors based on French research. (Faidy, 2012, 2014)

Scatter	Size	Temperature ¹	Cold work ¹	Biaxiality ¹	Hold time	Transient shape ¹	Roughness ¹	$F_{en,max}$	Factor on life	Factor on strain
2.5 ²	1.6	1	1	1	1	1	2	1.5	12.0	1.4
2.5 ³	1.2	1	1	1	1	1	2	1.5	9.0	1.4
2.0 ³	1.2	1	1	1	1	1	2	1.5	7.2	1.4

¹ongoing research program at time of publication (2014)

²From Faidy (2012)

³From Faidy (2014)

The listed values in Table 2 were simplified into three coefficient groups for

- material variability and data scatter (identical with the NUREG/CR-6909 definition),
- component effects (surface roughness, size, "structural effect" for thermal loading) and
- loading (multiaxiality, variable amplitude). (Métais et al., 2014)

Statistical analysis of French air data arrived at the same scatter factor on life (to one decimal accuracy) as in NUREG/CR-6909 by splitting the data for both $<10^4$ and $<10^5$ cycles. For component effects, the AREVA test campaign (Le Duff et al., 2010) demonstrated factors on life ranging between 1.5–2.5 in air for a rough surface finish. For conservatism, additional 0.5 to these coefficient ranges was added in the final proposal.

For the loading coefficient group, the range of 1.2–2.0 applied also in NUREG/CR-6909 Rev. 0 was established, but later adjusted to 1.0–2.0¹ (Métais et al., 2015). A more specific range could not be defined, recognizing that the numerous existing multiaxial data from French research institutes was too complex to transform into comparable uniaxial format.

The combined overall transferability factor on life from statistical analysis to French data, repeating the Monte Carlo based method used by ANL, was finally 7.0 (Métais et al., 2015). The revised factor for the US-Japanese database in NUREG/CR-6909 Rev.1 (draft) (O. K. Chopra & Stevens, 2014) was 9.6, which leaves a margin of $9.6/7.0 \approx 1.4$ in the final French proposal. This difference is of the order of magnitude of a size effect (see Table 1 and Table 2).

Despite French analyses finally demonstrating a factor of 7.0 on life, to be consistent with NUREG/CR-6909 Rev.0 (O. K. Chopra & Shack, 2007), a factor of 12 was at first suggested. This was to account for effects whose magnitude remained uncertain and too difficult to reliably quantify (Métais et al., 2014). In late 2014, the value of 10 was settled for when the request for modification of the RCC-M was formally submitted to AFCEN for review. This was still conservative relative to 9.6 in NUREG/CR-6909 Rev. 1, but it was intentional to partially account for environmental effects as part of the DFC. (Métais et al., 2015)

The transferability factor of strain was reduced from 2 to 1.4 by arguing that scatter is limited for the restricted number of RCC-M material grades (essentially 304L and 316L) and that the most recent experiments in HCF used were performed in strain control. Consequently, the proposed French design fatigue curve for stainless is very nearly identical with the 1963 ASME design fatigue curve at 10^6 cycles. (Faidy, 2012) Technical basis publications focused on supporting the selected factor of 1.4 on strain. Multiple statistical analysis methods were applied to confirm this. (Blatman et al., 2014, 2016)

The RCC-M 2016 edition (AFCEN, 2016) introduced a Rule in Probationary Phase (RPP) N° 2 with an alternative design fatigue curve for stainless steels, using the transferability factors 10 and 1.4. RPPs are comparable to Code Cases of the ASME Code. The RPP adopted the NUREG/CR-6909 mean curve as representative of French stainless steels due to the proximity of experimental data (Métais et al., 2013).

Figure 9 compares the design curves in RCC-M, RPP N° 2 and 2010 edition of ASME III. The S_a values are all adjusted to $E=179$ GPa, which is the paired modulus in RCC-M. The RPP N° 2 and ASME 2010 design curve deviate markedly after 10^4 cycles. The RPP N° 2 curve approaches the ASME 1963 design curve towards 10^6 cycles, which is effectively considered an endurance limit. In the other direction, the RPP N° 2 curve is conservative relative to the existing RCC-M DFC by a factor of about two in part of the low cycle range between 10^3 – 10^5 cycles.

¹ which coincidentally is the same range as in NUREG/CR-6909 Rev.1 of 2018.

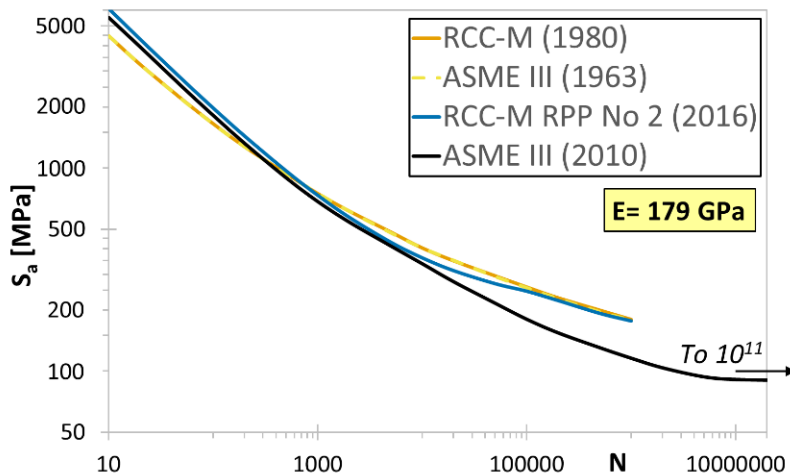


Figure 9. Comparison of RCC-M design curve and RPP N° 2 with ASME III design curves.

2.4.2 JSME (Japan)

The Japan Society of Mechanical Engineers (JSME) has been involved in nuclear code development since the Committee on Power Generation Facility Code was established in 1997. The first edition of ASME III equivalent Code, JSME S NC1 (JSME, 2001) was issued in 2001 and adopted DFCs from the 1983 ASME Code edition. (ASME, 2012) The Japanese codes and standards activities since then have concerned revisions of both the air best-fit and design curves.

The first Japanese best-fit curve was defined in the Environmental Fatigue Test (EFT) project. The so-called Tsutsumi best-fit curve, equation (23), was based on a mix of Japanese and US data. The best-fit curve was needed as a reference for modelling environmental effects, which is described later in chapter 3.

$$\varepsilon_a = 23 \cdot N_f^{-0.457} + 0.11$$

$$\ln(N_{25}) = 6.861 - 2.188 \cdot \ln(\varepsilon_a - 0.11) \quad (23)$$

Although the stainless steel design curves in JSME S NC1 Code remain adapted from the 1983 edition of ASME III (Langer's curve with extension curves A, B and C), efforts to develop revised design curves have been in progress for over a decade. Influenced by the revised design curve proposal in NUREG/CR-6909, the JSME Code Committee established in 2007 a task group on fatigue evaluation with many similar objectives as ANL research in the EAFLWR program.

The task group work commented that the proposed air DFC in U.S. NRC draft regulatory guide DG-1144 (U.S. NRC, 2006c), which is identical to NUREG/CR-6909 DFC (O. K. Chopra & Shack, 2007), did not include a review on the stress/strain transferability factor. Takahashi and Nakamura (2003) had performed a statistical analysis to show particularly small scatter of (both US and Japanese) air data in the strain amplitude direction, which may justify a reduced transferability factor (such as 1.5 instead of 2.0). This would have a remarkable effect in HCF.

Similar databases of air data were evaluated in both the Japanese and US programs, which not surprisingly led to similar conclusions of mean behaviour. The JSME task group proposed a best-fit mean air curve with the following equation (Nomura et al., 2009):

$$\varepsilon_a = 22.1 \cdot N_f^{-0.457} + 0.11$$

$$\ln(N_{25}) = 6.774 - 2.188 \cdot \ln(\varepsilon_a - 0.11) \quad (24)$$

The difference in databases used between equations (24) and (23) only results in a minor change of the leading constant (the LCF parameter) and consequently the Tsutsumi best-fit curve continued to be used.

According to Nomura et al. (2009) the endurance limit was a set rather than fitted parameter, but the specific technical basis is not explained. This is believed to be the decision also made in the Tsutsumi best-fit curve, though not explicitly explained in the original literature.

There is a distinct difference in the regression of Japanese best-fit curves such as equation (24) compared to the NUREG/CR-6909 mean curve, equation (21). In the former, regression was done on all data points of all heats rather than performing first an evaluation of the constant A of equation (12). Scarce details of the regression are provided by Nomura et al. (2009).

The JSME task group studied design curve margins, which are summarized in Table 3 and Table 4 (Nomura et al., 2009).

Table 3. 95 % confidence limit scatter factors on fatigue life and strain by stainless steel alloy type and cycle range. (Nomura et al., 2009)

Material	<10 ⁴ cycles		<10 ⁵ cycles	
	Factor on life	Factor on strain	Factor on life	Factor on strain
Type 304	2.90	1.49	4.16	1.55
Type 316	2.09	1.32	2.49	1.34
SCS14A	1.37	1.13	2.25	1.27
Weld	2.39	1.35	2.37	1.31
Total	2.74	1.47	3.44	1.47

Table 4. Stainless steel design fatigue curve transferability factors according to the JSME task group (Nomura et al., 2009). NUREG/CR-6909 rev.0 (O. K. Chopra & Shack, 2007) values in parentheses for comparison.

Parameter	Factor on life	Factor on strain
Scatter	2.7–3.4 (2.1–2.8)	1.47
Size effect	1.2–1.4 (same)	–
Surface roughness	2.0–3.5 (same)	1.0–1.5
Total	6.6–16 (6.0–27)	1.47–2.2
95 % confidence level	10–12 (12)	1.9

The JSME task group study acknowledged the lack of large-scale component verification tests and gigacycle data which would reduce uncertainty especially for defining the endurance limit. These kinds of studies were later performed in the Gigacycle Fatigue (GCF) subcommittee of the Japan Welding Engineering Society (JWES).

After the JSME task group work, Fukuta et al. (2013) reported separate best-fit curves by material type, equations (25)–(28). Only domestic data from the EFT project was used in the regression analysis and base metals 304 and 316 were grouped together. Based on the equations, the endurance limit constant was fixed and not fitted.

$$\varepsilon_a = 32.6 \cdot N_f^{-0.511} + 0.11$$

$$\ln(N_{25}) = 6.819 - 1.957 \cdot \ln(\varepsilon_a - 0.11) \quad \text{for base metal} \quad (25)$$

$$\varepsilon_a = 12.1 \cdot N_f^{-0.420} + 0.11$$

$$\ln(N_{25}) = 5.936 - 2.381 \cdot \ln(\varepsilon_a - 0.11) \quad \text{for 304 welds} \quad (26)$$

$$\varepsilon_a = 28.9 \cdot N_f^{-0.515} + 0.11$$

$$\ln(N_{25}) = 6.532 - 1.942 \cdot \ln(\varepsilon_a - 0.11) \quad \text{for 316 welds} \quad (27)$$

$$\varepsilon_a = 23.6 \cdot N_f^{-0.500} + 0.11$$

$$\ln(N_{25}) = 6.322 - 2 \cdot \ln(\varepsilon_a - 0.11) \quad \text{for CASS} \quad (28)$$

A comparison of the various Japanese stainless steel air best-fit curves is shown in Figure 10. Roughly speaking, the EFT best-fit curves (Tsutsumi and Higuchi) and the JSME task group best-fit curve (Nomura) lie between the Langer and NUREG/CR-6909 best-fit curves. On the contrary, weld and CASS best-fit curves of Fukuta et al. (2013) are mainly conservative relative to the rest. The base metal best-fit curve of Fukuta et al. (2013) agrees closely with NUREG/CR-6909.

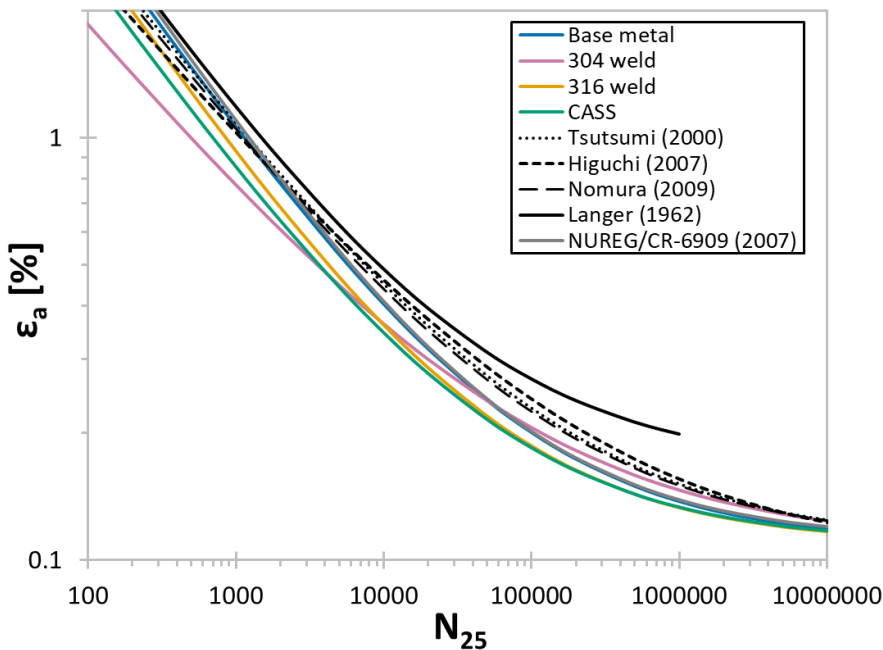


Figure 10. Comparison of Japanese (Fukuta et al., 2013; Higuchi, Sakaguchi, Nomura, et al., 2007; Nomura et al., 2009; Tsutsumi et al., 2000) and US (O. K. Chopra & Shack, 2007; Fukuta et al., 2013; Langer, 1962) best-fit curves.

Shortly after the JSME task group had summarized their findings, the Atomic Energy Research Committee of JWES established the Design Fatigue Curve (DFC) subcommittee with similar objectives of eliminating remaining uncertainties through new experimental studies (S. Asada et al., 2013).

The structure of JWES DFC subcommittee work was presented by Asada et al. (2013). Running between 2011 and 2016, the work was divided into the following tasks:

- Collection and analysis of existing small-scale fatigue test data for best-fit curves.
- Study on existing large-scale fatigue test data.
- Study of relevant fatigue evaluation codes and methods.
- Study of mean stress effect.
- Study on transferability factors.
- Development of design curves.
- Large-scale fatigue testing.
- Evaluation of current fatigue analysis method.

Table 5. JWES DFC subcommittee PVP papers on design fatigue curve development and application with the environmental fatigue evaluation method.

Paper title	Reference
PVP2013-97767 Plan and Status of Development of Design Fatigue Curves (Phase 1)	(S. Asada et al., 2013)
PVP2013-97770 Proposal of Fatigue Life Equations for Carbon and Low-Alloy Steels and Austenitic Stainless Steels as a Function of Tensile Strength	(Kanasaki et al., 2013)
PVP2014-28573 Study on Consideration of Size Effects on Design Fatigue Curve	(Hirano et al., 2014)
PVP2014-28601 Proposal of Surface Finish Factor on Fatigue Strength in Design Fatigue Curve	(Fukuta et al., 2014)
PVP2015-45089 Study on A New Design Fatigue Evaluation Method	(S. Asada et al., 2015)
PVP2016-63796 Study on Mean Stress Effects for Design Fatigue Curves	(S. Asada et al., 2016)
PVP2018-84052 Development of New Design Fatigue Curves in Japan: Discussion of Best-Fit Curves Based on Fatigue Test Data With Small-Scale Test Specimen	(Y. Wang et al., 2018)
PVP2018-84432 Development of New Design Fatigue Curves in Japan: Proposal of a New Fatigue Evaluation Method	(S. Asada et al., 2018)
PVP2018-84436 Development of New Design Fatigue Curves in Japan: Discussion of Best Fit Curves Based on Fatigue Test Data with Large Scale Piping	(Bodai et al., 2018)
PVP2019-93167 Development of New Design Fatigue Curves in Japan: Discussion of Effect of Surface Finish on Fatigue Strength of Nuclear Component Materials	(Nakane et al., 2019)
PVP2019-93272 Development of New Design Fatigue Curves in Japan: Discussion of Fatigue Crack Growth Based on Fatigue Test Data with Large Scale Piping	(Bodai et al., 2019)
PVP2019-93273 Study on Incorporation of a New Design Fatigue Curve into the JSME Environmental Fatigue Evaluation Method	(S. Asada et al., 2019)
PVP2019-93393 Development of New Design Fatigue Curves in Japan: Discussion of Crack Growth Behavior in Large-Scale Fatigue Tests of Carbon and Low-Alloy Steel Plates	(Takanashi et al., 2019)
PVP2020-21078 Study on Incorporation of New Design Fatigue Curves and a New Environmental Fatigue Correction Factor for PWR Environment into the JSME Environmental Fatigue Evaluation Method	(S. Asada et al., 2020)
PVP2021-60418 Development of New Design Fatigue Curves in Japan – Treatment of Variable Loading Amplitude Effect	(S. Asada & Nomura, 2021)
PVP2022-84695 Investigation of Surface Finish Effect on Fatigue Strength of Carbon and Low Alloy Steels	(S. Asada et al., 2022)

The PVP papers describing the JWES DFC subcommittee work on design fatigue curves and ensuing environmental fatigue evaluation method are listed in Table 5. Further material can be found on the JWES fatigue knowledge platform (JWES, 2023).

Small-scale fatigue data for stainless steels was collected from Japanese JNUFAD and FADAL (Fatigue Database for LWR materials) databases, NIMS (National Institute for Materials Science) datasheets and other open literature data sheets, resulting in approximately 750 data points for stainless steels. The best-fit curve evaluation methodology was based on the EN 13445-3 standard (CEN, 2009), where tensile strength (TS) is a curve parameter. In developing the TS dependence of the curves, austenitic stainless steels were divided into ten ranges representative of the collected data. Only finite fatigue life results at temperatures up to 200 °C were used for fitting.

The best-fit curve equations of all ten ranges of TS showed that there is no obvious effect of TS on any strain-life curve parameter besides the constant for endurance limit. Thus, the global best-fit curve applicable up to TS=950 MPa was defined by using the average constants A and B in equation (12) and the linear TS dependence of constant C. The equation, given by Kanasaki et al. (2013) is:

$$\varepsilon_a = 26.1 \cdot N_f^{-0.485} + \frac{0.488}{E_0} TS$$

$$\ln(N_{25}) = 6.726 - 2.062 \cdot \ln\left(\varepsilon_a - \frac{0.488}{E_0} TS\right) \quad (29)$$

From equation (29) it is easy to calculate that in order for the endurance limit to be the same as it is in the NUREG/CR-6909 best-fit curve, equation (21), TS<450 MPa would be necessary (using E=195 GPa for room temperature). This is well below typical room temperature minimum TS values tabulated in codes such as ASME II. Figure 11 shows how the endurance limit (blue line) term in equation (29) changes as a function of temperature due to the change in tensile strength (using ASME II tabulated values, black line) and elastic modulus (lavender line) as functions of temperature.

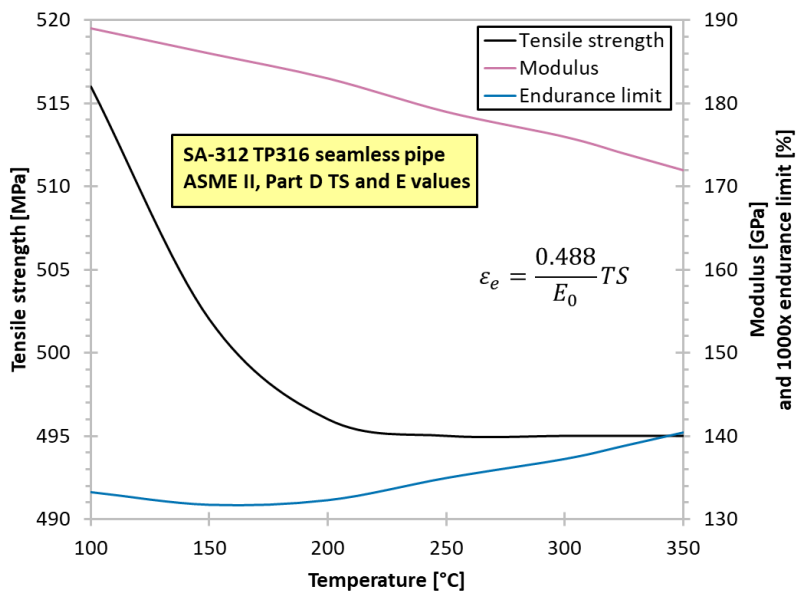


Figure 11. Influence of temperature on tensile strength, elastic modulus and endurance limit per equation (29). Endurance limit is scaled by 10^3 for plotting on the same common right axis with the modulus.

Scatter and material variability were evaluated for each of the ten ranges, both in terms of fatigue life (with data up to $4 \cdot 10^4$ cycles) and strain amplitude (with data greater than 10^4 cycles). A log-normal distribution was assumed when defining the standard deviation. For all data, mean minus two standard deviations translated to factors of 2.49 on fatigue life and 1.33 on strain amplitude. More details can be seen in Table 6.

The JWES DFC subcommittee recommendation was to not apply a size effect on either fatigue life or fatigue strength, based on the review by Hirano et al. (2014). The study concluded that size effects on endurance limit are dominated by stress gradient effects, which do not exist in the axially loaded smooth specimen data.

Table 6. Scatter by tensile strength, from data between room temperature and 200 °C. (Kanasaki et al., 2013)

Tensile strength [MPa]	10 ⁵ ≤ N ≤ 10 ⁴ cycles	10 ⁴ ≤ N cycles
	Factor on life	Factor on strain
516	2.987	–
529–550	2.712	1.300
552–578	2.361	1.355
586–595	2.999	1.553
600–619	2.520	1.495
628–650	2.205	1.436
665–682	2.451	1.377
693–712	2.546	1.216
745–756	2.793	1.181
951	1.632	1.139
Average	2.487	1.332

Similar conclusions on surface finish effects were made in the literature review collected by Fukuta et al. (2014). Geometric roughness, surface cold work and residual stress are identified as the three variables governing the magnitude of surface roughness effects. For stainless steels, evidence collected from earlier Japanese and international publications did not show conclusive detrimental surface roughness effect and the DFC proposal was to neglect it in the design curve.

Asada et al. (2015, 2018) provided the details of the JWES DFC proposed updated fatigue evaluation method. In addition to the changes discussed in previous paragraphs, the other two major details are the use of the Smith-Watson-Topper (SWT) method to account for mean stress and the applicability of design curves up to 10^8 cycles only. Where variable amplitude loading can be neglected, the JWES DFC proposed to use the endurance limit suggestion of $0.4 \cdot TS$ given in safety standard KHKS-0220 (KHK, 2010). Otherwise, variable amplitude loading is accounted for by using the Haibach approach, i.e. extrapolating the curve using a shallow slope after a specified number of cycles. The procedure proposed by JWES DFC comes from EN 13445-3. Between $2 \cdot 10^6$ and 10^8 cycles the slope of the curve is set to ten. (S. Asada & Nomura, 2021)

A typical design curve for SUS F316 stainless steel is shown in Figure 12. Because effects of size and surface roughness do not need to be considered for stainless steel, the only transferability factors are $\alpha=1.43$ on stress/strain and $\beta=2.48$ on fatigue life which are the final proposals to account for scatter and variability and differ slightly from Table 6 (S. Asada et al., 2018). For comparison, the proposal of the preceding JSME task group, with transferability factors of 12 and 1.9, is shown.

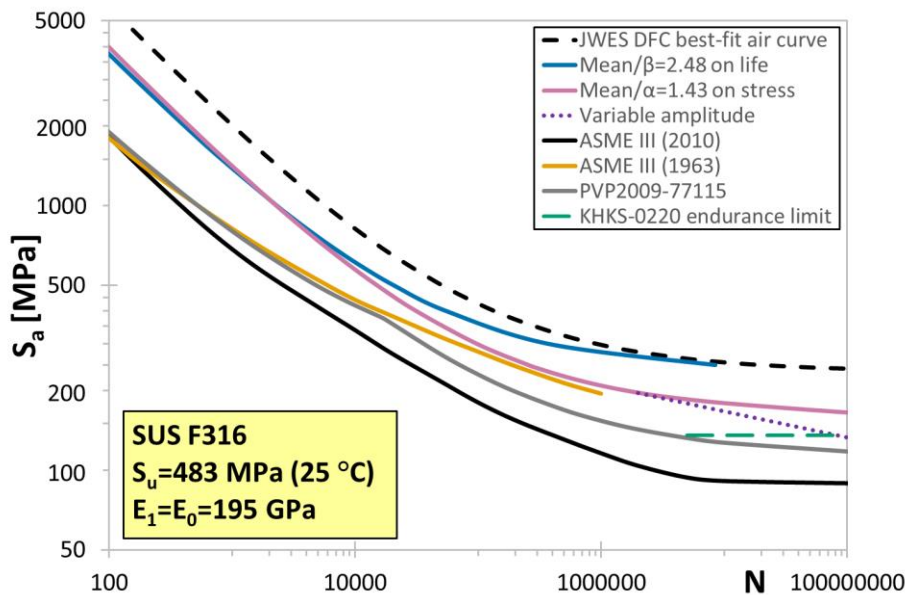


Figure 12. Typical mean and design curves proposed by DFC compared to other design curves and 2009 JSME task group proposal in PVP2009-77115 (Nomura et al., 2009).

Recently the JSME Main Committee on Power Generation Facility Codes approved the new design fatigue curve methodology with tensile strength as a curve parameter. The change was approved for the 2022 edition Japanese JSME Environmental Fatigue Evaluation Method Code JSME S NF1 (S. Asada et al., 2022, 2023).

2.4.3 KTA (Germany)

In Germany, Kerntechnischer Ausschuss, KTA (the Nuclear Safety Standards Commission) issues safety standards in nuclear technology topics. Design and analysis of LWR primary components is contained in KTA 3201.2, which was first issued in 1980 and strongly rooted in ASME III. Thus, the stainless steel design fatigue curve in KTA 3201.2 was identical to the 1963 ASME III design curve.

The most relevant KTA revision in terms of fatigue design is 2013-11 (KTA, 2013), in which KTA reflected the regulatory and ASME Code development in the USA, NRC endorsement of NUREG/CR-6909 and the change of ASME III design curve in 2009. On the other hand, for piping German plants apply stabilized stainless steel grades X6CrNiTi18-10S (equivalent to AISI 321) and X6CrNiNb18-10S (equivalent to AISI 347), which were not used to construct the ASME III 2010 DFC. This warranted an investigation on compatibility of German alloys with the ASME III DFC (Schuler et al., 2013).

Technical endurance limit at 10^7 cycles was evaluated with additional load-controlled test series at room temperature and 288 °C. A subset of the database had previously been demonstrated to deviate notably from the NUREG/CR-6909 Rev.0 best-fit curve in air, namely in HCF (J. Solin, Reese, et al., 2011). The additional data confirmed the observation.

Further efforts were made to examine effects of temperature, hold times, strain rate, and dynamic strain ageing. The conclusion from the elevated temperature database opposed the statement of negligible temperature effects in air up to 400 °C given by ANL. A continuous temperature dependency in HCF regime was demonstrated, but separate best-fit curves for data above or below 80 °C were presented using the same statistical approach selected by ANL. (Schuler et al., 2013). The equations of the two best-fit curves are

$$\ln(N_{25}) = 6.706 - 2.172 \cdot \ln(\varepsilon_a - 0.136) \text{ for } T \leq 80 \text{ } ^\circ\text{C} \quad (30)$$

$$\ln(N_{25}) = 6.850 - 2.255 \cdot \ln(\varepsilon_a - 0.078) \text{ for } T > 80 \text{ } ^\circ\text{C} \quad (31)$$

The equations were formulated to bound the load-controlled results at 10^7 cycles with an approximation of the endurance limit from tensile strength (Schuler et al., 2013). Due to limited availability of elevated temperature failure data points, equation (21) was adopted for the $>80 \text{ } ^\circ\text{C}$ curve beyond $2 \cdot 10^6$ cycles, with an offset defined by the strain amplitude difference between equations (21) and (31) at $2 \cdot 10^6$ cycles (a difference of 0.0193 %).

Design curves aimed for the stabilized steels 1.4550 and 1.4541 were determined based on the new reference curves (equations 30 and 31) and selected transferability margins for fatigue life and for strain amplitude.

A transferability margin with a factor of 12 in life had been justified to account for material variability and scatter in NUREG/CR-6909 Rev. 0. As the material variability and scatter was smaller in the KTA data, the factor of 12 in life was selected and considered at least as conservative as that for the ASME III. Smaller scatter in the KTA data is probably due to limited selection of alloys, extraction of samples from components manufactured for NPP use and testing in experienced fatigue laboratories.

The factor on stress/strain was analysed separately. The subfactors and resulting global factors are shown in Table 7. The subfactor on scatter is based on room temperature results only. This factor is less limiting than factor of 1.4 in the RCC-M RPP N° 2, but unlike in the French proposal, in KTA the global factor is conservatively derived from a multiplication of all subfactors shown in Table 7. (Schuler et al., 2013).

Table 7. Transferability factors on stress/strain in KTA 3201.2 design curves for stabilized stainless steels.

Parameter	T≤80 °C	T>80 °C	Factor based on:
Scatter	1.27	1.27	149 RT fatigue data
Surface roughness	1.23	1.27	$R_z = 20 \text{ } \mu\text{m}$
Size effect	1.09	1.09	thickness = 40 mm
Mean stress	1.05	1.07	$S_{\text{mean}} = 100 \text{ MPa}$
Total	1.79	1.88	all factors multiplied

The resulting DFCs are specified in the following equations where the strain amplitudes are transformed to stress intensity amplitudes:

$$\ln(N) = 4.400 - 2.450 \cdot \ln\left(\frac{S_a}{E/100} - 0.071\right) \text{ for } T \leq 80 \text{ } ^\circ\text{C} \quad (32)$$

$$\ln(N) = 4.500 - 2.365 \cdot \ln\left(\frac{S_a}{E/100} - 0.0478\right) \text{ for } T > 80 \text{ } ^\circ\text{C} \quad (33)$$

These KTA DFCs are plotted in Figure 13 along with the original and current ASME III design curves, the latter adjusted compatible with $E=179 \text{ GPa}$ as the paired elastic modulus. The room temperature KTA curve is not far removed from the 1963 ASME III curve, whereas the 2010 ASME curve and elevated temperature KTA curve are very similar.

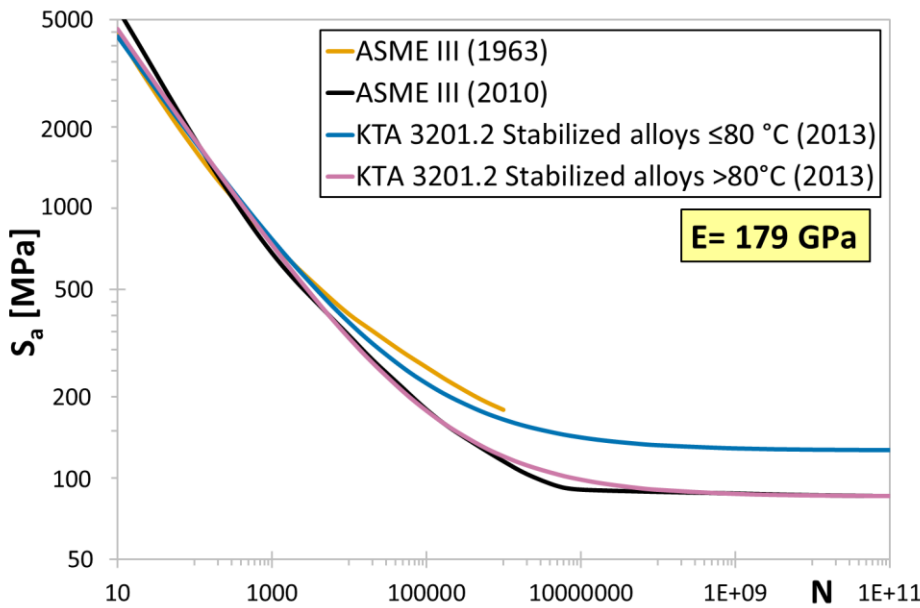


Figure 13. Comparison of KTA 3201.2 stabilized alloy design curves with ASME III design curves.

The 2013-11 revision of KTA 3201.2 also incorporated the ASME III 2010 design curve, which is to be applied for stainless steels not covered by the new curves provided in the KTA 3201.2. A difference between KTA and ASME III DFCs for non-stabilized stainless remains because KTA continues to use $E=179$ GPa as the paired elastic modulus, while it had been changed in 1983 to $E=195$ GPa in ASME III DFC for stainless steels. To illustrate this difference, the KTA and ASME III DFCs in Figure 13 are redrawn in Figure 14 paired with elastic moduli representative to RT and 300 °C.

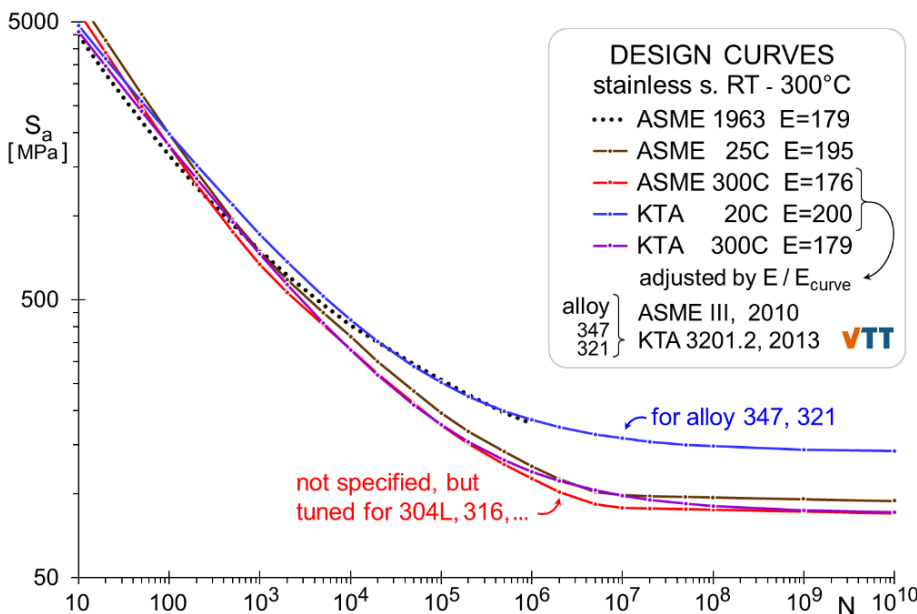


Figure 14. Comparison of KTA design fatigue curves with the original and current ASME III design curves, as in Figure 13, but adjusted to design temperatures 20 and 300°C. KTA and ASME 1963 curves are defined with $E_{curve}=179$ GPa, the ASME III (2010) curve with $E_{curve}=195$ GPa. Two of the curves are adjusted according to equation (9).

2.4.4 PNAE-G-7 (Russia)

Russian fatigue design curves are included in the document PNAE G-7-002-86 'Regulations of Strength Analysis of Equipment and Piping of Nuclear Power Facilities' (Energoatomizdat, 1989), effective from 1987. This document included unique features to the fatigue design curves already in the 1980's. Development of a modern VVER reactor code SPiR-WWER-2012 was started in 2010 but has yet to replace the PNAE G-7 series (ASME, 2012).

Mean and design curves in PNAE G-7 are defined differently to all other codes and standards referred in this report. Specified material properties are used to construct the parametric curves at a range of temperatures, which gives the designer flexibility compared to a fixed curve for all materials and conditions, including cyclic asymmetry ($R \neq -1$).

As a first approximation, a lower bound DFC with conservative parameters is provided for cumulative usage calculations. If CUF exceeds the allowable value based on this curve, the designer may at first apply tabulated mechanical properties to construct an alternative DFC. Since the observation of conservative curves even by using material properties rather than fitted values in equation (3) was already made by Coffin, an experimentally defined fatigue curve may be used as a final option in case CUF calculations are not satisfactory.

The basic curve equation is based on the Coffin-Manson-Basquin type. A fixed value of the anticipated endurance limit may be used to construct a DFC up to 10^6 cycles, but the more general case includes no fixed value for the endurance limit. Instead, the elastic stress/strain term includes a slope, as was suggested by Manson and Halford (1967).

Transferability factors for pressure boundary components are ten on fatigue life and two on stress/strain. Additional fatigue strength reduction factors are provided for welded joints. Although the factor of ten may seem less conservative than in other codes of the time, the BFC to which the factors are applied represents the lower bound of the experimental data for crack initiation and not the mean curve like in all other codes (Buckthorpe et al., 2003).

Investigating many of the details of the PNAE documents is complicated by the lack of public availability of relevant experimental data from Russian laboratories and lack of participation of relevant Russian parties in international activities. Limited data and further information on environmental effects of primary coolant can be found in Filatov and Zelensky (1990, 2003), but the DFC itself is not explicitly suggested to contain any margins for the reactor coolant.

Figure 15 shows examples of reference and design curves for titanium-stabilized 08KH18N10T stainless steel (\approx AISI 321) using tabulated material properties in PNAE G-7-002-86 at 20 °C and 300 °C. As mentioned, the DFC is generally conservative even with respect to the ASME 2010 design curve. Note that the DFCs also extend up to 10^{12} cycles, which is beyond all other codes. Due to the absence of a constant term for endurance limit, the curves do not asymptotically approach a horizontal line.

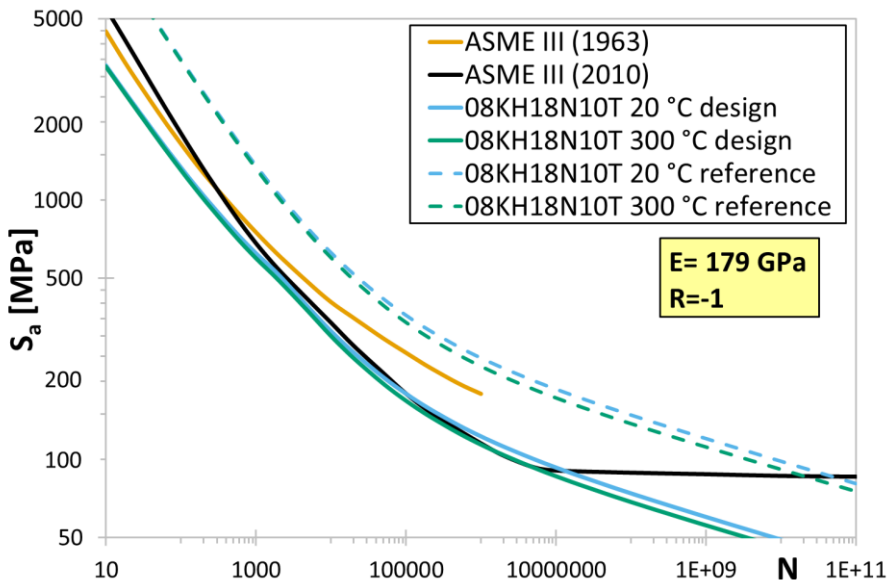


Figure 15. Comparison of PNAE G-7-002-86 design and reference curves for 08KH18N10T with ASME III design curves.

3. Explicit methods to account for EAF

3.1 Introduction to existing methodologies

3.1.1 EAF design curves

To account for reduction of fatigue lives in reactor coolant, engineering methodologies compatible with stress analysis were needed for practical implementation with Code fatigue usage calculations. There are two common existing methodologies when it comes to predicting fatigue lives in reactor coolant.

The first option is to develop fatigue curves which reflect the material behaviour in the specific environment and apply them for water-touching components in the same way as air fatigue curves are used. The EACLWR program favoured this approach until the late 1990's. Interim reactor coolant design curves based on Japanese and US data were published in NUREG/CR-5999 (Majumdar et al., 1993). The saturated curves, representing the most severe assumed environmental effects, are shown in Figure 16 for carbon, low-alloy and austenitic stainless steels. The stainless steel curve was constructed with a transferability factor of 1.5 (rather than 2) on stress/strain, based on real margins for actual material heats in HCF. At this early stage temperature, strain rate and dissolved oxygen effects were modelled for carbon steels only. Limited data on stainless steels was available, and the effects of low dissolved oxygen (DO) PWR water were considered bounded by 0.2 ppm DO results at 288 °C on 316NG stainless steel from Shack and Burke (1991). Those results indicated a reduction factor of only four on the best-fit air curve. Reduction on fatigue life relative to the ASME III design curve is shown in Figure 17 as a function of strain amplitude. Because the ASME III mean and heat-specific best-fit curves were not equivalent, the factor is a function of strain amplitude. Relatively soon after NUREG/CR-5999 was published, strain rate dependency was acknowledged and added to the stainless steel curves (O. K. Chopra, 1994), significantly influencing the factors as also demonstrated in Figure 17.

As more experimental data was generated in the early 1990's, improved statistical models were developed at ANL for carbon steels, low-alloy steels, austenitic stainless steels and nickel-based alloys (J. Keisler et al., 1994, 1995; J. Keisler & Chopra, 1995; J. M. Keisler et al., 1996). The water design curve for stainless steels in NUREG/CR-6335 (J. Keisler et al., 1995) was represented by the equation

$$\ln(N_{25}) = [6.69 - 1.98 \cdot \ln(\varepsilon_a - 0.12)] + I_W(0.134 \cdot \varepsilon^* - 0.359) + 0.382 \cdot I_{316NG} \quad (34)$$

where $I_W=1$ for water (and zero for air), ε^* is the transformed strain rate term and $I_{316NG}=1$ for type 316NG and zero otherwise. Equation (34) was applicable up to 10^6 cycles. The transformed strain rate term (note: based on carbon and low-alloy steel data) was equal to

$$\varepsilon^* = 0 \text{ for } \varepsilon > 1 \text{ \%}/s$$

$$\varepsilon^* = \ln(\dot{\varepsilon}) \text{ for } 0.001 \leq \dot{\varepsilon} \leq 1 \text{ \%}/s$$

$$\varepsilon^* = \ln(0.001) \text{ for } \dot{\varepsilon} < 0.001 \text{ \%}/s \quad (35)$$

The main benefit of design curves with built-in environmental effects is their simplicity of use for a desired failure probability. The major drawback is in the parametric nature of EAF. The reduction of fatigue crack initiation life of austenitic stainless steels in LWR water is a function of at least temperature, strain rate and DO of the coolant. For carbon and low-alloy steel, the material's sulfur (S) content also plays a role. (H. S. Mehta & Gosselin, 1995) What this means is that separate curves would be required for each combination of the critical parameters. Interpolation between slightly different curves is not straightforward due to non-linear effects on fatigue life. Additionally, application of several curves in fatigue usage evaluation is not efficient. However, if a first screening of CUF using the most limiting curve (representative of the highest

temperature, slowest strain rate and lowest DO combination for stainless steels) is sufficient to demonstrate $CUF < 1$, this approach can still be satisfactory.

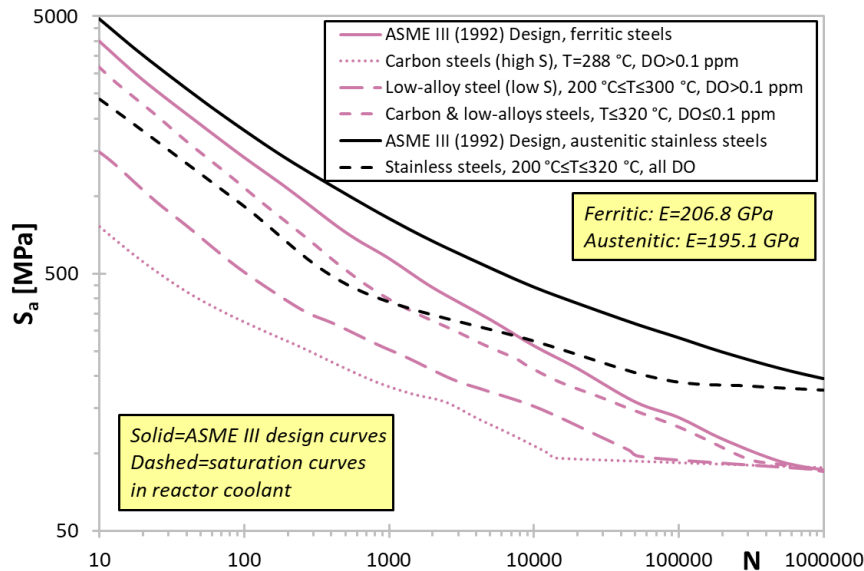


Figure 16. Interim design curves from NUREG/CR-5999 compared to ASME III design curves at the time. (Majumdar et al., 1993)

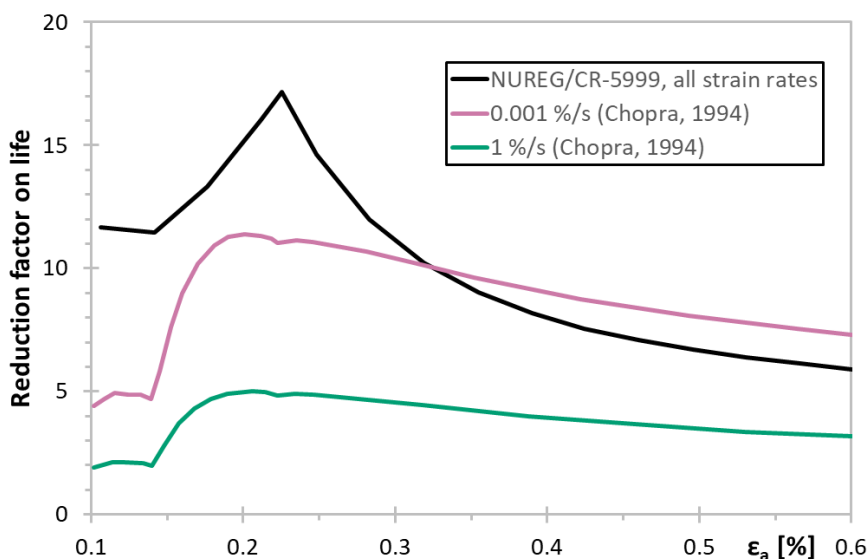


Figure 17. NUREG/CR-5999 (Majumdar et al., 1993) and Chopra (1994) stainless steel interim design curve reduction factor on life as a function of strain amplitude relative to the ASME III design curve.

3.1.2 F_{en} models

Where more detailed evaluation of environmental effects is needed to satisfy the CUF requirement, the fatigue life reduction factor or “ F_{en} ” methodology is more applicable. In fact the “design curves in LWR water” approach can be thought of as application of a particular set of parameters in a F_{en} equation. Explicit use of F_{en} factors was proposed by Mehta and Gosselin (1995) in a joint effort by EPRI (Electric Power Research Institute) and GE, Japanese researchers in the utility-funded EFD (Environmental Fatigue Data) project (Higuchi et al., 1995; Kishida et al., 1995), and later by ANL researchers (O. K. Chopra, 1999; O. K. Chopra & Shack, 1998a) in the EAFLWR project.

Much credit to the F_{en} approach is given to the paper published by Higuchi and Iida (1991), though earlier Japanese research by Higuchi and Sakamoto (1985), Iida et al. (1986) and Higuchi and Iida (1989) already explained the use of similar models for ferritic steels. Another, albeit less sophisticated, model proposal from EPRI sponsored work at GE was made by Ranganath et al. (1982a, 1982b) and Mehta et al. (1986). More specifically, these references propose a factor called K_{en} instead of F_{en} . Higuchi and Iida call this the fatigue strength correction factor for environmental effects, whereas the EPRI term is simply named the environmental correction factor. The Higuchi and Iida (1991) model is given in equation (36), using notation from equation (13).

$$K_{en} = \frac{\varepsilon_{a,RT\ air}}{\varepsilon_{a,HT\ water}} = 1 + (\dot{\varepsilon}_T^{-n_1 \cdot P} - 1) \left(1 - \frac{A_2}{\varepsilon_{a,HT\ water}} \right) \quad (36)$$

The term P describes the dependence of fatigue life on the strain rate and the term $\dot{\varepsilon}_T$ is the strain rate in the increasing strain part of a cycle. Note that the strain amplitude ratio compares room temperature air and high temperature water. Equation (36) is also readily applied in stress intensity units by replacing the strain terms according to equation (1).

The EPRI K_{en} model was based on comparing high temperature data in both air and water. Frequency (\approx strain rate) and temperature dependence were introduced via multiplication of K_{en} with an environmental correction modification factor, M . K_{en} also contains an empirical constant H , which is a function of the coolant environment. (H. S. Mehta et al., 1986) The German model by Bienusca and Schulz (1986) from the same era used the GE model as a basis, but further divided the K_{en} factor into two subfactors to account for separate effects of temperature and the environment.

Contrary to equation (36), the F_{en} methodology is based on the ratio of fatigue life in air (at room temperature, RT or high temperature, HT) and water, according to equation (37).

$$F_{en} = f(T, \dot{\varepsilon}_T, DO, S) = \frac{N_{RT\ (or\ HT)\ air}}{N_{HT, water}} \quad (37)$$

F_{en} expressions in the form of equation (37) could be derived by rearranging terms in the prior models of Higuchi and Iida (1991) and ANL (J. Keisler et al., 1995; Majumdar et al., 1993). This approach was selected in the EPRI/GE model (H. S. Mehta & Gosselin, 1995, 1996, 1998) and remains the dominant modelling approach for environmental effects. Stainless steel equations (10), (11) and (34) rearranged in the form of equation (37) become

$$F_{en} = \exp(-0.023 - 0.134 \cdot \varepsilon^*) \text{ for 316NG} \quad (38)$$

$$F_{en} = \exp(0.359 - 0.134 \cdot \varepsilon^*) \text{ for other SS} \quad (39)$$

The transformed strain rate term is calculated as in equation (35). The first models were calibrated in detail for ferritic steels only, which is a direct reflection of the relatively scarce EAF research on stainless steels until the latter half of the 1990's. Therefore, the only parameter affecting F_{en} in equations (38) and (39) is the strain rate.

Another key aspect of the EPRI/GE model was the addition of threshold criteria to the influential parameters. For example, strain rate equation (35) contains a threshold of 1 %/s. A strain rate higher than this would result in marginal environmental effects. The industry approach was to identify from the literature a set of threshold conditions, which result in $F_{en} \leq 4$ unless all conditions are simultaneously exceeded. Based on work done under the auspices of the PVRC, the values listed in Table 8 were identified and verified for a large database of ferritic steel EAF data. A factor of four on life was said to constitute regular laboratory scatter, temperature effects and other inbuilt conservatisms of the design curve.

Table 8. Tentative threshold criteria for moderate environmental effects in ferritic steels ($F_{en} \leq 4$). (Van Der Sluys, 1993; Yukawa & Van Der Sluys, 1995)

Parameter	Range
Strain amplitude	$\leq 0.1 \%$
Strain rate	$\geq 0.1 \%/s$
Dissolved oxygen	$\leq 0.1 \text{ ppm}$
Temperature	$\leq 150 \text{ }^\circ\text{C}$
Sulfur content*	$< 0.003 \%$
Flow rate	$> 3 \text{ m/s}$

*not applicable for stainless steel

The Japanese F_{en} proposal initially used the Higuchi-Iida equation (36) as a starting point. This work was assigned to the EFD project. For a more detailed account of EFD activities, refer to EFD Committee (1995). The early model (Kishida et al., 1995) was focused on carbon and low-alloy steels only, with equations given in the form:

$$F_{en} = \dot{\epsilon}^{-P} = \dot{\epsilon}^{-(0.1+M \cdot N)} \quad (40)$$

Where M and N are constants which depend on the DO and temperature, respectively. Both have a trilinear functional form.

The first Japanese F_{en} model for stainless steel was prepared in March 2000, see Tsutsumi, Kanasaki et al. (2000; 2001) as an outcome of the government-funded EFT project (1994–2007) of the Japan Power Engineering and Inspection Corporation (JAPEIC). EFT was a follow-up to the work of the TENPES funded Environmental Fatigue Design (EFD) committee (1991–1995), where the focus had been on carbon and low-alloy steels.

For stainless steel F_{en} was composed of two separate factors, as shown below:

$$F_{en} = F_{en1} \cdot F_{en2} \quad (41)$$

F_{en1} is equal to the reduction of fatigue life of the best-fit curve in environment (PWR water, 288–360 °C) to that in air at a strain rate 0.4 %/s. It has a constant value of 3.43 for all strain amplitudes and can also be expressed by equation (42).

$$\epsilon_a = 13.1 \cdot N_f^{-0.457} + 0.11$$

$$\ln(N_{25}) = 5.629 - 2.188 \cdot \ln(\epsilon_a - 0.11) \quad (42)$$

Tsutsumi, Kanasaki et al. (2000; 2001) explain that 0.4 %/s as the baseline was selected because it had the most experimental data. Equation (23) was used for the air best-fit curve, between 20–350 °C based on an assumed non-effect of temperature in air.

F_{en2} is the additive part to F_{en1} and has a larger magnitude with slower strain rate and/or higher temperature.

$$F_{en2} = (\dot{\epsilon}/0.4)^{-P} \quad (43)$$

The saturation strain rate for type 304 stainless steel was considered $4 \cdot 10^{-4} \%/s$ and for type 316 stainless steel $4 \cdot 10^{-3} \%/s$. Constant P is a trilinear term, called the strain rate dependency factor and it is calculated as:

$P = 0.04$ for $T < 100$ °C

$P = 9.33 \cdot 10^{-4}T - 0.053$ for $100 \leq T \leq 325$ °C

$P = 0.25$ for $T > 325$ °C (44)

Using the saturation strain rate yields a maximum F_{en} value of 19.28 for type 304 and 10.85 for type 316.

ANL began referring to the F_{en} methodology in 1997 (O. K. Chopra & Shack, 1998b), after previously expressing environmental effects through design curves in reactor coolant (though as mentioned it was mathematically possible to transform the design curves into F_{en} equations). The general form of the F_{en} expressions follows equation (45).

$$F_{en} = \exp(X - T^* \dot{\epsilon}^* O^*) \quad (45)$$

The leading term X has a constant value. The other parameters, called transformed temperature T^* , transformed strain rate $\dot{\epsilon}^*$, and transformed DO O^* each have their unique functional forms based on regression to experimental data. The first ANL EAF model for stainless steel written in F_{en} format was published in NUREG/CR-5704 (O. K. Chopra, 1999). Equation (17) for strain rate effects in air from the same report was identical to that proposed in water. The experimental vs. predicted data using the NUREG/CR-5704 F_{en} model followed the same general trend as for Japanese data, namely that scatter tends to increase for long lives at low strain amplitude.

O'Donnell and O'Donnell (2008) have argued that F_{en} is more relevant to operating reactors than use of EAF design curves. However, the latter approach is claimed more applicable in new reactor design since the relevance of pre-determined loading sequence, hold times and transient rates required as F_{en} inputs may be questioned.

All F_{en} models are empirically derived from laboratory data. In other words, the fatigue lives of laboratory specimens in water have been compared to laboratory specimens in air, and mathematical equations have been formulated to model the observed behaviour by regression analysis. This directly means that in laboratory experiments, the value of F_{en} always comes from a comparison to the best-fit curve which is supposed to give an accurate value of fatigue life for a polished laboratory specimen. In design calculations, however, the F_{en} factor is always applied with the design fatigue curve which contains the transferability margins to crack initiation in components, as shown in Figure 18. Inherently this includes the assumption that environmental effects are no different in laboratory specimens than in components. This is an area which has been challenged by research done in France and the UK.

Figure 18 illustrates how the transferability margins act in both directions, strain/stress intensity or number of cycles, but F_{en} is calculated for the allowable cycles only. The reference curve of NUREG/CR-6909 and design curve of ASME III are used for this schematic presentation, which also indicates a link between a F_{en} factor and an EAF design curve derived from identical EAF model, laboratory data and test parameters.

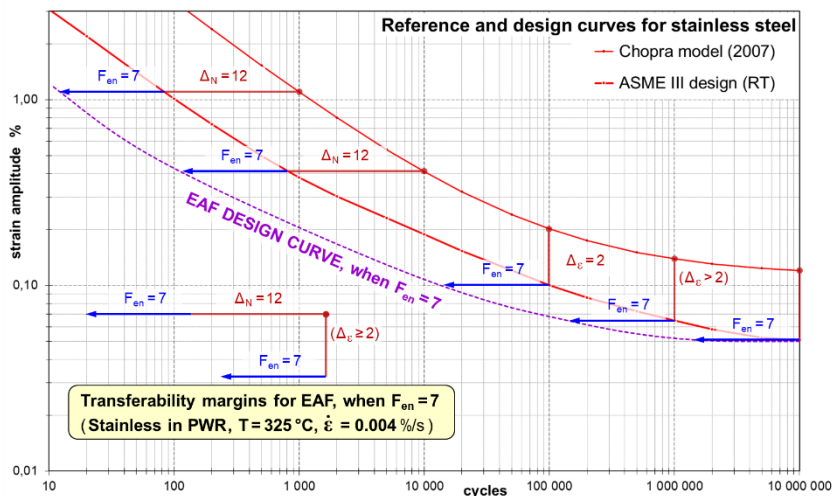


Figure 18. Schematic of F_{en} factor applied together with the transferability margins in ASME III.

3.2 Overview of EAF approaches in codes, standards and regulations

3.2.1 ASME (USA)

The U.S. NRC had taken an interest in fatigue and EAF already in the late 1970's after reports of suspected fatigue cracking in PWR feedwater piping (U.S. NRC, 1979). In the 1980's fatigue received further attention after steam generator cracking (U.S. NRC, 1988b), surge line stratification (U.S. NRC, 1988a) and thermal fatigue in unisolable reactor coolant system piping (U.S. NRC, 1988c), none of which were accounted for in the design basis. Laboratory evidence from the mid-1970's began to suggest detrimental effects on fatigue life in reactor coolant but it was not until the late 1980's to early 1990's when extensive databases became available and comprehensive methodology development began. Coincidentally, license renewal (LR) preparation beyond the original design life of 40 years of most generation II NPP's was becoming a timely discussion topic at the same time. Since fatigue design based on ASME III relied on a simple demonstration of $CUF < 1$ without the effect of environment explicitly accounted for, there was an increasing concern in the NRC over the actual design margins in plants licensed to 40 years. This concern was strengthened after Japanese data in the JNUFAD (Japanese Fatigue Database for Nuclear Materials) database (Iida et al., 1988) was presented to ASME Code Subgroup Fatigue Strength and the NRC in December 1988.

Frequent bilateral discussions on LR between NRC and the industry trade association Nuclear Management and Resources Council (NUMARC) started taking place in 1990 (Lee, 1990). A NUMARC working group on nuclear plant life extension had prepared an industry technical position to address fatigue for LR and implemented this into a series of industry reports (IR). These reports were intended to support LR and were submitted for NRC review between 1989–1991 with subsequent revisions based on feedback. IR titles concerning the most typical fatigue sensitive locations were BWR Primary Coolant Pressure Boundary (Braden & Stancavage, 1994) and PWR Reactor Coolant System (Robinson, 1994). These IRs did not explicitly account for effects of the coolant environment.

NRC staff drafted their own position on fatigue in January 1991 (Craig, 1991), with an obligation for licensees to account for environmental effects. Subsequently (Kuo, 1991) NUMARC referred to the existing K_{en} methodology (H. S. Mehta et al., 1986; Ranganath et al., 1982a, 1982b), which could be applied in extreme but rare cases where assumed margins of the DFCs are insufficient, namely for carbon steel in high DO water. Despite a general consensus on the roadmap to assess fatigue for extended operation (Griffing, 1991a), the industry criticized the NRC position of environmental effect evaluation for all ASME III stress analyses, as these were outside the scope of explicit Code requirements.

After a series of discussions by the end of 1991 (Craig, 1991; Griffing, 1991a, 1991b; Kuo, 1991), NRC formally published a draft Branch Technical Position (BTP) on EAF for LR to facilitate the ongoing technical discussions (U.S. NRC, 1991) and to aid preparation of the agency's Standard Review Plan (SRP) for LR. The BTP contained simple screening guidance to incorporate environmental effects into fatigue usage evaluation for 60 years, based on the best available knowledge from experimental data at the time. In practice, the 40-year design CUF (either the original design value, or recalculated) was first to be multiplied by 1.5 to account for 20 years life extension and then by a reasonably bounding environmental penalty factor. For stainless steel the factor was assumed equal to three, equating to a total multiplier on 40-year design CUF of 4.5. Provided this screening CUF remained below unity, more detailed evaluation such as actual transient reconstruction or refined stress analysis was not considered a necessity.

NRC and the industry had opposing positions regarding the continued service prerequisite of $CUF < 1$, which would often be violated when applying environmental penalty factors. The industry leaned heavily towards allowing flaw tolerance rules. NUMARC estimated tenfold costs of applying the BTP instead of the industry position (Craig, 1992). What at first started out as mutually productive discussion between the industry and NRC unfolded into disagreement, as evidenced by the quote by W.E. Cooper who described the NRC staff position on fatigue evaluation as "*an invitation to paralysis through analysis that won't do us much good at all*" (Ward & Shewmon, 1992).

The ASME Board of Nuclear Codes and Standards (BNCS) was aware of the fast-developing issue of EAF in the early 1990's, not least due to pressure from the NRC. In June 1991, in response to U.S. NRC concerns, it requested the PVRC to examine the matter in more detail. The Steering Committee on Cyclic Life and Environmental Effects (CLEE) was established. CLEE consisted of three working groups (WG S-N Data Analysis, WG Evaluation Methods and WG da/dN Crack Growth), each subdivided into Task Groups. (Hechmer, 1998) When the NRC issued the BTP in 1991, CLEE had barely started its work and was thus unable to contribute or influence its contents.

Subsequent to the fatigue BTP, generic safety issues (GSI) prompting immediate action were published by the NRC in the early 1990's. GSI-78 "Monitoring of Fatigue Transient Limits for Reactor Coolant System" was identified initially in a 1983 memorandum but developed more fully in 1992 (Beckjord, 1992; Murley & Beckjord, 1993). Old vintage plants designed to B31 piping rules had neither explicit fatigue analysis nor fatigue monitoring requirements. This lack of requirements had left open questions on actual cycle numbers and potential transients that were not included in the licensing basis. As an outcome of the license renewal discussions, the adequacy of metal fatigue in operating reactors (including EAF) had become a large enough concern that it was implemented as part of GSI-78 in parallel with the original monitoring issue.

After NRC staff had reviewed key license renewal issues in SECY-93-049 (Taylor, 1993), the Commission directed staff to consider fatigue as a potential generic safety issue also for operating reactors in June 1993. This led to the development of GSI-166 "Adequacy of Fatigue Life of Metal Components". Immediately after this the NRC's fatigue action plan (FAP) was approved in July 1993, replacing the fatigue BTP (Taylor, 1994). The FAP subsumed three major issues which had been highlighted in GSI-78 and GSI-166:

- Absence of explicit fatigue analyses for components designed to e.g. B31.1.
- Eroded margins of fatigue design curves when incorporating environmental effects.
- Exceedance of the current licensing basis requirement of $CUF < 1$.

The technical basis of the FAP closeout (Taylor, 1995) two years later was provided in interim fatigue design curves for LWR environments in NUREG/CR-5999 (Majumdar et al., 1993) and in their application to selected plant components in the generic study NUREG/CR-6260 (Ware et al., 1995). The latter study was partially undertaken in response to approximately 40 % of vintage plants containing primary piping without a formal fatigue analysis, as allowed by the respective design codes (Kalinousky & Muscara, 2001).

In parallel, an industry sponsored study at Sandia National Laboratories (Deardorff & Smith, 1994) focused on the same topics as NUREG/CR-6260 with comparable conclusions.

Meanwhile, and out of direct FAP scope, more detailed and revised statistical modelling of EAF continued in reports NUREG/CR-6237 (J. Keisler et al., 1994) and NUREG/CR-6335 (J. Keisler et al., 1995) prepared by ANL. As a subcontractor to the U.S. NRC, ANL focused throughout the 1990's and 2000's on improving statistical models for EAF as new data became available, one by one filling understanding gaps related to a variety of material, loading and environmental factors. The ANL reports are heavily research-oriented and not intended as such for design code incorporation.

Table 9 shows the full evolution of F_{en} parameters in ANL reports given in equation (45) format. An exception can be found in the NUREG/CR-5704 report (O. K. Chopra, 1999) where the air best-fit curve included a term accounting for the strain rate at temperatures exceeding 250°C. As can be seen from the equations (14–17), this term defines a penalty factor, much like F_{en} , but for air environment. Using notation $F_{en,air}$ for reduction of life in air, the equation (45) would get the format shown below.

$$F_{en,air} = \exp[-\dot{\epsilon}^*(T_1^*)]; F_{en} = \exp[X - \dot{\epsilon}^*(T_2^*O^*)]; X = 0.935 \text{ or } 0.509 \quad (46)$$

Since the ANL methodology for F_{en} proposes to use the air fatigue life at room temperature, the first $F_{en,air}$ factor vanishes from equation (46), reducing it to the more familiar equation (45) format. The separate temperature and strain rate dependent terms for air and water environments lead to surprising results in high temperatures ($T > 250^\circ\text{C}$), but the issue disappeared when the environmental term ($F_{en,air}$) was subsequently removed from the best-fit curve in air. The statistical models on EAF and F_{en} in the early reports from NUREG/CR-6335 (J. Keisler et al., 1995) to CR-6878 (O. Chopra et al., 2005) differentiated between the stainless alloy grades. The best-fit air curve and environmental effects were separately given for the 316NG. Only the reference air curves were different in NUREG/CR-6335. The follow up statistical models for fatigue endurance in environment resulted to environment dependent leading constants X in equation (46), starting from $X=0.935$ for alloys 304 & 316, but $X=0.509$ for 316NG in NUREG/CR-5704 and CR-6717 (O. K. Chopra & Shack, 2001). The difference was increased to $X=1.028$ for 304 & 316, and $X=0.311$ for 316NG in NUREG/CR-6787 (O. K. Chopra, 2002), CR-6815 (O. K. Chopra & Shack, 2003b) and CR-6878. However, the equations for calculating F_{en} “for austenitic stainless steels” were presented in these reports with X constant fitted for alloys 304 & 316 only. A careful reader was left wondering, whether to use the statistical model or the equation given for F_{en} in calculating environmental effects for 316NG.

Example graphs of F_{en} as a function of temperature, strain rate and dissolved oxygen are shown in the Appendices (chapter 7.1), where peculiarities in the EAF model in NUREG/CR-5704 are also demonstrated. The fundamental changes in the model up to the most recent one in NUREG/CR-6909 Rev.1 (O. K. Chopra & Stevens, 2018) have been:

- Single F_{en} expression for all stainless steels, rather than type 304 or 316NG specific.
- Removal of the leading constant, resulting in $F_{en}=1$ if any one of the threshold conditions is not exceeded.
- Separate treatment of high and low DO environments.

Table 9. F_{en} models developed by ANL in the EACLWR program 1995–2018, based on equation (45). Shaded cells indicate change of functions from the preceding reference. CASS is cast austenitic stainless steel.

	NUREG/CR-6335	NUREG/CR-5704	NUREG/CR-6717
Leading constant X	0.359 (separate air curve for 316NG)	0.935 or 0.509? (316NG) 0.935 (304)	0.935 or 0.509? (316NG) 0.935 (304)
T^*	1	$T_1^* = 0$ for $T < 250$ °C $T_1^* = [(T-250)/525]^{0.84}$ for $250 \leq T < 400$ °C $T_2^* = 0$ for $T < 200$ °C $T_2^* = 1$ for $T \geq 200$ °C	0 for $T < 180$ °C ($T-180$)/40 for $180 \leq T \leq 220$ °C 1 for $T \geq 220$ °C
$\dot{\epsilon}^*$	0 for $\dot{\epsilon} > 1$ %/s $0.134 \cdot \ln(\dot{\epsilon})$ for $0.001 \leq \dot{\epsilon} \leq 1$ %/s $0.134 \cdot \ln(0.001)$ for $\dot{\epsilon} < 0.001$ %/s	0 for $\dot{\epsilon} > 0.4$ %/s $\ln(\dot{\epsilon}/0.4)$ for $0.0004 \leq \dot{\epsilon} \leq 0.4$ %/s $\ln(0.001)$ for $\dot{\epsilon} < 0.0004$ %/s	0 for $\dot{\epsilon} > 0.4$ %/s $\ln(\dot{\epsilon}/0.4)$ for $0.0004 \leq \dot{\epsilon} \leq 0.4$ %/s $\ln(0.001)$ for $\dot{\epsilon} < 0.0004$ %/s
DO^*	1	0.260 for $DO < 0.05$ ppm 0.172 for $DO \geq 0.05$ ppm	0.260 for $DO < 0.05$ ppm 0 for $DO \geq 0.05$ ppm

	NUREG/CR-6787	Chopra & Shack (2003a)(2003a)	NUREG/CR -6815 and CR-6878
Leading constant X	1.028 or 0.311? (316NG) 1.028 (304)	0.935	1.028 or 0.311? (316NG) 1.028 (304)
T^*	0 for $T < 150$ °C ($T-150$)/175 for $150 \leq T \leq 325$ °C 1 for $T \geq 325$ °C	0 for $T < 150$ °C ($T-150$)/175 for $150 \leq T \leq 325$ °C 1 for $T \geq 325$ °C	0 for $T < 150$ °C ($T-150$)/175 for $150 \leq T \leq 325$ °C 1 for $T \geq 325$ °C
$\dot{\epsilon}^*$	0 for $\dot{\epsilon} > 0.4$ %/s $\ln(\dot{\epsilon}/0.4)$ for $0.0004 \leq \dot{\epsilon} \leq 0.4$ %/s $\ln(0.001)$ for $\dot{\epsilon} < 0.0004$ %/s	0 for $\dot{\epsilon} > 0.4$ %/s $\ln(\dot{\epsilon}/0.4)$ for $0.0004 \leq \dot{\epsilon} \leq 0.4$ %/s $\ln(0.001)$ for $\dot{\epsilon} < 0.0004$ %/s	0 for $\dot{\epsilon} > 0.4$ %/s $\ln(\dot{\epsilon}/0.4)$ for $0.0004 \leq \dot{\epsilon} \leq 0.4$ %/s $\ln(0.001)$ for $\dot{\epsilon} < 0.0004$ %/s
DO^*	0.281	0.26	0.281

	NUREG/CR-6909 Rev.0	NUREG/CR-6909 Rev.1 draft	NUREG/CR-6909 Rev.1
Leading constant X	0.734	0	0
T^*	0 for $T < 150$ °C ($T-150$)/175 for $150 \leq T \leq 325$ °C 1 for $T \geq 325$ °C	0 for $T < 100$ °C ($T-100$)/250 for $100 \leq T \leq 325$ °C	0 for $T < 100$ °C ($T-100$)/250 for $100 \leq T \leq 325$ °C
$\dot{\epsilon}^*$	0 for $\dot{\epsilon} > 0.4$ %/s $\ln(\dot{\epsilon}/0.4)$ for $0.0004 \leq \dot{\epsilon} \leq 0.4$ %/s $\ln(0.001)$ for $\dot{\epsilon} < 0.0004$ %/s	0 for $\dot{\epsilon} > 10$ %/s $\ln(\dot{\epsilon}/10)$ for $0.0004 \leq \dot{\epsilon} \leq 10$ %/s $\ln(0.0004)$ for $\dot{\epsilon} < 0.0004$ %/s	0 for $\dot{\epsilon} > 7$ %/s $\ln(\dot{\epsilon}/7)$ for $0.0004 \leq \dot{\epsilon} \leq 7$ %/s $\ln(0.0004/7)$ for $\dot{\epsilon} < 0.0004$ %/s
DO^*	0.281	0.29 for $DO < 0.1$ ppm 0.14 for $DO \geq 0.1$ ppm (non-sensitized wrought alloys) 0.29 for $DO \geq 0.1$ ppm (CASS and sensitized wrought alloys)	0.29 for $DO < 0.1$ ppm 0.14 for $DO \geq 0.1$ ppm (non-sensitized wrought alloys) 0.29 for $DO \geq 0.1$ ppm (CASS and sensitized wrought alloys)

As the series of ANL reports builds upon one another, not least due to the growing amount of experimental EAF data, the latest laboratory report NUREG/CR-6909 Rev.1 should be considered as up to date and having the most scientific relevance. Nevertheless, the older reports' contributions and historical context are valuable and should be acknowledged to build a full understanding of the present state of EAF in codes, standards and other regulations. The F_{en} models in the older reports are not recommended for application unless specifically required.

In the latter half of the 1990's ANL briefly experimented with the use of artificial neural networks for predicting environmental effects. A large set of carbon and low-alloy steel data was used as the training material and the results were compared to the ANL statistical models in air and water. The predictive capability of the artificial neural networks was good. Estimates were very similar to the statistical models. Their use, however, was discontinued due to limitations with model overtraining and extrapolation capability. The artificial neural networks do not produce functional forms of statistical models, which limits their practical use. Their greatest benefit was with using incomplete data sets to suggest statistical trends, which could then be transformed into mathematical language (Pleune & Chopra, 1997, 2000).

Both GSI-78 (Kress, 1996; U.S. NRC, 2011a) and GSI-166 (Speis, 1996; U.S. NRC, 2011b) were resolved during 1996–1997 (Morrison, 1997), after completion of the FAP and other remaining topical studies. Neither of the two resolutions considered backfitting of new requirements justified for a 40-year plant life. The outcome of the GSI-166 closure was that nearly always CUF_{en} (subscript “en” indicating environmental effects are included) reduced to <1 by eliminating one or more of the conservatisms inherent in the design basis. Where this could not be demonstrated, the increase in probabilistic core damage frequency (CDF) remained low enough to not warrant a backfit of analyses including environmental effects to older vintage plants for a 40-year design life.

As NRC staff are required to document resolutions of generic issues for license renewal, topics contained in the resolved 40-year GSIs would need to be re-evaluated for 60-year plant life. Thus, GSI-190 “Fatigue Evaluation of Metal Components for 60-Year Plant Life” was developed in 1996 as a LR spinoff from GSI-166. The main body of work in GSI-190 was to extend the leakage and CDF probability calculations from 40 to 60 years and based on the results define appropriate actions, if any, for LR applicants (Speis, 1996).

Throughout the 1990's, industry technical perspectives were expressed in a series of EPRI reports and other publications, which the Nuclear Energy Institute (NEI, of which NUMARC had become a part of in 1994) referred to in negotiations with the NRC. As explained, Mehta and Gosselin (1995, 1996, 1998) contributed the F_{en} methodology through the so-called EPRI/GE model. A nonmandatory ASME III Appendix was drafted on the matter in anticipation of Code implementation. Mehta (1998) demonstrated for NUREG/CR-6260 sample locations the significant relief on CUF_{en} from applying F_{en} penalty factors instead of the EAF design curves in NUREG/CR-5999 (Majumdar et al., 1993). In parallel with the F_{en} methodology itself, EPRI initiated multiple pilot studies on operating PWR and BWR plants to reinforce the industry solutions to residual concerns being explored in GSI-190 (EPRI, 1998a, 1998b; Gerber & Stevens, 1997; Stevens, 1998). All of these documents were submitted to the NRC for review, particularly since the first U.S. plants were seeking LR before GSI-190 was closed.

Whilst it was EPRI and GE who proposed the F_{en} methodology, the quantification of moderate environmental effects for fatigue under particular combinations of material, environment and loading was introduced via the CLEE (Van Der Sluys, 1993; Yukawa & Van Der Sluys, 1995). Arguments of moderate environmental effects as an inbuilt part of the design curve transferability factor on cycles were expressed in the industry-NRC discussions as early as 1991 (Griffing, 1991a). This can be traced back to interpretations made from the original ASME III criteria (ASME, 1969). To account for assumed built-in environmental effects in the DFCs, the EPRI/GE F_{en} model was revised with a moderation factor Z in equation (47) (H. S. Mehta, 1999)

$$F_{en,eff} = \max\left(\frac{F_{en}}{Z}, 1\right) \quad (47)$$

As a first screening, if one or more transient parameters fail to exceed the threshold condition for moderate effects, the effective $F_{en,eff}=1$ and no further analysis using the EPRI/GE methodology is required. Otherwise, $Z=4$ for carbon and low-alloy steels and $Z=2$ for stainless steels were assumed. The smaller factor for stainless steel was given based on discrepancy between mean curves of Langer (1962), Jaske and O'Donnell (1977) and ANL reports, leading to the conclusion of actual stainless steel design margins closer to 10 and 1.5 (instead of 20 and 2). $Z=2$ was argued to remain conservative (H. Mehta & Nickell, 1999) because:

- CUF is mainly accumulated through thermal transients with high amplitudes, where the margins on fatigue life remain close to 20 even with data published after Langer.
- The ANL F_{en} equation for stainless steel (in NUREG/CR-5704) results in a minimum F_{en} of 2.55 even if one or more threshold condition is not exceeded. This is because the equation includes a leading term $X=0.935$ in the exponent.
- Laboratory fatigue data in reactor coolant is from uniform gauge length specimens, but in plant components strain is typically more localized with less surface area and likelihood to encounter defects responsible for crack initiation.

Additional rationale for the application for Z factors was given by Mehta (2001) and later by Van Der Sluys (2003a). Namely, Chopra and Shack (1999) had discovered potentially negligible effects of surface roughness in LWR environments. Also, Cooper (1992) emphasized the average factor of three conservatism in the design curve for fatigue crack initiation in the 1960's PVRC pressure vessel tests at room temperature in water.

In April 1998 the Calvert Cliffs NPP submitted its LR application (Grimes, 1998) while GSI-190 was still an open issue. Oconee NPP followed soon after in July 1998. The EPRI pilot studies were referenced in the applications with the intention of demonstrating various EAF offsetting conservatisms for 60 years plant life. This could be thought of as repetition of what was concluded for a 40-year plant life when the FAP was closed in 1995. NRC staff requested additional information on several fatigue related evaluations for the Calvert Cliffs NPP (Grimes, 1998). Most of the questions were plant-specific, but there was a set of generic issues on the methodology which were directed at the industry to answer. The main NRC concerns and industry responses are summarized below:

- Values of strain thresholds needed clarification, since they deviated from the ANL proposals (O. K. Chopra & Smith, 1998). For stainless steel, there was only a marginal difference between 0.097 % suggested by ANL and 0.1 % proposed by industry.
- Recent findings of more severe environmental effects for stainless steel in low DO water (O. K. Chopra & Smith, 1998) were not sufficiently discussed. According to industry review, potential effects of low DO remain bounded by assumed moderate environmental effects and did not affect previous conclusions.
- Use of weighted methods to calculate effective F_{en} values for typical plant stress histories was unclear, particularly due to scatter in the reference data used to support the methods. The methods in the EPRI reports always applied maximum transient temperature, which is a conservative assumption. After this clarification, NRC considered this method adequate. (Grimes, 1999)
- The F_{en} equation (37) was assumed by industry to be a ratio between service temperature in air and service temperature in water. NRC interpreted instead the former to be room temperature in air. Further rationale was that high temperature air data was generated with such strain rates that the term T_1 in equation (46) reduces to zero anyhow (Grimes, 1999). Subsequent ANL best-fit curves in air after Chopra and Smith (1998) (identical with NUREG/CR-5704) no longer modelled any effects of temperature, making the industry interpretation irrelevant. NRC reasoning was that since ASME III DFCs are intended as room temperature curves, this ratio would maintain the same margins between BFC and DFC (Grimes, 1998). A non-negligible share of BFC data was generated above room temperature, but if the curves in question are limited to LCF any temperature effects below creep regime should be marginal. The industry did not agree with the requirement, instead

suggesting that all factors outside of environmental effects were already included in the DFC margins (Grimes, 1998).

- A more in-depth review of transferability factors on fatigue life was requested in support of the Z-factors proposed by industry. NRC accepted the factors $Z=3$ and 1.5 for carbon/low-alloy steels and stainless steels, respectively based on Chopra and Smith (1998) findings.

Because of the multiple technical concerns listed previously, the NRC did not approve the generic resolution to EAF for LR which was proposed by the industry when the Calvert Cliffs LR application was being reviewed. Instead for the time being the NRC expected plant-specific evaluation a necessity (Thadani, 1999).

GSI-190 was resolved by the end of 1999 (Powers, 1999; Thadani, 1999; U.S. NRC, 2011c). Technical basis supporting the resolution was documented in NUREG/CR-6674 (Khaleel et al., 2000), in which probabilistic calculations were performed to evaluate whether LR from 40 to 60 years of operation would influence CDF. NUREG/CR-6674 heavily referenced NUREG/CR-6260 for input information on the component locations and loads. The more recent EAF statistical models from NUREG/CR-6335 were applied. The report concluded negligible increases in the CDF for 20 additional years of operation. However, the expected pipe leak frequency increase for continued operation led NRC staff to conclude the need for EAF ageing management programs (AMP) in support of LR (Kalinousky & Muscara, 2001). As this was already consistent with requirements of 10 CFR part 54.21 "Requirements for Renewal of Operating Licenses for Nuclear Power Plants: Contents of Application -Technical Information", no new or revised requirements were associated with the closure of GSI-190. This outcome was welcomed by the nuclear industry (Hou, 2000).

In 1998, the CLEE formally proposed the EPRI/GE F_{en} methodology for use with ASME III fatigue evaluations (Yukawa, 1998). The PVRC forwarded this proposal to the ASME BNCS in 1999 for consideration as a nonmandatory Code appendix (Karcher, 1999; Yukawa, 1999). Also in 1999 the NRC formally requested the ASME Code to explicitly address environmental effects and also to update the stainless steel design curve (Craig, 1999) The ASME III Subgroup on Fatigue Strength subsequently started a process to revise the DFCs, whereas the reconvened ASME XI Task Group on Operating Plant Fatigue Assessments considered inclusion of an EAF methodology in a revision to nonmandatory Appendix L (Kalinousky & Muscara, 2001; H. S. Mehta, 2001).

The CLEE F_{en} proposal included revised Z factors and thresholds (Van Der Sluys & Yukawa, 1998). The Z factor for stainless steel was reduced to 1.5 to be conservative and to match the NRC approved value. The strain rate threshold was defined as ≥ 0.4 %/s, in accordance with the most recent ANL model (O. K. Chopra & Smith, 1998) (this identical model was later reprinted in NUREG/CR-5704). The CLEE proposal, however, modified the temperature term to a ramp function and reduced the threshold to ≤ 180 °C. ANL would adopt this temperature function in NUREG/CR-6717. To ensure a smooth transition near the strain amplitude threshold of 0.1 %, a ramp function was also proposed wherein the full F_{en} is effective at 0.11 %. Between 0.1 % and 0.11 % linear interpolation may be used. The transformed strain rate and transformed DO terms of the CLEE model were directly adopted from the ANL model, as it had NRC approval.

Both the industry and NRC understood the burden of detailed plant-specific approaches to fatigue. After GSI-190 closure a common interest was to develop guidance documentation with approved EAF methodologies to minimize the overall effort for acceptable fatigue management. On the regulator side, it was important for staff to have a consistent plan for reviewing upcoming applications and to inform licensees what is expected from them.

To achieve this, NRC published in 2001 the Standard Review Plan for LR, NUREG-1800 (U.S. NRC, 2001c), and the Generic Aging Lessons Learned (GALL) report, NUREG-1801 (U.S. NRC, 2001a, 2001b), to summarize generically staff views on existing and forthcoming time-limited ageing analyses (TLAA)/AMPs associated with LR. The staff considered an AMP necessary to resolve EAF as per 10 CFR

Part 54.21 (c)(1)(iii) and had taken an action in 2000 to develop a suitable description in the GALL format (Grimes, 2000). The AMP description is given in NUREG-1801 Vol. 2 chapter X.M1. It shall as a minimum consist of a set of sample locations (identified in NUREG/CR-6260), whose cumulative fatigue usage is calculated using the F_{en} methodology with equations from NUREG/CR-6583 (carbon and low-alloy steels) or NUREG/CR-5704 (stainless steels), which do not take credit for Z factors. That is, the CLEE recommendation was not endorsed. Practically, NUREG-1801 guided licensees towards an ASME XI Appendix L type of requalification of the design cumulative usage factors, with adverse effects of the reactor coolant included in the analysis. There was no mention of acceptable flaw tolerance approaches for EAF.

In principle, the resolution of the TLAA concerning fatigue could be adequately supported by using monitoring data to demonstrate that 40-year design basis transient numbers are also bounding for 60 years [option (i)]. Then, if the projected 60-year cumulative usage remains below unity, the particular location is considered to satisfy requirements [option (ii)]. If $CUF_{en} > 1$, the licensee is required to provide a more detailed demonstration through an AMP on how the issue is managed [option (iii)]. Options (i)–(iii) are provided in 10 CFR Part 54.21 (c)(1) for LR applicants to resolve TLAAs. Obviously, the most economically attractive scenario involves demonstrating bounding transient count and severity of the 40-year design basis up to 60 years, thus eliminating the need to revise the existing fatigue TLAA. However, since environmental effects were not inherent in the original design basis, options (i) and (ii) as such would not suffice without additional technical evaluation. (Nickell et al., 2001)

Partly because generally approved guidance was initially not available when the LR process started in 1998, licensees in the USA used various amounts of effort to account for EAF and thermal fatigue. A beneficial discussion forum between industry, regulators and researchers in this regard was the trio of international conferences on fatigue of reactor components (2000, 2002 and 2004) organized by EPRI within the Materials Reliability Program (MRP). The program had been established by the U.S. nuclear industry to respond to LR requirements imposed by the NRC. Recall also that not all U.S. licensees had the benefit of the GSI-190 closeout in their LR applications. Influenced by this, both implicit and explicit approaches to EAF were used. (Nickell et al., 2001)

An example of implicit application is the use of conservative factors to reduce the number of design-basis transients or design-basis CUF, which triggers the start of more comprehensive AMPs. This approach is reminiscent of the NRC fatigue BTP from 1991. The value of the conservative factor is subject to negotiation and could typically fall within the range of 2–10. These kinds of approaches require the least effort from the licensee in the LR process but are expected to trigger AMPs sooner than explicit approaches. (Nickell et al., 2001)

The two explicit approaches relevant to crack initiation involve either the application of DFCs with built-in environmental effects or the use of F_{en} penalty factors to recalculate the CUF of critical locations (or inversely, to reduce the allowable CUF). To offset environmental effects, LR applicants in the USA typically used monitoring data to eliminate the most common conservatisms in design basis transient severity and numbers. The third explicit option is to resort to a flaw tolerance approach and initiate a risk-informed in-service inspection (RI-ISI) program. Generic studies suggested the most likely applications for RI-ISI programs to be at PWR pressurizer surge line welds, nozzles or elbows and at various Class 1 branch piping locations. (Nickell et al., 2001)

At EPRI, the short-term task of developing EAF guidance for LR was given in 2000 to the Fatigue Issue Task Group (ITG), operating within the MRP (M. Robinson & Rosinski, 2003). This guidance was collected into EPRI report MRP-47, for which a working draft was published in December 2000. The approach selected for this guidance was to assume the need for environmental fatigue assessment using F_{en} penalty factors (EPRI, 2003). In practice, the PVRC CLEE work evolved hand in hand with EPRI work by this time, not least due to similar membership in both groups. As examples of concession with NRC comments, the PVRC (and EPRI) accepted to use the most recent ANL statistical models and room temperature air fatigue life as the basis for F_{en} (H. S. Mehta, 2000, 2001). Several draft versions of MRP-47 were prepared (Olshan, 2001; Walters, 2001), reviewed and revised prior to official publication. Revision 0 of MRP-47

was published in October 2001 (EPRI, 2001a) and was considered of high importance for near future LR applications (Walters, 2001). Revision 0 of MRP-47 received review comments from NRC the following year (Kuo, 2002), but EPRI responses were deferred based on progress with long-term tasks of the Fatigue ITG (M. R. Robinson, 2002).

The long-term task of the Fatigue ITG was to directly assess the technical issues of experimental EAF data and determine the need for considering environmental effects as part of fatigue analyses (EPRI, 2003). The early 2000's was a period of evolving perspectives on EAF from new laboratory data. Of major importance was the NRC's sudden disapproval of Z factors greater than 1 (Kalinousky & Muscara, 2001). This was built into Rev. 0 of the SRP LR and GALL documents. The argument for no longer crediting a part of the transferability factor for moderate environmental effects relied on laboratory data e.g. from NUREG/CR-6583 (O. K. Chopra & Shack, 1998a). Even if a moderate effect were to exist, NRC believed that more pronounced scatter in LWR environments (about a factor of ± 5) than in air (about a factor of ± 2) could fully offset any potential benefits. In agreement with ANL data, Japanese reviews (Higuchi, 2001; Tsutsumi et al., 2000; Tsutsumi, Kanasaki, et al., 2001) suggested greater scatter in water.

Responding to these critical views, EPRI released the report MRP-49 (EPRI, 2001b) in December 2001. It contained a technical review of available laboratory and component EAF data. MRP-49 argues that there is a comparable scatter in water and air environments. EPRI's analysis relied on normalizing the effect of strain rate on fatigue life. Shorter lives at lower strain rates were not considered to be due to scatter but more correctly due to the effect of the environment. By correcting Japanese PWR water data to account for temperature and strain rate effects, Takahashi and Nakamura (2003) also demonstrated that scatter is comparable between Japanese air and water data. Solomon and Amzallag (2005) used Weibull statistics to demonstrate less scatter in PWR water than in air, arguing that environmental effects enhance crack initiation and overcome the effects of metallurgical variation.

MRP-49 continued to build on the EPRI/GE model, which combines F_{en} factors with Z factors for moderate effects ($Z=3$ for carbon and low-alloy steels, $Z=1.5$ for stainless steels). It was expected that NRC would reapprove the use of Z factors. A comprehensive review of available laboratory specimen and component data not only supported existing arguments justifying use of Z factors, but a further significant conservatism in laboratory EAF data was identified: near-stagnant water flow rate. The difference to plant-relevant flow rate is typically three orders of magnitude. However, since laboratory data was insufficient there was not a sound technical basis to justify a threshold flow rate value for moderate effects and it was withdrawn. The threshold for sulfur content (applicable for carbon and low-alloy steels) was also withdrawn, as 0.003 % was considered too low to provide any practical relief for vessel and piping materials.

Further parallel content of MRP-49 and CLEE involved the evaluation of other transferability factors for DFCs (size, surface finish etc.). These efforts were also aimed at justifying the use of Z factors. The final report of CLEE, WRC Bulletin 487 (Van Der Sluys, 2003b), was published in December 2003 with similar discussion and conclusions as MRP-49. The recommendations by CLEE were intended to form the basis for ASME III Code revisions to include EAF guidance.

From a computational perspective, the industry's argument against the expected increase in pipe through-wall cracking between 40 and 60 years (as suggested in NUREG/CR-6674) was that the probabilistic calculations made use of conservative boundary conditions not representing the actual plant conditions and encountered loading. Criticism was pointed towards the assumed through-wall stress distributions, component dimensions and the scatter associated with material endurance limits in fatigue (M. Robinson & Rosinski, 2003). To prove this, in report MRP-74 EPRI performed re-evaluations of carbon and low-alloy steel locations with assumed realistic input values (EPRI, 2002). Similar recalculations for stainless steel components were later published in EPRI report MRP-172 (EPRI, 2005b). The revised calculations were a part of the Fatigue ITG longer-term efforts to try and justify why EAF would not need explicit consideration. The outcome in MRP-74 was typically several orders of magnitude reduction in crack initiation and leakage probabilities, as shown in Figure 19 (Deardorff et al., 2003). This Figure shows two sets of revised calculations, either using the reference best-fit curves from NUREG/CR-6335 or NUREG/CR-6717. A major difference in the revised predictions was the reduction of standard deviation

on endurance limit. In MRP-74 the standard deviation assumption was 10 % of the mean endurance limit, which is a typical handbook value (Wirsching, 1995). On the contrary the standard deviation in the NUREG statistical models was such that the low percentile probabilistic fatigue curves ended up having a physically impossible negative endurance limit value. In the revised predictions no attempts were made to remove all known conservatisms by using e.g. realistic strain rates or detailed finite element analysis. (Deardorff et al., 2003)

The NRC agreed that conservative assumptions were used in NUREG/CR-6674, but at the same time argued that the probabilistic study was intended only to increase generic knowledge of the issue rather than attempting to manage it. The explicit use of F_{en} factors remained as the NRC endorsed methodology (Grimes, 2000). It is noteworthy that, although revised F_{en} models were frequently being published, there was a certain lag in applying them in plant level analyses. Furthermore, references to seemingly old models appear in documents even after more recent updates had been published.

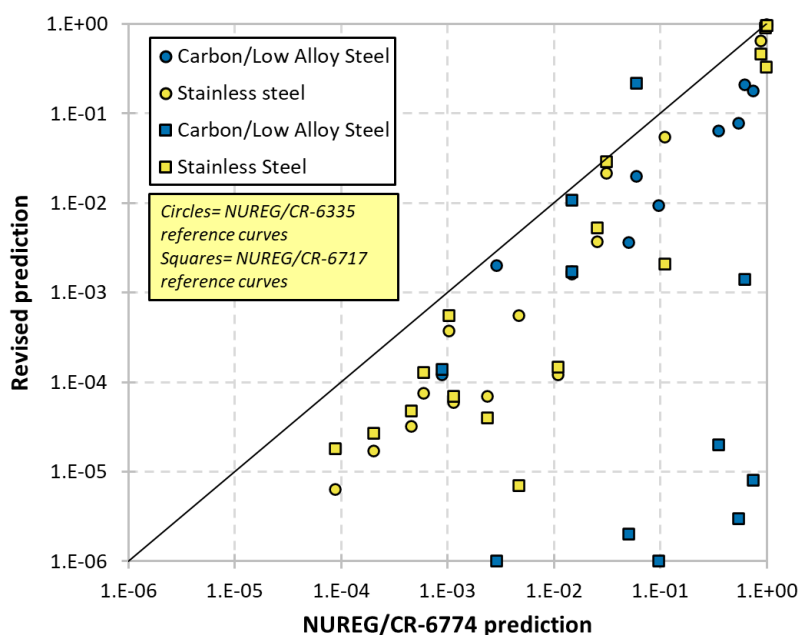


Figure 19. Leakage probability from NUREG/CR-6674 (Khaleel et al., 2000) calculations compared to revised calculations of EPRI Fatigue ITG. Data from Deardorff et al. (2003)

From the industry perspective, the MRP-74 conclusions were convincing enough for the EPRI Fatigue ITG to propose an Interim Staff Guidance (ISG) to the NRC. This ISG suggested dropping the requirement for the license renewal applicants to explicitly account for EAF for carbon and low-alloy steels. This ISG-11 referred to MRP-49 and MRP-74 reports as the technical basis. Changes were also proposed to NUREG-1800 and NUREG-1801 to enable existing fatigue management programs to be continued in place of explicit environmental effects. (Nelson, 2003) Despite a later revision to ISG-11 (Marion, 2003) after the first NRC review (Kuo, 2003), the NRC rejected the proposed guidance on the grounds of inadequate technical basis to support certain industry arguments (Kuo, 2004). A point of major disagreement was the experimental scatter in HCF. Sensitivity analysis for the probabilistic calculations also suggested significant influence on the result based on input values. (Kuo, 2004) As an outcome, concerning EAF, Revision 1 of the NUREG-1800 SRP (U.S. NRC, 2005b) NUREG-1801 GALL reports (U.S. NRC, 2005a) were published with practically only editorial changes to Revision 0.

Recognizing that the NRC would not endorse industry proposals omitting explicit EAF evaluation for LR, EPRI returned to developing guidance on how to apply F_{en} penalty factors in practice through Revision 1 to report MRP-47 (EPRI, 2005a). The recommended best practice was to perform evaluations for the set of component locations identified in NUREG/CR-6260. Depending on the outcome, the set of sample locations for assessment could be extended to other susceptible components. As the NRC no longer

endorsed the use of Z factors at this time, they were omitted in the EPRI guidance. MRP-47 Rev.1 contained a summary of the multitude of EAF approaches which LR applicants had committed to by the time. Several applicants had chosen to “wait-and-see” where scientific consensus would lead to before actually performing the needed analyses, which were due by the end of 40 operating years.

The ASME III Task Group Environmental Effects on Fatigue had been formed in 2003 as a step towards incorporating EAF into design rules. Technical discussions within ASME III committees resulted in a list of three future approaches to choose from (Balkey, 2006):

- Do not revise ASME III design rules. Environmental effects would rather be treated as an operating plant fatigue issue. Positive operating experience supports this approach.
- Develop Code Case (CC) with EAF fatigue curves which bound all data. This is the most conservative approach.
- Develop Code Case utilizing F_{en} methodology. This is the most flexible approach if environmental effects are to be considered, but reaching a consensus on the details in order for approval in the multiple Code committee levels is a long iterative process. Additional difficulty arises from the continuous evolution of F_{en} formulas (see e.g. Table 9).

The task group was closed in 2006, but from an outside perspective no changes in the Code had occurred. Instead, the NRC reacted.

The NRC publishes so-called regulatory guides (RG) as guidance documents for licensees to implement acceptable methods for specific problem areas (U.S. NRC, 2006c). An intra-agency user need request for EAF guidance for new reactors was documented in January 2005. High priority was given to this task, with the final RG to be completed by March 2007. (Gonzalez & Chopra, 2006)

The EAF draft RG numbered DG-1144 was published for comment in mid-2006 after consideration at the 532nd ACRS meeting in May (Larkins, 2006). The main message of DG-1144 was the endorsement of upcoming NUREG/CR-6909 Rev. 0 F_{en} equations and for stainless steel an alternative design curve to what ASME III contained in 2006. The NRC staff did also consider not publishing regulatory guidance or to endorse the appropriate ASME Code Case on the matter as alternatives. The former was believed to overburden staff due to the need to request additional information on plant-specific application and the need for reanalysis. The latter was not a viable option, since as mentioned lack of consensus even in the ASME committees prevailed. (U.S. NRC, 2006c)

Based on previously discussed conservative findings for the existing fleet licensed to 40 years, the guidance was applicable for fatigue design of new reactors only with no backfitting intended. New reactor types specifically referred to the EPR (internationally short for Evolutionary Power Reactor) and ESBWR (Economic Simplified Boiling Water Reactor) designs, for which the NRC expected to receive new construction license applications (U.S. NRC, 2006b).

DG-1144 collected much feedback during the public commenting period. Mainly the comments criticized the guidelines for being overly conservative with respect to operating experience, detailed instructions (like in MRP-47) not being given for practical application, lack of rules for Ni-Cr-Fe alloys and the notion that similar efforts were already in process within ASME. Some of the comments were addressed in the final guidance document, but most were rejected by the NRC. The conservative design rules of plants constructed in the 1970's were not believed to fully apply to modern plants, which means smaller margins against environmental effects. The NRC perspective remained firmly in necessitating EAF evaluation as part of design. This did not rule out eventual endorsement of an ASME Code Case as part of RG 1.84 (the regulatory guide containing NRC endorsed Code Cases), provided a suitable one was eventually accepted into a future revision of ASME III (U.S. NRC, 2007b).

After the December 2006 meetings of the ACRS Subcommittee on Materials, Metallurgy and Reactor Fuels (U.S. NRC, 2006b) and full ACRC Committee (U.S. NRC, 2006a, 2006d), the final publication of DG-1144 as RG 1.207 was recommended (Wallis, 2006a). One ACRC member voted against approving

RG 1.207 until NRC staff could demonstrate and justify the safety improvement which its implementation would lead to (for example through an identified event which application of RG 1.207 would have prevented) (Wallis, 2006b). In March 2007, RG 1.207 was published (U.S. NRC, 2007a). The technical basis document NUREG/CR-6909 Rev. 0 (O. K. Chopra & Shack, 2007) was published a month earlier.

In the December 2006 ACRS meetings ASME representatives indicated their interest in working with NRC staff towards a Code Case to supersede RG 1.207. However, reaching consensus remained challenging. Before a single EAF Code Case was published, the stainless steel DFC from NUREG/CR-6909 was adopted in the 2009 addenda to ASME III.

Responsibility for developing rules incorporating EAF into ASME III was assigned to Subgroup on Design, which developed an Environmental Fatigue Action Plan. The main elements in this plan were Code Cases on acceptable evaluation methods and more general implementation guidance for users. Code Committees encountered difficulties in achieving consensus, which is evident from the lengthy processing time for FAP actions. A potential reason for internal disagreement was the wide range of industry practices which had been used by this time due to lack of general guidance. Consequently, the FAP target was not limited to a single approach or a single Code Case. (Cole & Minichiello, 2010)

The first Code Case, N-761, was developed by the ASME III Subgroup Fatigue Strength and eventually approved in 2010 (ASME, 2013a). This CC contained EAF design curves which could be used in place of the air DFC. At an early stage of development, the curves were simplified as applicable up to the maximum expected temperature, making them conservative. Practically, the only parameter influencing the curves was strain rate. If expected threshold conditions were violated, the proposed air DFC was assumed applicable even in reactor water. (O'Donnell et al., 2005a, 2005b) In the final Code Case, temperature effects on the EAF design curves were included as described by O'Donnell and O'Donnell (2008).

Code Case N-792 includes users the option of applying F_{en} factors. The original version was published in 2010, with Revision 1 following in 2012 (ASME, 2013b). CC N-792-1 adopts the NUREG/CR-6909 Rev.0 F_{en} models but does not take credit for strain threshold. Neither of these Code Cases was approved by NRC (U.S. NRC, 2017). The EAF design curve technical basis was considered insufficient by the NRC. Disapproval of the F_{en} CC was based on the outdated F_{en} models from NUREG/CR-6909 Rev. 0. Rev. 1 models should be the basis for an approved F_{en} CC (U.S. NRC, 2019), which NRC staff continues to be engaged in as part of ASME Code activities (McCree, 2017).

3.2.2 JSME (Japan)

In terms of EAF rules, the Agency of Natural Resources and Energy within MITI (MITI, 2000), published in September 2000 a guideline, which was globally the first formal regulatory document including an acceptable methodology for plant life management (PLM) of NPPs already in operation (i.e. not in design stage). The guidelines contained a separate set of F_{en} equations for carbon/low-alloy steels and austenitic stainless steels. Note that having a single expression for the ferritic steels was different to US models of the time. The definition of F_{en} was the ratio of fatigue life in air (at room temperature) to fatigue life in high temperature reactor coolant.

Before the existence of regulatory guidance and specific requirements on EAF, a range of evaluation methods were in use side-by-side, as they were in the USA. NUREG reports, among others, were referenced as the technical basis for EAF PLM (Iwasaki et al., 2005). One case example of multiple method application to Japan's oldest LWR can be found in Ohata (2001).

The MITI Guideline F_{en} flowchart for stainless steels is shown in Figure 20. The method and F_{en} equations are exactly the same as proposed by Tsutsumi, Kanasaki et al. (2000; 2001), equations (41)–(44), for PWR environment (but also permissible for BWR environment). There is no modelled dependence of F_{en} on the dissolved oxygen content due to the wide scatter bands of data, particularly at 325 °C (Iida, 2001). This made the F_{en} model conservative relative to NUREG/CR-6717 (O. K. Chopra & Shack, 2001) and

particularly to EPRI (H. S. Mehta, 1999, 2001) at high DO representative of BWRs. The reason for the latter comes from Z factors, which the EPRI model used but the Japanese did not apply due to scatter concerns in water. The basis for leaving out Z factors in the Japanese models is given in Table 10. Higuchi (2001) assumed low and high F_{en} conditions to result in different effective Z factors (probably based on carbon and low-alloy steel data only) and by omitting its use, non-conservatism should be avoided for the low F_{en} case, which probably has more relevance with real plant transients.

Table 10. Interpretation of transferability subfactors and Z factors in air and water. (Higuchi, 2001)

	Air	Water	
		Low F_{en}	High F_{en}
Data scatter	2	5	5
Size effect	2.5	2	1
Environment and roughness	4	2	1.4
Total	20	20	7
Z factor	1	1	3

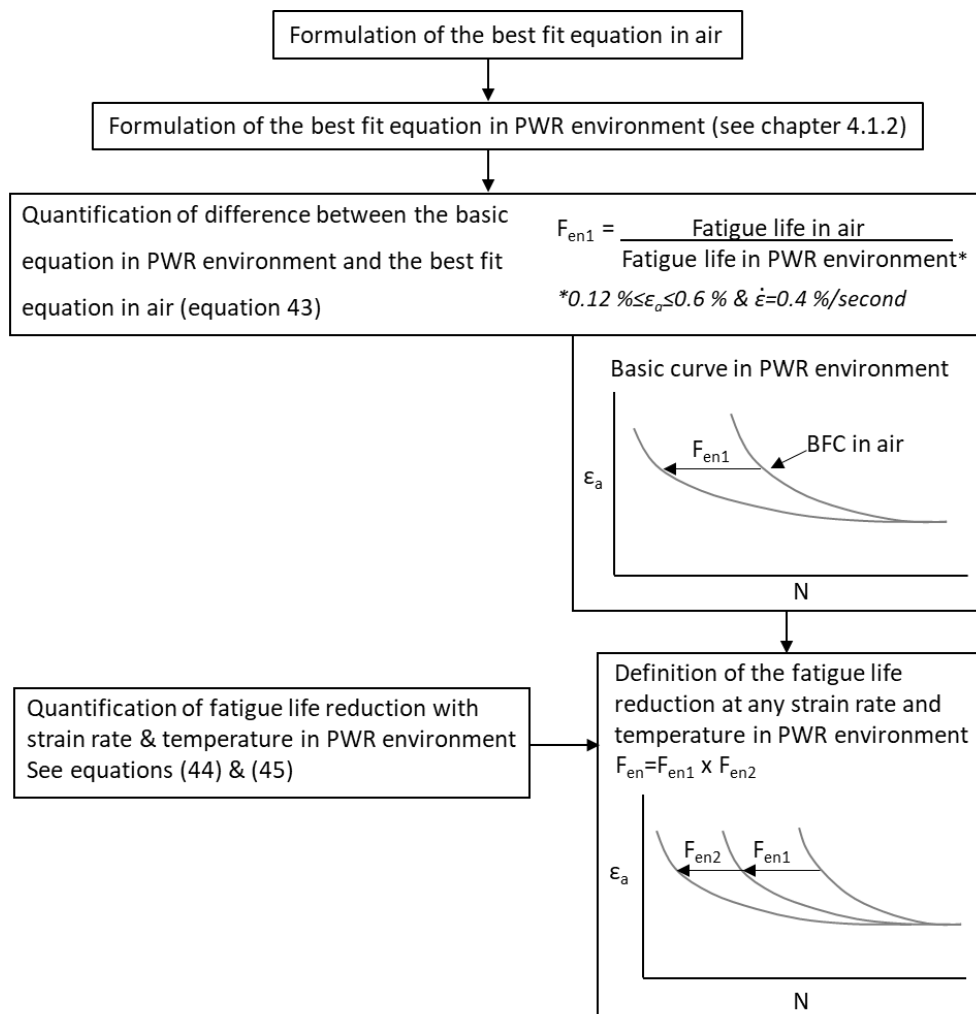


Figure 20. Flowchart for EAF evaluation method of stainless steels in the MITI Guideline. (Tsutsumi et al., 2000; Tsutsumi, Kanasaki, et al., 2001)

Wide scatter bands of Japanese data were also evident for the dependence of F_{en} on both temperature and strain rate, but general trends could nevertheless be seen and regression curve fitting was plausible.

The fatigue endurance limit in the MITI Guideline was assumed equal to the strain amplitude threshold for environmental effects, $\varepsilon_a=0.11\%$, which is almost identical with Chopra's (2001) threshold $\varepsilon_a=0.1\%$. The identical saturation strain rate (0.0004 %/s) was assumed in both Japanese and US models. Outside of a temperature range approximately 200–250 °C, the MITI Guideline F_{en} values were more severe in comparison with the US models. However, it should also be remembered that the best-fit curves in air were different. Equations 18 & 19 were used to define the experimental F_{en} of laboratory specimens in USA and equation 23 in Japan. Despite the differences, the net outcome measured in environmental fatigue life is typically quite similar and serves as a reminder that F_{en} models and best-fit (and design) curves are not interchangeable but rather need to be paired.

The MITI Guideline did not include a detailed evaluation method of EAF for practical application, such as determination of strain rate. Adoption of laboratory data-based F_{en} models to plant pressure vessel and piping components had been discussed by Kishida (1997; 1995) but were not fully mature in time for the MITI Guideline.

In April 2001, a study was started to establish a regulatory procedure, with both F_{en} equations and practical user guidance, within the Committee for Environmental Fatigue Evaluation Guidelines of TENPES (Thermal and Nuclear Power Engineering Society). The finished product became known as the TENPES Guidelines, which were published in June 2002 (TENPES, 2002) in Japanese. The technical content is summarized by Nakamura et al. (2003). The Guidelines contain separate sections for vessels, piping, pumps, valves and core internals. The guidance on piping is particularly important because conventional stress analysis lacks time-dependent information on stress/strain change.

The F_{en} equations of the TENPES Guidelines are directly adopted from the MITI Guideline (Nishimura et al., 2003). For plant application, three different alternatives methods are permitted: the factor multiplication method, the simplified method, and the detailed method. These are listed in order of decreasing conservatism but increasing complexity. The detailed method, commonly known as the modified rate approach (MRA), has been extensively validated using experimental data for carbon/low-alloy steels (Higuchi et al., 1995, 1997; Higuchi, Sakaguchi, & Nomura, 2007; Hirano & Sakaguchi, 2006; Kanasaki et al., 1995; Kanasaki, Hirano, et al., 1997) and for stainless steels (Higuchi, Sakaguchi, & Nomura, 2007; Kanasaki, Umehara, et al., 1997a; Nomura et al., 2004, 2010; Sakaguchi, Nomura, Suzuki, & Kanasaki, 2006; Tsutsumi, Dodo, et al., 2001). An overall description is given by Tsutsumi et al. (2002, 2003). Originally the method was known as the improved rate approach (Y. Asada, 1993).

More thorough descriptions of the three methods in practical use are given in chapter 5.2. Any of the methods may be combined so that in the end the usage factor (UF) in air of each particular load set pair is multiplied by a F_{en} value. An exception is earthquake loads, where environmental effects can be ignored due to the high strain rate and short duration. The sum of all UFs with environmental effects is the cumulative usage CUF_{en} (or U_{en}).

In addition to the MRA method for changing strain rate conditions, logarithmic average strain rate and the time-based integral methods have been experimented but with less accurate outcomes than MRA (Higuchi et al., 2004). The time-based integral method, suggested originally by Mehta and Gosselin (1995), is similar to MRA but weighted by time segments rather than strain.

TENPES Guidelines were targeted for application to PLM but are from a user's point of view just as well applicable to new plant design. In parallel with the Finnish YVL Guide 3.5 (STUK, 2002) published in April 2002, the TENPES Guidelines are thus the first regulatory documents containing EAF rules for use in operating plants and new designs, though in Japan the obligation did not extend to new designs yet and left as optional. A simple flowchart of fatigue evaluation for PLM in the TENPES Guidelines is shown in Figure 21.

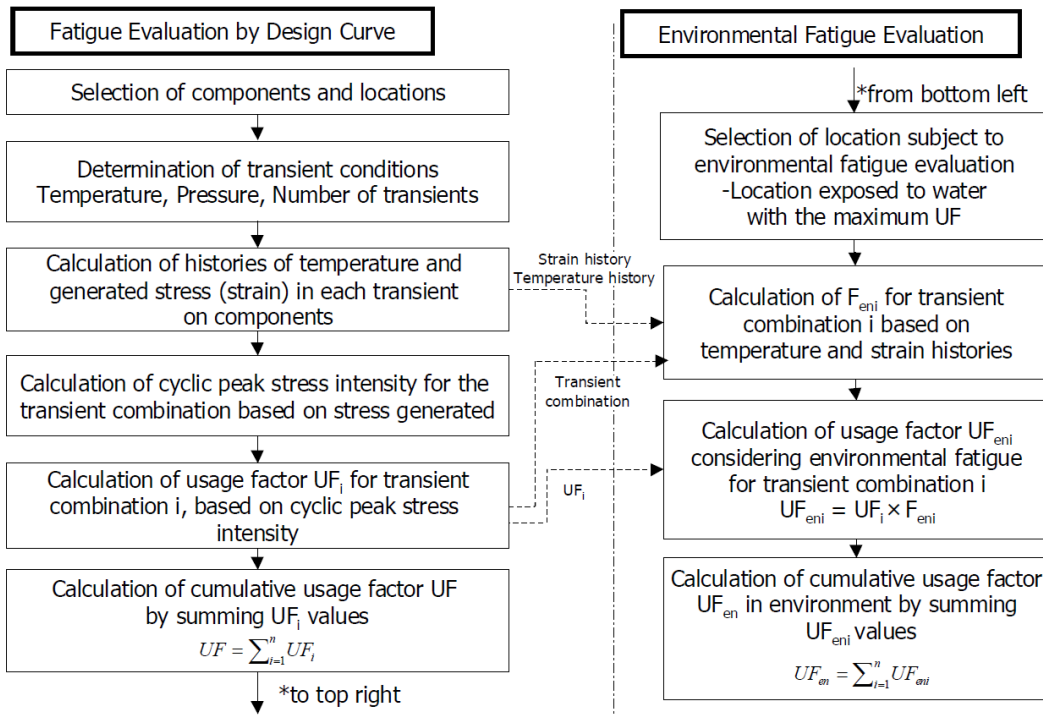


Figure 21. TENPES Guidelines flowchart for environmental fatigue evaluation in PLM. (Nakamura & Madarame, 2005)

The reason for EAF analysis requirement for only PLM is explained by the extensive margins in fatigue design for 40 years of operation, in particular from conservatism in stress analysis and transient definitions. For 60 years of operation, the actual plant transients are used instead of design transients to evaluate CUF and in parallel, to reflect the reduced margins, F_{en} calculations are required. (Iwasaki et al., 2005)

As more Japanese laboratory data continued to accumulate, a major revision to the stainless steel F_{en} model was proposed in 2002 (Higuchi et al., 2002; Higuchi, Iida, et al., 2003; Higuchi, Tsutsumi, et al., 2003). Contrary to the model used in the MITI and TENPES Guidelines, the new data indicated that BWR environments were (as US models had assumed) less harmful than PWR environments. The revised Japanese $F_{en(A)}$ model is given in equations (48)–(50). Slightly different notation is used here than in the original sources to remain consistent within this report.

$$F_{en(A)} = \exp[(X - \dot{\epsilon}^*)T^*] \quad (48)$$

For BWRs X , $\dot{\epsilon}^*$ and T^* are defined as follows.

$$X = 1.182$$

$$\dot{\epsilon}^* = \ln(3.26) \text{ for } \dot{\epsilon} > 3.26 \%/\text{s}$$

$$\dot{\epsilon}^* = \ln(\dot{\epsilon}) \text{ for } 0.0004 \leq \dot{\epsilon} \leq 3.26 \%/\text{s}$$

$$\dot{\epsilon}^* = \ln(0.0004) \text{ for } \dot{\epsilon} < 0.0004 \%/\text{s}$$

$$T^* = 0 \text{ for } \epsilon_a \leq 0.11 \%$$

$$T^* = 0.000813T \text{ for } \epsilon_a > 0.11 \% \quad (49)$$

For PWRs X , $\dot{\epsilon}^*$ and T^* are defined as follows.

$$X = 3.910$$

$$\dot{\epsilon}^* = \ln(49.9) \text{ for } \dot{\epsilon} > 49.9 \text{ \%}/s$$

$$\dot{\epsilon}^* = \ln(\dot{\epsilon}) \text{ for } 0.0004 \leq \dot{\epsilon} \leq 49.9 \text{ \%}/s$$

$$\dot{\epsilon}^* = \ln(0.0004) \text{ for } \dot{\epsilon} < 0.0004 \text{ \%}/s$$

$$T^* = 0 \text{ for } \epsilon_a \leq 0.11 \text{ \%}$$

$$T^* = 0.000782T \text{ for } \epsilon_a > 0.11 \text{ \%} \ \& \ T \leq 325 \text{ }^\circ\text{C}$$

$$T^* = 0.254 \text{ for } \epsilon_a > 0.11 \text{ \%} \ \& \ T > 325 \text{ }^\circ\text{C} \quad (50)$$

In case of earthquake loading, $F_{en(A)}=1.0$ for both BWR and PWR. Note that the 2002 Higuchi model does not contain a threshold temperature for environmental effects, unlike the MITI/TENPES, ANL or EPRI models. In fact, the temperature effect is modelled in such a way that that regression leads to $F_{en}=1.0$ at 0 $^\circ\text{C}$, which is a major difference to US EAF models.

Analysis of the data, despite scatter, tended to show more pronounced environmental effects at low strain amplitudes ($\epsilon_a < 0.16 \text{ \%}$) which prompted an alternative $F_{en(B)}$ model to be developed. This model includes a strain amplitude correction term A^* and is calculated using equations (49)–(53).

$$F_{en(B)} = \exp[(X - \dot{\epsilon}^*)T^*] \cdot A^* = F_{en(A)} \cdot A^* \quad (51)$$

For BWRs A^* is defined as follows.

$$A^* = 1.0 \text{ for } \epsilon_a \leq 0.11 \text{ \%}$$

$$A^* = \frac{0.178\epsilon_a^{-1.105} + 1}{1.637} \text{ for } \epsilon_a > 0.11 \text{ \%} \quad (52)$$

For PWRs A^* is defined as follows.

$$A^* = 1.0 \text{ for } \epsilon_a \leq 0.11 \text{ \%}$$

$$A^* = \frac{0.723\epsilon_a^{-1.157} + 1}{3.407} \text{ for } \epsilon_a > 0.11 \text{ \%} \quad (53)$$

In case of earthquake loading, $F_{en(B)}=1.0$ for both BWR and PWR.

Some examples of F_{en} modified best-fit curves using $F_{en(A)}$ or $F_{en(B)}$ in PWR water are shown in Figure 22. All coloured curves are applied together with the Tsutsumi best-fit mean curve, equation (23), to which the F_{en} models are paired. All other (black) mean curves are simply for reference. Figure 23 shows the magnitude of the strain amplitude correction term A^* , equations (52) and (53), as a function of strain amplitude for BWR and PWR environments, respectively. Note that above 0.3–0.35 % strain amplitude, the correction factor reduces $F_{en(B)}$ relative to $F_{en(A)}$ in order to correct a slight conservative bias in laboratory EAF lives. Between the threshold 0.11 % and 1 % strain amplitude, roughly a six-fold difference exists for the correction factor in PWRs.

Application of the $F_{en(B)}$ model to EFT experimental data positively affected the accuracy of fatigue life prediction in low strain amplitude tests, where some results estimated with $F_{en(A)}$ were outside the bounds of design curve margins. However, later Japanese publications no longer refer to the strain amplitude dependent $F_{en(B)}$ model, though the matter continues to be considered a knowledge gap in the recent EPRI report (EPRI, 2018c).

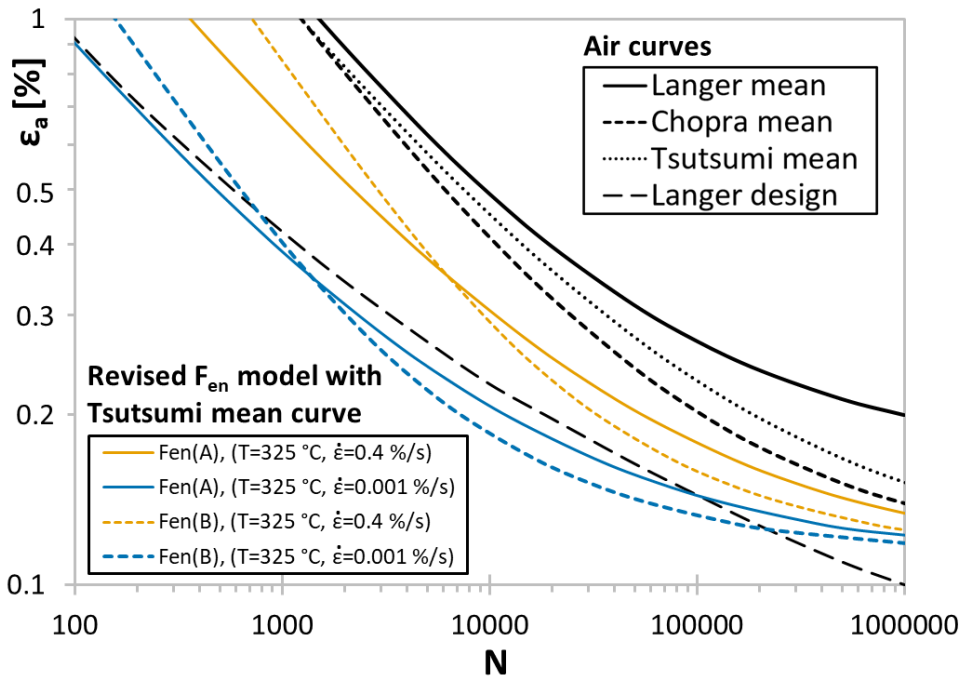


Figure 22. Comparison of $F_{en(A)}$ and $F_{en(B)}$ models in PWR water.

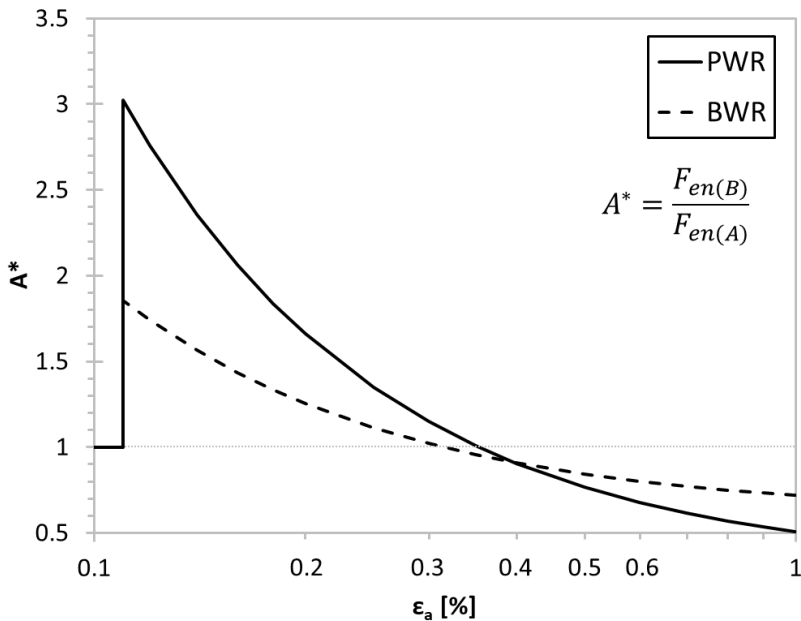


Figure 23. Strain amplitude correction term A^* in PWR or BWR environment as a function of strain amplitude.

Practical application of the TENPES Guidelines was refined gradually based on new experimental data as well as user experience (Higuchi et al., 2004). Continuous review of the F_{en} equations [e.g. equations (48)–(50)] was done within the EFT project committee, operating under the Japan Nuclear Energy Safety Organization (JNES, successor of JAPEIC). The simplified method for F_{en} calculation was also updated from the so-called combined model, where the average strain rate is calculated for the transient combination. As this was observed to result in excess conservatism, the so-called separate model includes calculation of the average strain rate for each transient individually and only then combines the result. (Nakamura & Madarame, 2005)

It was decided that the guidelines should become a part of the JSME Codes for Power Generation Facilities and in March 2004 the JSME Subgroup on Environmental Fatigue was formed. This policy change towards performance-based voluntary technical consensus codes and standards had taken place in 2002 (Nakamura & Sugie, 2011). During the draft phase of the new JSME Code, an ongoing discussion revolved around the necessity of EAF assessment for plant design to 40 years, in addition to PLM, which covers an extension to 60 years. The arguments against this referred to the lack of EAF related failure in existing plants, which was attributed to the considerable design margin coming from conservative transient definitions, for example. Probably influenced by this discussion, the JSME decided that the EAF draft Code would be independent of both the design & construction Code and fitness-for-service Code (Nakamura & Madarame, 2005).

Some remaining uncertainties in the procedure remained when the JSME Subgroup on Environmental Fatigue started to review the draft Code. Experiments below the assumed saturation strain rate for stainless steel (<0.0004 %/s), particularly for cast stainless steel, remained unconservative. Because of the slow strain rate, test durations for investigating such effects are very long. Some data had been generated to study the influence of hold periods and water flow rate, but results were initially inconclusive. Lastly, there was a general lack of data for Ni-based alloys to develop a unique F_{en} model. (Higuchi, 2005)

An acceptable answer to the open question on Miner's rule applicability in the case of combined fast and slow strain rates was obtained by demonstrating similar influence of the environment on both fatigue crack initiation and propagation. This was confirmed only with constant amplitude block load testing far from the endurance limit. In the case of random spectrum loading, the potentially detrimental influence of periodic high strain amplitude cycles on the endurance limit was not experimentally investigated but is assumed to be enveloped within the transferability margin on stress/strain in HCF. (Higuchi & Sakaguchi, 2005)

Based on the most recent findings from EFT it became clear that the draft Environmental Fatigue Evaluation Method (EFEM) being reviewed at JSME would not only make modifications to the general TENPES Guidelines but also to the F_{en} models published since 2002, including stainless steel (Nakamura et al., 2006):

- The transformed strain rate term in equations (49) and (50) for BWR and PWR water, respectively, was modified for cast stainless steels by reducing the saturation strain rate by an order of magnitude down to 0.00004 %/s. No change was suggested for wrought alloys.
- When using the factor multiplication method, the maximum temperature of a particular component location may be used instead of the temperature for maximum F_{en} in general.
- When using the simplified method, the F_{en} values of two transients making up a stress cycle are separately calculated and weighted together for the overall F_{en} . This reduces excess conservatism from using an average strain rate of the combined stress cycle.
- When using the detailed method (MRA), the maximum temperature and DO of each segment shall be used instead of the mean values of each segment to remain conservative.
- When applying K_e penalty factors on the alternating stress intensity, the strain rate shall nevertheless be based on no K_e factor applied to remain conservative.
- Piping equations to evaluate strain rate were revised.

It was concluded that no modification to stainless steel F_{en} models was needed to incorporate factors for strain hold periods, mean strain or water flow rate (Sakaguchi, Nomura, Suzuki, Tsutsumi, et al., 2006).

The EFEM was published as standalone code JSME S NF1-2006 (JSME, 2006) using the above listed modifications and based on data accumulated in the EFT project up to the year 2004 (Nakamura & Sugie, 2011). The English version was made available in October 2006. The BWR and PWR F_{en} models for stainless steels are shown in equations (54) and (55), respectively.

BWR

$$X = 1.182$$

$$\dot{\epsilon}^* = \ln(3.26) \text{ for } \dot{\epsilon} > 3.26 \text{ \%/s}$$

$$\dot{\epsilon}^* = \ln(\dot{\epsilon}) \text{ for } 0.0004 \leq \dot{\epsilon} \leq 3.26 \text{ \%/s for wrought alloys}$$

$$\dot{\epsilon}^* = \ln(0.0004) \text{ for } \dot{\epsilon} < 0.0004 \text{ \%/s for wrought alloys}$$

$$\dot{\epsilon}^* = \ln(\dot{\epsilon}) \text{ for } 0.00004 \leq \dot{\epsilon} \leq 3.26 \text{ \%/s for cast alloys}$$

$$\dot{\epsilon}^* = \ln(0.00004) \text{ for } \dot{\epsilon} < 0.00004 \text{ \%/s for cast alloys}$$

$$T^* = 0 \text{ for } \epsilon_a \leq 0.11 \%$$

$$T^* = 0.000813T \text{ for } \epsilon_a > 0.11 \% \quad (54)$$

PWR

$$X = 3.910$$

$$\dot{\epsilon}^* = \ln(49.9) \text{ for } \dot{\epsilon} > 49.9 \text{ \%/s}$$

$$\dot{\epsilon}^* = \ln(\dot{\epsilon}) \text{ for } 0.0004 \leq \dot{\epsilon} \leq 49.9 \text{ \%/s for wrought alloys}$$

$$\dot{\epsilon}^* = \ln(0.0004) \text{ for } \dot{\epsilon} < 0.0004 \text{ \%/s for wrought alloys}$$

$$\dot{\epsilon}^* = \ln(\dot{\epsilon}) \text{ for } 0.00004 \leq \dot{\epsilon} \leq 49.9 \text{ \%/s for cast alloys}$$

$$\dot{\epsilon}^* = \ln(0.00004) \text{ for } \dot{\epsilon} < 0.00004 \text{ \%/s for cast alloys}$$

$$T^* = 0 \text{ for } \epsilon_a \leq 0.11 \%$$

$$T^* = 0.000782T \text{ for } \epsilon_a > 0.11 \% \text{ \& } T \leq 325 \text{ }^\circ\text{C}$$

$$T^* = 0.254 \text{ for } \epsilon_a > 0.11 \% \text{ \& } T > 325 \text{ }^\circ\text{C} \quad (55)$$

Since the EFT project continued until closure in March 2007, new developments in F_{en} models continued to occur. The major modification for stainless steel is in the BWR F_{en} model, as shown in equation (56). The PWR F_{en} model, equation (55), was considered satisfactory without a change need. The consistency of additional air data with equation (23) was checked at the end of the EFT project. Thus, the JSME F_{en} models remained paired to that particular best-fit curve (Higuchi, Sakaguchi, Nomura, et al., 2007).

$$X = 0.992$$

$$\dot{\epsilon}^* = \ln(2.69) \text{ for } \dot{\epsilon} > 2.69 \text{ \%/s}$$

$$\dot{\epsilon}^* = \ln(\dot{\epsilon}) \text{ for } 0.00004 \leq \dot{\epsilon} \leq 2.69 \text{ \%/s}$$

$$\dot{\epsilon}^* = \ln(0.00004) \text{ for } \dot{\epsilon} < 0.00004 \text{ \%/s}$$

$$T^* = 0 \text{ for } \epsilon_a \leq 0.11 \%$$

$$T^* = 0.000969T \text{ for } \epsilon_a > 0.11 \% \quad (56)$$

In 2009, a revision to the EFEM code was published, JSME S NF1-2009 (JSME, 2009). The BWR and PWR F_{en} models within this code are equations (56) and (55), respectively. Note that regardless of wrought, weld or cast alloy, the saturation strain rate in BWR water is universal.

The summary of improvement items to the 2006 edition is given in the final report of the EFT project published in April 2007 (JNES, 2007). For the 2009 EFEM Code update, data from outside the EFT project developed in the meantime was also reviewed but the main influences were from domestic experiments (Higuchi, Sakaguchi, Nomura, et al., 2007):

- Studies on dissolved oxygen effects separately in BWR and PWR water did not warrant a parameter to be added to the F_{en} model. The main difference in stainless steel EAF behaviour between the two environments was speculated to be due to the water chemistry and electric conductivity.
- Additional water flow rate studies in BWR water consistently demonstrated a lower fatigue life at higher flow rate in the studied range up to about 10 m/s. As most laboratory data is based on near stagnant flow several orders of magnitude less than this, the apparent aggravating effect was considered when revising the BWR strain rate term in the F_{en} equation.
- A limited study on sensitization effects in BWR water did not reveal trends which would need to be incorporated into the F_{en} model.
- Strain holding experiments in BWR water suggested detrimental effects at a slow strain rate ≤ 0.004 %/s when the hold was timed at the peak strain. No saturation was seen when the holds were 2000 seconds long. However, if the hold location was overshoot to strains 0.03–0.06 % lower than the peak strain, the detrimental effect no longer took place. For thermal transients in plants, a peak strain hold is not a realistic expectation and thus a non-issue. For other specific BWR transients where holds may occur at the peak strain in a transient, the EFEM states that a saturation strain rate value should be used in place of the actual strain rate. In PWR water, a hold effect was not observed. (Higuchi et al., 2009; Higuchi, Sakaguchi, & Nomura, 2007; JSME, 2009)
- Use of the modified rate approach was examined for slow-fast-fast and fast-slow-fast partitioned waveforms as well as sine waveforms to confirm applicability. (Higuchi, Sakaguchi, & Nomura, 2007)

Primarily two open questions remained after publication of JSME S NF1-2009. The first was to gain a better understanding of the reasons why nonlinear sine waveforms are overconservatively predicted using MRA. This has plant relevance, where waveforms are typically irregular and not consisting of linear parts typical in laboratory experiments. The second open issue was the potential contribution of stress-corrosion cracking in very slow strain rate conditions in BWR water. The SCC component is difficult to differentiate from the EAF component of damage. The lowered saturation strain rate in the revised BWR F_{en} model, equation (56), closely approximates laboratory results which show both transgranular and intergranular fracture, but a mechanistic understanding was not developed. (Higuchi, Sakaguchi, Nomura, et al., 2007)

Nakamura and Sugie (2011) describe several planned follow-up topics related to fatigue and EAF after JSME S NF1-2009 was issued, but at least in the public domain not all have been addressed. The aforementioned and other open questions, such as overlapping effects of fatigue and stress corrosion (SCC) mechanisms, remain awaiting resolution and may become a future priority once more, perhaps after the revision work on the air DFC is completed, and depending on the nuclear energy policy in Japan.

As part of PLM the EFEM F_{en} models are used to multiply a usage factor in air, which is based on the 1963 ASME III design fatigue curve which is copied in the JSME S NC1 Design and Construction Code. On the contrary, the F_{en} models themselves use the Tsutsumi, Kanasaki et al. (2000; 2001) best-fit air curve to Japanese data, equation (23), and not the Langer best-fit air curve, equation (8), as their reference. The difference between these two best-fit curves can be seen in Figure 10, for example. This introduces an inconsistency to the JSME S NF1 evaluation methods.

Figure 24 and Figure 25 visualize the effect this has on the design curve margins. As the 1963 ASME III design fatigue curve is an offset of Langer’s best-fit curve by factors of 20 and 2 on fatigue life and strain, respectively, these margins appear as straight lines in these Figures up to the crossover point where fatigue life and strain margins are equally bounding. On the other hand, the margin of the design fatigue curve to the Japanese (dashed) best-fit curve is at its lowest less than a factor of eight. Similarly the margin on strain in HCF approaches a factor of 1.5 for the Japanese best-fit curve. Note that the margins on the NUREG/CR-6909 best-fit curve are even less (about 5 and 1.4 at minimum).

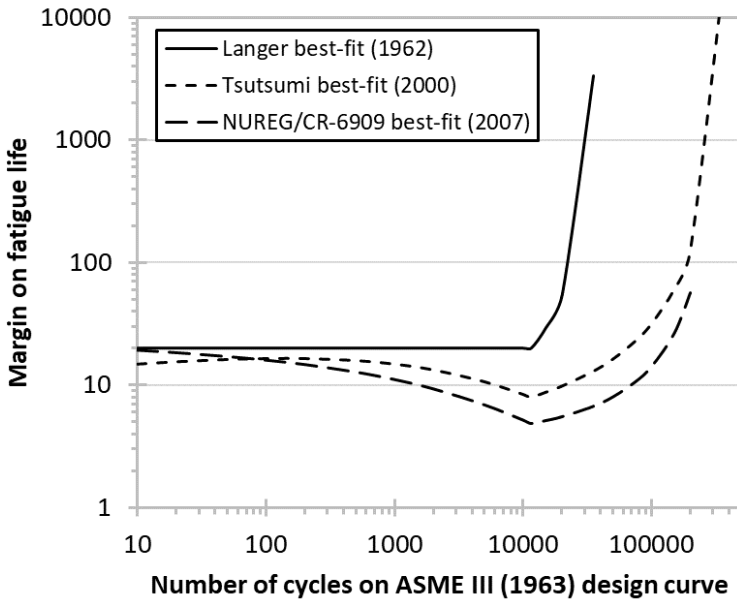


Figure 24. Margin comparison on fatigue life in the ASME III 1963 stainless steel DFC by choice of best-fit curve.

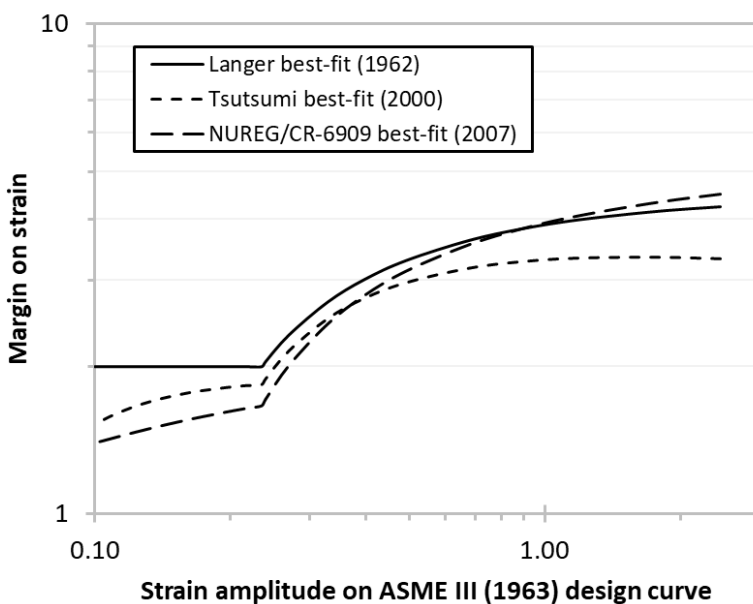


Figure 25. Margin comparison on strain (or stress) in the ASME III 1963 stainless steel DFC by choice of best-fit curve.

The JSME S NF1 (JSME, 2006, 2009) stainless steel F_{en} equations contain a very high threshold strain rate for environmental effects, up to 49.9 %/s in PWR water. This is an artefact of extrapolating experimental data to a strain rate where $F_{en}=1$. On the contrary, the guidance states that for seismic transients, environmental effects are not necessary. The US models (see Table 9) contain much lower thresholds (typically 0.4 %/s), above which environmental effects disappear. This leads to the issue of not having a well-defined threshold for practical application when using the JSME EFEM code. Secondly, if a practical threshold was considered in the neighbourhood of 1 %/s a considerable discontinuity in F_{en} value at this point would exist.

High strain rate effects were studied in more detail by Fukuta et al. (2013) to investigate if the transformed strain rate term could be adjusted to resolve these practical issues. High strain rate data was added to the existing EFT database. The three F_{en} models based on regression at 325 °C in PWR water (base metal, CASS and weld metal) are shown in equations (57), (58) and (59). (Fukuta et al., 2013) Material specific best-fit curves in air, equations (25)–(28), were used to define the experimental F_{en} values. Due to the variation between the best-fit curves in air (see Figure 10), this has major significance. A further modification to the weld metal F_{en} was later done (S. Asada et al., 2020) and is shown in equation (60). All the models below have considerably reduced threshold strain rates, between 0.25–2.74 %/s. In BWR, the JSME S NF1 threshold is a more reasonable 2.69 %/s and a re-evaluation has not been done.

$$F_{en} = 1.38 \cdot \dot{\epsilon}^{-0.346} \text{ for base metal} \quad (57)$$

$$F_{en} = 0.62 \cdot \dot{\epsilon}^{-0.342} \text{ for CASS} \quad (58)$$

$$F_{en} = 1.27 \cdot \dot{\epsilon}^{-0.237} \text{ for weld metal} \quad (59)$$

$$F_{en} = 1.11 \cdot \dot{\epsilon}^{-0.224} \text{ for weld metal (JWES DFC revision)} \quad (60)$$

Since all evaluated EAF data was in PWR water, no dissolved oxygen parameter is necessary. Presumably the material specific air best-fit curves were derived on material heat(s) with similar tensile strength. As the common endurance limit 0.11 % in equation (25)–(28) reveals, this value was fixed rather than fitted. For quantifying environmental effects in LCF however, the result is not very sensitive to the endurance limit parameter.

A comparison of the new stainless steel F_{en} models (PWR, 325 °C), equations (57)–(61) to those of Higuchi et al. (2002) (same as 2006 and 2009 JSME EFEM Code equation), Higuchi, Sakaguchi, Nomura et al. (2007)2(O. K. Chopra & Stevens, 2018) (O. K. Chopra & Stevens, 2018) is shown in Figure 26. As mentioned, the choice of best-fit curve is very influential and the range of saturated F_{en} at very slow strain rate varies between 6.4 to 39.5. More than two orders of magnitude difference exists on the threshold strain rate between models (0.25 %/s to 49.9 %/s).

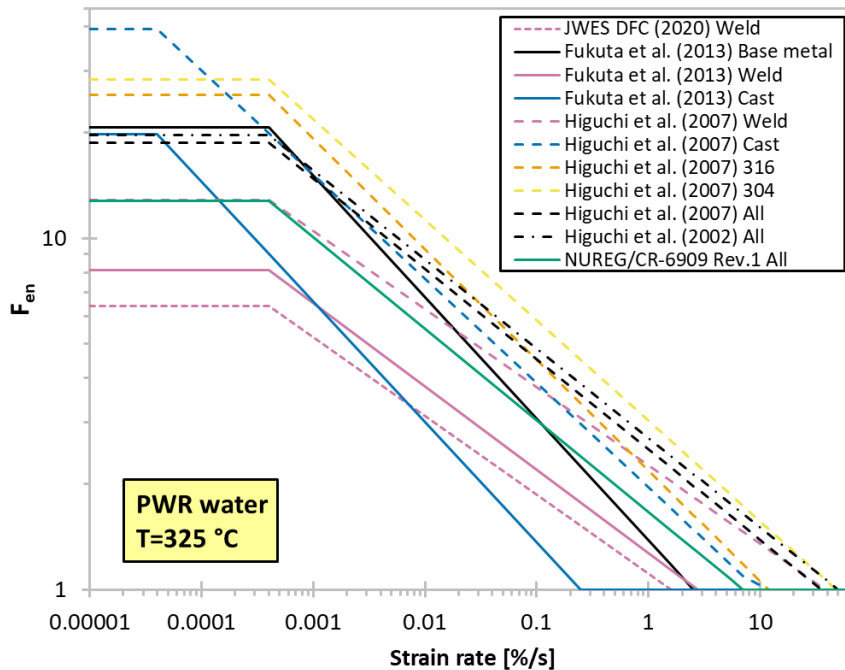


Figure 26. Comparison of F_{en} models in PWR water at 325 °C. (S. Asada et al., 2020; O. K. Chopra & Stevens, 2018; Fukuta et al., 2013; Higuchi et al., 2002; Higuchi, Sakaguchi, Nomura, et al., 2007)

An activity in the recent JWES DFC subcommittee has been to evaluate the applicability of the new tensile strength dependent stainless steel fatigue curves together with an F_{en} model. Because the most conservative F_{en} is calculated with the base metal model, equation (57), it was applied with all other materials as well. By considering the transferability factors on material scatter, all data was evaluated either accurately or with conservatism (S. Asada et al., 2020). Though this is strictly not consistent with the both F_{en} and design curve being based on the same reference best-fit curve in air, the experimental data does not suggest any potential non-conservatism in LCF. It should nevertheless be remembered that the overall margin in the new Japanese design fatigue curves (2.8/1.43) is much less than in either the old (20/12) or new (12/2) ASME design curves and any loss of margin is relatively speaking more significant.

3.2.3 RCC-M (France)

Like the ASME Code, RCC-M explicitly states that the design fatigue curves were not constructed using EAF data. This can be found in paragraph B3173, which reads:

“It should be noted that the group of tests on which the fatigue curves in figures Z I 4.0 are based, do not include tests performed in a corrosive environment which might accelerate fatigue damage.”

Consideration of environmental effects as part of fatigue usage calculations formed the second major planned modification to the RCC-M after the design fatigue curve for stainless steel in air. Though the ASME Code Case N-792 gave a method to account for EAF in fatigue evaluations, the preference in France was to integrate environmental effects directly into the RCC-M by using additional data from French research programs (Courtin et al., 2012).

EDF’s road map for EAF consisted of partial reduction (transferability) factors in PWR water on fatigue life. Quantifying more accurate formulas for each subfactor was intended after further research. Subfactors in water would be analogous to those in air and they would be supplemented with an explicit F_{en} equation. Faigy (2012) gives details of the proposed subfactors and F_{en} equations. These particular F_{en} equations yield values which are roughly between NUREG/CR-6909 Rev.0 and Rev.1 (Draft) in magnitude.

Meanwhile, AREVA suggested an EAF approach which shared features with the EDF road map but was simpler to adapt with an existing design curve (Courtin et al., 2012). This same method was proposed by AREVA to Finnish Nuclear Regulator STUK (Säteilyturvakeskus) for the Olkiluoto 3 EPR (European Pressurized water Reactor) project in Finland (Hytönen, 2011). The experimental background to the AREVA proposal is in the publications by Le Duff et al. (2008, 2009, 2010).

This chapter presents the technical details of the assessment method, which together with the revised design fatigue curve were sent to AFCEN as requests for modification of the RCC-M. Evolution of the technical justification for EAF assessment method is described in the series of annual PVP conference papers from 2012 to 2016 (Courtin et al., 2012, 2016; Métais et al., 2013, 2014, 2015).

The AREVA EAF assessment method was built on two assumptions:

- F_{en} equations, such as those developed by ANL in the EACLWR program, can accurately predict the severity of environmental effects for the case of polished surface finish and triangular waveform i.e. the standard laboratory experiment (Le Duff et al., 2010).
- For plant-relevant conditions where surface finish of real components is not polished and loading waveforms are complex, interaction of various factors influences the magnitude of environmental effects. Observations suggest that the design fatigue curve in air, applied for PWR conditions, includes an appreciable margin for environmental effects which should counterbalance F_{en} penalty factors. (Courtin et al., 2012)

The AREVA experimental program suggested that it is specifically the combination of PWR environment with industrial (non-polished) surface finish and realistic loading transients, which limits their total influence on fatigue life, thus resulting in additional margin of the design curve when associated with a PWR water environment. Figure 27 illustrates an example waveform simulating a safety injection system (SIS) transient, during which injection of cooler water induces a surface tensile strain, and reversed flow of warmer water induces a compressive strain.

In a nutshell, what the French experimental data suggested was that the transferability factor on life between design curve and best-fit curve is specific to the environment. In this case, the argument is for a smaller transferability factor on fatigue life in PWR water than in air. The proposed solution to normalize the differences between environment was to not modify already existing air DFC, but to instead reclaim a part of the transferability factor on life in PWR water in the opposite direction (i.e. reduce the usage factor).

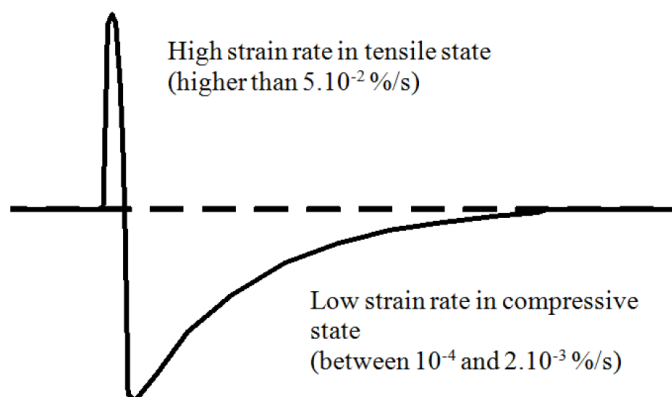


Figure 27. Schematic of simulated SIS transient. (Métais et al., 2015)

The potential margin for environmental effects in the design curve was initially called $F_{en, allowable}$ but the term was renamed $F_{en-integrated}$. In principle, the combined effect of four factors is assumed between the best-fit and design curves (for application to PWR water), as schematically shown in Figure 28. These factors are (a) scatter, (b) size, (c) surface finish and (d) reserve environmental effect (additive to what F_{en} factors already account for). Practically, this leads to equation (62).

$$N_{design} = \frac{N_{best-fit}}{a \cdot b \cdot c \cdot d} \quad (62)$$

N_{design} and $N_{best-fit}$ are the number of cycles from the design and best-fit curves in air, respectively.

Note that in the design fatigue curve for application in air, factor (d) should not have meaning apart from being an extra margin through $F_{en,max}$ as Table 2 demonstrates. In the absence of further differences between air and PWR water, factor (c) in air should be assumed equal to the combined effect of (c) and (d) in PWR water. This implies that the surface finish effect in PWR water is argued to be less than in air. It is not evident why $F_{en,max}$ is included as an extra margin in the total transferability factor on fatigue life in the air design curve (Table 2), only to be erased in the process of calculating fatigue usage in PWR water.

The quantification of $F_{en-integrated}$ from experimental studies is based on the notion that the margins for scatter and size can be assumed (also in a PWR environment) as known quantities derived from extensive data in air, whilst the combination of surface finish and environmental effect is unknown.

Rearranging equation (62) by replacing with $N_{best-fit}=F_{en,test} \cdot N_{25}$ and $F_{en-integrated}=c \cdot d$, we end up with equation (63).

$$F_{en-integrated} = F_{en,test} \cdot \frac{N_{25}}{N_{design}} \cdot \frac{1}{a \cdot b} \quad (63)$$

$F_{en,test}$ is evaluated using the equations in NUREG/CR-6909 Rev.1 (draft) (O. K. Chopra & Stevens, 2014) and N_{25} is the experimental fatigue life. For consistency, the use of this approach necessitates the adoption of NUREG/CR-6909 best-fit fatigue curve, design fatigue curve and F_{en} model which the French approach does.

Mathematically, the design curve is argued to contain an allowable margin for environmental effects ($F_{en-integrated} > F_{en,test}$) on the condition that

$$\frac{N_{test}}{N_{design}} > a \cdot b \quad (64)$$

This case is represented in Figure 28. Conversely, if N_{test} were to fall within the range defined by the arrows indicating subfactors a and b in Figure 28, the allowable margin would be exceeded, and the environmental effect in PWR water would be more severe than what the design fatigue curve alone could account for.

The publicly available technical basis documentation does not explain in-depth, why the loading type coefficient group (for multiaxiality, variable amplitude loading etc.) is not part of the margin in PWR water as it was for constructing the design curve in air. The other two coefficient groups for material variability and component effects are taken into account through the factors (a) through (c). Courtin et al. (2012) state that loading history can be covered conservatively as part of the stress analysis itself by for example transient combination and/or use of the plasticity correction factor. While this is true, the minimum design margin consequently becomes user-dependent and influenced by the level of detail of a user's fatigue analysis. Métais et al. (2013) indicate that further conclusions on other parameters' influence (temperature, multiaxiality and mean stress) in PWR water are awaited from future research. To date, these factors are not yet included in the $F_{en-integrated}$ methodology. If any of the aforementioned parameters are eventually confirmed to be detrimental, they would in effect decrease the value of $F_{en-integrated}$ by growing the denominator in equation (63). Other simultaneous beneficial factors, such as hold time effects, may balance the overall effect.

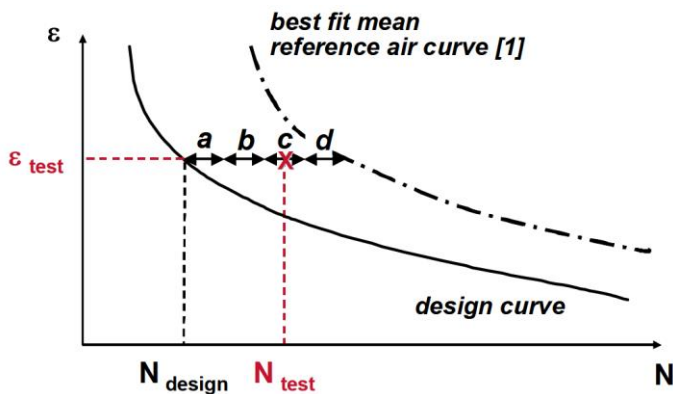


Figure 28. PWR transferability subfactors between best-fit and design fatigue curves: material variability (a), size (b), surface finish (c) and environmental effect (d). (Courtin et al., 2012)

The summarized analysis steps consist of:

- Using screening criteria to identify and limit the locations to be analyzed further for CUF_{en} , the cumulative usage factor inclusive of environmental effects.
- Limiting the transient combinations to be further analyzed by excluding the least severe ones.
- A global F_{en} is evaluated for each remaining transient combination by weighting the partial usage factors of each transient combination by their associated partial F_{en} factors.
- If $F_{en} \leq F_{en-integrated}$, no further analysis is needed and the existing CUF calculation is applicable as CUF_{en} .
- If $F_{en} > F_{en-integrated}$, further analysis is required. (Courtin et al., 2012)

A flow chart of the analysis steps is shown in Figure 29. For ferritic steels, the regular very low oxygen operating environment in PWRs rules out the need for EAF assessment.

Screening for the components and locations was suggested with the following limitations:

- Minimum total usage factor (in air) of e.g. 0.1.
- Surface is in contact with reactor water.
- Selecting sentinel location from a group of similar geometries undergoing similar transient histories.
- Certain exemption criteria can be applied e.g. transients below a limiting temperature, where F_{en} does not under any circumstances exceed $F_{en-integrated}$.

It was suggested by Courtin et al. (2012) that after sorting transient combinations in order of decreasing partial usage factor, the group consisting at least 40 % of the total usage is selected for the next steps. This leaves an element of subjectivity to the analysis.

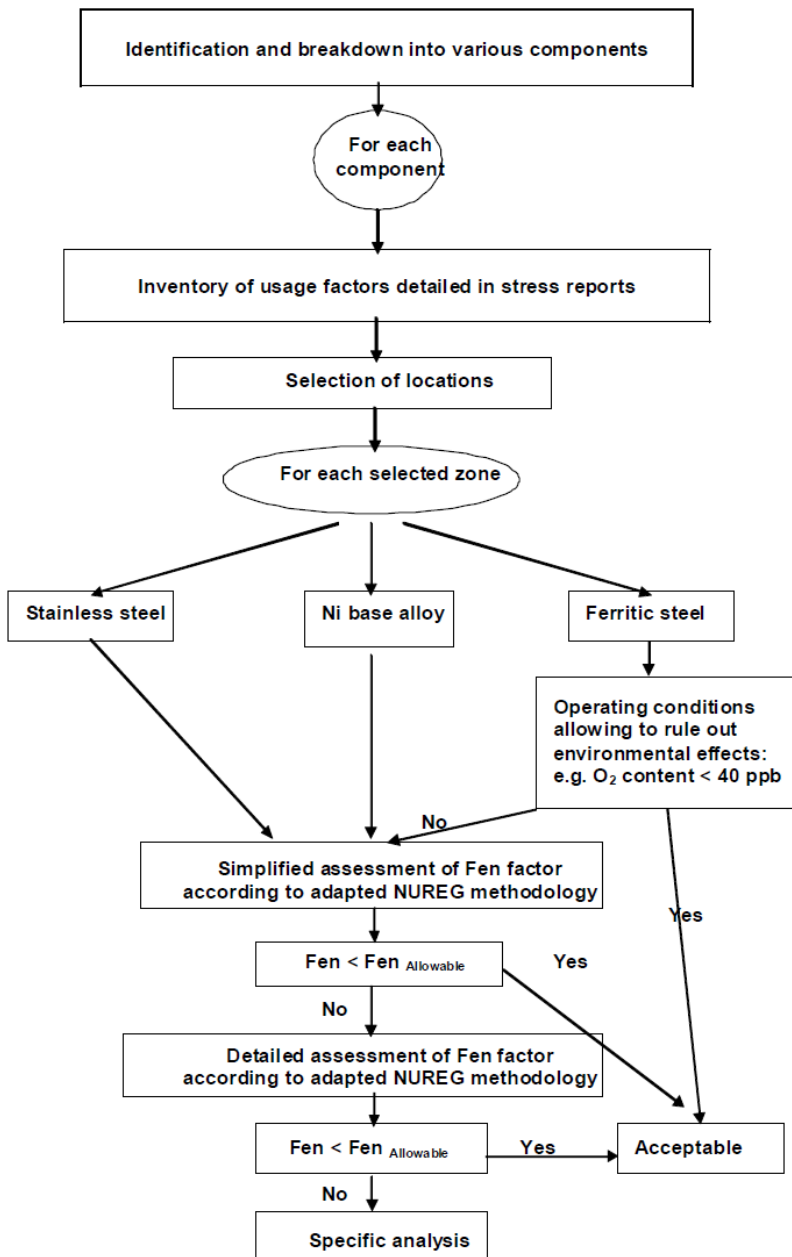


Figure 29. Flow chart of EAF assessment in the AREVA method. (Courtin et al., 2012)

The global F_{en} is defined as the average of each combination, weighted by their partial usage factor, equation (65).

$$F_{en} = \frac{\sum_1^n F_{en,partial,j} \cdot UF_{partial,j}}{\sum_1^n UF_{partial,j}} \quad (65)$$

where $F_{en,partial,j}$ and $UF_{partial,j}$ are the EAF penalty factor and partial usage factor of the j^{th} transient combination, respectively, and n is the number of selected transient combinations. Note that the global F_{en} value may thus contain transient combinations, which on their own can both exceed and be less than $F_{en-integrated}$. Nevertheless, sensitivity of the global value to the choice of which transient combinations are included and which ones omitted is probably not severe.

Only the parts of a transient consisting of a positive strain rate are used to calculate F_{en} . Time history gaps between combined transients can be ignored in the proposal. Long time gaps influence the strain rate

parameter for F_{en} . Issues of transient linking have been discussed further e.g. in an EPRI guidance report (EPRI, 2012).

As per code requirements, the K_e plasticity correction factors are to be applied to correct the strain amplitude. Two different methods are suggested, both of which use the mechanical and thermal contributions to K_e . To evaluate strain rate, the plasticity corrected strain is used rather than the elastic assumption, to remain consistent with the fatigue usage definition without environmental effects. The elasto-plastic strain rate with K_e is higher than the elastic strain rate and thus yields lower F_{en} values.

If globally $F_{en} < F_{en-integrated}$, no further EAF analysis is necessary. Otherwise, the total usage in PWR water is as a first step recalculated based on the ratio of equation (65) to $F_{en-integrated}$, equation (66).

$$CUF_{en} = CUF \cdot \frac{F_{en}}{F_{en-integrated}} \quad (66)$$

Two different values have been determined for $F_{en-integrated}$, based on average experimental values from the AREVA test program. The default option is to apply a value of 3. If after this step $CUF_{en} < 1$, no further analysis is needed. If the CUF_{en} requirement is not met and the simplified method (with conservative strain rate and temperature) was previously used to calculate F_{en} for the transient combinations, the detailed method (effectively the modified rate approach) can be used instead, and equation (66) re-evaluated. For zones undergoing mainly thermal transients, $F_{en-integrated}=5$ may be used in lieu of 3. It is also permitted to use the larger value for only a subset of all transients which it may concern, if necessary, to satisfy the CUF_{en} requirement.

If the detailed method cannot successfully demonstrate $CUF_{en} < 1$, additional refinement of the fatigue analysis is needed (e.g. elastic-plastic finite element analysis).

The methodology was evaluated by AFCEN GTFE together with the modification request for the design fatigue curve. It was approved as RPP N° 3, at the same time as RPP N° 2, for the RCC-M 2016 edition. The rules were specifically included in RPP form, as the RCC-M subcommittee board did not find the needed user experience to justify inclusion into the main body of the code at the time. Additionally, the RPP text states that *“the text and the retention of this RPP will be reviewed annually by AFCEN”*. Between leaving the modification request and a favourable technical opinion from the AFCEN GTFE, revisions were made to clarify the procedure, namely:

- The strain threshold $\epsilon_a=0.1$ % was removed on the basis that oxide film rupture in variable amplitude loading could make cycles below the threshold damaging. Note however, that the endurance limit in the RPP N° 2 design fatigue curve effectively negates the influence of the removal.
- Clear user guidance on when the $F_{en-integrated}$ value of 3 or 5 is used was added to avoid confusion.

Internationally published data from the UK (Platts et al., 2015) during the review period included similar conclusions as the AREVA experimental program, which positively influenced the opinion of the GTFE working group (Courtin et al., 2016).

Since RPP N° 3 is based on the design fatigue curve given in RPP N° 2, these exact $F_{en-integrated}$ values cannot be applied together with any other DFC as such. In order to be applicable, the quantification of potentially built-in environmental effects would need to be repeated for each separate DFC. Keeping consistency for RPP N° 2 at the same time also requires the adoption of the NUREG/CR-6909 best-fit curve and exact F_{en} equations. RPP N° 3 is consistent by adopting equation (21) rather than equation (22). It is not evident from public documentation how this consistency matter has been resolved for licensing of the Finnish EPR project, whose design basis is the RCC-M design curve (and thus Langer best-fit curve) rather than RPP N° 2 curve (with NUREG/CR-6909 best-fit curve).

RPP N° 3 does not comment on applicability of the methodology to HCF, where the margin on stress or strain is more bounding than the transferability factor on cycles. In practice, the margin on cycles grows

beyond the crossover between the two factors. The transition point in the RPP N° 3 DFC is at approximately $1.33 \cdot 10^5$ cycles (where $\varepsilon_a \approx 0.135$ %). On the best-fit curve, $\varepsilon_a \approx 0.190$ % at this point. Data from the AREVA experimental program exists in the range $\varepsilon_a = 0.3$ %– 0.6 %.

Lastly, on the discussion on incorporated environmental effects in design fatigue curves: the ASME DFC should on the basis of RPP N° 2 and 3 intuitively contain a larger margin for environmental effects in PWR water than a factor of 3 as it has larger margins on fatigue life with respect to the NUREG/CR-6909 BFC.

3.2.4 KTA (Germany)

The 2013 revision of KTA 3201.2 (KTA, 2013) adopted environmental effects in fatigue assessment of safety class 1 components in contact with primary cooling water. A new formulation was included in chapter 7.8 'Fatigue analysis' to require that the "fluid effects" on component fatigue are to be considered to the state of science and technology.

To mitigate abrupt burden of work, a threshold for cumulative damage of $D = 0.4$ was set. Where this threshold is exceeded and a reduction of fatigue strength due to fluid effects cannot be excluded, then the following measures shall be taken to ensure consideration of fluid influence on the fatigue behaviour:

- a) the components considered shall be included in a monitoring program to KTA 3201.4, or
- b) experiments simulating operating conditions shall be performed, or
- c) verifications by calculation shall be made in due consideration of fluid-effected reduction factors and realistic boundary conditions.

The wordings in KTA 3201.2 (KTA, 2013) are quite distant from the NUREG/CR-6909 reports and JSME S NF1-2009 code. KTA states that that fluid effects may reduce the "fatigue strength", where reduction of fatigue life or acceleration of fatigue usage is considered in the US and Japanese approaches – and even stated that environmental effects can be excluded below a threshold amplitude. Despite this, it is obvious that the measures for option c) would probably be based on assessment of F_{en} factors and increased fatigue usage – and perhaps, application of the latest NUREG/CR-6909 report for determining the F_{en} factors. But the EAF methodology to be used was left open and experimental approaches (option b) are also welcomed. The option a) is in line with already earlier in KTA adopted strategy: The calculated fatigue usage may exceed the limit set at unity ($UF < 1$), but such condition requires additional measures for in-service inspection.

The method applied for determining F_{en} factors shall be compatible with the fatigue curves used for fatigue assessment. This compatibility would be severely compromised if F_{en} factors according to NUREG/CR-6909 reports were applied together with the KTA 3201.2 (KTA, 2013). The problems arising from conflicting assumptions concerning the effects of temperature without the water environment (in air) are illustrated in Figure 30.

The effects of design temperature are acknowledged in the KTA 3201.2, but neglected in the NUREG/CR-6909 reports for fatigue in air. Figure 30 a) introduces a factor F_{temp} representing the increase of fatigue usage at 300 °C in relation to the room temperature design curve of KTA and as function of stress intensity amplitude. The F_{en} factors according to NUREG/CR-6909, rev.1 represent combined effects of temperature and environment. They are functions of temperature and strain rate, but not depending on the amplitude of strain or stress intensity.

The fatigue assessment according to the KTA 3201.2 (KTA, 2013) without effect of environment result to 8.9 times higher fatigue usage at 300 °C than at room temperature when the stress intensity (S_a) is 195 MPa. The same factor for usage at 300 °C in PWR water is obtained according to NUREG/CR-6909, rev.1, if the strain rate is almost saturated at 0.00057 %/s. In other words, $F_{temp} = F_{en} = 8.9$ at that point in Figure 30 a). An increase of amplitude would decrease the F_{temp} factor and the strain rate resulting to a matching F_{en} factor, but a minor decrease in the amplitude to $S_a = 190$ MPa would result to $F_{temp} = 10.15$ and $F_{en} =$

1, because the amplitude drops below the threshold for environmental effects ($S_a < 195$ MPa) provided in NUREG/CR-6909, rev.1. Thus, an inert fatigue assessment according to the KTA 3201.2 (KTA, 2013) results now to ten times higher usage than if moving to an EAF assessment, where a F_{en} factor is calculated exactly as instructed in the NUREG/CR-6909, rev.1. This is because the F_{en} factor is defined as the ratio of fatigue endurance in RT air over that in hot water and the F_{en} factor is applicable only with a design fatigue curve for room temperature. Literally following the instructions would lead to replacing the $F_{temp} = 10.15$ by $F_{en} = 1$.

Figure 30 b) illustrates another comparison between the F_{temp} and F_{en} at 200 °C. Because the KTA design curve is common for elevated temperatures, the difference between 200 and 300 °C is limited to temperature dependent elastic modulus values. A change in design temperature affects F_{en} factor more than F_{temp} . This means that at 200 °C the F_{temp} exceeds the saturated F_{en} factor already above the threshold applied for calculation of the F_{en} factor. And the difference reaches a maximum at 100 °C, where $F_{en} = 1$ according to the NUREG/CR-6909, rev.1 and the KTA design fatigue curve for $T > 80$ °C still applies.

It is obvious that engineering judgement is needed when considering different codes or versions of fatigue assessment and procedures for estimating the environmental effects and penalty factors. The compared cases in Figure 30 are extreme and problems easy to detect, but similar concerns can be met better hidden in other combinations of rules for EAF assessment.

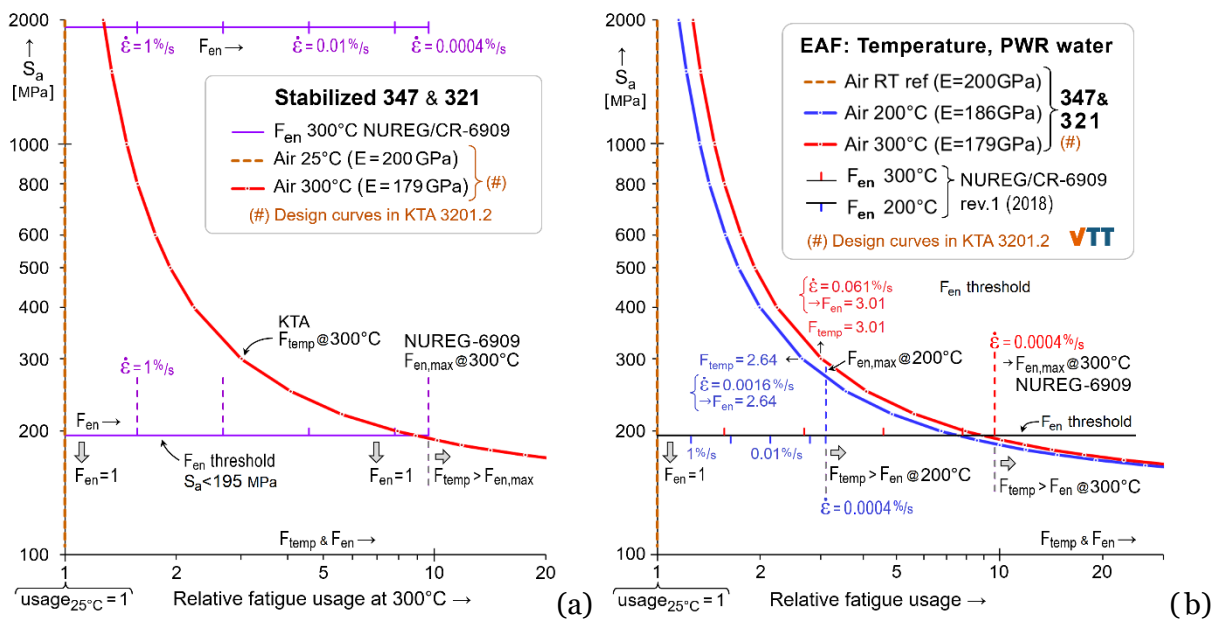


Figure 30. Comparison of the F_{en} factors in PWR water according to NUREG/CR-6909, rev.1 and the effect of design temperature as acknowledged in the KTA 3201.2. A factor F_{temp} represents the increase of fatigue usage at temperatures of 300°C (a) and also 200°C (b) in relation to the room temperature design curve of KTA. The effect of temperature is pronounced for small strain amplitudes in HCF, where the F_{temp} grows even beyond the most severe F_{en} factors.

3.3 Recent and emerging approaches

Internationally, revisions of the NUREG/CR-6909 report (O. K. Chopra & Shack, 2007; O. K. Chopra & Stevens, 2014, 2018) practically remain a default reference for methods to take into account environmental effects in fatigue. Evidently, vast amounts of research have been conducted since the EACLWR program concluded but in the space of Codes and Standards there is relatively little change to reflect this. Only in recent years have the numbers of approved Code Cases started growing. This is a testimony of the difficulty in reaching consensus, which is a prerequisite in Code activities. On the other hand, regulatory approval of ASME Code Cases is not always self-evident, even though it is an obvious goal.

This following will describe the recently approved EAF & fatigue relevant Code Cases in ASME Section III as well as outline ongoing activities in the various Working Groups. The maturity of the various emerging approaches ranges from infancy to fully developed. Depending on the context (particular regulator, end user, specific application etc.) there may be considerable differences in practical application of certain emerging approaches.

Regarding EAF and fatigue analysis, the development of Code Cases N-761 (2013a) and N-792 (ASME, 2013b) were mentioned previously. As of January 2023, N-761 and N-792-1 remain unapproved by U.S. NRC (U.S. NRC, 2023b).

The most recent Code editions (latest in 2023) have seen an increasing number of fatigue Code Cases approved, reflecting the wide-ranging scope of work which the working groups have had on their agendas.

The most relevant Section III working groups are WG Environmental Fatigue Evaluation Methods (WGEFEM) and WG Fatigue Strength (WGFS). WGFS has a long history, and its charter is as follows:

“To develop advanced fatigue design criteria, analysis methods, and their associated physical and thermo-mechanical properties for application to Section III of the ASME BPV Code. The WG will provide support to other Sections as requested.”

WGEFEM was formed about a decade ago and it operates under the following charter:

“The Working Group will evaluate recognized methods of assessing cyclic life of components that are subject to a wetted environment. The life assessment includes traditional fatigue usage evaluations, crack growth evaluation and other approaches to provide appropriate design margins when a usage factor or an equivalent criterion is determined.”

Wright (2017) explains the intentionally provoking wording choices of this charter, namely the use of “crack growth”. Historical interpretations and Code language in Section III contain inconsistencies in what the failure criteria (CUF=1) exactly means. A conservative view of a design Code is that flaws should not be permitted. However, if the fatigue usage factor is considered exhausted when an engineering crack (of roughly 3 mm) has developed in a component, this is far from defect-free. Through-wall cracking in component tests as a failure condition, as found in Section III Mandatory Appendix II adds to the confusion. Ultimately, Wright (2017) considers the charter to contain a paradigm shift in the design Code.

Within WGEFEM an internal action plan was proposed to tackle the various EAF issues. The objective was to have in Section III methods considered acceptable to regulators with an ultimate goal of providing a non-mandatory EAF appendix. In the interim, Code Cases would define milestones in reaching this objective. An overview of the action plan options for EAF, ordered from simplest to most complex is given below (Wright, 2017):

1. Use of exclusion clauses for cyclic analysis in a water environment.
2. Simplified screening criteria for piping components designed to NB-3600, with F_{en} .
3. Use of water adjusted design S-N curves for strain rate (CC N-761 approach).
4. Use of a F_{en} correction to air design curves (CC N-792 approach).
5. Use of curve correction factor for strain gradient versus membrane loading.
6. Use of flaw tolerance approach for postulated defect at start of life.
7. Use of a F_{en} threshold method that considers the integrated effect of surface finish and environment, as per RCC-M proposal ($F_{en-integrated}$).
8. Total life prediction (initiation plus growth) with consequence-based design factor.

Options 1–4 were already in existence and would not provide any additional reduction of CUF_{en} unless e.g. the F_{en} models themselves were to be revised. Options 5–8 were seen as ambitious future evolutions.

As there were ongoing and partially overlapping action plans within Section III, a fatigue steering committee was formed in 2017 to coordinate activities. The work of this steering committee was completed in 2019 with the adoption of a Section III Fatigue Action Plan (FAP). Implementation of the plan has since been a priority of Section III Standards Committee. (McKillop et al., 2021)

The original FAP contained 27 actions spread across four WGs under Subgroup Design Methods: WGEFEM, WGFS, WG Design Methods (WGDM) and WG Probabilistic Methods in Design (WGPMD). These are listed in Table 11. New items have since been added, reflecting the evolving nature of the topic. Management of the FAP is the responsibility of Subgroup Design Methods. (McKillop et al., 2021)

In Section XI, the WG Flaw Evaluation Reference Curves (WGFERC) is involved with EAF through fatigue crack growth curves. This has relevance to the total fatigue life prediction method listed above, but the activities in Section XI will not be further discussed in this report which focuses on Section III.

Table 11. Original Section III Fatigue Action Plan contents. (McKillop et al., 2021)

Task description	Responsible WG	Target date	Code Case
Code Case with revised simplified elastic-plastic analysis to reduce conservatism	WGDM	2020	N-904
Code Case to allow temperature dependent mean stress correction to air fatigue design curve	WGDM	2021	N-920
Revise procedure for use of results from plastic analysis (strain) to calculate alternating stress intensity	WGDM	2023	
Develop method to account for through thickness stress gradient and actual thickness in piping	WGDM	2020	N-902
Evaluate alternate methods for cycle counting in design	WGDM	2023	
Develop method to account for stress gradient and actual thickness in geometries other than piping	WGDM	2025	
Develop a strain-based fatigue analysis	WGDM	2025	
Code Case for test procedure and minimum data requirements for new fatigue design curve	WGFS	2021	
Code Case for alternate design curves for carbon and low alloy steels in NUREG/CR 6909-1	WGFS	2020	N-905
Present plan for upgrading air design fatigue curves including items listed below	WGFS	2021	
- <i>Develop multiple best fit curves for carbon and low alloy steels based on material spec. or ultimate tensile strength</i>	WGFS	2022–2030	
- <i>Develop multiple best fit curves for Ni-Cr-Fe alloys and stainless steels</i>	WGFS	2022–2030	
- <i>Evaluate and select method for adjustment for mean stress effect; change modified Goodman</i>	WGFS	2021	
- <i>Evaluate and select proposed factor on cycles; Using 95 % confidence interval applied on the mean curve for example</i>	WGFS	2022	
- <i>Evaluate tensile strength effects on fatigue curves; using tensile strength to develop new fatigue curves</i>	WGFS	2021	
Evaluate approach to high cycle fatigue and select proposed factor on stress	WGFS	2025	
Code Case to calculate strain rate for an EAF evaluation when using NB-3200/App XIII	WGEFEM	2018	N-884
Code Case to calculate strain rate for an EAF evaluation for piping and valves	WGEFEM	2022	
Fatigue evaluations considering environmental effects: strategy for using operational fatigue assessment to assist in meeting fatigue usage when considering EAF	WGEFEM	2021	N-919
Update Code Case N-792 to incorporate changes below			
- <i>Update CC N-792 based on NUREG/CR 6909-1 and more recent test data</i>	WGEFEM	2023	
- <i>Review justification for strain amplitude threshold</i>	WGEFEM		
- <i>Review RCC-M F_{en} threshold approach for possible incorporation in CC N-792</i>	WGEFEM	2023	
Consideration of Strain-Life Weighted method (SNW) as an approach to calculate F_{en}	WGEFEM	2022	
Evaluate the use of the Total Life Methodology to account for crack initiation and growth	WGEFEM	>2025	
Form reliability steering committee	WGPMD	2025	
Define methodology for determining reliability of the pressure boundary for fatigue	WGPMD	2025	
Interface with Plant System's Design Committee	WGPMD	2025	

3.3.1 Recent ASME Code Cases

Code Case N-884 Procedure to Determine Strain Rate for Use with the Environmental Fatigue Design Curve Method and the Environmental Fatigue Correction Factor, F_{en} , Method as Part of an Environmental Fatigue Evaluation for Components Analyzed per the NB-3200 Rules

This Code Case was approved in 2018 and included in the 2019 Code (ASME, 2019). It was classified as one of the highest priority FAP items in an effort to immediately regain some of the fatigue usage factor margin of the existing LWR fleet (McKillop et al., 2021).

The premise behind this Code Case is the highly influential strain rate factor in defining F_{en} . By defining a common procedure, Code users can be more confident that EAF rules are applied in a more consistent basis. The enclosed methodology is applicable with both the F_{en} factors as well as environmental fatigue design curves. The technical background is in JSME research and the NUREG/CR-6909 report. Practical guidance on strain rate calculation (e.g. transient overlapping, asymptotically reached peaks or valleys) is provided. Seismic events can be screened out due to the high strain rate. Some of the same guidance was earlier published in an EPRI report (EPRI, 2012). In the first place, the Code Case should be paired with an elastic or simplified elastic-plastic stress analysis. If the nonlinearity between stress and strain is considered, fully elastic-plastic analysis is also permitted. The overall F_{en} of a transient pair may be determined using the simplified method or modified rate approach (see chapter 5.2).

The applicability of this Code Case is only together with analyses performed using the Mandatory Appendix XIII, Article XIII-3000, XIII-3520(e) [formerly NB-3222.4(e)(5) before the 2017 Code] approach.

U.S. NRC (2023a) approves the use of Code Case N-884 as an alternative to compliance with ASME Code rules.

Code Case N-902 Thickness and Gradient Factors for Piping Fatigue Analyses

This Code Case was approved in 2020 and included in the 2021 Code edition (ASME, 2021a). It was classified as one of the highest priority FAP items in an effort to immediately regain some of the fatigue usage factor margin of the existing LWR fleet (McKillop et al., 2021).

The attainable relief in fatigue usage factors originates from accounting for the actual wall thickness (compared to smaller laboratory specimens) and the non-uniform through-wall stress distribution of components (compared to membrane stress in laboratory specimens). The thickness and gradient factors are essentially multipliers (with values <1) to the regular Appendix XIII, Article XIII-3000, XIII-3520(e) fatigue usage. The thickness (TF) and gradient factors (GF) are mathematically expressed in the form given in equations (67) and (68), respectively.

$$TF = \{A + B \cdot \ln(t/25.4) + C \cdot [\ln(t/25.4)]^2 + D \cdot [\ln(t/25.4)]^3\}/1000 \quad (67)$$

$$GF = 1 - \left(1 - \frac{\sigma_m}{\sigma_m + \sigma_b + \sigma_g}\right) (W + X + Y + Z)/1000 \quad (68)$$

A, B and C are material specific parameters which depend on the strain range. D is a material specific constant.

σ_m is the uniform membrane linear elastic stress range. σ_b and σ_g are the linear and nonlinear through-thickness bending linear elastic stress ranges, respectively. W, X, Y and Z are parameters which depend on the wall thickness as well as all three stress ranges σ_b , σ_g and σ_m .

For piping, a relief in usage factor of 10–40 % has been claimed in the technical basis document for a set of sample problems (EPRI, 2018b).

The Code Case provides alternative rules, currently restricted to piping components analyzed per Mandatory Appendix XIII, Article XIII-3000, XIII-3520(e) but is intended to be validated to expand the scope to other components (McKillop et al., 2021). The methodology is not only restricted to EAF analysis, but is also applicable to structures not subjected to environmental effects.

U.S. NRC (2023a) approves the use of Code Case N-902 as an alternative to compliance with ASME Code rules.

Code Case N-904 Alternative Rules for Simplified Elastic-Plastic Analysis

This Code Case was approved in 2020 and included in the 2021 Code edition (ASME, 2021b). It was classified as one of the highest priority FAP items in an effort to immediately regain some of the fatigue usage factor margin of the existing LWR fleet (McKillop et al., 2021).

The essence of this Code Case is providing a more realistic value of the simplified elastic-plastic fatigue penalty factor K_e which would approach those calculated using other international Codes (RCC-M, JSME). The technical basis to the alternative rules is given in an EPRI report (EPRI, 2018a). The alternative rules may be used for vessels (or piping) evaluated using the design by analysis principles (Mandatory Appendix XIII) or for piping evaluated by the design by rule principle (NB-3600). A third use is for core support structures. The benefit of the rules is that existing stress analysis results may be used as such. As with N-904, the rules can be applied generically regardless of environmental effects or not.

U.S. NRC (2023a) approves the use of Code Case N-904 as an alternative to compliance with ASME Code rules.

Code Case N-905 Alternate Design Fatigue Curves to Those Given in For Section III Appendices, Mandatory Appendix I, Figures I-9.1 and I-9.1M

This Code Case was approved in 2020 and included in the 2021 Code edition (ASME, 2021c). It was classified as one of the highest priority FAP items in an effort to immediately regain some of the fatigue usage factor margin of the existing LWR fleet (McKillop et al., 2021).

The origin of this Code Case was that the carbon and low alloy steel DFCs from NUREG/CR-6909 were not adopted in the Code, unlike the stainless steel DFC in 2009. Therefore, this Code Case permits the use of the NUREG/CR-6909 DFCs for carbon and low alloy steels. These curves use a factor of 12 on cycles, rather than 20 in the main body of the Code in Mandatory Appendix I. The Code Case curves are less conservative than those in Mandatory Appendix I, partially due to the differences in transferability factors.

U.S. NRC (2023a) approves the use of Code Case N-905 as an alternative to compliance with ASME Code rules. Currently, within WGFS there is an effort to incorporate N-905 directly into Mandatory Appendix I.

Code Case N-919 Alternative Fatigue Evaluation Method to Consider Environmental Effects on Class 1 Components

This Code Case was approved in 2021 and included in the 2023 Code edition (ASME, 2023a). The content of this Code Case is very simple. As the text in NB-3121 states that the design fatigue curves are not inclusive of environmental effects, the permitted method to account for EAF is to apply the usage factors defined from the DFC in air and simply multiply the partial usage factors in air by the respective F_{en} factors to obtain the cumulative usage in a water environment, U_{en} .

Interestingly, the Code Case specifies that the $U_{en} \leq 1$ requirement shall apply as a minimum for the first 10 years of operating service, and not the entire service life. For the remaining service cycles beyond reaching $U_{en} = 1$, establishment of an operating plant fatigue assessment is the responsibility of the Owner.

U.S. NRC (2023a) approves the use of Code Case N-919 as an alternative to compliance with ASME Code rules.

Code Case N-920 Alternative Fatigue Design Curves for Ferritic Steels With Ultimate Tensile Strengths (UTS) \leq 80 ksi (552 MPa) and Austenitic Steels

This Code Case was approved in 2021 and included in the 2023 Code edition (ASME, 2023b). It was classified as one of the highest priority FAP items in an effort to immediately regain some of the fatigue usage factor margin of the existing LWR fleet (McKillop et al., 2021).

The reasoning behind this Code Case is the conservatism introduced by assuming the mean stress correction in the high cycle end of the DFCs to be based on room temperature mechanical properties fed into the Modified Goodman equation. As an alternative, this Code Case permits the use of temperature dependent properties to scale the DFCs at elevated temperature and offset effects of the modulus correction [equation (9)]. The net outcome is a 10–40 % higher fatigue strength (dependent on the material and temperature) than the current Code DFCs in Mandatory Appendix I have. It is unclear if N-920 can be used in parallel with N-905 for ferritic steels.

The technical basis to this Code Case is provided in an EPRI report (EPRI, 2019).

U.S. NRC (2023a) approves the use of Code Case N-920 as an alternative to compliance with ASME Code rules.

3.3.2 ASME Working Group ongoing activities

Code Case N-792-2

The U.S. NRC has not approved (and is not intending to approve) the F_{en} Code Case N-792-1 due to the methodology not representing the latest research activities i.e. the later revisions of NUREG/CR-6909 (U.S. NRC, 2023b). In order to eventually incorporate a general Code Case with the F_{en} equations, WGEFEM has been developing a revision N-792-2 which addresses the basis for disapproval of N-792-1.

There have been numerous iterations of the draft Code Case, stretching back several years, and it has not yet passed the ballot in the WG to be considered ready for submission to the next level in the committees. Many detailed comments have been addressed and in the back and forth exchanges some sections have even been reinstated after being removed at an earlier time (such as the modified rate approach). As the Code Case has taken several years to progress beyond WGEFEM, recent modifications include adding references to other Code Cases such as N-884 which have been approved by both ASME and U.S. NRC (K. Wang, 2023).

Code Case Proposal on Strain Rate for Piping and Valves

This proposal has been developed in WGEFEM for close to a decade and can be thought of as a sibling of N-884, but with application to NB-3600/NB-3650 analyses for piping and valves rather than the design by analysis methods of former NB-3200.

This proposal has been circulated at several WGs and up to the Subgroup level, but in order to address the disapproval votes and comments has each time been returned back to WGEFEM. The received comments are more or less detailed technical questions or requests for clarification. The concept of having a Code Case with strain rate calculation guidance itself is not being challenged. At the August 2023

WGEFEM meeting, it was suggested that a first version of this Code Case could be limited to piping only, as there are more open comments related to valves (Hirano, 2023).

Code Case Proposal on $F_{en-threshold}$

This Code Case proposal is targeting to bring into the ASME Code a similar methodology as the French $F_{en-integrated}$ RPP N° 3 in RCC-M (see chapter 3.2.3). Despite the slightly different terminology, the principle is identical. This item has been on the WGEFEM agenda since 2016, which is the same year RCC-M adopted the rule in probationary phase. In WGEFEM this item is led by EDF and is being supported by Rolls-Royce.

The proposal has received regular criticism from U.S. NRC and progress over the last couple of years has been marginal due to disapproved votes, which is a major difference to RCC-M where the technical basis was reviewed and approved in much shorter time. Mainly, the data from ANL has been reference by U.S. NRC as demonstrating a consistent surface roughness effect in both air and PWR water. Meanwhile, the proposal writers refer to the since generated test data in France, UK and the rest of Europe (Cuvilliez et al., 2020) as proof of integrated environmental effects in the design fatigue curve. The use of mean $F_{en-integrated}$ values (which has a factor of three in the proposal) from the more recent data does not appear acceptable to the U.S. NRC.

Another cause for concern is that as previously discussed for the $F_{en-integrated}$ methodology, its use is always restricted to a particular combination of best-fit curve, design fatigue curve and the numerical value of the integrated environmental effect factor. As a way to recover detrimental effects of EAF partially or fully, it lacks the flexibility to be paired with alternative combinations of BFC and DFC, which are another ongoing development in ASME III.

Alternative F_{en} integration method

Based on the UK R&D program involving fatigue crack initiation testing with non-standard waveforms, the strain-life weighted (SNW) method (Currie et al., 2017, 2018) has been developed into a Code Case proposal in WGEFEM. The method takes a similar approach as the weighted stress intensity factor rate (WKR) method (Emslie et al., 2016, 2017) to determine an effective value of the environmental effect, $F_{en,eff}$. The technical basis in the developed method refers to experimental work, in which complex waveforms are not necessarily predicted accurately using the MRA method. Some of the referenced data from outside of the UK R&D programs includes that from Japan (Tsutsumi, Dodo, et al., 2001), France (Le Duff et al., 2010) and Finland (Seppänen et al., 2017). In all of these references, the empirical observation has been that a slow strain rate near the peak (or “top”) of a hysteresis loop is more damaging than an equal fraction of slow strain rate near the valley (or “bottom”) of a loop.

The weighting curve is derived by using the ratio of fatigue lives at the full strain range ($\epsilon_{max}-\epsilon_{min}$) to that at the instantaneous fatigue life N_ϵ for a given point within the rising part of a load cycle.

N_ϵ can obviously be calculated only when the strain range exceeds twice the endurance limit. Therefore, for $\epsilon > (\epsilon_{min} + 2C)$ the weighting factor is defined as by equation (69).

$$w_{SN} = \frac{N}{N_\epsilon} = \frac{\exp\{A-B \cdot \ln[0.5(\epsilon_{max}-\epsilon_{min})-C]\}}{\exp\{A-B \cdot \ln[0.5(\epsilon-\epsilon_{min})-C]\}} = \exp\left\{B \cdot \ln\left[\frac{0.5(\epsilon-\epsilon_{min})-C}{\epsilon_a-C}\right]\right\} \quad (69)$$

Otherwise $w_{SN}=0$. The values A, B and C in equation (69) come from the selected fatigue curve, which must have the same form as equation (12).

The effective value of F_{en} , taking into account the weighting, is calculated using equation (70).

$$F_{en,eff} = \sum_{i=0}^{n-1} F_{en,i \rightarrow i+1} \cdot (w_{i+1} - w_i) \quad (70)$$

Due to the nonlinearity of strain-life curves, the weighting according to SNW is nonlinear throughout a cycle. This is demonstrated in Figure 31, where different detailed F_{en} calculation models are compared for an example cycle with $\varepsilon_a=0.6\%$ and $R=-1$. The MRA method weights the cycle equally throughout, giving a straight line. The Tsutsumi binary weighting (TBW) method (Tsutsumi, Dodo, et al., 2001) is similar, but the weighting factor is zero until a pre-defined threshold strain range is exceeded. The plastic strain weighting (PSW) method is similar to SNW, but requires knowledge of the distribution between elastic and plastic strain during a cycle, which is not necessarily available. PSW and SNW emphasize the damage occurring near the peak of a cycle.

As with many of the other emerging Code Cases, there is a need with SNW to maintain consistency when applied in order to not mix and match fatigue curves and F_{en} models which are not derived based on each other. This can potentially become an issue, if new fatigue curves are introduced into the ASME Code without parallel F_{en} models following with each new curve.

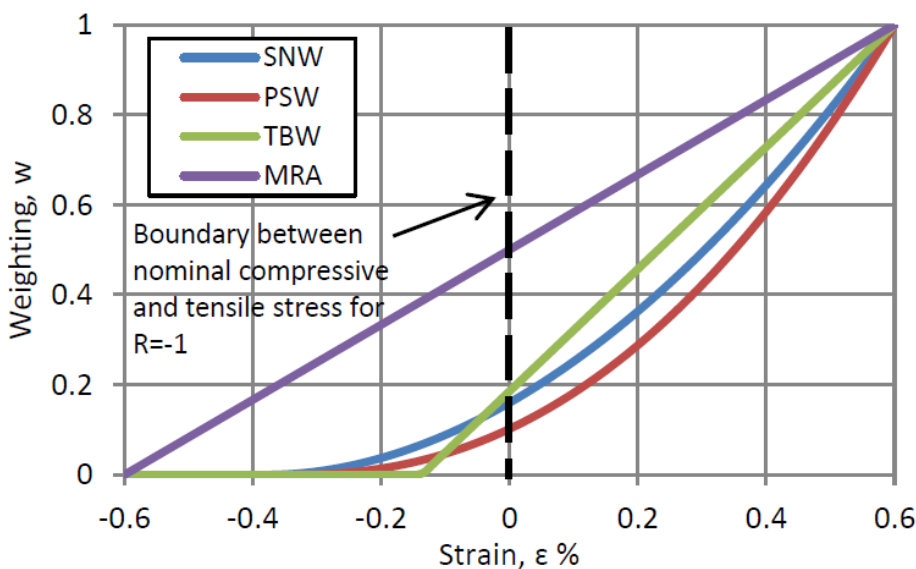


Figure 31. Schematic of SNW weighting factor compared to other detailed F_{en} calculation models (Currie et al., 2017)

This Code Case proposal was balloted at Section III Committee level but received a negative vote. The negative vote was not due to the technical content but caused by a general observation about the large number of approved and upcoming (and partially interacting) Code Cases on EAF, which may add to confusion for those aiming to use them.

Alternate Procedure for Providing Fatigue Strength Values in Air to Appendices, Mandatory Appendix III-1300 Fatigue Strength Values for All Materials

ASME Section III Mandatory Appendix III-1300 states the basis on which the Mandatory Appendix I design fatigue curves were constructed: regression of uniaxial strain cycling data for a best-fit curve followed by the mean stress correction and application of transferability factors for stress and cycles. This item is being developed in WGFS (originally as a Code Case, but since November 2022 as a White Paper) to give users an option to alternatively perform fatigue testing in air on which to base application-specific fatigue curves.

A guidance document was written in 1994 by William O'Donnell and David Jones to give a procedure containing the experimental procedures and data requirements which would adequately characterize a material's fatigue curves. The now ongoing work intends to update this document while keeping it principle-based, rather than e.g. relying solely on particular national standards or specifications such as ASTM. The document includes general requirements on the execution of tests and minimum numbers of tests to perform (21–42 depending on need to investigate temperature or mean stress effects). Use of three

different material heats in equal testing numbers is required. The comments received during balloting of the draft White Paper have aimed to clear up consistency issues which may otherwise result in conflicting requirements.

No matter which format the White Paper may eventually take, it will be susceptible to inconsistency issues with existing F_{en} models which are for use with entirely different design fatigue curves.

Design fatigue curves using the tensile strength of materials

The recent Japanese work on fatigue curves with tensile strength dependency has been prepared into a Code Case proposal in WGFS. Background to this work is described in chapter 2.4.2 and an ASME technical basis document more than 100 pages in length has been written. Approval of these methods in ASME has been sluggish compared to JSME, where the curves are already incorporated into use with the environmental fatigue evaluation method Code. A specific discussion point remains on the considerably reduced transferability factors on fatigue life and stress. U.S. NRC does not approve on e.g. neglecting the surface finish or size effect in air.

There are further details than only surface roughness effects, which in this proposal may be confusing and inconsistent together with other ongoing Code Case activities. This includes the fact that although the proposed DFCs are in air, they are in the JSME Code intended for use in EAF evaluations, but not in air fatigue usage calculation. MHI has commented that this is due to potential loss of margin with the proposed DFCs in the case of seismic loading and ratcheting. This restriction was removed for the ASME Code Case proposal in 2023. Another boundary condition is that by introducing a range of DFCs through this Code Case (and any others aiming to do so too), each should be paired with a unique F_{en} expression which adds WGEFEM as an important stakeholder for any future developments. Reflecting on the rate of progress on EAF and DFCs in the working groups over the last few years, this may become a source of significant delay over technical details.

Total fatigue life approach

A philosophical change in the design life to fatigue crack initiation is in progress within WGEFEM. Across many safety critical industries (such as aerospace), damage tolerant design approach has been in use successfully for decades. Compared to these industries, nuclear has remained conservative and hesitant to revise its safe-life view on fatigue design.

Initially in 2015, a record in WGEFEM was registered on assuming a postulated defect at the start of operation and doing design fatigue calculations entirely based on fatigue crack growth. This suggestion subsequently evolved into Code Case N-919, which states that an operating plant fatigue assessment shall be established after fatigue usage reaches a value of 1.0. The MHI (Japan) total life approach, introduced at the May 2021 meeting, developed this by assuming a postulated flaw to exist at the time when U_{en} (fatigue usage including environmental effects) reaches a value of 1.0, but in addition already in design calculations also accounting for the ensuing lifetime spent in growing the crack and ensuring that it remains smaller than the allowable flaw depth for the specified service life (see Figure 32). Although the U.S. NRC commented that a flaw tolerance approach at the time was not acceptable to them for design based on ASME Section III, they did support further development of the approach. (S. Asada, 2021)

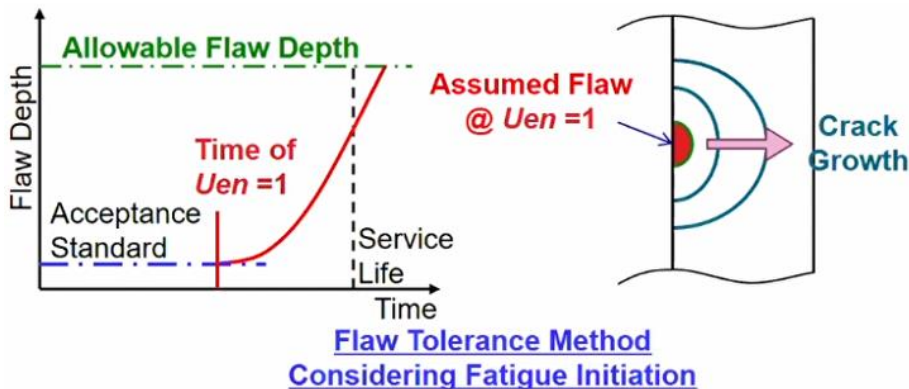


Figure 32. Total fatigue life principle. (S. Asada, 2021)

Rolls-Royce presented in parallel to MHI their approach to total fatigue life, bearing in mind the additional design requirements which UK regulations necessitate e.g. in terms of defect tolerance of the highest risk components (Pellereau, 2021). Outside of direct ASME activities, Rolls-Royce has also been active in developing their deterministic approach towards a probabilistic direction, where a target reliability level could be associated with a specific total life (Batten et al., 2020). Much of the recent UK R&D work e.g. on short crack growth (Griffiths et al., 2021) and multiaxial fatigue (Gill et al., 2021) aims to support the various aspects of the total life approach.

The independent proposals for total life approaches by MHI and Rolls-Royce are not identical as Table 12 shows, but in recognition of the similarities and a common interest, the action items were combined into one in 2022. Note from Table 12 the many existing links between the MHI proposed approach and approved Code Case N-919, which could suggest a future revision of N-919 evolving towards a total life approach. On the contrary, the Rolls-Royce approach leans on applying other state-of-the-art methods such as $F_{en-threshold}$ and weighted stress intensity factor rate (WKR) method (Emslie et al., 2016, 2017), some of which are not yet approved as ASME Code Cases but may have national endorsement on a case-by-case basis. Since the two separate action items were combined, there have been no new updates at the WGEFEM meetings.

Table 12. Comparison of MHI (Asada) and Rolls-Royce (Pellereau) approaches to total fatigue life. (S. Asada, 2022)

	Asada's Proposal	Pellereau's Proposal
U in air ≤ 1	Same as N-919/#15-352	Not required
$U_{en} \leq 1$ for min. 10 years	Same as N-919/#15-352	Not required
Establish an operating plant fatigue assessment	[Time of $U_{Fen}=1$] U_{Fen} with F_{en} by N-792-X	$U_{Fen} = U_{F6909}$ with F_{en} -threshold
	[Postulate crack at time of $U_{Fen}=1$] Sec.XI App. L; L-3200 Flaw Model	3 mm-depth crack
	[da/dN] JSME Fitness-for-Service (95% confidence limit)	N-809 (~2x mean) with WKR, no K threshold
	[Analytical evaluation procedure] Sec.XI App. C (App. L refers App. C)	R6 FAD approach
	[At operation] Successive examination of IWB-2410 & Operating plant fatigue assessment	Not required
Way forward	Revise N-919 to add fracture analysis assessment for the rest of life after $U_{Fen}=1$	A new code case is developed as a generic total fatigue life approach.

A critical path forward for any total life approach will require future collaboration between working groups in Sections III and XI to discuss over the overlapping elements, assumptions etc. between the design and operating Codes. One obvious example is the choice the fatigue crack growth curves which to use: ASME XI for flaw evaluation is based on mean curves whereas the common philosophy for design is to include margin by using upper bound curves. If eventually reaching a consensus on a total life approach including environmental effects, it should in principle be applicable to situations where EAF is not in effect.

In summary, a total life approach sums together the life spent in initiating a crack (CUF limits, ASME III) and the remaining life spent in growth of that crack to a critical length (periodic inspection requirements, ASME XI), all whilst retaining the appropriate margins. Philosophically this does not automatically mean removing known conservatism which some recent Code Cases address, but in its rawest form simply accounting for the additional life spent in crack growth. Considering that many components of the primary circuit are thick-walled, this has the potential to significantly alter the safe design cycles, particularly if simultaneously using some of the already existing or planned Code Cases explained in this chapter and proposed by MHI and Rolls-Royce.

Non-mandatory EAF Appendix

A longer term vision in ASME III is to introduce a comprehensive non-mandatory appendix, which provides users overall and most importantly, practical guidance on how to address EAF as part of design. Currently there is a brief description of EAF phenomena in Nonmandatory Appendix W-2700, but actual guidance is not given and the chapter is more of a generic placeholder than an actual reference, even though the subchapter headings “W-2730 Design” and “W-2740 Mitigating Actions” contain a lot of promise.

The non-mandatory EAF appendix should be published at a time, when not too much change is expected over a regular two-year Code interval between editions. At the moment it does not appear likely that it will yet become a part of the 2025 Code, as there are too many outstanding action items pending approval which would significantly undermine the value of adding the expanded non-mandatory appendix.

Additionally, a longer-term strategy is to not have the appendix reference individual Code Cases but instead incorporate them directly into the appendix and retire the Code Cases entirely. This is to avoid the issue of keeping cross-referencing between documents up to date.

Design fatigue curve transition to Section II

WGFS has been in contact with ASME Section II to discuss eventual migration of the current ASME III, Mandatory Appendix I design fatigue curves into Section II, which contains material properties for design use. It is already common practice for the ASME III DFCs to be used by industries outside of nuclear energy, which would justify moving them into a common Code book. This would have implications for many of the activities ongoing in both WGFS and WGEFEM and may set back completion of some items. One example is the fatigue testing requirements White Paper, whose eventual location in the Code relies on understanding where fatigue curves will in future Codes be placed.

3.3.3 VTT plastic strain-based approach

Mission for science based and transferable EAF research

The EPRI & OECD organized conferences on ‘Fatigue of Reactor Components’ in 2000, 2002, 2004 and progress in Japan as explained by Makoto Higuchi of IHI (Higuchi, 2001) attested that EAF of stainless steel in PWR is a particularly hot topic, so far addressed by regression fitting of non-standard experimental data. The need of ASME III and ASTM E606 compliant fatigue data and developing of EAF models founded on mechanisms became obvious. Focusing on stainless steel in PWR water chemistry was justified by scientific arguments and stakeholder’s interest in France and Germany and later confirmed by launch of

the OL3 project as an EPR. It became the first reactor design subjected to regulatory requirement on accounting for EAF already in the design phase.

The Regulatory Guide YVL 3.5 (STUK, 2002) was well in phase with the early guidelines prepared in the USA and Japan, but being a formal Regulatory Guide, the revised YVL 3.5 put the Finnish license holders (TVO & Fortum) and designer of the OL3 (Areva NP) in the frontline of applying environmental fatigue models and results in practise. The Guide stated that “fatigue assessment shall be based on S-N -curves applicable to each material and conditions” and required justification, if design fatigue curves of ASME III were to be used for assessing EAF in primary coolant boundaries. This statement was explainable by the fact that the referred report NUREG/CR-6717 proposed solving the issue by parametrised design curves for environmental fatigue conditions. However, the utilities Fortum and TVO responded in 2004 referring to a VTT report which recommended adoption of F_{en} approach.

Moving from regression fitting of non-standard data to scientific modelling based on calibrated results was considered necessary to improve transferability of EAF to fatigue assessment of NPP components. The General Electric Global Research Center was the only laboratory which performed strain controlled EAF tests in PWR water (Solomon, Amzallag, DeLair, et al., 2005a). Their setup shown in Figure 81 was soon dismantled, but VTT adopted another approach for reliably measuring calibrated strain inside autoclaves and performing EAF tests with constant strain amplitudes and rates (J. Solin, Alhainen, et al., 2011). The primary target was a capability to verify that the fatigue assessments made for OL3 and operating reactors meet the requirements set in the Regulatory Guide YVL 3.5, but ability to control the applied strains and track the material cyclic response (hardening/softening) opened possibilities for advances in F_{en} modelling.

Thorough review and efforts for understanding the evolution, status and expected progress in international Codes and Standards related to EAF guided into paying respect to the original ideas of modelling fatigue for the 1963 ASME III. Coffin and Manson (Coffin, 1953, 1954; Manson, 1953, 1954) introduced a useful correlation between cyclic plastic strain and fatigue endurance and or amplitude, equation (2). It is also logical to assume that reversible elastic strain does not accumulate damage. Furthermore, the difference between LCF data obtained at different temperatures was smaller when plastic strain was used instead of stress or total strain. Would plastic strain fit as a parameter for modelling EAF?

Elastic-plastic stress analysis was not considered the most attractive solution when aiming for a convenient engineering code at the time of using a slide rule for calculation. But it was realized that, when ductile steels are used and limited numbers of fatigue cycles are subjected for the designed pressure equipment, the elastic strains can be approximated constant and be represented by an endurance limit, a minimum amplitude of strain when the plastic strain is zero. This justified the stress analysis concept by Langer (1962), where total strain amplitude ε_a is used as the parameter in laboratory and translated to ‘stress intensity’ S_a for the designer ($S_a = E_T \cdot \varepsilon_a$).

The state-of-the-art F_{en} approaches consider environmental effects in a similar manner: the total strain amplitude ε_a in laboratory and ‘stress intensity’ S_a for design, but without addressing the temperature or temperature dependent modulus E_T as a factor affecting transferability of the lab results. Momentary strain rates during the increasing strain part of a cycle are used as a parameter in detailed calculation of the F_{en} factor without differentiation between elastic and plastic strains. As a result, the F_{en} factors fitted to constant rate lab data are not well transferable to variable rate plant transients, and the effects of temperature without environment “in air” are not properly modelled. Questions arise, would it be better to acknowledge elastic plastic material behaviour in research laboratory and then carefully consider all aspects affecting transferability of the results to assessment of EAF in reactor components.

Range and rate of plastic strain in EAF

Referring to the pioneering research by Coffin and Manson (Coffin, 1953; Manson, 1953) and some EAF research, e.g., (Kanasaki, Umehara, et al., 1997a; Tsutsumi, Dodo, et al., 2001) suggesting that elastic strain may have negligible effects also in LWR coolant, a hypothesis for an improved F_{en} model was

selected: “plasticity is the cause of fatigue damage and plastic strain rate affects experimental fatigue life in environment” (Seppänen et al., 2017).

A model based on plastic strain would probably present a challenge for transferring it to design, but from a mechanistic point of view it is the key to an improved understanding of EAF. Calculation of environmental factors as a function of plastic strain rate $F_{en} = f(\dot{\epsilon}_{pl})$ may also help in improving transferability of the factor to plant transients associated with notable changes in the increase rate of stress intensity. The laboratory experiments conducted to simulate safety injection (SIS) transients in a PWR have demonstrated the bias caused by calculation of F_{en} as function of total strain rate $F_{en} = f(\dot{\epsilon}_{total})$ (Le Duff et al., 2010; Seppänen et al., 2017, 2019). When calculating F_{en} using the ‘Detailed Method’ as explained in chapter 5.2.3, bias originates from two sources:

- incremental rates of total vs. plastic strain, which affect the incremental factor ($F_{en,k}$), and
- increments of total vs. plastic strain ($\Delta\epsilon_k$), affecting the weights of ($F_{en,k}$) factors in averaging.

Differences appear even during a constant amplitude total strain-controlled test. The range of plastic strain within a cycle varies due to cyclic hardening and softening. Within a single cycle, the rate of plastic strain varies from essentially zero at the valley of the hysteresis loop and approaches the total strain rate as a function of strain, Figure 33.

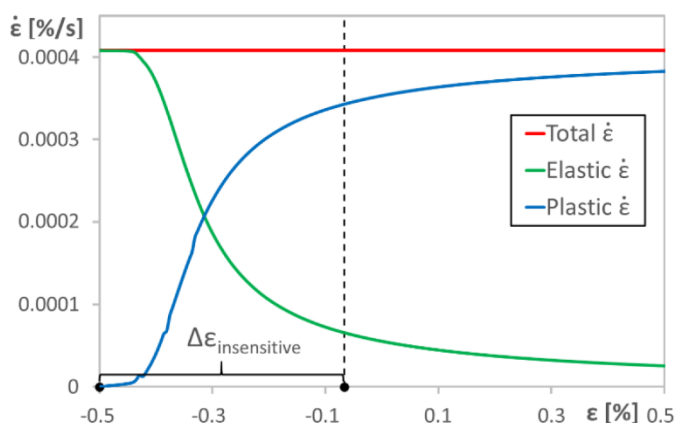


Figure 33. Components of strain rate as function of strain during an increasing half cycle ramp.

A scientific model based on plastic strain rate may be unattractive to apply in design calculations. In practice, a total strain rate model based on mechanistic understanding from $F_{en} = f(\dot{\epsilon}_{pl})$ may be a tempting alternative. Seppänen et al. (2018) developed a model based on the assumption that F_{en} is a function of temperature, water chemistry and plastic strain rate, but using total strain rate as the parameter in calculation. This is realized by introducing an “insensitive strain range” to improve the correlation between the resulting F_{en} factors and plastic components of strain.

This approach is actually comparable to the way strain-life curves were constructed: LCF was explained as function of plastic strain – $N_f = f(\epsilon_{a,pl})$ (Coffin, 1953, 1954; Manson, 1953, 1954), but the design curve itself was based on total strain amplitude, which is simpler to apply in the design by analysis procedure. A constant strain amplitude was inserted to the ϵ - N curve (Langer, 1962). It was named as ‘endurance limit’, but one might call it also as an “insensitive” strain because from mechanism and model point of view it is an add-on strain amplitude which does not contribute to fatigue. In similitude, our proposed F_{en} model splits the increasing strain path into “insensitive” and “ F_{en} effective” strain portions to account for reduced role of the elastic strain. However, the “insensitive strain range” is not proposed as a constant. It depends on the total strain amplitude. The portion of “insensitive strain range” ($\Delta\epsilon_{in}/2\epsilon_a$) is approximated as $\Delta\epsilon_{in}/2\epsilon_a = -0.44 \cdot \epsilon_a + 0.65$, which means that the “ F_{en} effective” part of a cycle increases from 35% to 100% (when $\epsilon_a \leq 1.48\%$) as linear function of the strain amplitude.

Another new element in the proposed EAF model was to redefine and measure the F_{en} factor as product of two components ($F_{en} = F_{en,T} * F_{en,water}$). Separation of the effects of temperature ($F_{en,T}$) and water environment ($F_{en,water}$) plays an increasing role with low strain amplitudes because the assumption of no temperature effect in NUREG/CR-6909 (O. K. Chopra & Shack, 2007) is false for HCF (Coffin, 1978). An overview of the proposed model structure is shown in Figure 34.

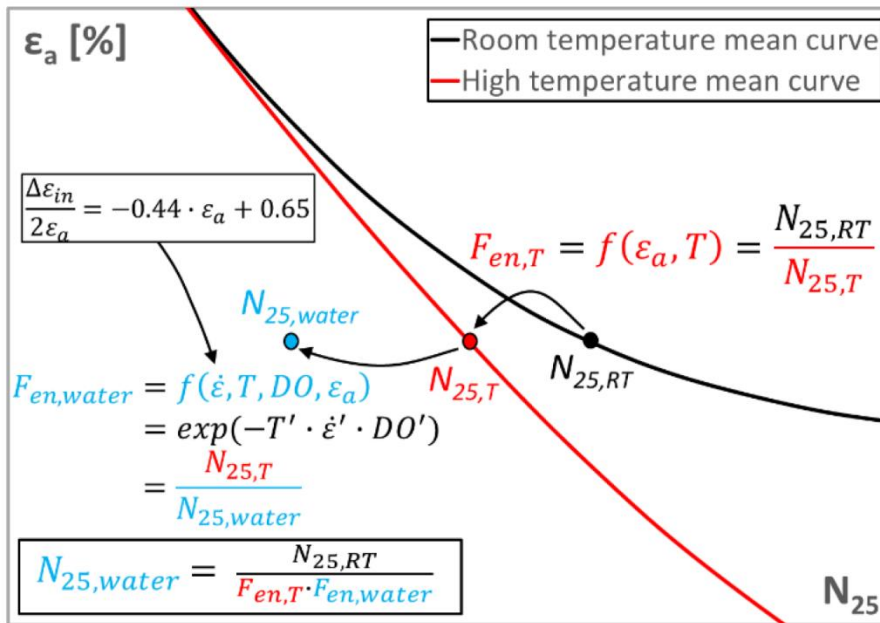


Figure 34. Overview of the proposed EAF model.

Results and comparison of total and plastic strain based EAF models

Seppänen et al. studied the environmental effects in simulated PWR coolant water at 325 °C applying normal constant amplitude cycles and linearized ramps representing typical thermal transients in PWR operation (Figure 35) and for comparison the same with reversed order of slow/faster strain rate to obtain an unrealistic conservative test condition. The results obtained in experimental campaigns using two different types of stainless steels are plotted in Figure 36 (vertical scale) in comparison with the predictions according to the NUREG/CR-6909, Rev. 1 (O. K. Chopra & Stevens, 2018) and a tentative model based on assessment with plastic strains (on horizontal scale).

The results summarized in PVP2019-93279 paper (Seppänen et al., 2019) showed that significant improvement to prediction can be achieved if the effect of plastic strain and strain rate are considered together with material specific reference fatigue lives for relevant temperatures and an “insensitive strain range” concept. The F_{en} model used in this study does not include plastic strain rate as a parameter. It was translated to application using total strains through calculation of an “insensitive strain range” to approximately represent the difference between plastic and total strains. The detrimental effect of PWR environment on fatigue life is relatively well predicted by the VTT model, but most often overestimated using the F_{en} methodology presented in NUREG/CR-6909 Rev.1.

The parameters and results of these experiments will be further explained in the following chapter 4 on ‘Laboratory evidence of environmental effects’ in Finland (see topic 4.5.6).

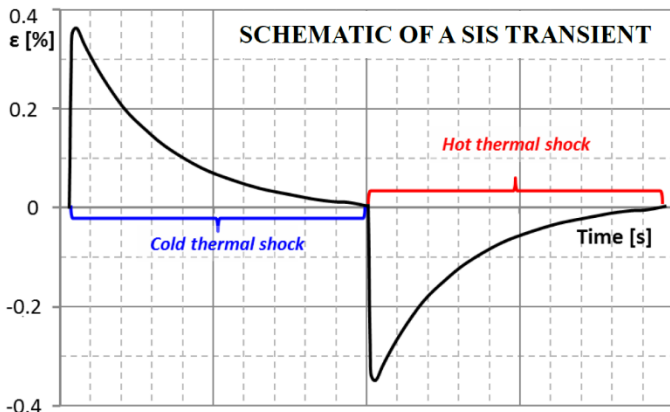


Figure 35. Schematic of SIS transients during cold and hot flow in safety injection system of a PWR.

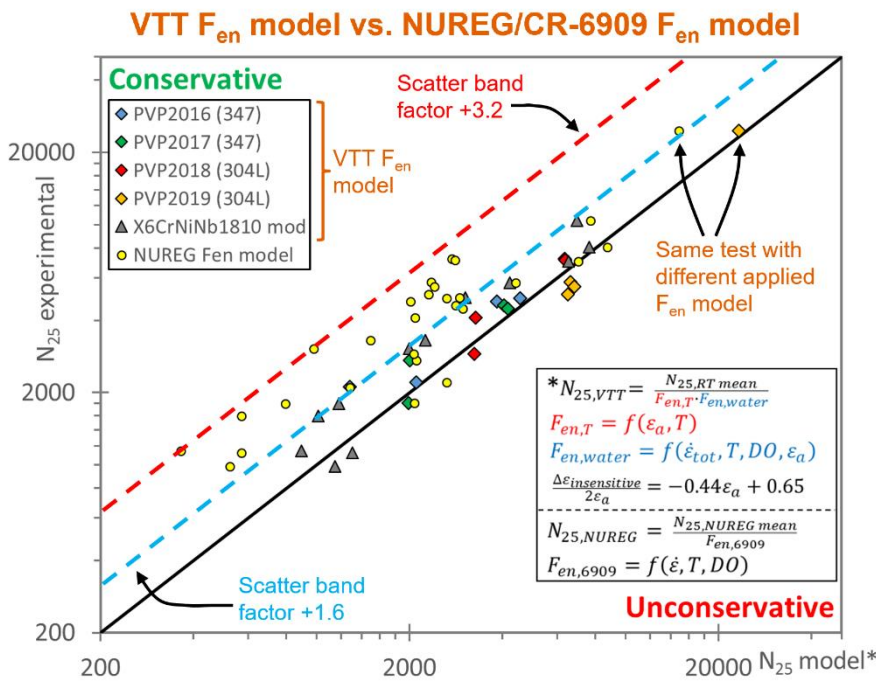


Figure 36. VTT experimental data from EAF research campaigns with stabilized and non-stabilized stainless steel batches and linearized representations of SIS transients in PWR water at 325 °C. (Seppänen et al., 2019)

4. Laboratory evidence of environmental effects

4.1 USA

Soon after publication of ASME III in 1963, the U.S. Atomic Energy Commission (AEC, succeeded by U.S. NRC since 1975) sponsored reactor pipe rupture study was initiated to investigate the reliability of piping systems in water-cooled reactors. Based on an industry survey (Kilsby Jr., 1964), a review of design considerations (Tagart Jr., 1964) as well as other reports, the AEC sponsored program's experimental topic recommendations were heavily focused on fatigue, with effects of the environment also being mentioned (Klepfer, 1965). Nuclear piping design at this time was still based on the B31.1 Code (published by the American Standards Association) and not the B&PV Code.

AEC-sponsored work on environmental effects in fatigue commenced in the latter half of the 1960's with design of an experimental facility to be built in a corrosion test loop at the Dresden I BWR plant. Positioning of the test rig within a primary circuit loop placed the materials in direct contact with reactor coolant. The major difficulty was designing the mechanical loading and instrumentation setup to obtain as quantitative data as possible, a challenge which remains valid still to this day. Experiments in the coolant were performed from September 1970 until decommissioning of the loop in June 1975. The materials studied included A-516 carbon steel, types 304 and 304L stainless steels, as well as Inconel 600 plate materials. The results were published in a series of progress reports and summarized by Hale et al. (1977, 1981).

The importance and innovativeness of the EAF campaign at Dresden I cannot be overstated, even if by today's standards the results' applicability for design purposes can be challenged. As the loading was performed in displacement control, using thin bending specimens, the compatibility of results with ASME III mean and design curves can be questioned. However, the parallel testing of identical bend specimens in an air environment did provide a useful baseline to which assess the extent of environmental effects.

Stainless steel results (types 304 and 304L) in 260 °C air and BWR water are shown in Figure 37 and Figure 38. It is worth noting that among the various materials and experimental conditions employed, the sensitized condition was most adversely affected by the environment. This outcome was expected due to their susceptibility to stress corrosion cracking (SCC) and the lengthy hold times at maximum deflection. The furnace sensitized low-carbon 304L displayed a more obvious strain amplitude dependence on fatigue life than the regular 304 alloy, confirming improved SCC resistance. The reference condition, on which the Code fatigue curves are also based, generally showed no adverse effect of the BWR water. On the contrary, in some conditions the tests in reactor coolant had longer fatigue lives.

Behavior of carbon steel A-516 was quite different, as a clear detrimental environmental effect was observed, and all specimens failed before being classified as runouts. A fatigue strength reduction factor of 7.6 was reported for the carbon steel test series. As this was within the transferability factor of 20 on life inherent in the ASME III design curve and since size effect was the only subfactor not considered in the experiments, the Code design methodology was considered to remain adequately conservative even for ferritic steels. (Hale et al., 1977, 1981) In the 1950's and 1960's the design curve was widely considered to cover a factor of only two for environmental effects (O'Donnell, 2014).

It should be mentioned that the number of cycles accumulated in individual tests was limited to about 35 000, after which a runout was recorded. The limitation reflected the loop operation being dependent on factors such as maintenance outages of the hosting NPP. Although the fatigue cycles were accumulated over 17 separate operating periods totalling 381 calendar days, the test strain rates were much faster than the nominal frequency indicates. A square waveform with a rise time of 10 to 20 s was used due to the structure of the test rig (Hale et al., 1977, 1981). Considering the applied strain amplitudes, the range of average strain rates was therefore approximately 0.025–0.1 %/s. Using today's knowledge of the strain rate effect in EAF, the applied rates are not expected to result in the most severe possible effect.

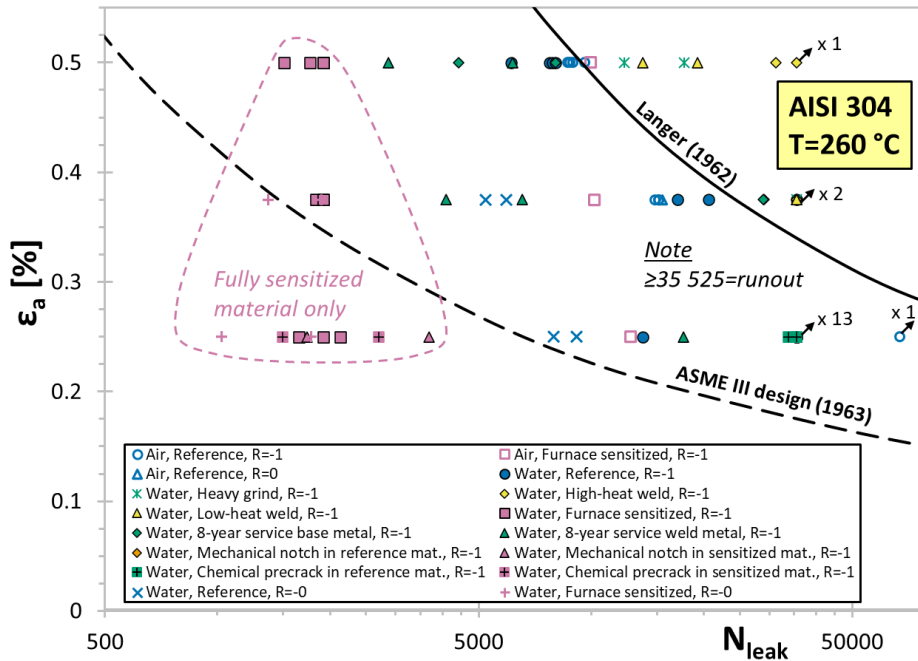


Figure 37. AISI 304 results from Dresden I BWR reactor experimental loop studies. Also shown for comparison are test results from air. Legend refers to environment, material state and load ratio. Data points without accurately known failure cycles are omitted. (Hale et al., 1977)

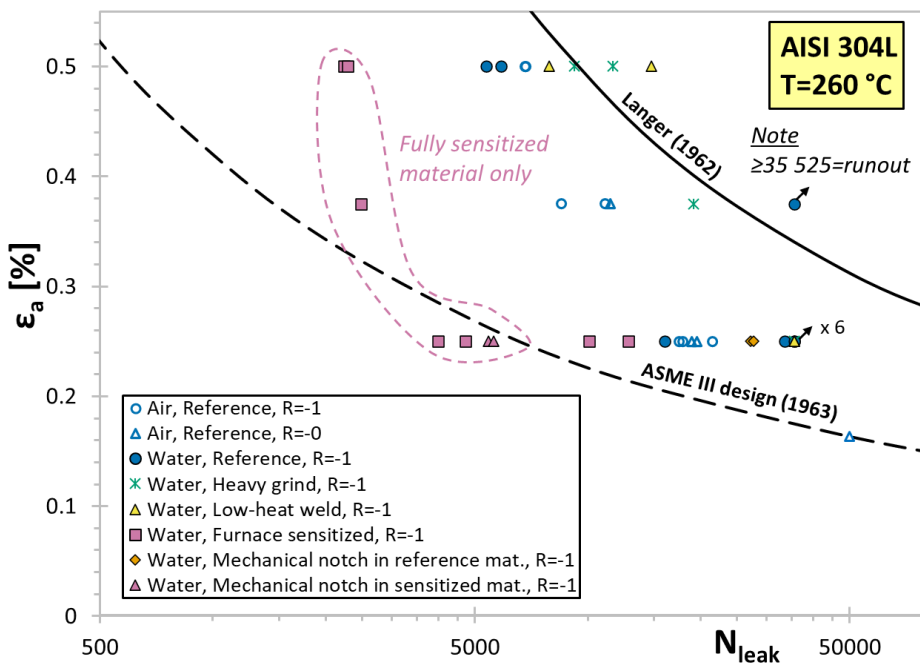


Figure 38. AISI 304L results from Dresden I BWR reactor experimental loop studies. Also shown for comparison are test results from air. Legend refers to environment, material state and load ratio. Data points without accurately known failure cycles are omitted. (Hale et al., 1977)

The EACLWR program started during the following decade from the Dresden I experimental campaign. ANL initially focused on type 316NG stainless steel (Shack & Burke, 1988) and only later performed testing on carbon piping steels A106-Gr.B (Hicks & Shack, 1992) and A333-Gr.6 (O. K. Chopra, Gavenda, et al., 1995a) and low-alloy pressure vessel steels A533-Gr.B (Hicks & Shack, 1992) and A302-Gr.B (O. K. Chopra, Michaud, et al., 1995).

Other stainless steels included in EACLWR EAF tests later on were type 304 (O. K. Chopra & Gavenda, 1997) and CF-8M cast alloy (O. K. Chopra & Smith, 1998). ANL testing started in simulated BWR water and expanded to PWR environments in 1996 (Gavenda & Chopra, 1996). Rather than using hollow tubular specimens, ANL opted to develop the so-called companion specimen method for solid specimens. Results from ANL EAF experiments on stainless steel are shown in Figure 39 for a wide range of nominal strain rates as low as 0.0001 %/s. Several results are to the left of the ASME III design curve at the time. The deionized water chemistry is presumably equivalent to the deoxygenated ($\approx 1\text{--}2$ ppb) PWR water prior to addition of boric acid and lithium hydroxide (O. K. Chopra, 1999). Figure 40 gives a more direct comparison of EAF results with the air data from ANL. Not all these results are referred to as part of the NUREG/CR-6909 final report.

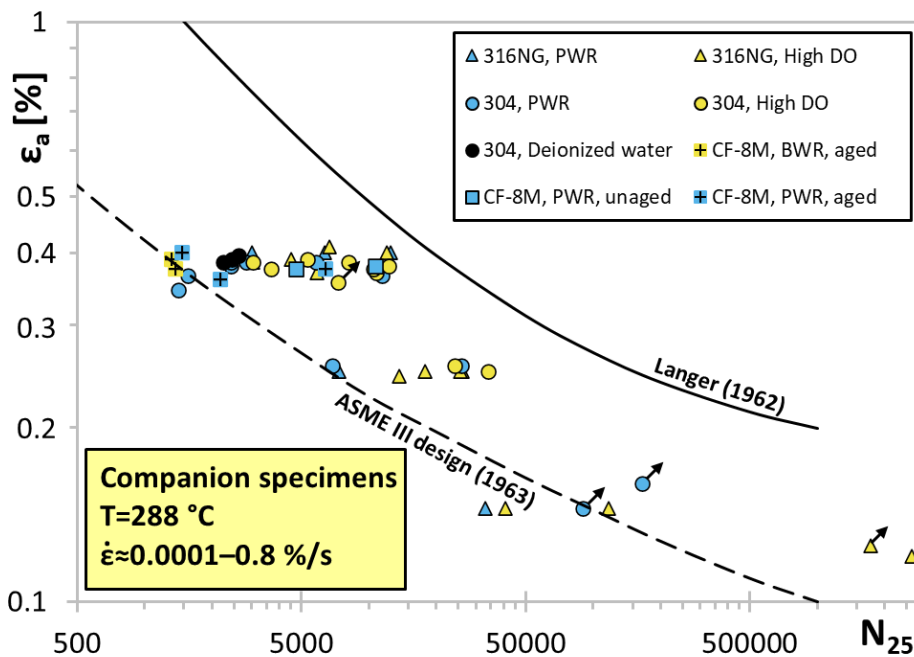


Figure 39. ANL stainless steel EAF results in low and high DO water with companion specimens at 288 °C. (O. K. Chopra & Shack, 2001)

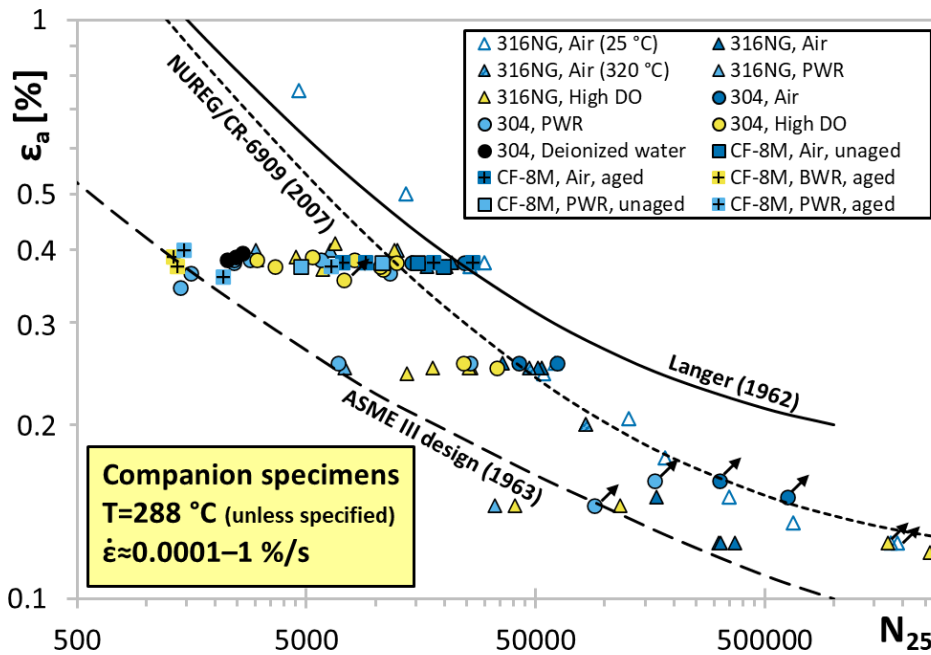


Figure 40. Expansion of Figure 39 EAF data with ANL air data for comparison. (O. K. Chopra & Shack, 2001)

A comparison of ANL's low DO and high DO EAF data with respective F_{en} models from NUREG/CR-6909 Rev.1 are shown in Figure 41 and Figure 42, respectively. In low DO water, the F_{en} model is most non-conservative for a result at a low strain amplitude (0.145 %) and most conservative for unaged CF8M stainless steel as a material group. The limited available data suggests detrimental effects of aging on endurance of cast austenitic stainless steel in low DO water, but this is not accounted for in the F_{en} model. The PWR dissolved oxygen term is applied for cast austenitic stainless steels also in high DO water. This results to higher F_{en} factors, which more closely predict the experimental results for aged CF8M in high DO water (Figure 42). However, there is no ANL data to indicate if aging has an influence in high DO water, i.e., whether the low oxygen term is applicable also for unaged CF8M stainless. Once again, the low strain amplitude data in high DO water is non-conservatively predicted by the F_{en} model, which does not include a strain amplitude correction term.

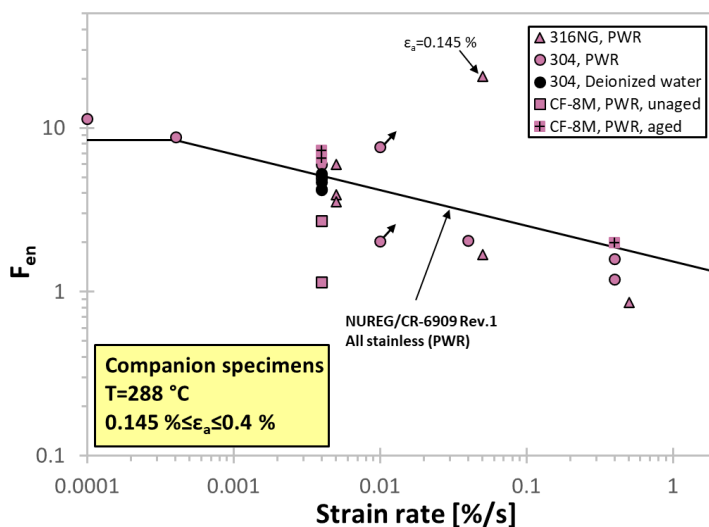


Figure 41. ANL low DO data F_{en} as a function of strain rate. (O. K. Chopra & Shack, 2001)

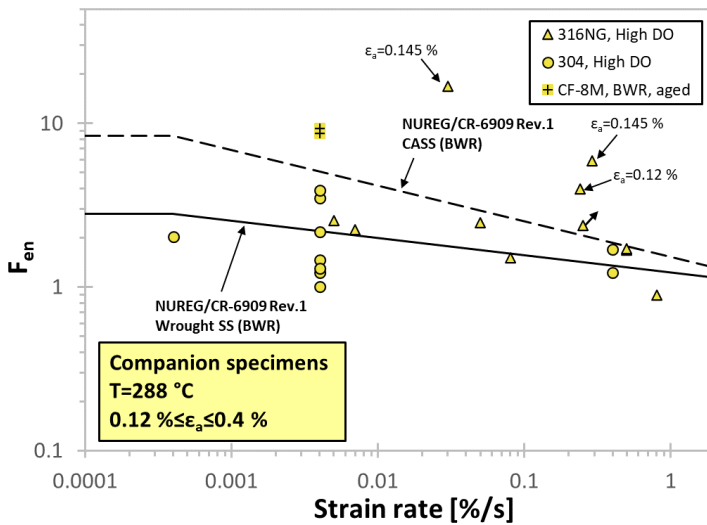


Figure 42. ANL high DO data F_{en} as a function of strain rate. (O. K. Chopra & Shack, 2001)

Effects of surface roughness were studied with a small test matrix (O. K. Chopra & Shack, 2003b), with results shown in Figure 43. The manually performed roughening in a lathe resulted in average surface roughness $R_a=1.2 \mu\text{m}$ and root-mean-square roughness $R_q=1.6 \mu\text{m}$. The measured roughness is well below e.g. the allowable surface roughness $R_a \leq 6.3 \mu\text{m}$ (cold-finished) or $R_a \leq 12.5 \mu\text{m}$ (hot-finished) in RCC-M (article M3304 for pipe and tube products, for example).

The factor of a rough surface on life in air and PWR water for 304 and 316NG stainless steels is fairly constant in ANL data, about three. In BWR water the results are not indicative of a surface finish effect. Drawing conclusions from this available data set should be done cautiously. The results are all at a constant strain amplitude and tensile strain rate and the test matrix does not include repeat tests. Considering this, conclusions in NUREG/CR-6909 have been made on a very limited body of evidence. Surface roughness effects are expected to be more severe at the tested strain amplitude level 0.25 % than say, 0.6 %. A constant surface roughness factor is thus not mechanistically speaking anticipated to exist but was concluded by ANL.

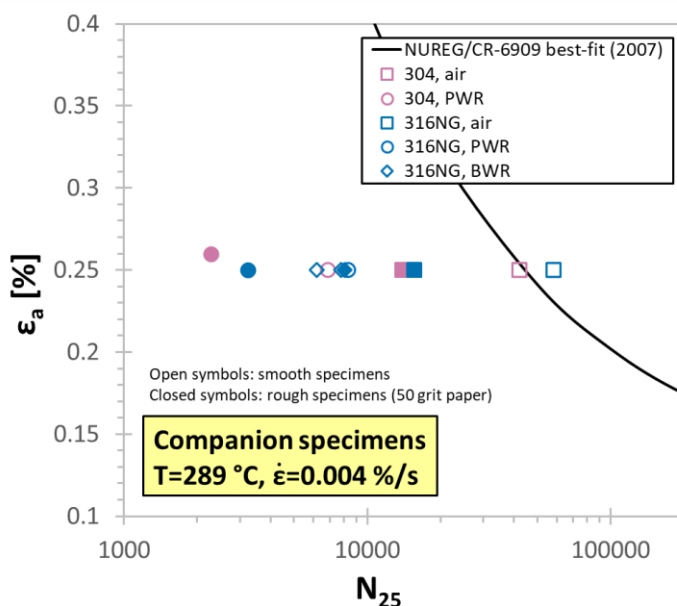


Figure 43. Surface roughness effects in air and water for 304 and 316NG. (O. K. Chopra & Shack, 2003b)

Effects of heat treatment were studied with a small test matrix (O. Chopra et al., 2005), with results shown in Figure 44. More precisely, 304 stainless steel was sensitized to a non-desirable condition. Effects in air appear negligible. In high DO BWR water sensitization adds to EAF susceptibility, which also manifested as partially intergranular fracture morphology. In low DO PWR water, there was little effect of a sensitization heat treatment following annealing. As with the surface roughness studies at ANL, the matrix is limited to practically a single strain amplitude and strain rate, but conclusions were extrapolated to apply as such across the range of strain rates and amplitudes in the F_{en} model.

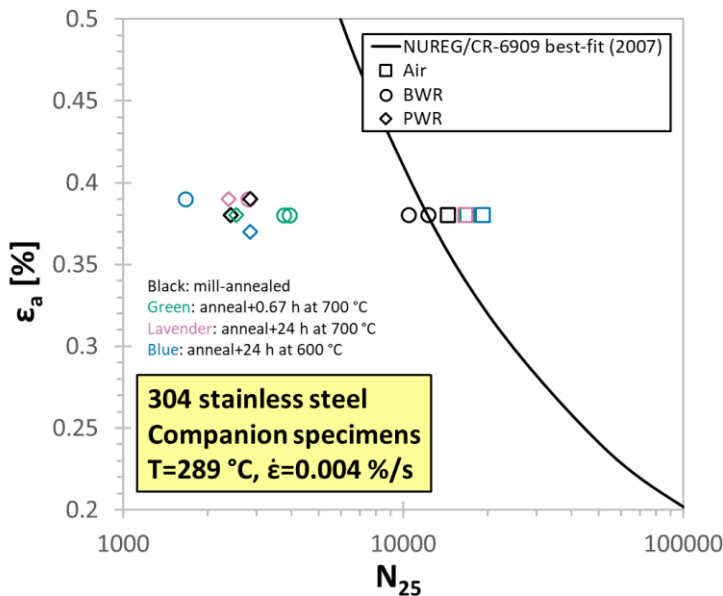


Figure 44. Effect of heat treatment on fatigue life in air, BWR and PWR environment. (O. Chopra et al., 2005)

All of the ANL EAF data was performed in indirect strain control, using the companion specimen method. The companion specimen method involves running reference fatigue tests in the air environment, where gauge length strain and displacement (from specimen shoulders or beyond) are simultaneously measured. Subsequently, the EAF testing inside an autoclave is performed by using the calibrated displacement history obtained from the companion specimen. Gauge length strain is not measured in this phase, primary due to concerns related to signal stability and potential early crack initiation at knife-edge attachment points, for example.

The specimen design, with key dimensions added in metric units, is shown in Figure 45. The long and slender design is needed to accommodate the gauge length inside a 12 mL autoclave, whilst specimen ends are gripped outside of the autoclave in hydraulic collet grips (O. K. Chopra et al., 1993). ANL justified this arrangement by referring to the difficulty of specimen alignment using threaded specimens. The large length/diameter ratio exposes the specimen to a higher risk of buckling. Strain gauge measurements were done to demonstrate relative bending (bending strain to axial strain ratio) to be less than or equal to 2.2 % for the 0.75 inch gauge length design at a strain range of 1.644 %. Another design with a 0.9375 inch gauge length was not selected based on a 6.1 % relative bending (Shack & Burke, 1988). The details of the calibration do not reveal the measurement scheme of the strain gauges, nor do they investigate the effects outside of the first few cycles of a test, where cyclic hardening takes place. The check was supposedly performed at room temperature in air, which leaves out the potential influence of the autoclave during EAF experiments.

The ANL test equipment for EAF testing was not tailored for purpose, but transformed from its original purpose of stress corrosion cracking studies using constant extension rate tensile testing, which was an original focus area in the EACLWR program (Shack et al., 1986; Shack & Burke, 1988). The experimental setup is shown in Figure 46.

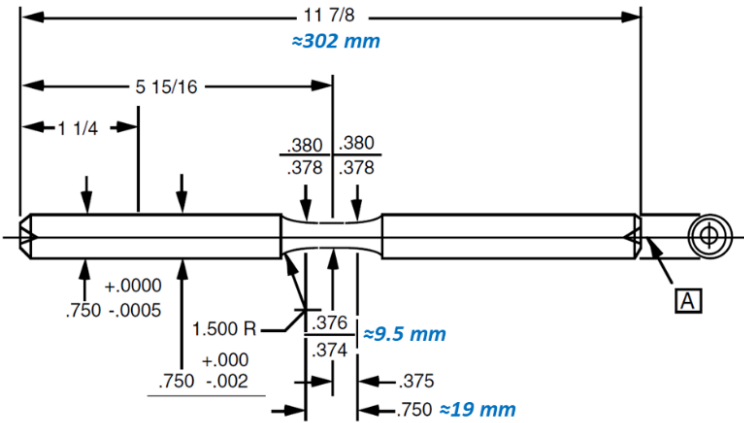


Figure 45. ANL companion specimen design. Modified from Chopra (1999)

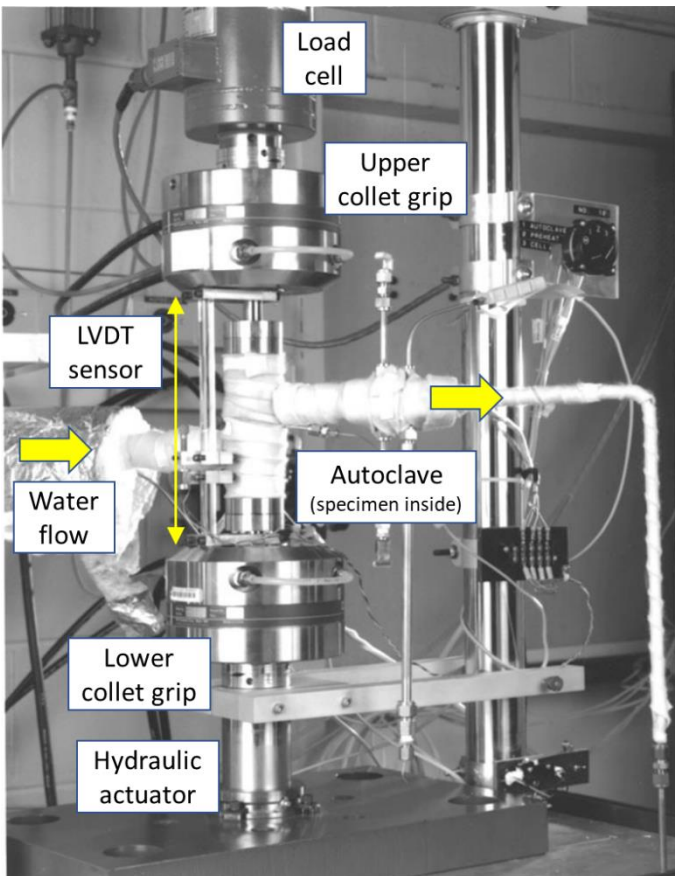


Figure 46. ANL autoclave system for EAF testing. Modified from Chopra et al. (2005)

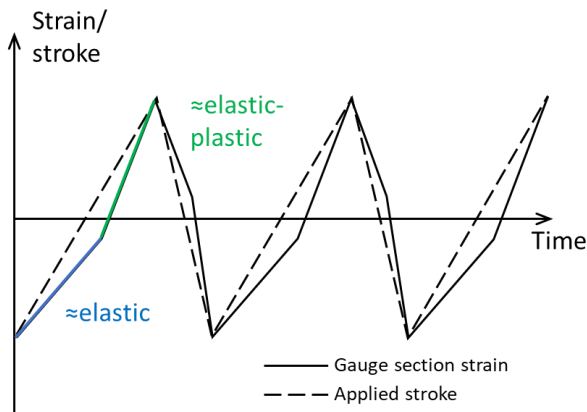


Figure 47. Applied stroke and measured strain in ANL companion tests. Modified from Chopra, Gavenda et al. (1995b)

The first companion specimen tests were performed on carbon and low-alloy steels. An accuracy of both $\pm 5\%$ (O. K. Chopra, Gavenda, et al., 1995b) and $\pm 2\%$ (O. K. Chopra & Shack, 1995) has been reported for the stroke control of these steel types. The stroke for practical purposes means displacement over a distance which covers most of the 302 mm specimen length. The ANL laboratory reports do not quote a particular accuracy for stainless steel specimens. The stroke is controlled with a sawtooth waveform (constant rate), which ANL researchers note does not result in a constant strain rate as Figure 47 shows. This is because not all of the displacement from the stroke goes to the specimen gauge length. Only when the elastic limit is exceeded and strain begins to localize does the change in stroke approach the change in gauge length strain. In elastic loading, the strain rate at the gauge length is below the target level and vice versa for elastic-plastic loading (O. K. Chopra, Gavenda, et al., 1995b).

From a resourcing perspective, a technical limitation of the companion specimen method is the time that it takes, in principle, to duplicate at first each EAF experiment in air. Depending on the test loading parameters, this can easily take months. In the early history of the EACLWR program, stainless steel companion tests in air were done at a frequency of 0.33 or 0.5 Hz and EAF experiments as low as 0.005 Hz, indicating that exact calibration data was missing. Later ANL reports reveal that only a small fraction of the EAF tests have had exact companion specimen tests done to pre-check the stroke calibration. This information is shown in Table 13 and Table 14 for 316NG and 304 stainless steels.

If measured throughout the test, the complete stroke and strain history should theoretically be repeatable when switching from strain to stroke control in a repeat test. However, most EAF tests at ANL were done by averaging the applied stroke over ranges (cycles 10^0 – 10^3 , 10^3 – 10^4 etc.) rather than on a cycle-by-cycle basis. (Shack & Burke, 1990) This makes the EAF tests both variable (strain) amplitude and variable strain rate, as the block averages do not reflect the cyclic hardening and softening tendencies. In cyclic softening for example, strain localization accelerates, driving crack growth and leading to a smaller N_{25} value than under strain control. In some tests, namely on cast CF8M stainless steel, compressive ratcheting was noticed at the specimen shoulders in the air companion test and the stroke-controlled EAF experiment was conducted with a mean tensile strain to prevent this (O. K. Chopra et al., 1998). This example violates the principles of companion specimen testing by deliberately modifying test parameters. The consequences on strain (rate and amplitude) and thus fatigue life cannot be predicted in such circumstances.

Table 13. ANL companion specimen strain amplitude and strain rate data for 316NG alloy. (O. K. Chopra & Shack, 2001, 2003b)

In water

ϵ_a [%]	0.41	0.4	0.39	0.385	0.37	0.25	0.245	0.145	0.125	0.12
$\dot{\epsilon}$ [%/s]	0.08	0.8	0.0005	0.005 ²	0.007 ²	0.5 ¹	0.005 ²	0.29 ²	0.25 ²	0.24 ²
		0.5				0.05		0.05		
		0.05				0.005		0.03		
		0.005				0.004 ¹				

In air (companion specimens)

ϵ_a [%]	0.38	0.375	0.255	0.25	0.2	0.15	0.125
$\dot{\epsilon}$ [%/s]	0.5	0.005	0.005	0.5	0.27	0.2	0.17
				0.004			0.16

¹Exact strain amplitude and strain rate companion specimen test exists

²Companion specimen test within 0.01 % amplitude and factor of two on strain rate exists

Table 14. ANL companion specimen strain amplitude and strain rate data for 304 alloy. (O. K. Chopra & Shack, 2001)

In water

ϵ_a [%]	0.395	0.39	0.385	0.38	0.375	0.37	0.365	0.355	0.345	0.255	0.25	0.16	0.145
$\dot{\epsilon}$ [%/s]	0.004	0.004 ²	0.004 ²	0.004 ¹	0.004 ²	0.4 ²	0.4	0.0004	0.0004	0.4 ¹	0.004 ²	0.01	0.01
			0.04 ²				0.0004			0.004 ¹			

In air (companion specimens)

ϵ_a [%]	0.38	0.255	0.16	0.15
$\dot{\epsilon}$ [%/s]	0.4	0.4	0.04	0.04
	0.004	0.004		

¹Exact strain amplitude and strain rate companion specimen test exists

²Companion specimen test within 0.01 % amplitude and factor of two on strain rate exists

Another uncertainty in the ANL experimental setup is the effect of thermal gradients on displacement in the axial direction. This is because the only a part of the specimen is contained within the autoclave at test temperature, and the gripped ends are in water-cooled collet grips, close to the LVDT measuring location. Unfortunately, there is no technical information on such measurements on the test setup for EACLWR program data. However, some indicative information can be deduced from a modified test setup used for more recent experiments at ANL, as described by Mohanty et al. (2015, 2016) and schematically shown in Figure 48. In this test setup, the 4" long specimen is threaded onto pullrods on either end. In the companion test in air, induction is used to heat the specimen. In water, the specimen is at the temperature of water circulating inside the autoclave.

Temperature measurements on the specimen and pull rods were done in both the air and PWR water tests targeting 300 °C. These are shown in Figure 49, where the specimen location is also indicated. A rough estimate for the total thermal expansion of both pull rods, based on the measurement data and assuming a linear thermal expansion coefficient of $11 \cdot 10^{-6} \text{ }^\circ\text{C}^{-1}$ would make approximately 0.5 mm and 0.6 mm in air and EAF tests, respectively. The 0.1 mm difference is of the order of the target stroke level (0.1313 mm) for a test with strain amplitude 0.5 %.

As stated, there are no details on temperature measurement in the EACLWR test setup, but considering the combined effect of a shorter thermal gradient distance (\approx specimen length, Figure 45) with the higher thermal expansion coefficient of stainless steel ($17 \cdot 10^{-6} \text{ }^\circ\text{C}^{-1}$) the net result may be fairly similar as in the setup shown in Figure 48. In light of this, the reported uncertainty of $\pm 2\text{--}5\%$ in stroke control may be underestimated.

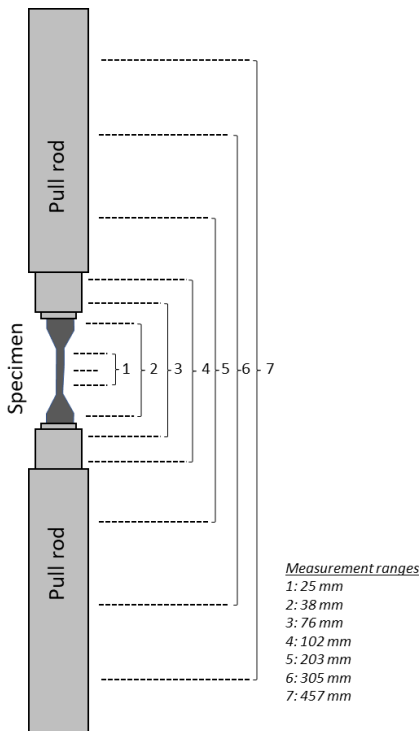


Figure 48. Schematic of recent ANL companion air test setup with temperature measurement locations. Modified from Mohanty et al. (2015)

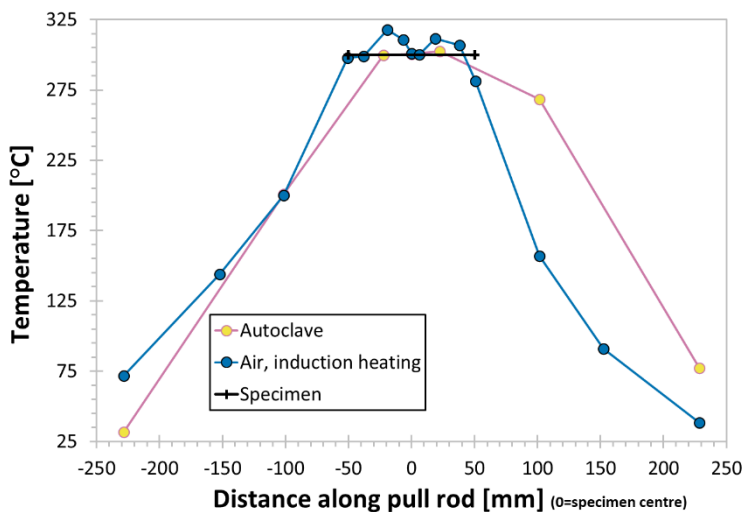


Figure 49. Measured temperature gradient in pull rod of ANL experimental setup for companion tests in air and EAF tests in water. Data from Mohanty et al. (2015)

4.2 Japan

In Japan, EAF research began in 1980 but initially focusing on smooth solid axial specimens of ferritic carbon steel A333-Gr6 for piping (Higuchi & Sakamoto, 1985) and low-alloy steel A508-C13 for RPV nozzles (Iida et al., 1986) with testing done inside an autoclave. A508-C13 and A533B-C11 results were also published by Nagata et al. (1989, 1991) and Sato et al. (1989). As in U.S. studies, a considerable decrease in fatigue life was observed in simulated BWR water. Solid specimen testing of types 304 and 316NG stainless steels was also performed by multiple laboratories (Hitachi, Ishikawajima Heavy Industries and Toshiba) (JAERI, 1992). A summary of 1980's solid specimen data at 288 °C is shown in

Figure 50. Most of the testing was done in high DO BWR water. Note that all results are bound by the ASME III design curve at the time.

In the mid-1980's, the hollow tubular specimens were adopted by Mitsubishi Heavy Industries (MHI) in Japan to overcome difficulties of strain control within an autoclave (Endo et al., 1985; Fujiwara et al., 1986). The tubular specimen design is also advantageous for application of non-isothermal temperature waveforms (Kanasaki et al., 1995; Tsutsumi et al., 2002) and for flow rate studies (Hirano et al., 2002). Hollow specimen research started with type 304 stainless steel. The results suggested that in the sensitized condition (in both high and low DO water) and in the solution annealed condition (high DO water) environmental effects could fully use up and even exceed the design curve margin on fatigue life. (Endo et al., 1985; Fujiwara et al., 1986) These results are shown in Figure 51.

Application of direct strain control is likely a key reason why more severe environmental effects could be observed by Endo et al. (1985) but not by Hale et al. (1977). Other reasons include push-pull loading as opposed to bending, a higher temperature (300 °C vs. 260 °C) and slower applied tensile strain rates which were used in the Japanese study.

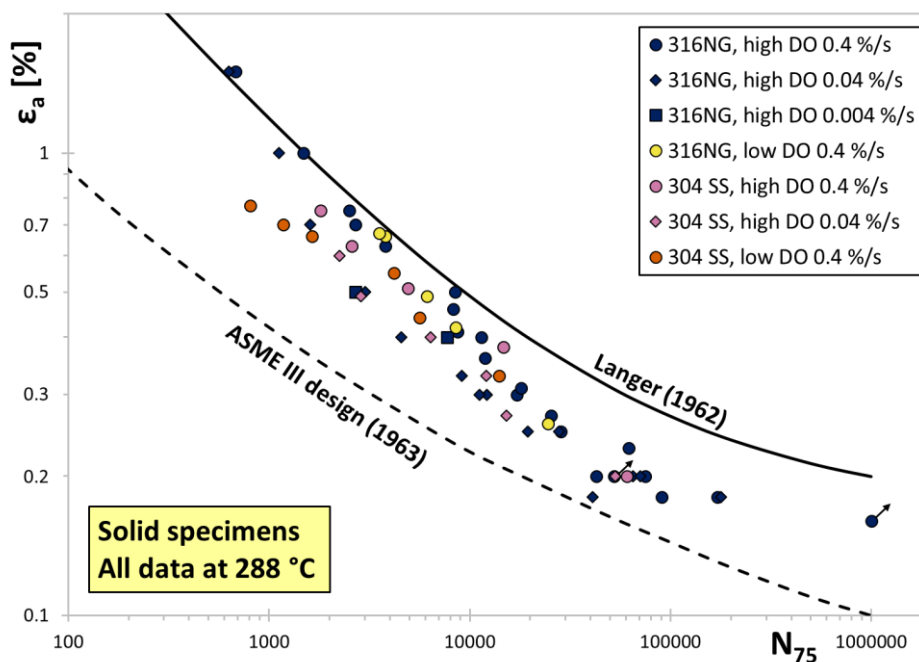


Figure 50. Japanese stainless steel EAF results in low and high DO water with solid specimens at 288 °C. (JAERI, 1992)

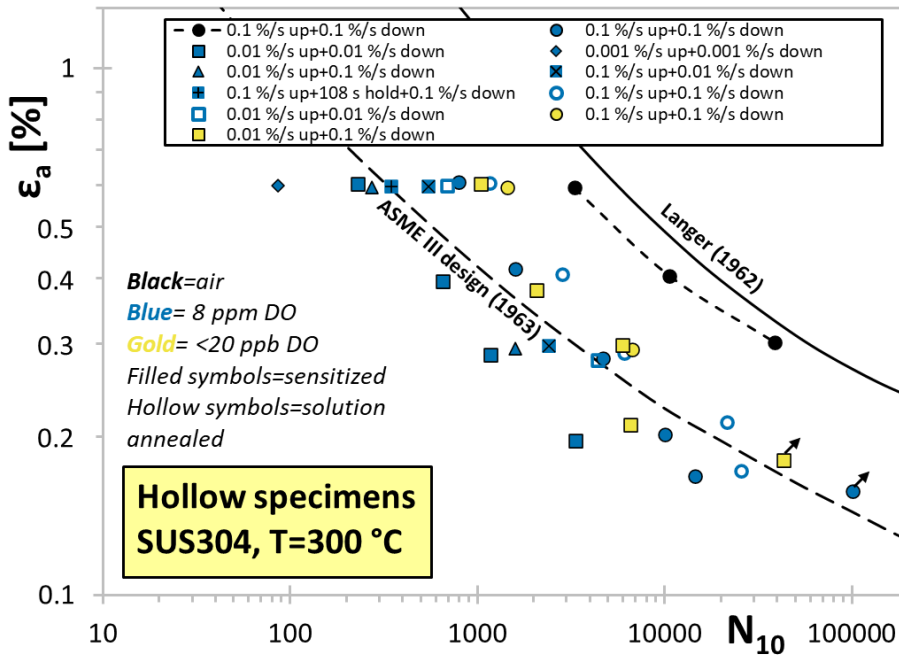


Figure 51. Hollow specimen stainless steel EAF results for various strain rates in high and low DO water. Data extracted from Endo et al. (1985) and Fujiwara et al. (1986).

Globally, most experimental EAF research conducted in the 1990's was done in Japan, using the hollow tubular specimen technique for all materials and solid specimens mostly for non-stainless steels. A wide range of materials was studied in addition to those already mentioned in the previous paragraphs. These included A516 carbon steel, A508 low-alloy steel, 304L and 316 wrought stainless steels and weld metals of 308 and 316 type stainless steels. Ni-based alloys were also studied for the first time, including Alloy 600 and Alloy 690 base metals as well as Alloy 132, 152 and 182 welds. Stainless steel data at 325 °C is shown in Figure 52 with multiple data points to the left of the ASME III design curve at the time. Fatigue life is defined by N_{leak} , the number of cycles to cause through-wall leakage. The material SCS14A is a cast alloy equivalent to CF-8M. Note that contrary to most of the data from 1980's, the 1990's stainless steel data is mainly in low DO water. A later refocus on BWR environment in Japan around the year 2000 resulted in the proposed differentiation of BWR and PWR environment environmental effects for stainless steel. Data numbers from the EFT project between approximately 1994 and 2002 are shown in Table 15. By the end of the project in March 2007, the numbers had improved considerably. For stainless steel 216 BWR and 380 PWR results are reported though it is not clear if this number includes data obtained from other projects outside of EFT as well (Higuchi, Sakaguchi, Nomura, et al., 2007).

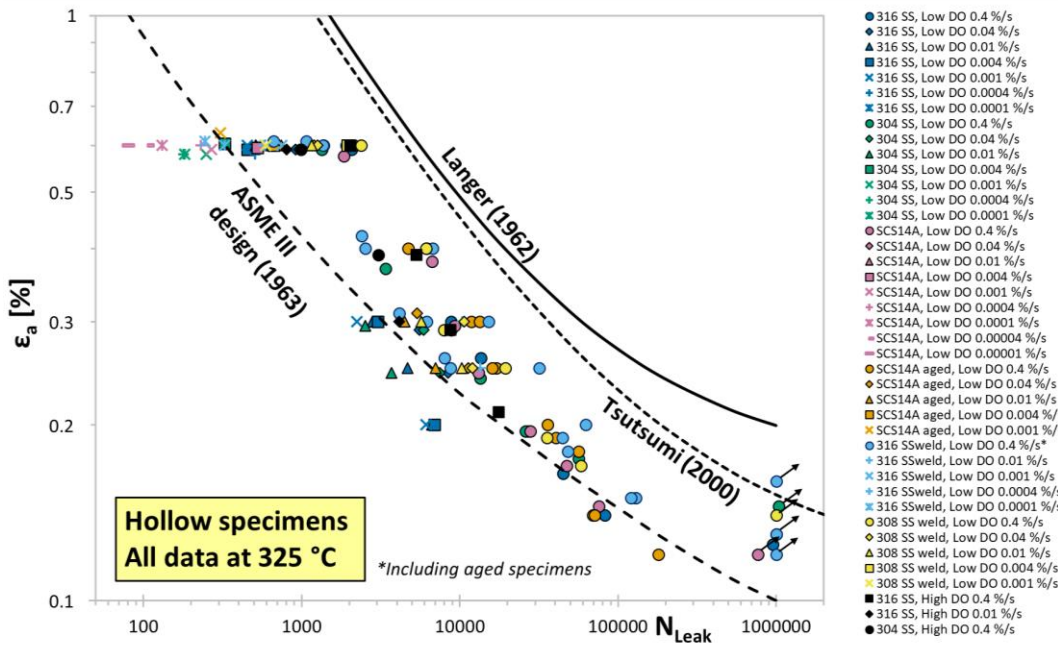


Figure 52. Japanese stainless steel EAF results in low and high DO water with hollow specimens at 325 °C (Kanasaki, Umehara, et al., 1997b; Tsutsumi et al., 2000; Tsutsumi, Kanasaki, et al., 2001).

Table 15. EFT project test numbers between approximately 1994 and 2002. (Sayano et al., 2002)

Environment	Material	Data points	Total
BWR	Carbon steel	236	275
	Stainless steel	30	
	Low-alloy steel	9	
PWR	Carbon steel	21	113
	Stainless steel	92	
Air	Carbon steel	71	112
	Stainless steel	41	
Total			500

Environmental effects in single material heats by alloy type in simulated PWR water are shown in Figure 53. The data is from the EFT project (Sakaguchi, Nomura, Suzuki, & Kanasaki, 2006). The influence of strain rate at 325 °C is clearly visible, though there is a lack of low strain amplitude data at very slow strain rate due to excessively long test durations. At an equivalent strain rate between air and PWR water (0.4 %/s) the design curve margins just barely bound all PWR data.

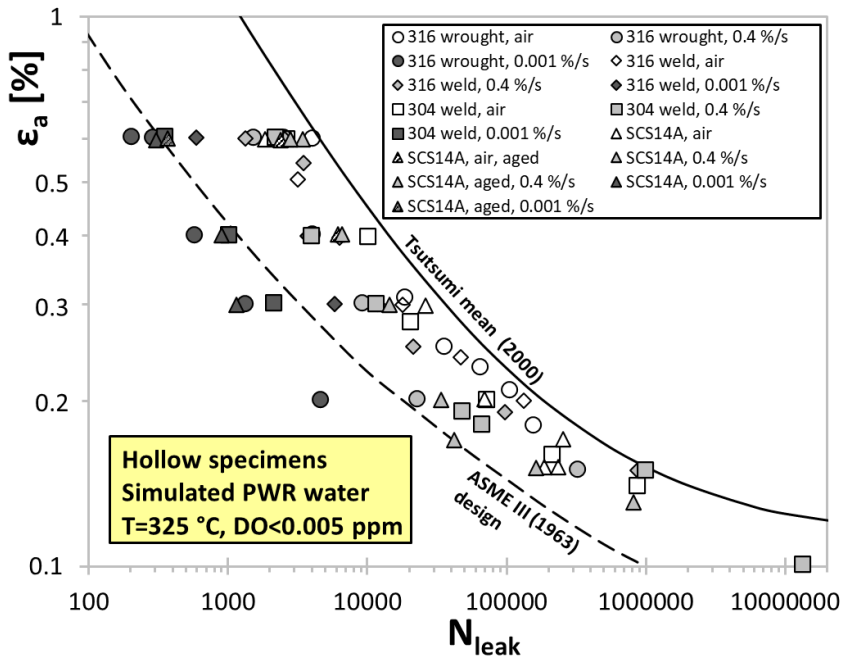


Figure 53. EFT data on PWR water effects on wrought, welded and cast austenitic stainless steels. (Sakaguchi, Nomura, Suzuki, Tsutsumi, et al., 2006)

Effects of temperature in PWR water on a single heat of type 316 stainless steel are shown in Figure 54. Again, this data is from the EFT project (Sakaguchi, Nomura, Suzuki, & Kanasaki, 2006). At 100 °C the environmental effect is already significantly reduced and strain rate seems to have a negligible influence. Temperature effects on cast SCS14A alloy are shown in Figure 55. Similarly to type 316, there is a consistency at $\epsilon_a \geq 0.3$ % but below that the datasets are not as complete and include more scatter. More broadly, the relation between temperature and F_{en} in BWR and PWR environments is shown in Figure 56 and Figure 57, respectively, as collected by Higuchi, Sakaguchi, Nomura et al. (2007). Note that the BWR data is on solid specimens and PWR data on hollow tubular specimens. In both Figures the 2009 EFEM model assumes extrapolation to $F_{en}=1.0$ at $T=0$ °C. The rationale behind this choice has not been explained in the open literature. In BWR water the experimental data does not seem to support this modelling choice, but it is conservative. In PWR water the extrapolation is in better agreement with the data despite the scatter.

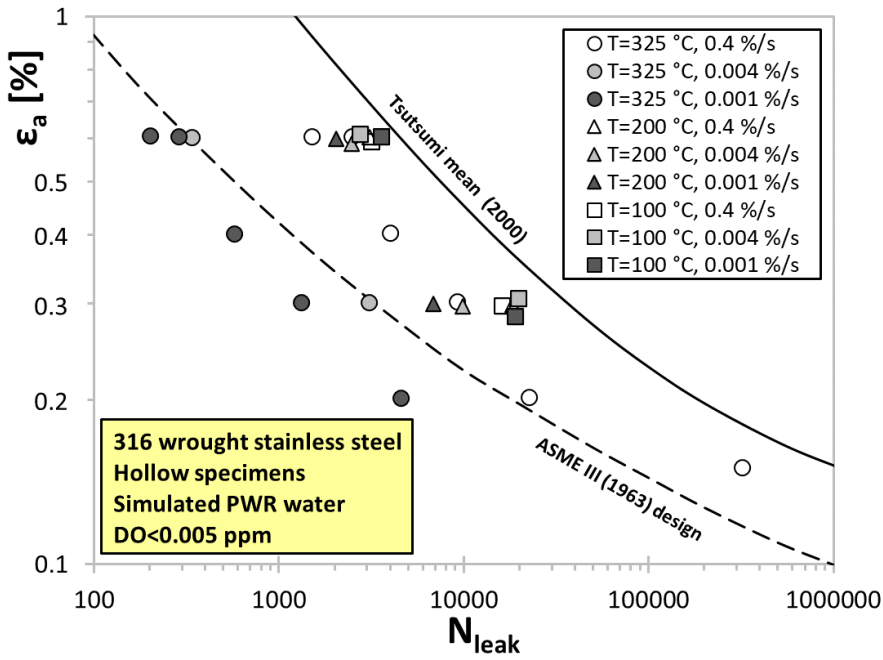


Figure 54. Temperature effect on type 316 stainless steel in PWR water. (Sakaguchi, Nomura, Suzuki, Tsutsumi, et al., 2006)

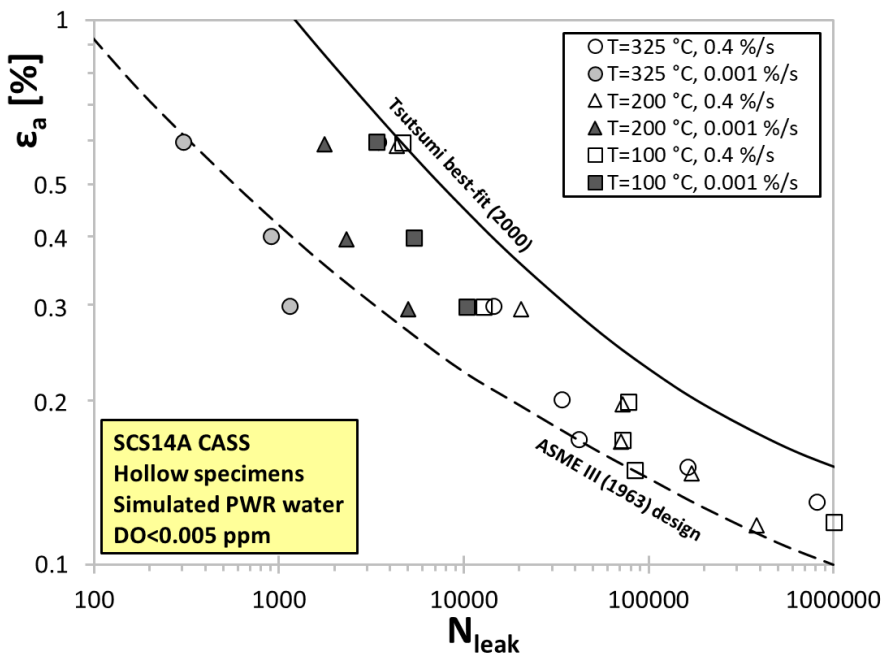


Figure 55. Temperature effect on SCS14A CASS in PWR water. (Sakaguchi, Nomura, Suzuki, Tsutsumi, et al., 2006)

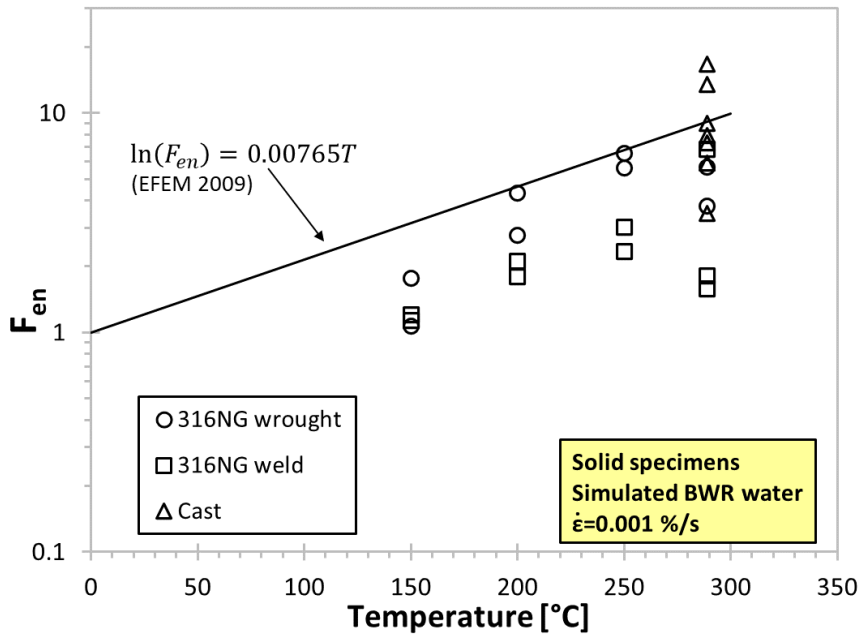


Figure 56. Relation between temperature and F_{en} in BWR water. (Higuchi, Sakaguchi, Nomura, et al., 2007)

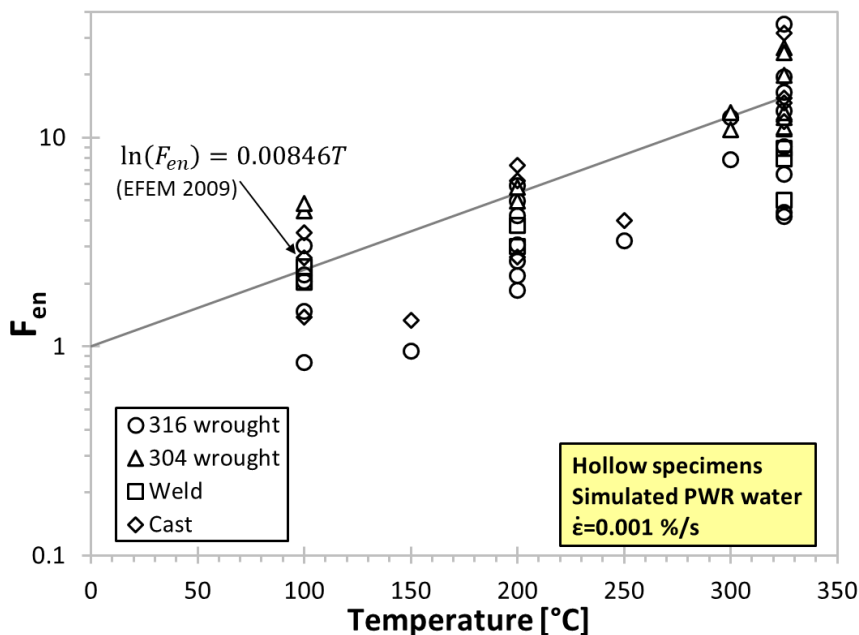


Figure 57. Relation between temperature and F_{en} in PWR water. (Higuchi, Sakaguchi, Nomura, et al., 2007)

The relation between strain rate and F_{en} in BWR and PWR environments is shown in Figure 58 and Figure 59, respectively, as collected by Higuchi, Sakaguchi, Nomura et al. (2007). The 2006 and 2009 EFEM models in the JSME S NF1 Code are shown in both Figures for reference. The models represent regression to all data, but notable differences exist between the materials. They can be attributed to differences in the best-fit curves in air, the actual environmental effects, or a combination of the two. For some materials, e.g. CASS in BWR water, the F_{en} models seem consistently unconservative.

No definite effect of sensitization was on the BWR F_{en} model was assumed based on a study on type 304 stainless steel (Higuchi, Sakaguchi, Nomura, et al., 2007). The strain amplitude was not reported for this study. Data is shown in Figure 60. The sensitization heat treatment consisted of 100 minutes at 750 °C, followed by furnace cooling and a further 1700 hours at 400 °C and air cooling. Additional data would have been useful to confirm the assumption, as the 0.001 %/s strain rate data is non-conservative for the sensitized data. This could indicate that a stress-corrosion cracking mechanism is acting in parallel with EAF.

Susceptibility of a type 316NG alloy to a combined SCC+EAF damage mechanism through very slow strain rate testing was studied as a knowledge gap after the EFT project was completed (Higuchi et al., 2009). The results are shown in Figure 61. Intergranular fracture appearance was taken as a sign of SCC being active. The same kind of intergranular fracture was observed in some of the testing done at ANL. The 2009 EFEM F_{en} equation was not specifically fit to the very slow strain rate data but seems to capture reasonably well the combined effect with a potential SCC mechanism. To better understand overlapping mechanisms, further data at strain amplitudes lower than 0.6 % would be valuable but take considerable testing time to generate.

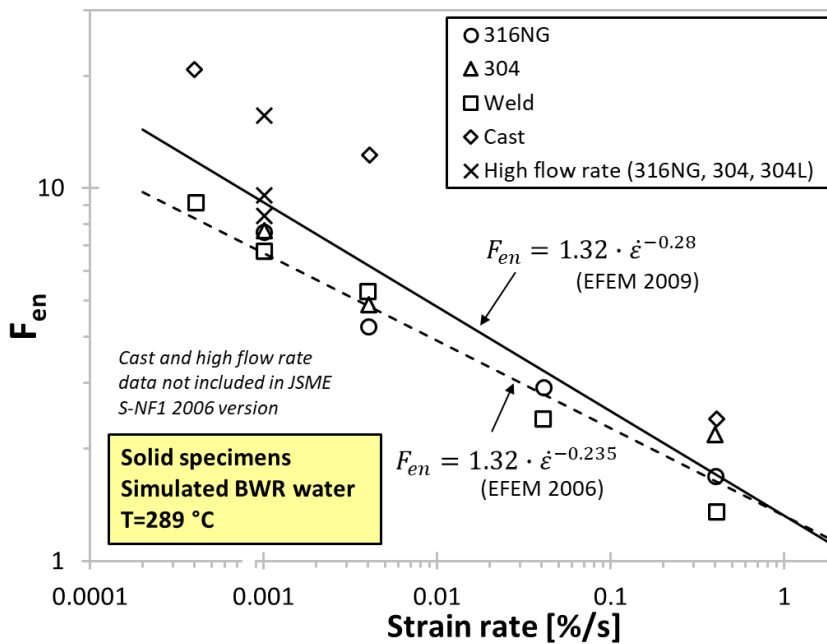


Figure 58. Relation between strain rate and F_{en} in BWR water. (Higuchi, Sakaguchi, Nomura, et al., 2007)

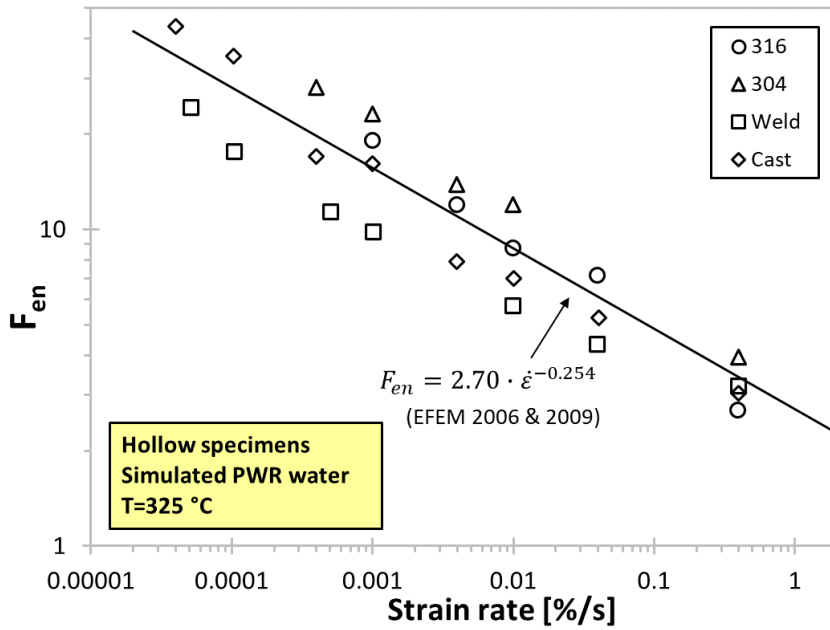


Figure 59. Relation between strain rate and F_{en} in PWR water. (Higuchi, Sakaguchi, Nomura, et al., 2007)

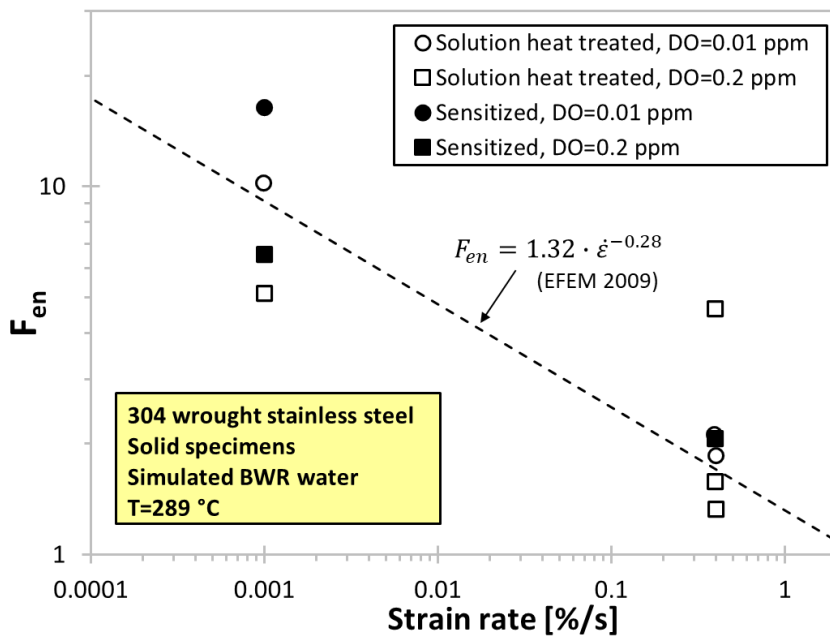


Figure 60. Influence of sensitization in type 304 stainless steel on F_{en} in BWR water. (Higuchi, Sakaguchi, Nomura, et al., 2007)

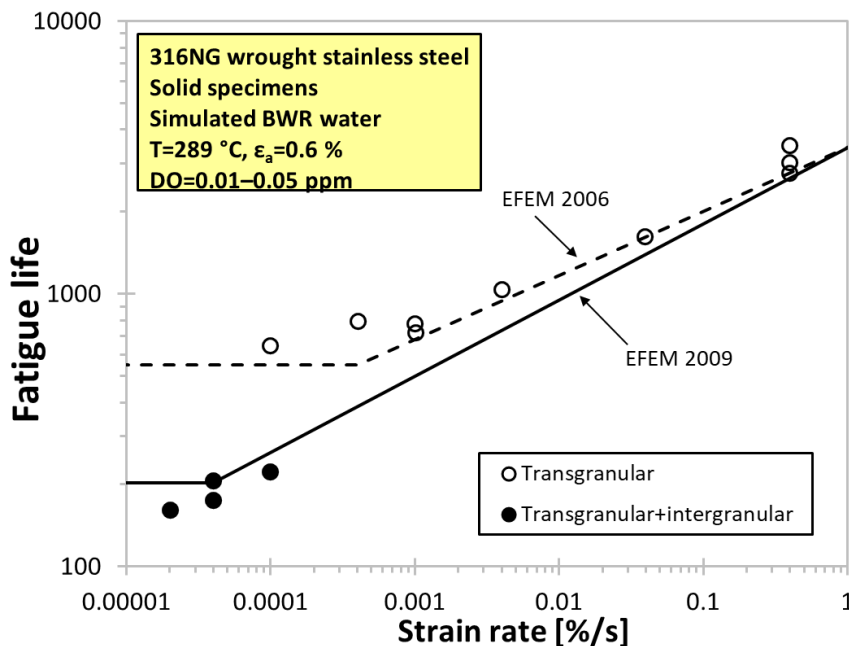


Figure 61. Effect of very slow strain rate on type 316NG stainless steel fracture morphology and fatigue life in BWR water. (Higuchi et al., 2009)

The influence of water flow rate on F_{en} of 304 and 316 types of stainless steel in BWR and PWR water are shown in Figure 62 and Figure 63, respectively, as collected by Higuchi, Sakaguchi, Nomura et al. (2007). All testing with accelerated flow rate was done using tubular specimens, in which the flow rate can conveniently be adjusted by inserting a mandrel inside the tube. In BWR water, there is a slight tendency of higher environmental effects for higher flow rate. On the contrary, no particular effect exists in PWR water. As most EAF data is at near stagnant flow condition, the 2009 EFEM BWR F_{en} equation revision used the high flow rate data in regression. The average high flow rate F_{en} factors for three wrought stainless steels was also plotted in Figure 58, where there is a better agreement with the 2009 EFEM model than 2006 model. Since at least in BWR water the stagnant flow rate testing was done using solid specimens, an uncertainty remains on the influence of specimen type. Also, the BWR data is limited to a single strain amplitude and strain rate.

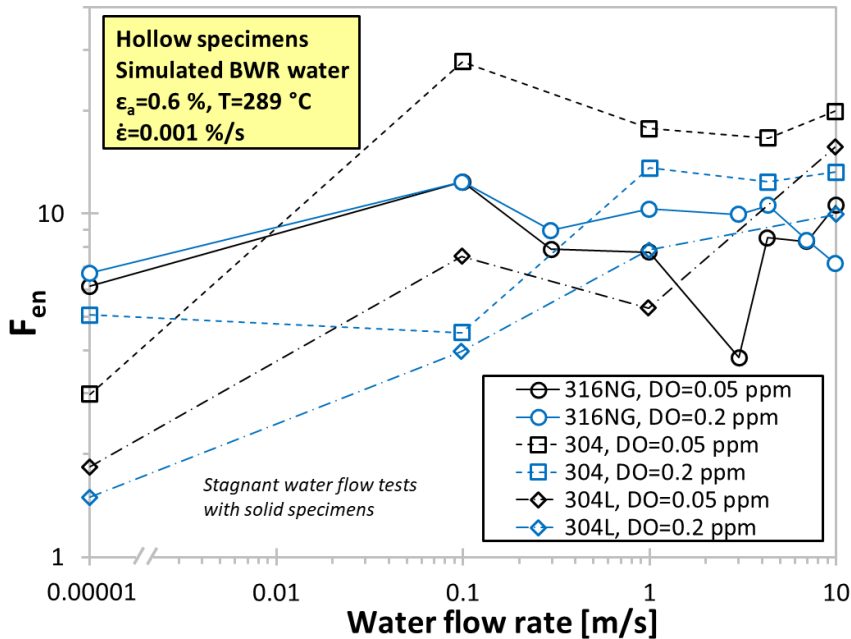


Figure 62. Relation between water flow rate and F_{en} in BWR water. (Higuchi, Sakaguchi, Nomura, et al., 2007)

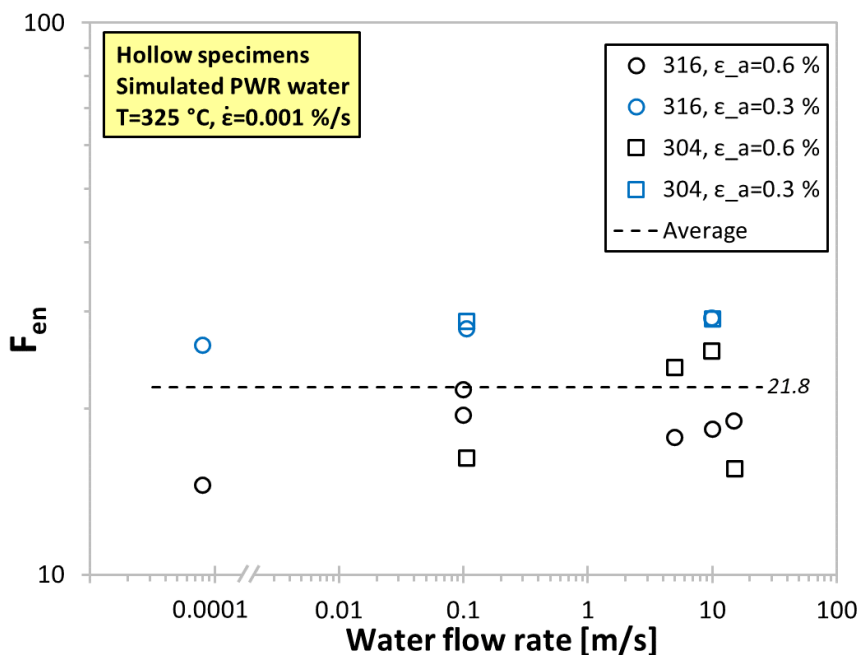


Figure 63. Relation between water flow rate and F_{en} in PWR water. (Higuchi, Sakaguchi, Nomura, et al., 2007)

Effects of dissolved oxygen were separately investigated in BWR and PWR water (Higuchi et al., 2002; Higuchi, Sakaguchi, Nomura, et al., 2007). The data from these investigations is shown in Figure 64 and Figure 65 for BWR and PWR water, respectively. The conclusion was consistent in both environments: there is no clear tendency with regard to DO. In BWR water, the lack of data at exactly the same strain rate and strain amplitude may conceal effects, because the data is normalized to a certain assumed F_{en} . This normalization may create bias, such as the seemingly more severe environmental effects for CASS for lower DO in BWR water.

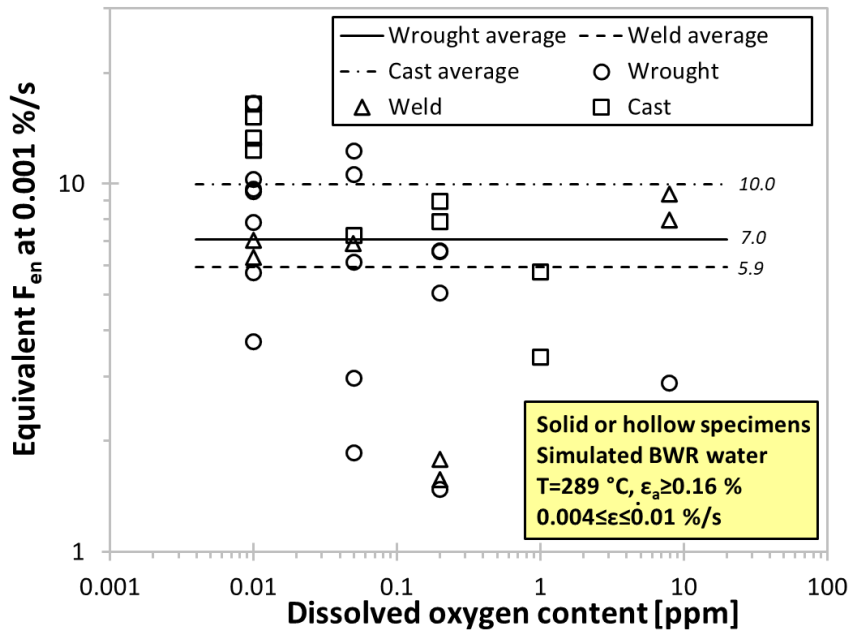


Figure 64. Relation between dissolved oxygen and equivalent F_{en} in BWR water. (Higuchi et al., 2002; Higuchi, Sakaguchi, Nomura, et al., 2007)

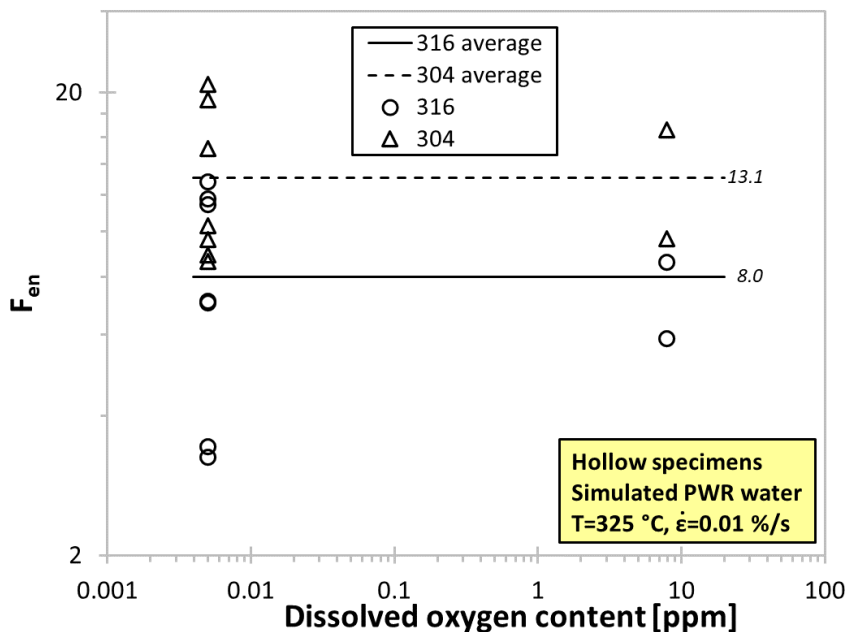


Figure 65. Relation between dissolved oxygen and F_{en} in PWR water. (Higuchi, Sakaguchi, Nomura, et al., 2007)

Results of a study on strain ratio effects in PWR water by Sakaguchi, Nomura, Suzuki, Tsutsumi, et al. (2006) are shown in Figure 66. Conventionally, standard tests are fully-reversed ($R=-1$) with the cyclic strain minima and maxima having equal magnitudes but of opposite sign. With a mean tensile strain ($R=0.1$) there appears to be no obvious effect at strain amplitudes above 0.2 %. At lower amplitudes there is insufficient data for quantitative conclusions and it is not known, if such effects were further investigated in the EFT project or other Japanese research.

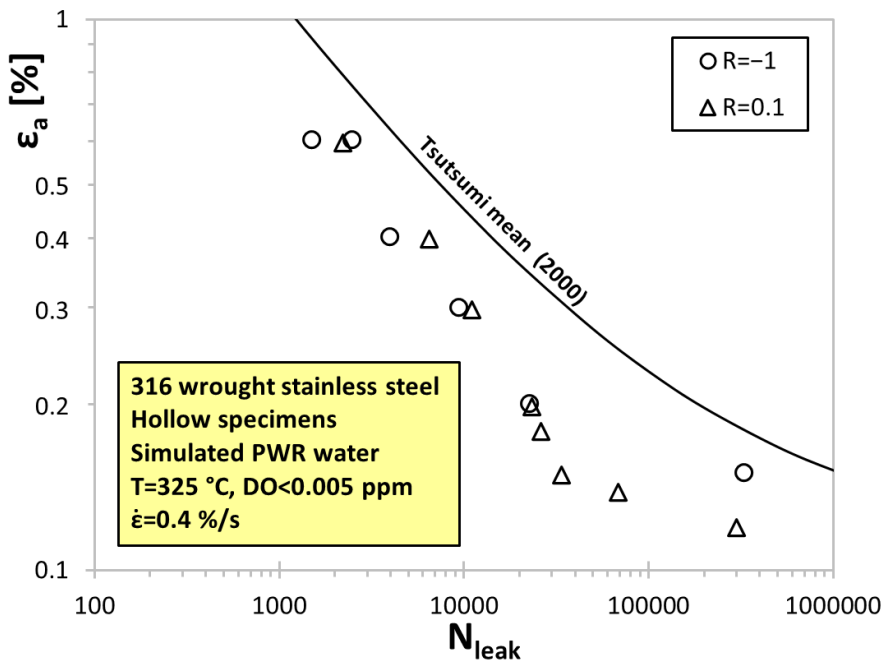


Figure 66. Strain ratio effect on type 316 stainless steel in PWR water. (Sakaguchi, Nomura, Suzuki, Tsutsumi, et al., 2006)

Research on hold time effect at or near peak strain is summarized in Figure 67 and Figure 68 for BWR and PWR environments, respectively, as reported by Higuchi, Sakaguchi and Nomura (2007). In BWR water, there was no indication of hold effects at 0.4 %/s and 0.04 %/s strain rates. However, at a lower strain rate, a trend emerged, showing a decrease in fatigue life with longer hold time when the hold period occurred at the peak of the cycle, specifically at 0.6 % tensile strain. With even a slight offset in the hold location in the hysteresis loop, the detrimental effects were mitigated. In PWR water no detrimental hold time effect was observed at the peak strain but no sub-peak strain hold data has been presented, which could be useful to confirm that the same still applies considering most NPP transients are not representative of the peak strain hold condition. In both BWR and PWR environments all the data is limited to 0.6 % strain amplitude. The hold times are also relatively short, only up to 2000 seconds, which may not be realistic of the length of steady-state operation between plant transients.

The modified rate approach (or detailed method) has been validated repeatedly with a growing set of data, including non-isothermal experiments. The main set of literature references have been listed in chapter 3.2.2. Figure 69 is a summary of accumulated BWR data at the end of the EFT project, including results with a non-linear sine waveform (Higuchi, Sakaguchi, & Nomura, 2007). The other data are for waveforms with a trilinear ramp consisting of slow-fast-fast (S-F-F) or fast-slow-fast (F-S-F) strain rate parts. For the selected conditions, the trilinear waveform experimental $F_{en,test}$ is approximated reasonably well and consistently using the MRA approach ($F_{en,det}$). However, the fatigue life of sine waveforms is underpredicted. For application to NPP components this is not an immediate concern as the detailed method should thus result in conservative estimates. As plant transients more often than not include irregular and nonlinear strain rates throughout a cycle, there remains room for improvement with the detailed method.

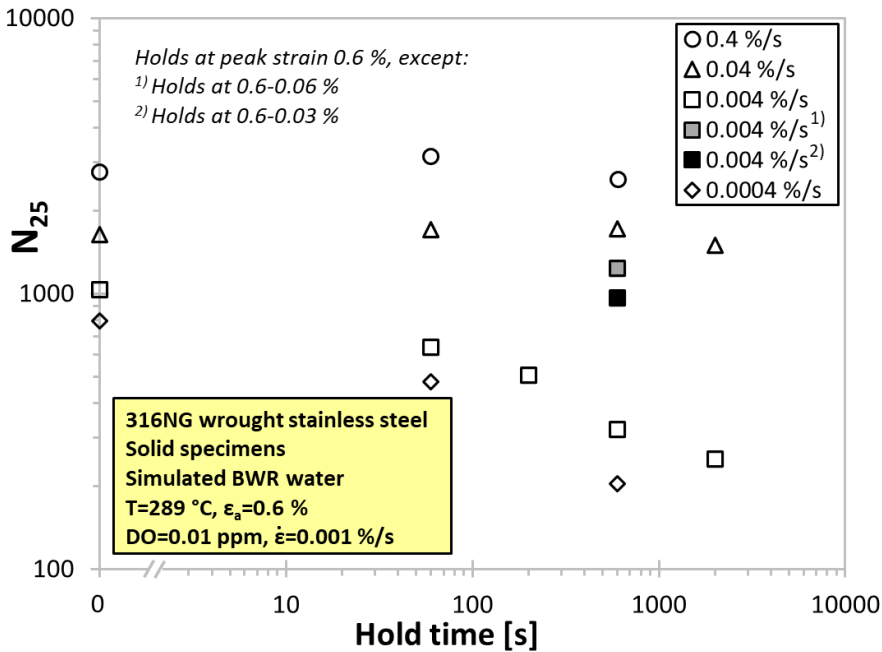


Figure 67. Effect of hold time on fatigue life of type 316NG stainless steel in BWR water. (Higuchi, Sakaguchi, & Nomura, 2007)

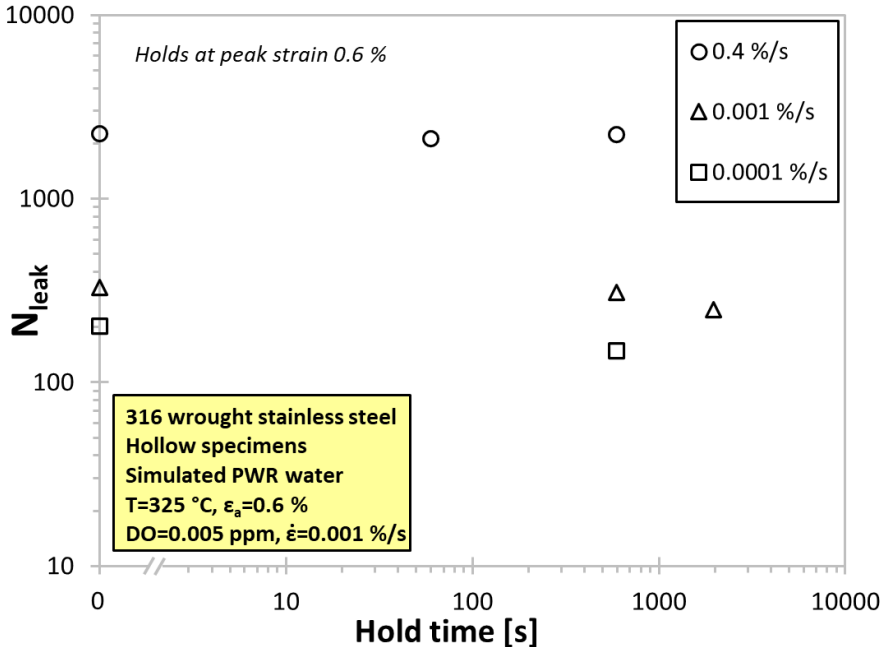


Figure 68. Effect of hold time on fatigue life of type 316 stainless steel in PWR water. (Higuchi, Sakaguchi, & Nomura, 2007)

Block loading has been studied on type 316 NG in simulated BWR water by Japanese researchers (Higuchi & Sakaguchi, 2005). All blocks were done at the same strain amplitude 0.3 %, but the order in which the faster and slower tensile strain rates (0.4 %/s and 0.004 %/s) were applied was varied. This was done to evaluate if there was a greater influence of the environment on crack initiation or growth of a mechanically small crack to engineering size. The results in Table 16 suggest that there is an approximately equal effect on the N_{25} no matter which order the strain rate blocks are applied. Certainly,

beyond the obvious

any variation in the total CUF is well within the scatter of EAF results. A broader test matrix using carbon steel STS410 ended up with the same conclusion. The STS410 matrix included tests with strain amplitudes 0.3 % and 0.6 % separately and within the same test. The conclusions only apply when all strain blocks are well above the endurance limit.

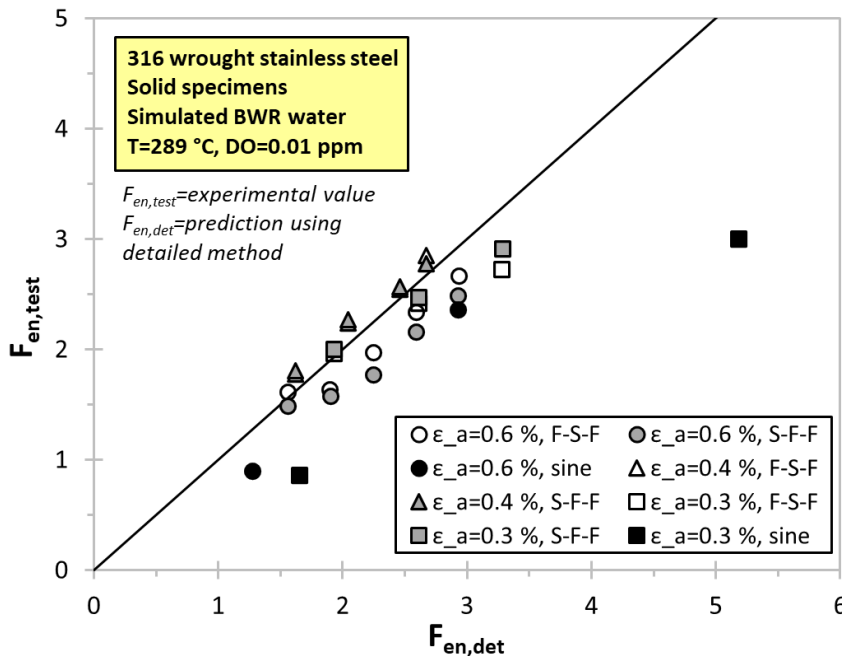


Figure 69. Relation between experimental F_{en} with predicted F_{en} using the detailed method for changing strain rate tests. (Higuchi, Sakaguchi, & Nomura, 2007)

Table 16. Block loading fatigue test results for type 316NG at $\epsilon_a=0.3\%$, $R=-1$. Simulated BWR water at 289 °C, DO=0.01 ppm. (Higuchi & Sakaguchi, 2005)

Step	Tensile strain rate [%/s]	Step cycles	N ₂₅	CUF
1/1	0.4	12645	12645	1
1/1	0.004	4024	4024	1
1/4	0.004	1000	8742	0.25
2/4	0.4	3000		0.49
3/4	0.4	3000		0.72
4/4	0.4	1742		0.86
1/4	0.4	3000	10945	0.24
2/4	0.004	1000		0.49
3/4	0.4	3000		0.72
4/4	0.4	3945		1.03
1/4	0.4	3000	14745	0.24
2/4	0.4	3000		0.47
3/4	0.004	1000		0.72
4/4	0.4	7745		1.34
1/4	0.4	3000	9848	0.24
2/4	0.4	3000		0.47
3/4	0.4	3000		0.71
4/4	0.004	848		0.92

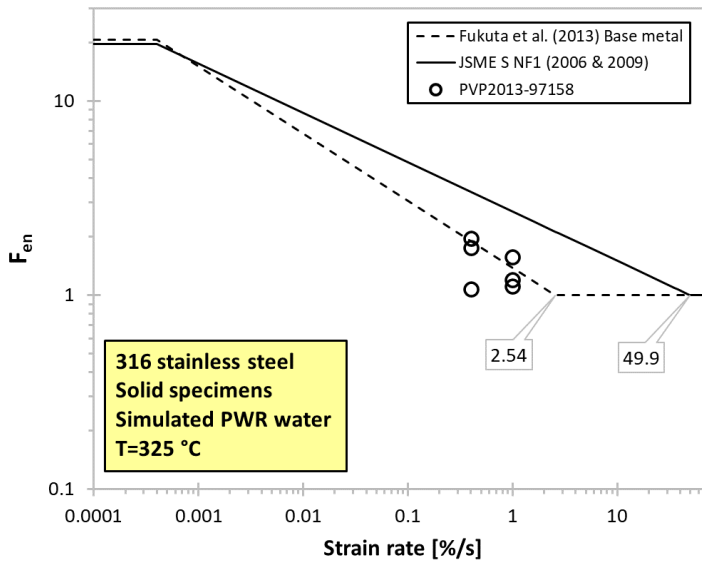


Figure 70. EAF data on type 316 stainless steel at high strain rate. (Fukuta et al., 2013)

Asada et al. (2020) evaluated the applicability of EAF data together with the new design fatigue curves which are based on tensile strength and revised transferability margins. The evaluated data set is shown in Figure 71. The predicted fatigue life in air is based on equation (29), with transferability factors on cycles or strain (2.48 or 1.43) applied to take into account material scatter. The predicted life in water is obtained from the air prediction, divided by the revised F_{en} model for base metal, equation (57). The base metal equation was chosen as it was the most conservative of all revised equations (57)–(60). With these assumptions made, the data is predicted accurately or conservatively by a factor of seven (with one single data point by a factor of 12). Although this approach strictly speaking violates the pairing of specific fatigue curves and F_{en} models, the conservative choices in the process appear to lead to a net conservative result. For the different material groups, linear regression of the data in Figure 71 (coloured dashed lines) gives differing levels of conservatism. A small consistent bias towards extra conservatism in the low cycle end also seems to exist via the regression curve slopes. This is consistent with the strain amplitude dependency proposed by Higuchi et al. (2002), which is not included in current Japanese F_{en} models.

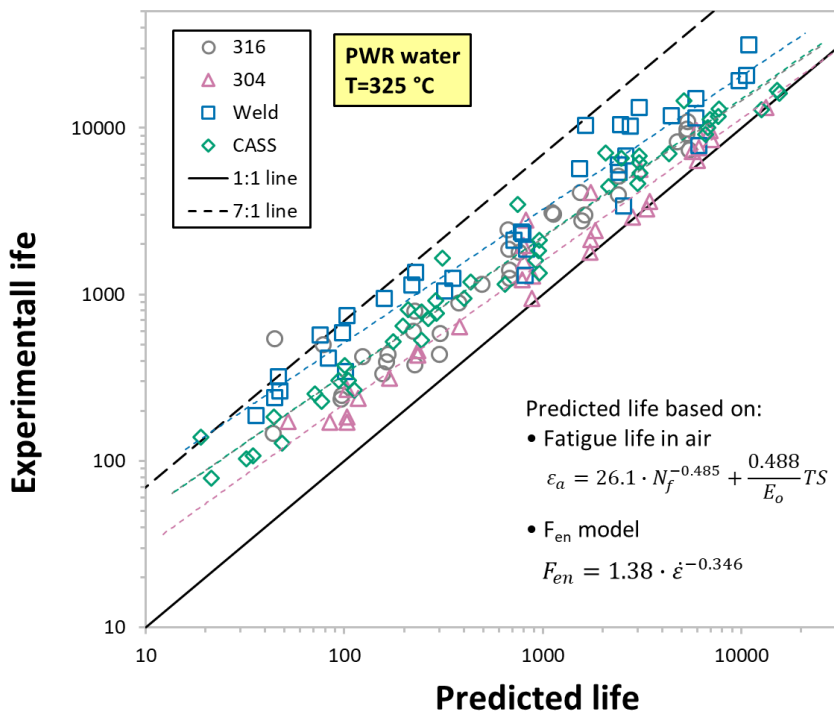


Figure 71. Experimental fatigue lives of stainless steels in PWR compared to predicted lives using the tensile strength dependent best-fit curves, new transferability margins and revised F_{en} model. (S. Asada et al., 2020)

The use of hollow tubular specimens for much of the Japanese EAF testing of stainless steel has led to discussion on the applicability of results in direct comparison to solid specimens. The tubular specimen design used at Mitsubishi Heavy Industries is shown in Figure 72 and the design at Hitachi (for flow rate studies) in Figure 73. The major benefits of hollow specimens include the ability to control strain directly using an external extensometer, the option to adjust flow rate, and the easier realization of non-isothermal conditions. Disadvantages include the difficulty of maintaining a constant and uniform temperature (particularly if outer induction heating is not used), difficulty of observing crack initiation prior to leakage and challenges associated with honing the inner bore to an equivalent polish as solid specimens.

Examples of Japanese solid specimen designs, which have also been used in stainless steel testing, are shown in Figure 74–Figure 76. Note that in the solid specimen designs, the uniform test section length does not adhere to the recommendation in ASTM E606 (ASTM, 2021) strain-controlled fatigue testing standard (2–4 x specimen diameter).

In a review by Twite et al. (2016) existing literature on hollow specimen data was collected, analyzed and possible reasons identified for why some authors report shorter lives using the hollow specimens. It is also worthwhile noting that ASTM E606 states that “Lives determined using tubular specimens are less than those for solid specimens, the extent of which depends on the failure criteria and specimen configuration. Differences in excess of a factor of two are not unusual for failure criteria based on separation, whereas for failure defined by crack size contained within the tube wall there will be much less difference” (ASTM, 2021).

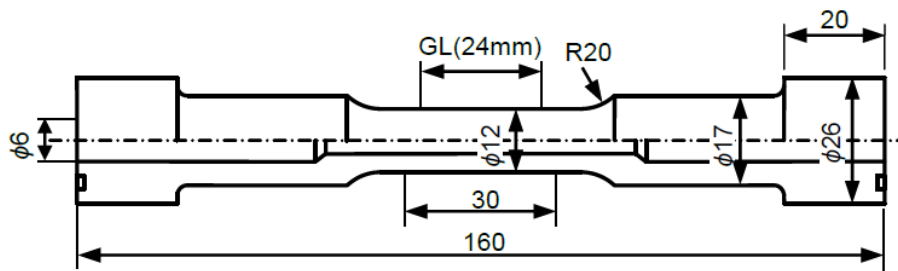


Figure 72. Tubular hollow specimen design at MHI. (S. Asada et al., 2017)

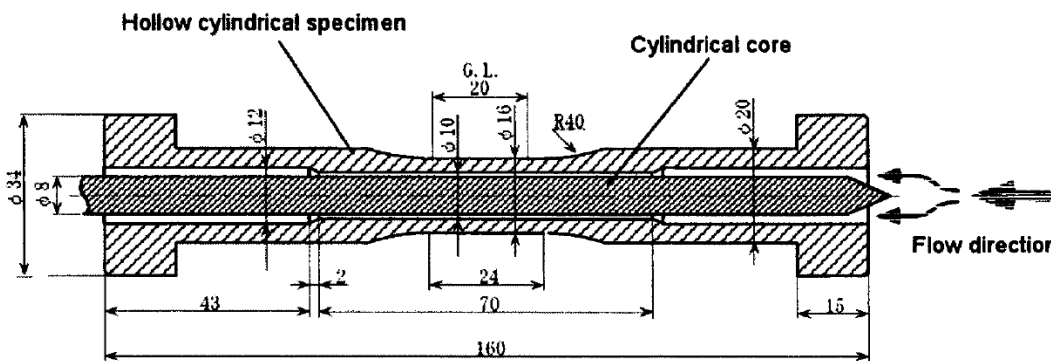


Figure 73. Tubular hollow specimen design at Hitachi. Note the inserted mandrel to adjust water flow rate. (Hirano et al., 2004)

The review by Twite et al. (2016) suggests that in the literature where no difference between solid and hollow specimens is reported, test related factors such as using a single strain amplitude may be influential. Further experimental evidence was collected in testing done at Jacobs and is shown in Figure 77. Potential reasons for the observed factor of about 1.8 between solid and hollow specimens in PWR water were suspected to be differences in the fatigue crack growth mechanism, definition of failure criteria and/or the internal pressure which induces a multiaxial stress state.

Asada et al. (2017) defended the applicability of the hollow specimen by describing the experimental procedure and its merits in detail. Verification data was shown to argue equivalence between hollow and solid specimens. The 316 stainless steel verification data in air is shown in Figure 77. While the absolute factors on life appear to be less in the Japanese verification data with respect to the data from Jacobs, there is still arguably a consistently shorter fatigue life in the hollow tubular specimens.

For now the potential mechanisms and reasons behind the debate on solid versus hollow specimens has not been fully resolved. However, it is worth bearing in mind that much of the technical basis of both the ANL/NRC and JSME F_{en} models leans heavily on hollow specimens. If a consistent “hollow specimen factor” can be proven and subsequently applied to revisit existing F_{en} models, the value of this extensive data as valid would not be lost whilst improving the general understanding of EAF and its applicability in plant fatigue assessments.

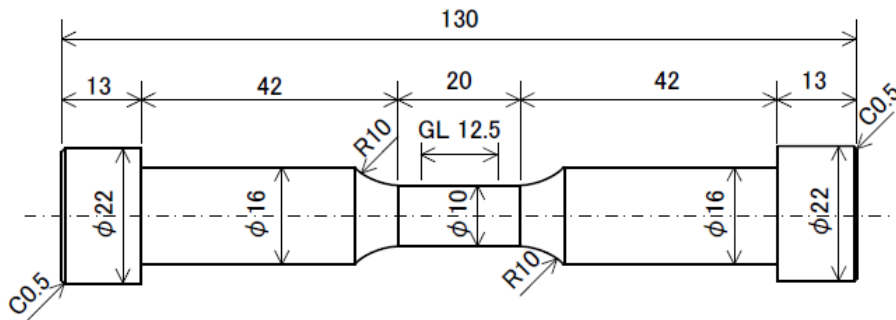


Figure 74. Solid specimen design at MHI. (Fukuta et al., 2013)

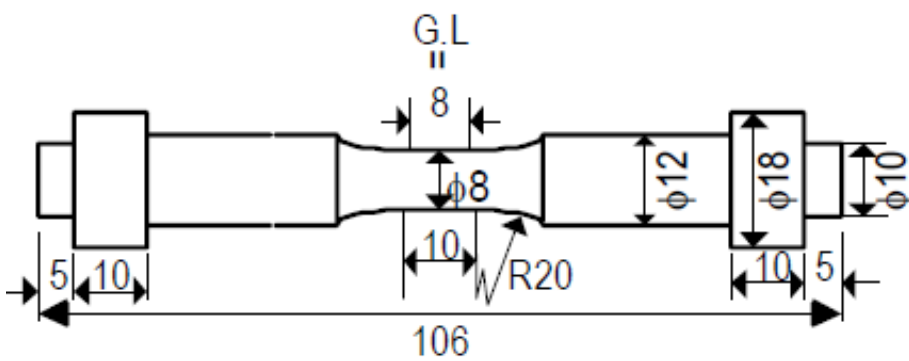


Figure 75. Solid specimen design at IHI. (Higuchi, Sakaguchi, & Nomura, 2007)

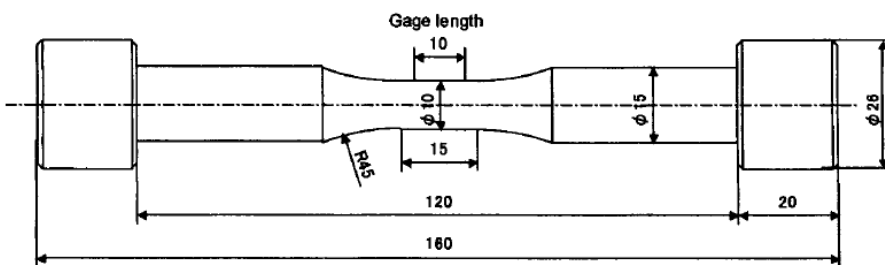


Figure 76. Solid specimen design at Hitachi. (Hirano et al., 2004)

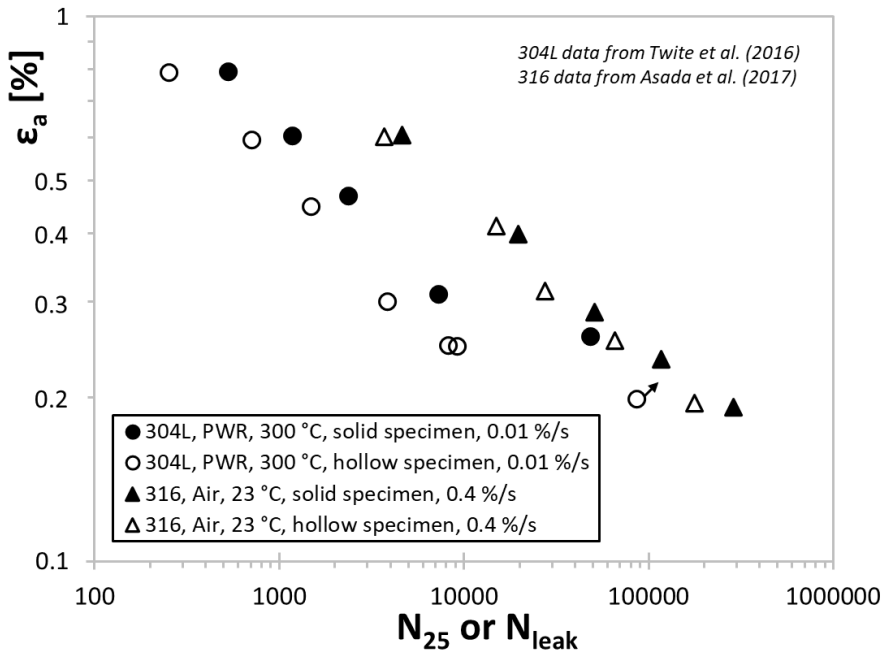


Figure 77. Comparison of solid and hollow specimen data in air and PWR. (S. Asada et al., 2017; Twite et al., 2016)

4.3 France

Shortly after the Dresden I experiments were started, a pioneering French research program into environmental effects in PWR environments was initiated based on the 1974 decree regulating the construction of pressure components in NPPs. The laboratory studies were reported by Garnier et al. (1975, 1979) and Barrachin et al. (1981) and used a pressurized laboratory scale loop with circulating low DO water. As in the AEC study, loading was applied by bending of slender 2 mm thick specimens in deflection control. The results are collected in Figure 78 for a range of stainless steel materials at two temperatures. In general, the environment reduced fatigue lives to a greater extent than in the AEC study: the best-fit curve for normal operation ($Cl^- \leq 200$ ppb) has a fatigue reduction factor life between four and five. Specific reasons are likely to be the higher test temperature, deoxygenated PWR water and lower tensile strain rate in the French program: all factors now understood to increase severity of environmental effects in laboratory experiments.

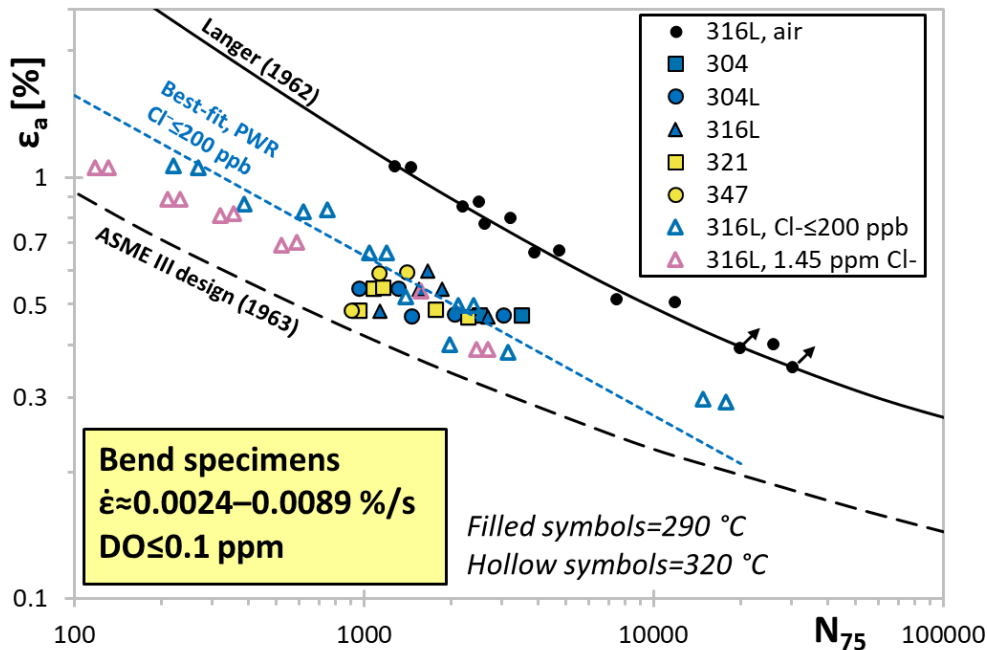


Figure 78. Bend specimen EAF results for various strain rates, materials and temperatures in low DO water. Data extracted from Garnier et al. (1975, 1979) and Barrachin et al. (1981).

In the early 2000's EDF partnered with General Electric Global Research Center for fatigue studies on 304L stainless steel (RCC-M designation Z2 CN 18-10) both in air and PWR water (Solomon, Amzallag, DeLair, et al., 2005a). The strain-controlled data in air and PWR water from this research is shown in Figure 79. Also shown is 304L and 316L reference data in air at the same temperatures from EDF's own laboratories (Amzallag, 2003).

Most of the data was generated with a strain rate of 0.4 %/s, which enabled high cycle data up to 10^7 cycles to be generated in PWR water within a reasonable time. To this day it remains the only EAF data to such cycle numbers. Fewer EAF experiments (at higher amplitudes) were done at strain rates 0.027 %/s and 0.004 %/s with an expected trend of decreasing fatigue lives at the lower rates.

An influence of temperature on the endurance limit in strain-controlled tests was found by Solomon, Amzallag, DeLair and Vallee (2005a), namely that at 300 °C in both air and PWR water an effective limit was greater than at 150 °C. This was attributed to a secondary hardening mechanism, which at low strains at 300 °C produced a dislocation structure resembling corduroy.

Several specimens, mainly at 150 °C in PWR water, exhibited crack initiation at the extensometry knife-edge contact points. Although this leaves some uncertainty in the results, secondary cracks were also observed within the uniform length between the knife-edges. This observation implies that in the absence of knife-edge cracks, other cracks would eventually have grown to cause failure (Solomon, Amzallag, DeLair, et al., 2005a).

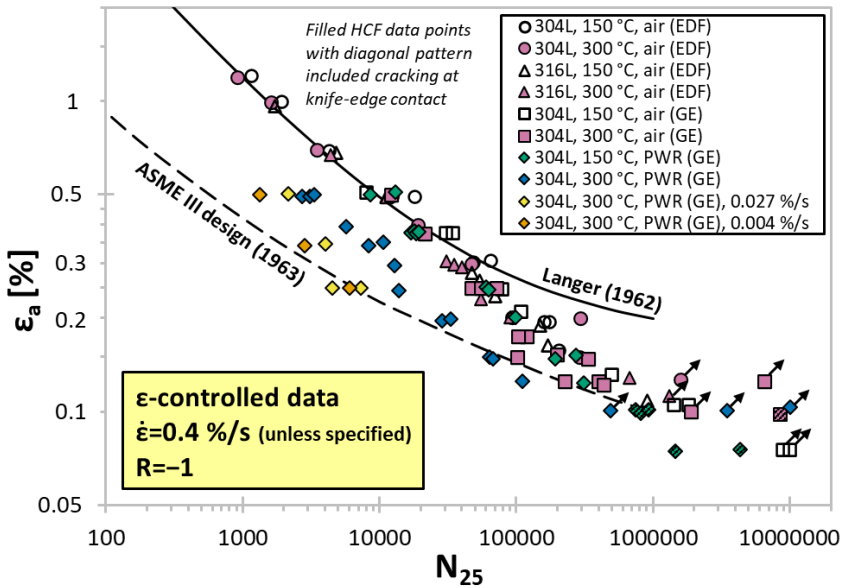


Figure 79. Strain-controlled fatigue data in air and PWR water, at 150 °C and 300 °C, from EDF and GE laboratories. (Amzallag, 2003; Solomon, Amzallag, DeLair, et al., 2005a)

A merit of the experiments performed at GE include the direct control of strain from the uniform gauge length of the specimens. The specimen design is shown in Figure 80. The experimental EAF setup is shown in Figure 81. Note that specimen shoulder extensometry was initially investigated but abandoned in favour of direct strain control because of the considerable difficulty in correlating the shoulder-to-gauge displacements during the complex sequence of softening and hardening (Amzallag, 2003).

Examples of the hardening and softening stress response in air and PWR water are shown in Figure 82 and Figure 83 at 300 °C and 150 °C, respectively. The plotted pairs of air and PWR tests in terms of strain amplitude were selected to be as close as possible. The strain rate for all curves is 0.4 %/s. The figures clearly demonstrate that in otherwise identical experiments the stress response is not the same in air and PWR water. The difference is more notable at 300 °C. An unconfirmed mechanism is responsible for hardening the material more in PWR water than in air.

This evidence contradicts the assumption made in the ANL companion specimen experiments of stress response not being influenced by the environment. Considering further that De Baglion and Mendez (2010) demonstrated a consistent influence of strain rate on the stress response of 304L stainless steel in high temperature air and subsequently in PWR water (De Baglion et al., 2012) as part of AREVA research, the overall uncertainty of the ANL data becomes very difficult to quantify.

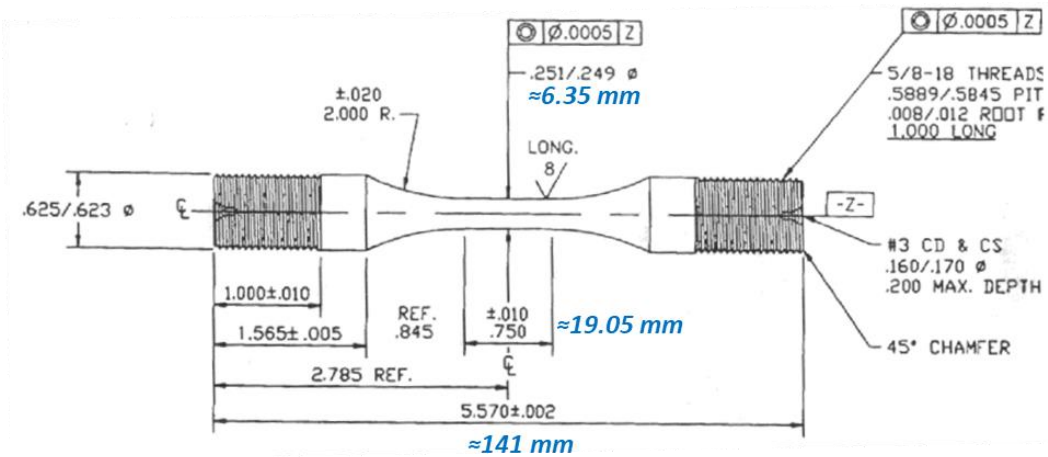


Figure 80. GE fatigue specimen geometry. Modified from Solomon, Amzallag, DeLair, et al. (2005a).

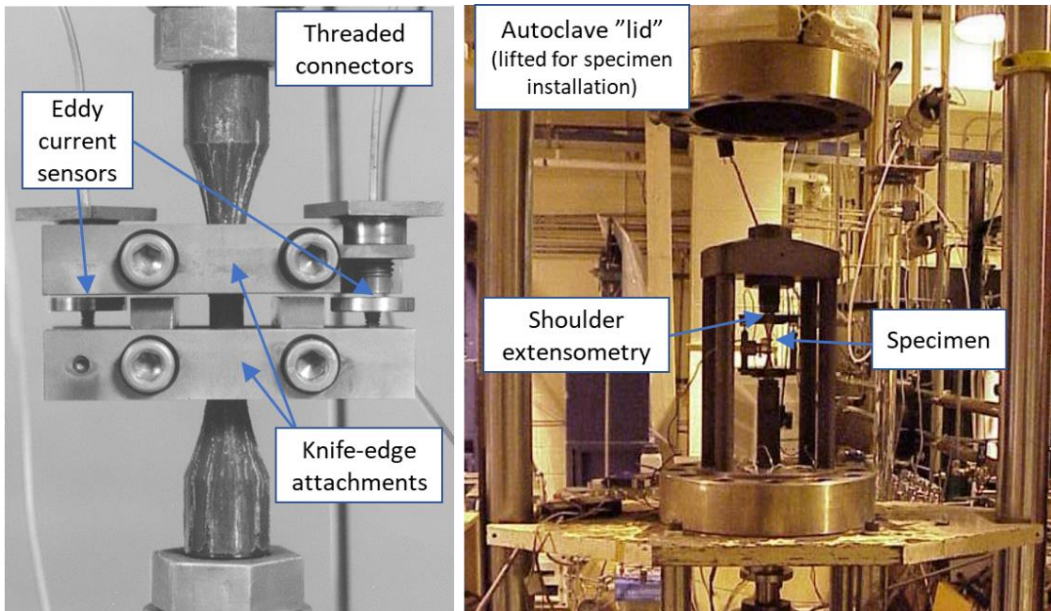


Figure 81. GE EAF test rig. Direct strain-control extensometry can be seen on the left. Shoulder extensometry seen on the right was investigated but abandoned. Modified from Amzallag (2003).

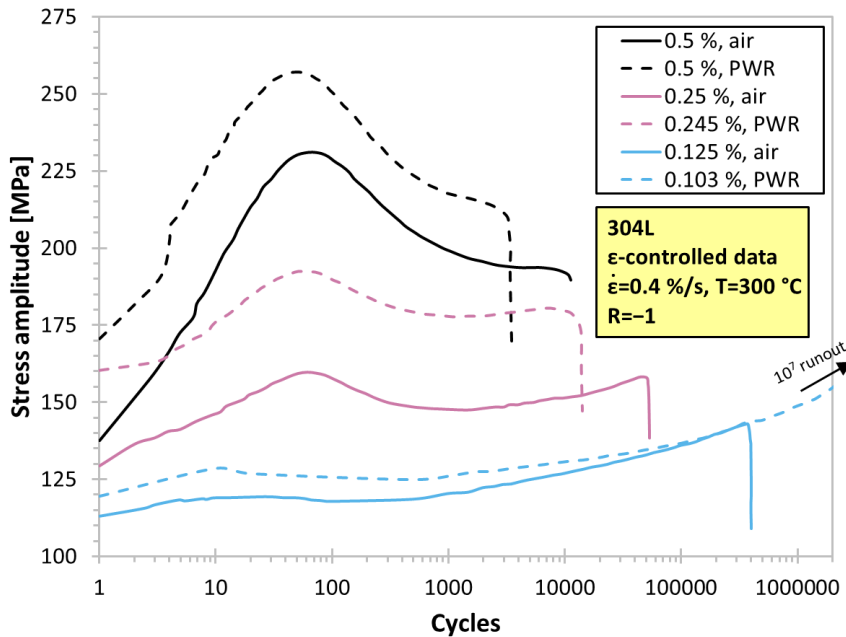


Figure 82. Stress response in 300 °C air and PWR water at near equivalent strain amplitudes. (Solomon, Amzallag, DeLair, et al., 2005a)

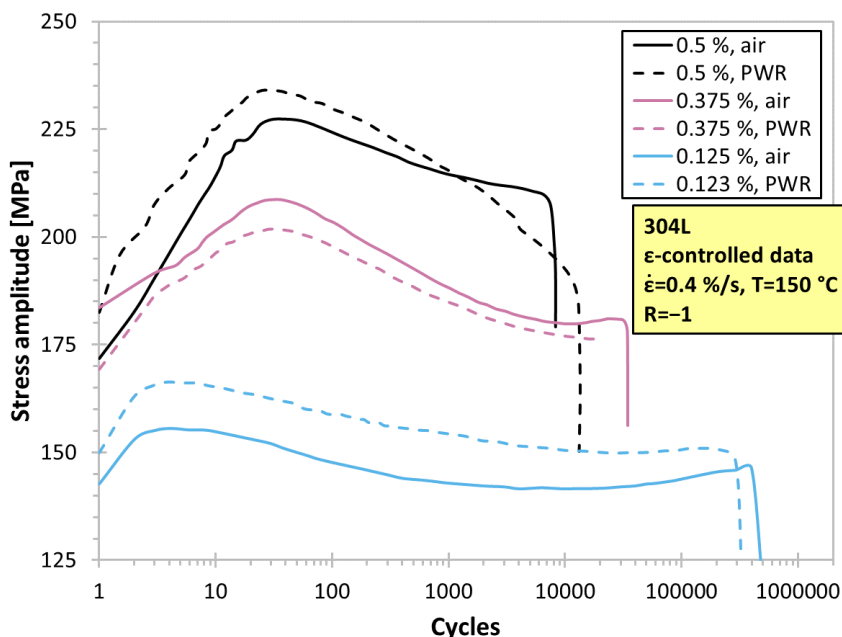


Figure 83. Stress response in 150 °C air and PWR water at near equivalent strain amplitudes. (Solomon, Amzallag, DeLair, et al., 2005a)

In other related research on 304L, Solomon, Amzallag, Vallee, et al. (2005b) studied the effect of a moderate 100 MPa mean stress on the fatigue behaviour in air and PWR water. The chosen temperatures were 150 °C and 300 °C. The results are summarized in Figure 84. At 300 °C in both air and PWR water the influence of the tensile mean stress was surprisingly to raise the fatigue limit at 10^7 cycles. The observation was attributed to the hardening, which the mean stress induces. This subsequently suppresses the plastic strain and enables secondary hardening to occur as in the strain-controlled experiments at low strain amplitude.

On the contrary, at 150 °C the mean stress lowered the fatigue limit in both air and PWR water, supposedly due to the lack of hardening effects. In PWR water the fatigue limit was reduced considerably more than either the Goodman or Gerber models predict. These results suggest that a sustained tensile mean stress may under certain circumstances accelerate environmental effects in a way which is not conservatively predicted by codified methods. The authors did not speculate further on the mechanisms behind such effects.

Ignoring the mean stress effects, the highest 10^7 fatigue limit in Figure 84, based on the staircase method, is for 150 °C in air and the lowest is for 300 °C in PWR water. Solomon, Amzallag, Vallee, et al. (2005a) compared the fatigue limit values in air to those in a non-public EDF research report, where a cyclic frequency of 30 Hz was applied. Both at 150 °C and 300 °C the effect of the higher frequency was to raise the fatigue limit by as much as 10 MPa. This was hypothesized to be due to suppression of plastic strain amplitude (and thus total strain amplitude) at 30 Hz compared to 1.818–2 Hz. Implications of self-heating of the stainless steel specimens due to a finite width of hysteresis loops was not discussed in the context of frequency effects.

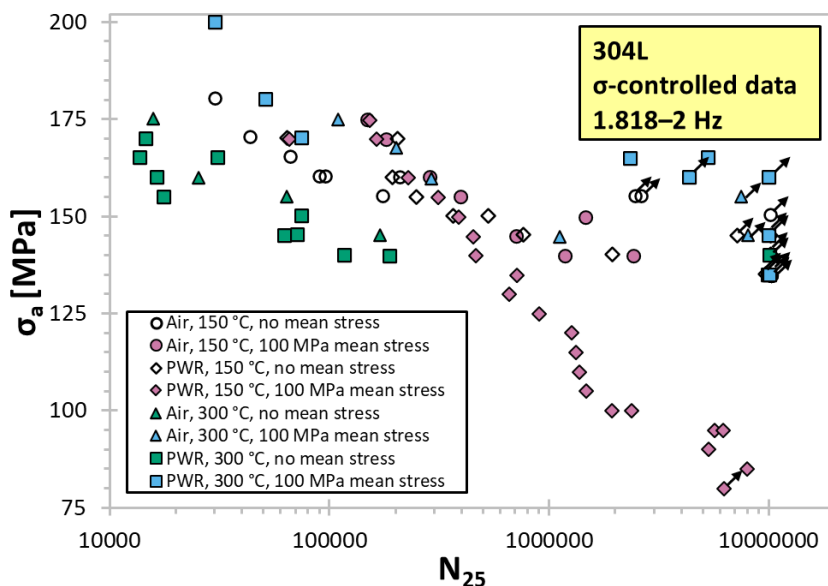


Figure 84. Effect of 100 MPa mean stress in load control in air and PWR water at 150 °C and 300 °C. (Solomon, Amzallag, Vallee, et al., 2005b)

With the available strain- and load-controlled data, Solomon, Amzallag, DeLair, et al. (2005b) performed transformations of either strain or stress such that all results could be plotted together for comparison. In Figure 85 and Figure 86 the half-life strain amplitude has been plotted for the load-controlled data at 150 °C and 300 °C, respectively. Because of the complex stress and strain evolution in cyclic loading, it is generally not advisable to make far-reaching conclusions from such comparisons, which is also acknowledged by the authors of the paper. Much of the load-controlled data aligns surprisingly well within the scatter band of strain-controlled data, but for example in the endurance limit at 150 °C there is a discrepancy. Particularly at the higher stress amplitude levels, ratcheting of the specimens (increase of average strain) comes into play. Also note that in the PWR load-controlled data the strain rate varies because the frequency is kept constant across the range of amplitudes.

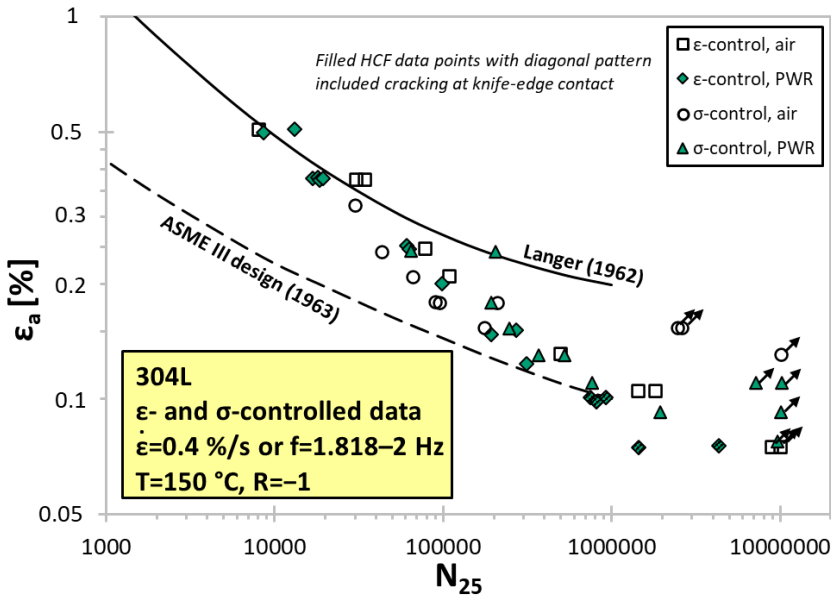


Figure 85. Comparison of strain-controlled data with transformed load-controlled data in air and PWR water at 150 °C. (Solomon, Amzallag, DeLair, et al., 2005b)

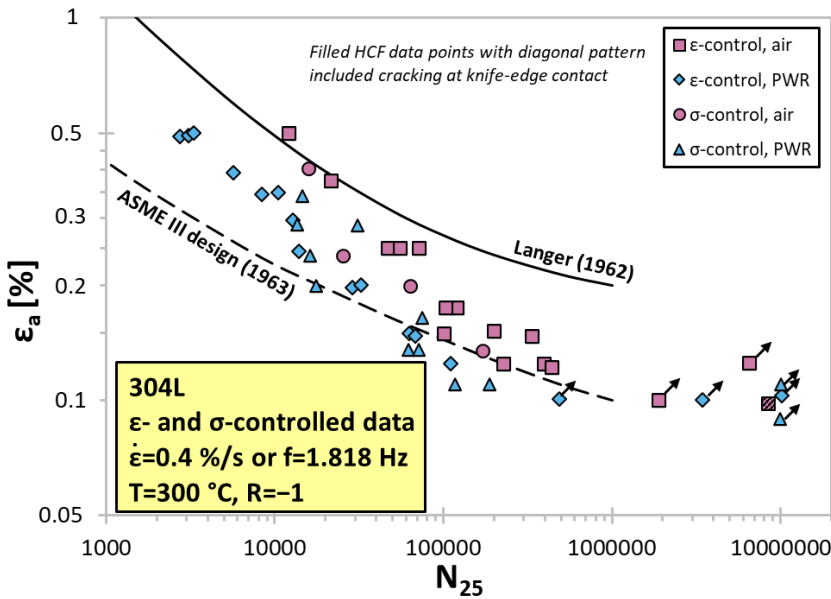


Figure 86. Comparison of strain-controlled data with transformed load-controlled data in air and PWR water at 300 °C. (Solomon, Amzallag, DeLair, et al., 2005b)

Data sources which were used to inform the more recent development work of RPP N° 2 and N° 3 proposed to the RCC-M code are listed in Table 17. Not all are public references.

Table 17. French stainless steel data sources, as indicated by Métais et al. (2015).

Lab	Alloy	RCC-M alloy	Air/PWR data	Reference
EDF Les Renardières	304L 316L CASS	Z2 CN 18-10 Z2 CND 17-12 Z2 CND 17-13 Z3 CN 20-09M	173/0	(Le Pêcheur, 2009)
Creusot Loire Unieux	316L	Z2 CND 17-12 Z2 CND 17-13	81/0	
CEA SRMA	304L 316L	Z2 CND 17-13 Z2 CND 18-10 Z2 CN 18-10	98/0	(Vincent et al., 2012)
CEAT	304L 316L	Z2 CN 18-10 Z2 CND 17-12	42/0	
GE (USA)	304L	Z2 CN 18-10	22/32	(Solomon, Amzallag, Vallee, et al., 2005b)
CETIM	CASS	Z3 CN 20-09M	10/0	
INSA Rouen	304L	Z2 CN 18-10	17/0	
UT Compiègne	304L	Z2 CN 18-10	5/0	
Toledo Univ. (USA)	304L	Z2 CN 18-10	52/0	(Colin, 2009)
LMT Cachan	304L	Z2 CN 18-10	14/0	
MHI (Japan)	304L	Z2 CN 18-10	0/13	
ENSMA	304L	Z2 CN 18-10	22/7	(De Baglion et al., 2014)
AREVA CT Le Creusot	304L	Z2 CN 18-10	24/31	(Le Duff et al., 2008, 2009, 2010)
		TOTAL	560/83	

The AREVA test program data in air and PWR water is shown in Figure 87 with additional data from De Baglion (2011). In total, 22 PWR test results were used to quantify $F_{en-integrated}$ (Courtin et al., 2012). Note that the reductions to the best-fit curve in air in this figure are based on the F_{en} equations in NUREG/CR-6909 Rev.0 (O. K. Chopra & Shack, 2007)

Supplementary experiments were performed using variations of the SIS transient, Figure 88. This was done by rearranging four equally sized (in strain amplitude) sections of the positive strain rate ramp such that the slower strain rates occurred either near the bottom of the cycle (Types A and D) or near the top of the cycle (Types B and C). By not accounting for the order in which the strain rates occur in a cycle, the modified rate approach (see chapter 5.2) results in identical F_{en} prediction for all four types of waveforms.

However, the experimental fatigue lives depicted in Figure 89 suggest that the more realistic transient Types A and D result in less severe environmental effects, potentially by a factor of up to two. Le Duff et al. (2010) have suggested that mechanistically this is because fatigue cracks are closed in the part of the cycle with the slowest, most damaging strain rate.

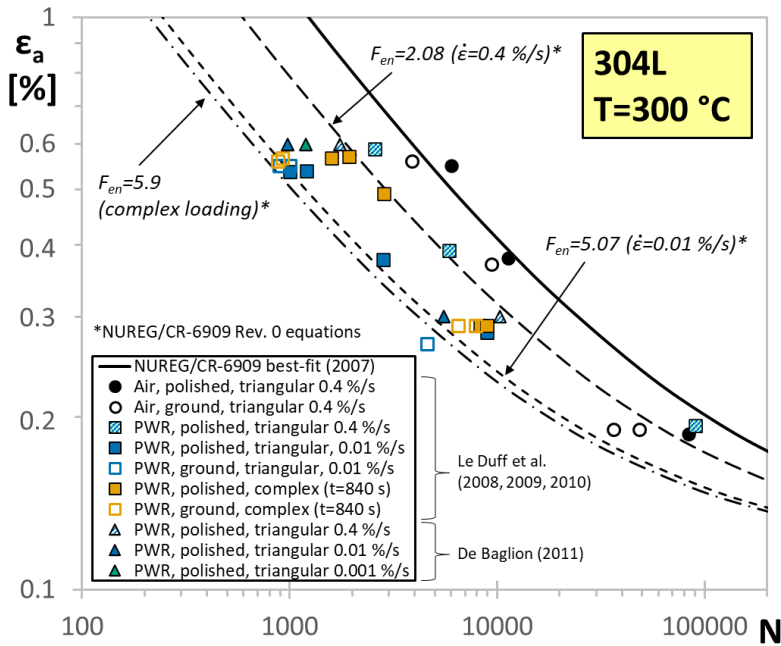


Figure 87. AREVA experimental program data in air and PWR water. (De Baglion, 2011; Le Duff et al., 2008, 2009, 2010)

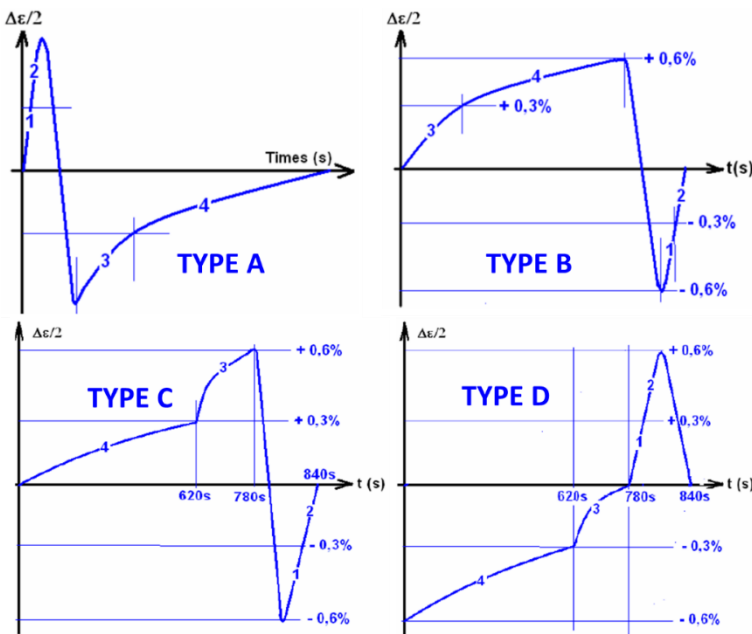


Figure 88. Complex loading variants used in AREVA experiments. (Le Duff et al., 2010)

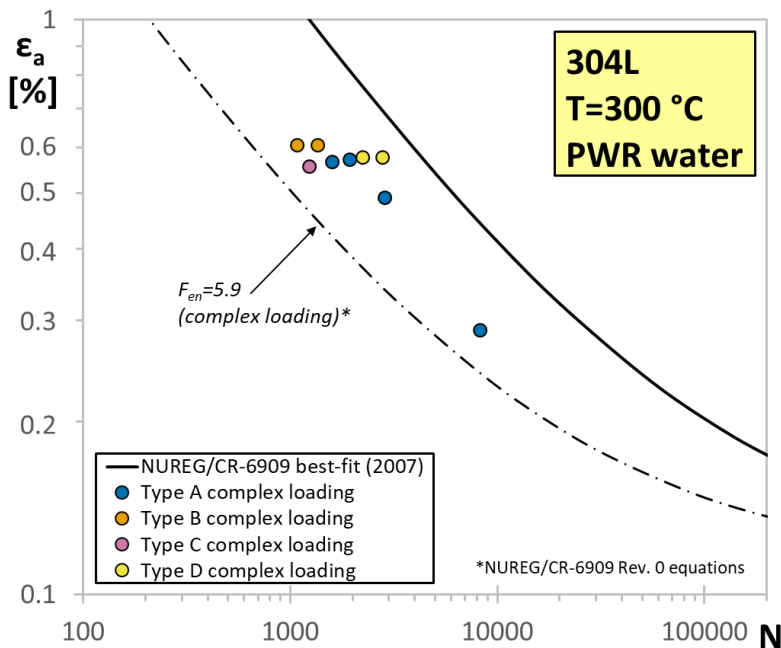


Figure 89. Complex loading experimental data from AREVA program. (Le Duff et al., 2010)

Results in PWR water in support of the $F_{en-integrated}$ methodology are shown in Figure 90. Not all of the data has been made public, such as an AREVA (Framatome Reactors Owners Group) program on CASS material. Métais et al. (2018) have indicated that over 200 data points (about 2/3 in air and 1/3 in PWR water), some of which are from labs in the UK, USA and Japan, have been collected as the technical basis. Details of precisely which data sets are included in Figure 90 are not available. Neither is the information on strain rate, which complicates interpretation. In general, the scatter band of the ground surface finish data appears to overlap with the polished data with somewhat lower mean fatigue lives.

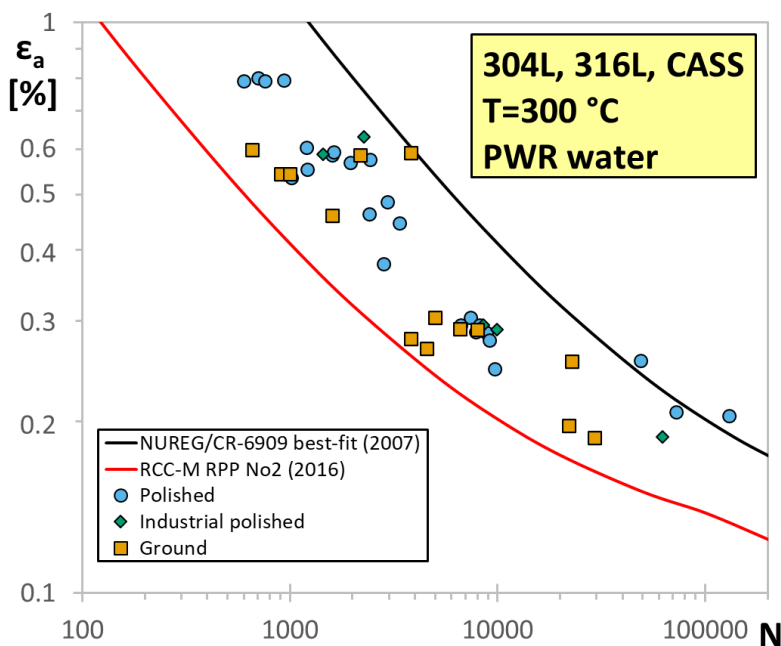


Figure 90. Data on polished and ground austenitic stainless steels in PWR water in support of an $F_{en-integrated}$ methodology and Code Case. (Métais et al., 2017)

The fatigue specimen used in AREVA's experiments is shown in Figure 91 and the strain measurement and control solution in Figure 92. The Le Creusot laboratory achieved technical readiness for EAF experiments in 2005 (Le Duff et al., 2008).

Displacement is measured using linear variable differential transformers (LVDT) attached to machined flanges on the specimen shoulders. Shoulders were preferred over the uniform gauge length to avoid issues of cracking at knife-edge contact points (Le Duff et al., 2008). Initially a single LVDT was used, but more recently a two-sided measurement was employed. This setup of averaging readings 180° can help mitigate the influence of bending strains. Note that the measuring length at the shoulders is about an order of magnitude shorter than that used by ANL in their companion specimen method. Furthermore, installing the LVDT inside the hot autoclave eliminates uncertainty related to thermal gradients within the load train, making this an overall improvement over the rigs used by ANL.

Le Duff et al. (2008) have described the calibration process for shoulder extensometry. An equivalent length of 23.5 mm when $\epsilon_a=0.6\%$ is assumed for the LVDT (displacement of ± 140 microns) which actually has attachment points 38 mm apart. This means that about 58 % of the displacement occurs in the uniform gauge length and about 42 % in the rounding and shoulders up to the LVDT attachment points. It is not indicated if the displacement value is calibrated at peak hardness, half-life or by some other definition. De Baglion (2011) acknowledges that the shoulder control mode cannot strictly replicate the intended strain history due to complex hardening and softening. However, considering that the EAF results fall within the general scatter of 3 % on stress response and 10 % on fatigue life, this level of inaccuracy is considered acceptable.

Certainly, the equivalent gauge length assumption for shoulder displacement control remains a simplification. Outside of the uniform gauge length each part of the specimen having a diameter >9 mm undergoes a different stress and strain history. If the rounding and shoulders of the specimen undergo secondary hardening at low strain amplitude, strain begins to concentrate at the $\varnothing 9$ mm diameter gauge length, leading to early cracking. A similar consequence may result, depending which cyclic hardening or softening phase the shoulder displacement is fixed to.

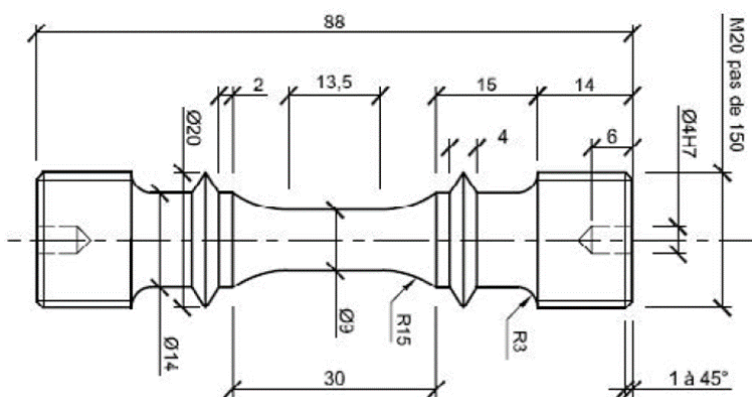


Figure 91. AREVA fatigue specimen dimensions. (De Baglion & Mendez, 2010)

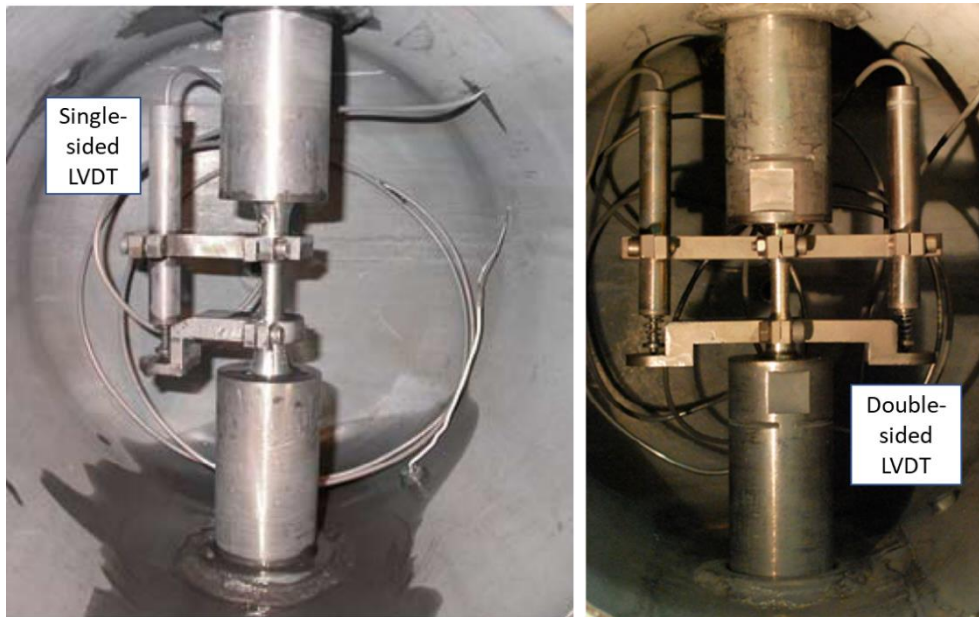


Figure 92. AREVA EAF test rig with single LVDT attachment at specimen shoulders (Le Duff et al., 2008) and later setup with double-sided LVDT measurement (Poulain et al., 2019). Modified from originals.

4.4 UK

A long history of fatigue research and development projects related to nuclear materials exists in the UK, see for example Tice (1985). Results have been published particularly actively and regularly in the 21st century. Most of the publications have concerned fatigue crack growth in PWR water rather than fatigue crack initiation. The relevant references on crack initiation work from about the last decade are shown in

Table 18. Based on the extensive research programs, suggestions to improve existing life assessment methods have been made and were discussed in chapter 3.3 on emerging approaches.

Much of the UK research on fatigue crack initiation has also been on complex topics and method development rather than generation of basic data. In the community of EAF stakeholders, Rolls-Royce is a leading organization in developing advanced evaluation methods for plant application together with its supplier of experimental data, Jacobs (formerly known as Wood, AMEC Foster Wheeler, and Serco). The main motivation behind the research projects has been the underlying criticism towards some of the conclusions made in NUREG/CR-6909.

An investigated topic in UK research has been the effect of surface roughness in both air and PWR water. The research interests align with French research and a common position has been published (McLennan et al., 2020; Métais et al., 2018). A selection of results are shown in Figure 93. Most of the published data is based on a batch of “MT643” 304L stainless steel, which is a hot-rolled plate. An alternative batch “AS216” is also 304L, but from a pipe segment. (Platts, Tice, Stairmand, et al., 2015)

Table 18. UK R&D related publications from last decade on fatigue crack initiation of stainless steels for light water reactors.

Paper title	Conference	Reference
PVP2015-45029 Effect of Surface Condition on the Fatigue Life of Austenitic Stainless Steels in High Temperature Water Environments	ASME PVP2015	(Platts, Tice, Stairmand, et al., 2015)
PVP2015-45844 Study of Fatigue Initiation of Austenitic Stainless Steel in a High Temperature Water Environment and in Air Using Blunt Notch Compact Tension Specimens	ASME PVP2015	(Platts, Tice, & Nicholls, 2015)
Effect of Shoulder Extension Control on Fatigue Endurance Testing of Stainless Steels	4 th Intl. Conf. on Fatigue in Reactor Components	(EPRI MRP) (McLennan et al., 2017)
PVP2016-63584 Variations in Measured Fatigue Life in LWR Coolant Environments due to Different Small Specimen Geometries	ASME PVP2016	(Twite et al., 2016)
PVP2017-65975 An Investigation Into the Lifetimes of Solid and Hollow Fatigue Endurance Specimens Using Cyclic Hardening Material Models in Finite Element Analysis	ASME PVP2017	(Gill, James, et al., 2017)
PVP2017-66030 Models for Calculating the Effect of Environment on Fatigue Life (Fen) for Complex Waveforms and/or Non-Isothermal Conditions	ASME PVP2017	(Currie et al., 2017)
PVP2018-84240 Explicit Quantification of the Interaction Between the PWR Environment and Component Surface Finish in Environmental Fatigue Evaluation Methods for Austenitic Stainless Steels	ASME PVP2018	(T. Métais et al., 2018)
PVP2018-84251 Effect of Surface Condition on the Fatigue Life of Austenitic Stainless Steels in High Temperature Water Environments	ASME PVP2018	(Morley et al., 2018)
PVP2018-84879 Further Validation of the Strain-Life Weighted (SNW) Fen Method for Plant Realistic Strain and Temperature Waveforms	ASME PVP2018	(Currie et al., 2018)
PVP2019-93847 Scaling of SN Curves for Varying 'Initiation' Crack Definitions From Striation Counted Environmental Fatigue Specimens A 250 Micron Austenitic Stainless Steel SN Curve	ASME PVP2019	(Batten et al., 2019)
PVP2020-21262 Further Evidence of Margin for Environmental Effects, Termed Fen-Threshold, in the ASME Section III Design Fatigue Curve for Austenitic Stainless Steels Through the Interaction Between the PWR Environment and Surface Finish	ASME PVP2020	(McLennan et al., 2020)
PVP2020-21373 Strain Control Correction for Fatigue Testing in LWR Environments	ASME PVP2020	(Vankeerberghen et al., 2020)
PVP2022-84249 Statistical Analyses of Austenitic Stainless Steel High Cycle Fatigue Data to Support a Revised Design Factor for Design Fatigue Curve Development	ASME PVP2022	(Morley & McLennan, 2022)
PVP2023-107205 Shoulder Control for Fatigue Endurance Tests Carried Out Under Variable Amplitude Loading Conditions	ASME PVP2023	(Meldrum et al., 2023)

Initiation of very short cracks and their growth has been studied with blunt compact tension C(T) specimens having notch root radii of 0.3 or 0.5 mm. Finite element analysis was done to understand the strain field and gradient near the root of the notch, where cracks initiate. Despite a load ratio of $R=0.05$, the notch root strain field quickly approaches a condition of $R=-1$ for strain. The size of the fully-reversed strain zone is as large as 1 mm for a 10 kN applied load. (Platts, Tice, & Nicholls, 2015)

The direct current potential drop technique was used to evaluate the initiation of cracks. Note that the definition of initiation here is orders of magnitude smaller cracks than typically associated with N_{25} fatigue lives (engineering cracks of about 3 mm depth). Crack initiation between air and PWR tests, Figure 94, shows an expected trend. It is worth mentioning that in-air C(T) specimen data suggested the initiation criteria of the NUREG/CR-6909 best-fit curve to corresponds to crack lengths of the order of 300 μm which is an order of magnitude less than expected and likely explainable by an influence of the strain gradient.

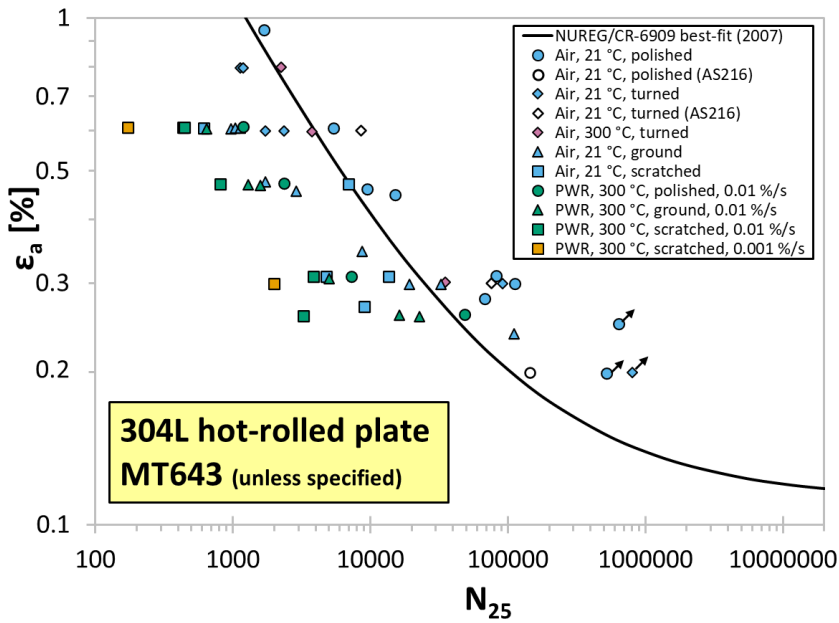


Figure 93. Effect of surface roughness in air and PWR water in Jacobs’ experiments on solid specimens. (McLennan et al., 2017; Platts, Tice, Stairmand, et al., 2015)

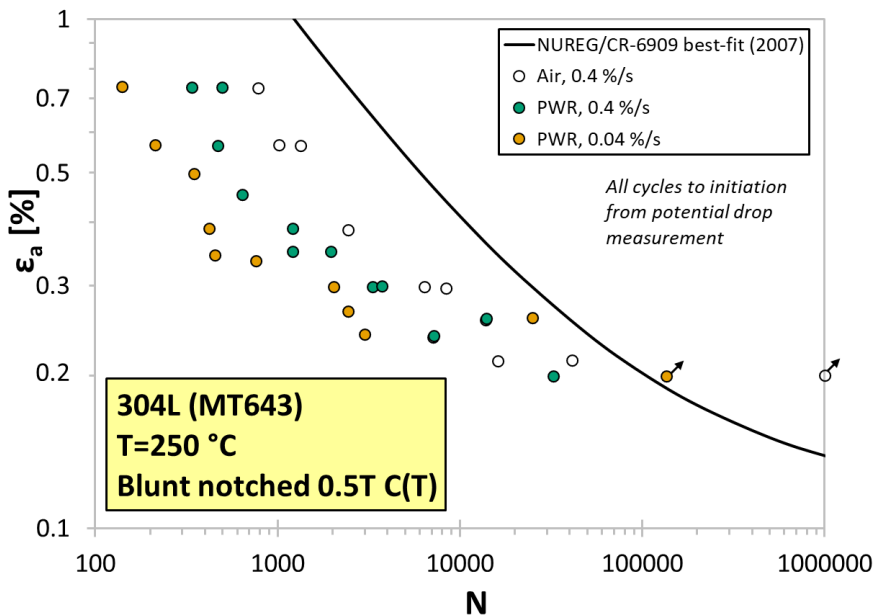


Figure 94. Cycles to very early crack initiation in air and PWR water, as measured from linear deviation in potential drop. (Platts, Tice, & Nicholls, 2015)

Much of the more recent experimental data from the UK has focused on complex waveforms and validation of advanced evaluation methods that take into account nonlinear damage accumulation within a hysteresis loop. For further details, the specific papers listed in

Table 18 should be referred. Results on domestic stainless steel batches are summarized in Figure 95 for a range of waveforms, using the so-called strain-life weighted (SNW) method. The results include in- and out-of-phase (IP & OOP) thermomechanical fatigue (TMF), realistic SIS transients and multilinear 4-stage waveforms. Though not shown here, the SNW prediction is an improvement over MRA for the complex waveforms. This work is associated with emerging approaches for EAF, which were discussed in chapter 3.3. Note that the predicted lives are based on the cast-specific fatigue curves in air, which are strictly speaking not compatible with the NUREG/CR-6909 F_{en} models.

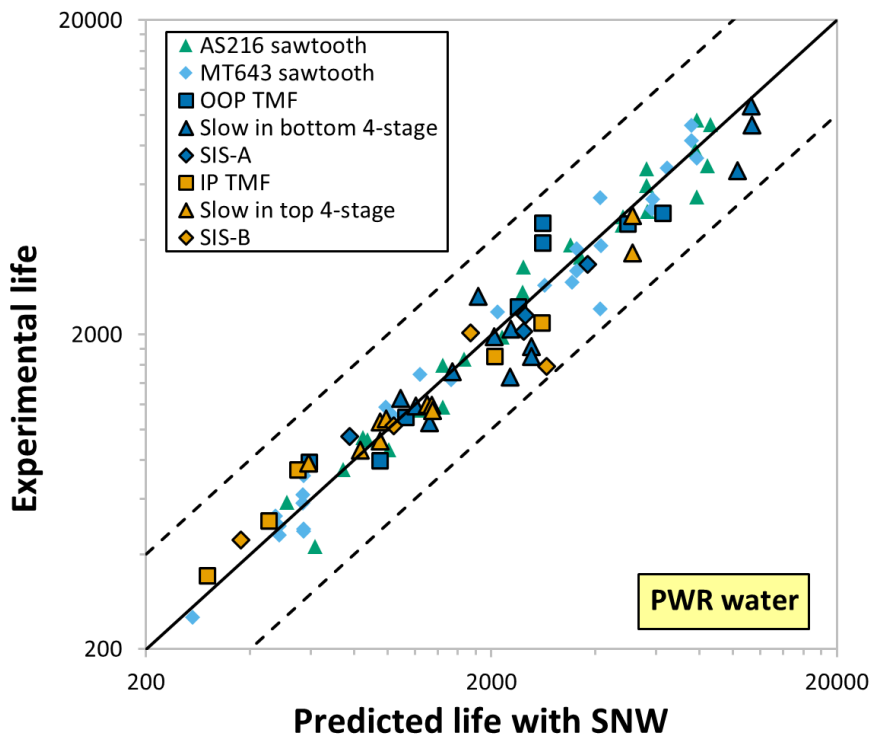


Figure 95. Comparison of complex waveform experimental lives with SNW predicted lives based on the cast-specific air curve and NUREG/CR-6909 Rev. 1 draft. (Currie et al., 2018)

During the past several years a test facility capable of thermal shock loading in simulated PWR water has been developed at Jacobs. The benefit of thermal shock loading is its relevance to actual plant loading. The hollow thermomechanical fatigue specimen has a wall thickness of 15 mm with a 6 mm inner diameter. Loading between about 300 °C and 40 °C has been reported. More details of the equipment and experimental results can be found in the publications listed in Table 19.

Table 19. UK R&D publications on a thermal shock fatigue test facility.

Paper title	Conference	Reference
PVP2016-63161 Development of a New Thermo-Mechanical Environmental Fatigue Testing Facility to Investigate the Impact of Thermal Strain Gradients on Fatigue Initiation	ASME PVP2016	(Platts et al., 2016)
Thermomechanical fatigue of hollow specimens in a light water reactor environment - latest test results and analysis	SMiRT24	(Gill, Madew, et al., 2017)
PVP2018-84923 A Thermomechanical PWR Test Facility to Investigate Thermal Shock Loading on a Small Scale Tubular Specimen	ASME PVP2018	(Gill et al., 2018)
PVP2019-93923 Fatigue Initiation of 304L Stainless Steel Subject to Thermal Shock Loading in a PWR Environment	ASME PVP2019	(Gill et al., 2019)

PVP2022-84760 Thermomechanical fatigue initiation in nuclear grades of austenitic stainless steel using plant realistic loading	ASME PVP2022	(Trownson et al., 2022)
---	--------------	-------------------------

UK partners have during the last decade had a strong presence as part of European consortiums studying EAF. Two projects have been funded by the European Atomic Energy Community. The INCEFA-PLUS (Increasing Safety in NPPs by Covering Gaps in Environmental Fatigue Assessment) project generated over 200 experimental results in air and simulated PWR water with such focus areas as mean strain, hold time and surface roughness effects. Part of the test data was generated at Jacobs' Warrington laboratory. A summary of the whole project is given in Mottershead et al. (2020) and lessons learned from the data in Cuvilliez et al. (2020). The follow-up project INCEFA-SCALE (Increasing Safety in NPPs by Covering Gaps in Environmental Fatigue Assessment - Focusing on Gaps Between Laboratory Data and Component-Scale) is in progress and focuses on transferability issues between small specimens and plant components. A summary of project contents is given in McLennan et al. (2022). In this project Jacobs is again one of the partners generating experimental data.

The ongoing project INCEFA-SCALE is strongly linked to the component testing program, which is coordinated by EPRI (Steininger et al., 2017). Data from the component testing will be used to benchmark the proposed methods developed in the European project.

The solid specimen design used by Jacobs is shown in Figure 96. Similarly to the AREVA specimen design, there are machined flanges at the specimen shoulders for LVDT attachment. The LVDT measuring distance is about 54.5 mm. Figure 97 shows the test setup. The average value of the two LVDT outputs is used for displacement control, which is based on calibration tests in air using dual extensometry (Platts, Tice, Stairmand, et al., 2015).

A limited amount of testing using a hollow specimen design has also been done. Those results were presented as part of the discussion on tubular specimen use in chapter 4.2. Further discussion on the potential reasons for specimen type effects between solid and hollow can be found in Gill, James et al. (2017).

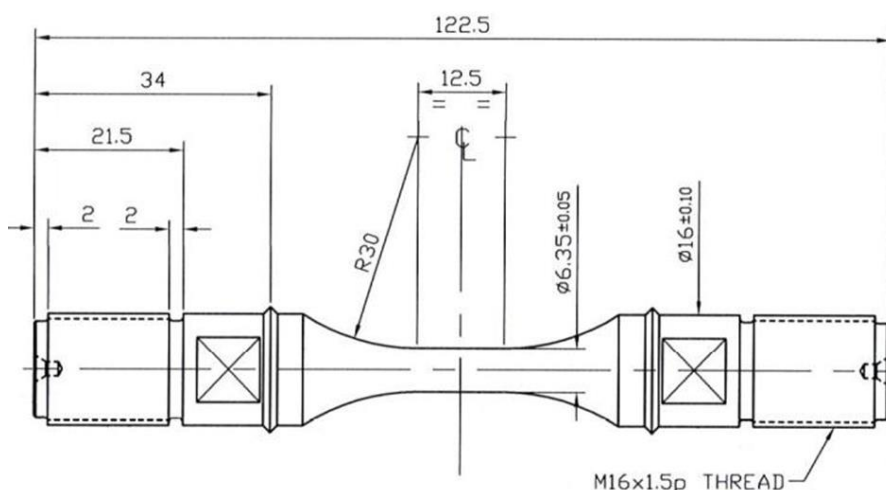


Figure 96. Jacobs EAF specimen design. (Twite et al., 2016)

Representative data from one of the shoulder displacement-to-gauge strain calibration tests is shown in Figure 98 and Figure 99. The data is digitized and should not be taken as absolute. For constant strain amplitude 0.3 % (with $R=-1$) at the gauge length, the shoulder displacement is non-constant and non-symmetric. McLennan et al. (2017) explain that the half-life shoulder displacement minimum and maximum values were used to control EAF tests. For the tests at room temperature in air, at $\epsilon_a=0.3$ % on material heat MT643 the half-life amplitude was measured to be 71.9 μm .

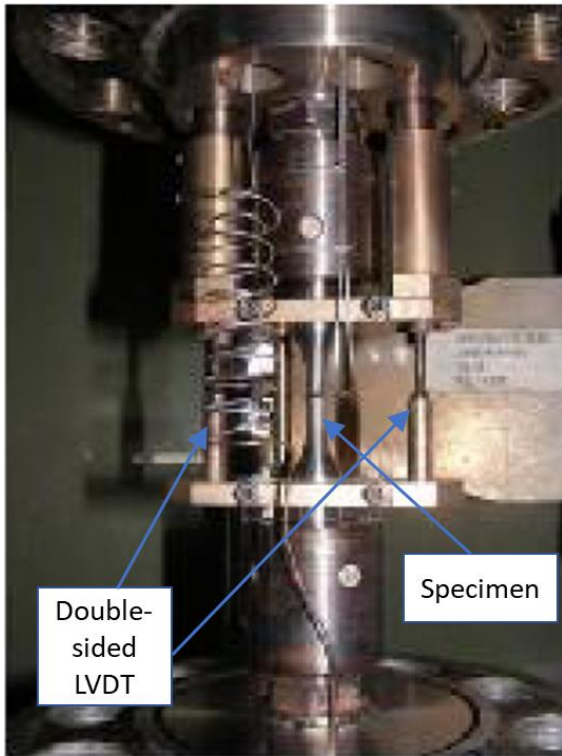


Figure 97. Jacobs shoulder displacement measurement for EAF testing. Modified from Platts, Tice, Stairmand, et al. (2015).

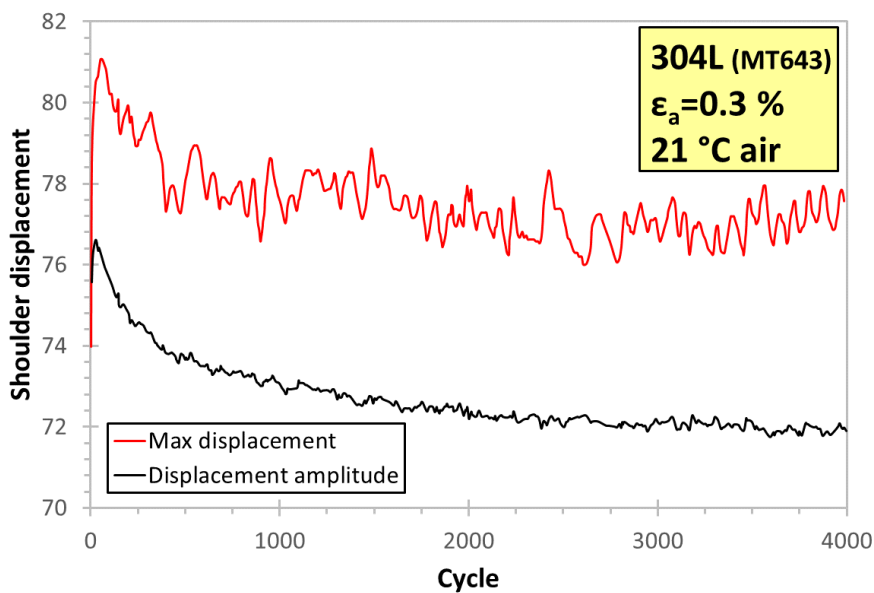


Figure 98. Shoulder displacement in a Jacobs calibration test with dual extensometry. (McLennan et al., 2017)

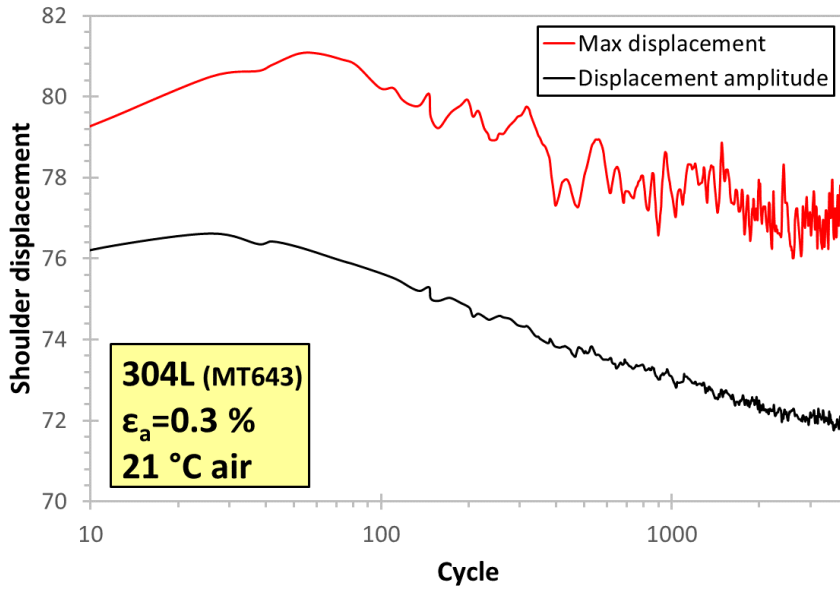


Figure 99. Same as Figure 98 but with logarithmic cycle scale.

Shoulder calibration values and a trend for materials beyond stainless steel is shown in Figure 100. Error bands of $\pm 10\%$ have been added to this figure to indicate residual uncertainty in the half-life shoulder displacement, despite careful dual extensometer tests. With the best-fit calibration curve, the strain-amplitude may be off-target by as much as 20% (relatively) in the presented data. The blue curve in Figure 100 represents the theoretical displacement in the 12.5 mm uniform gauge length and the green curve the remaining displacement, which spreads over the rounding of the specimens up to the LVDT attachment points on the shoulders. The effective gauge length, based on the shoulder displacement best-fit curve up to 1% strain amplitude, is between 21–25 mm. In practice this means that 50–60% of displacement applied at the shoulders translates to strain in the uniform gauge length.

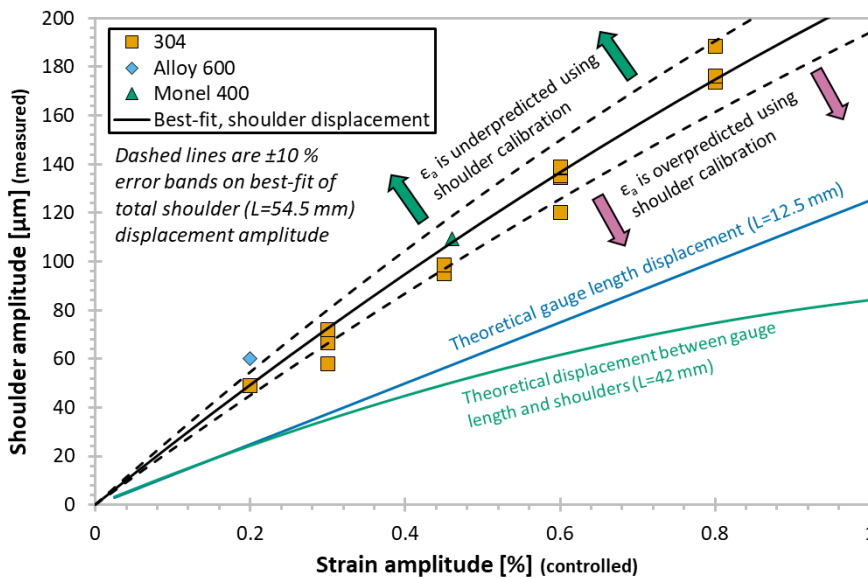


Figure 100. Comparison between gauge strain amplitude and shoulder displacement for a range of materials. Modified from Vankeerberghen et al. (2020). L =measuring distance.

4.5 Finland

4.5.1 Research of environmental fatigue in Finland – 50 years of experience

A Reactor Materials Research Division (RMR) was founded in 1970 by the Ministry of Trade and Industry and soon organized within VTT to provide scientific and technical support for licensing and operation of the first four nuclear reactors in Finland to be commissioned in 1977 – 1982. The first critical research capabilities were ramped up during the 70's. A key facility consisting of three autoclaves with circulation of controlled water chemistry was operable by year 1978. One of the autoclaves was used for fatigue research, Figure 101. The early research in simulated reactor coolant environments focused on corrosion performance of zirconium in fuel cladding and stainless steel in cladding of reactor pressure vessel. Testing of crack growth by corrosion fatigue and/or stress corrosion mechanisms in pre-cracked compact tension C(T) specimens increased preparedness for safe operation and inspection approaches in accordance with the ASME Code Section XI. Material performance in real environmental and loading conditions became a strategic mission of the RMR group and the Metals Laboratory as a whole.

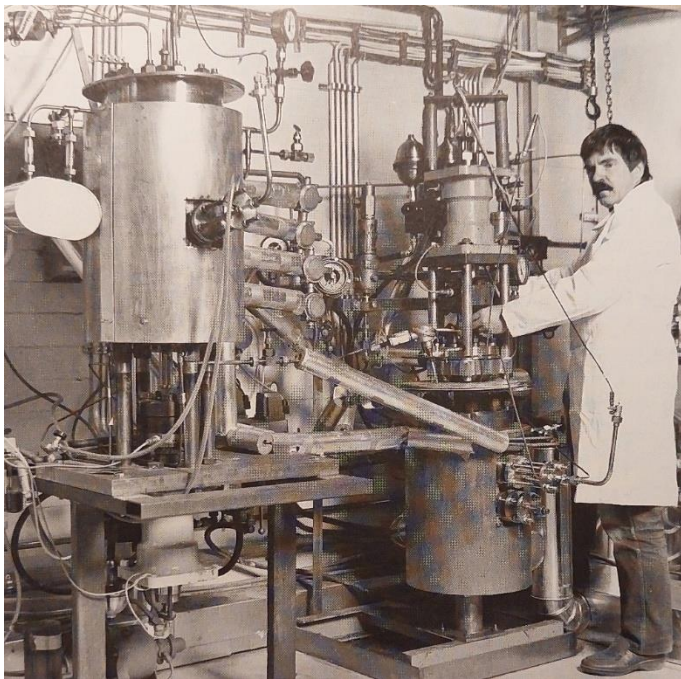


Figure 101. VTT Metals Laboratory's fatigue autoclave facility in late 1970's; Lauri Selin adjusting the VA1.

After about 20 years of research on fatigue crack growth in BWR and VVER coolant water chemistries, the focus into crack growth (ASME XI) turned to EAF in fatigue design and usage assessment (ASME III). A wide range of autoclave facilities and long experience in conducting fatigue crack growth testing in simulated reactor coolant environments formed a solid basis in developing an experimental capability for strain controlled axial fatigue (LCF). The first prototype EAF device was commissioned in 1999 (J. Solin et al., 2003), but a need for further development was soon emphasized when STUK issued the updated YVL Guide 3.5 (STUK, 2002). The target was set into meeting the essential requirements of LCF standard test method in ASTM E606 (ASTM, 2021), to obtain EAF data which is compatible with the ASME III, RCC-M and similar design codes. As a result, the 'FaBello' facility was commissioned in 2010 (J. Solin, Alhainen, et al., 2011).

VTT has adopted an active role, not only in developing experimental capabilities, but also in improving the transferability of laboratory results to NPP components through understanding the history, status and expected progress in international Codes and Standards related to management of fatigue in general, and environmental assisted fatigue (EAF) in design and operation of reactors. Today, the experimental

campaigns on EAF have been paused for a major revision and capacity upgrade of the facility, but they are expected to continue soon. The pause in experimental research has enabled addressing resources in closer review and reporting of the evolution of Codes and Standards and current research efforts internationally – also for writing the current report.

Strain controlled axial fatigue in environment and air – 25 years in focus

The first strain controlled EAF tests were conducted using miniature specimens of 316NG alloy in four prototype EAF devices immersed in a common autoclave circulated with simulated PWR coolant at 320°C. These results were published in the 3rd Int. Conference on Fatigue of Reactor Components (Solin, J. et al., 2005) and again in the ASME PVP, Pressure Vessel and Piping Conference (J. P. Solin, 2006) supplemented by results for titanium stabilized alloy 321 in simulated VVER coolant at 293°C. Those results are not repeated here, because they could not be considered valid according to the ASTM E606 procedure. Miniature 4mm diameter specimens (ASTM E606: “d≥6”) were used in turned condition without polishing, because mounting of the strain measuring LVDT required a grooved surface. The obtained fatigue lives were conservative, but to an unknown extent. However, comparisons between the steel batches within the same test campaign can be justified and one difference is worth of mentioning: the alloy 321 showed tendency for secondary cyclic hardening at room temperature in air, not in hot water; but the alloy 316NG showed an opposite tendency by secondary hardening in hot water and not at room temperature in air.

The first EAF tests using standard sized polished specimens in the upgraded ‘FaBello’ facility were part of the “*Technical Programme of EON Case on Thermal Transients – Environmental Fatigue*” commissioned by the EON Kernkraft GmbH. At the time, accounting for the environmental effects in the fatigue concept for Olkiluoto 3 remained a responsibility of the vendor. Research on EAF performance of the OL3 primary piping materials is planned to be conducted also at VTT after commissioning of the ‘FaVite’ facility which replaces the ‘FaBello’ with improved design and capacity. Meanwhile, VTT has performed EAF research also on non-stabilized 304L and 316L steels within domestic and European research projects.

In following an overview of the results and lessons learned within the EAF research at VTT will be given. We begin with selected parts of the German EON Kernkraft program (2008-2020). All results were made public and presented in 17 papers in the annual ASME PVP Conferences 2009-2020, as summarized by Solin, Seppänen and Mayinger (2020). Selected results on the non-stabilized steels and SIS transient simulations with alloys 304L and 347 will then follow. The results of ongoing research on the non-stabilized steels, including 316L sampled from piping manufactured for the EPR-1600 primary piping, will be summarized in near future. Annual progress of the research has been reported in ASME PVP Conferences 2016-2013 (Seppänen et al., 2023) and will continue next summer. The related PVP papers can be easily found by naming Seppänen as the first author.

4.5.2 Niobium stabilized alloy 1.4550 (comparable to AISI 347)

The U.S. NRC Regulatory Guide 1.207 Rev.0 (U.S. NRC, 2007a) referred to the environmental penalty factors and new design fatigue curve for stainless steels proposed in the NUREG/CR-6909 Rev.0 (O. K. Chopra & Shack, 2007). This raised concerns on eventual need of related updates in the German Kerntechnischer Ausschuss, KTA. The terms of fatigue design were revised in the KTA Standard issue 2013-11 (KTA, 2013) based on extensive experimental research focused on the stabilized stainless steels applied as primary piping in German NPP’s. EON Kernkraft shipped to VTT three meters of pipe cut from a surge line spare part and 2.5m of it was used for research on fatigue, EAF and effects of constant power operation versus load follow. The latter topic, referred as “effects of holds” occupied a major part of the experiments, but is omitted here.

Fatigue specimens were sampled longitudinally from a solution annealed 1.4550 (comparable to AISI 347) stabilized austenitic stainless steel pipe manufactured to $\phi 360 \times 32$ mm cross section. The microstructure consists of variable grain sizes typical for a heavy component. Niobium carbides are segregated to grain boundaries and only small droplets of delta ferrite were found sparsely distributed. Chemical composition

and tensile test results are shown in Table 20 and Table 21. The specimens were turned and polished to dimensions shown in Figure 102.

Table 20. Composition of the test material 1.4550 (X6CrNiNb1810 mod; \approx AISI 347) wt. %.

C	N	Si	Mn	Cr	Ni	Mo	Nb	P	S
0.031	0.021	0.235	1.885	17.30	10.29	0.405	0.357	0.030	0.004

Table 21. Tensile test results from the material report and measured at VTT. (J. Solin et al., 2009).

Data source	E [GPa]	R _{p0.2} [MPa]	R _m [MPa]
VTT: minimum of 5 tests	195	224	535
VTT: maximum of 5 tests	201	249	559
VTT: average of 5 tests	197	238	544
material report / pipe	-	239	548
material report / melt	-	251	544

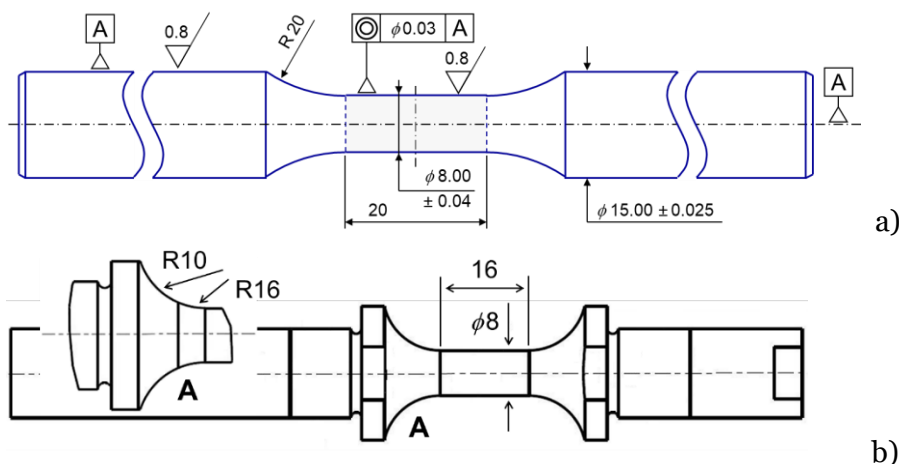


Figure 102. The specimen geometries; a) for tests in air, b) for EAF tests in 'FaBello'.

Reference curve and cyclic hardening

An experimental strain-life reference curve was determined at room temperature and fitted to the Coffin-Manson-Basquin model which suited well for the LCF regime and revealed that the Langer model with an endurance limit instead of a horizontal line (exponent $b \geq -0.001$) would have worked as well. A solid endurance limit was observed at $\epsilon_a \leq 0.19\%$, but it was conservatively estimated to $\epsilon_e = 0.18\%$ which matches with the regression curve value at $N_{25} \approx 10^6$ and is 1.6 times the value $\epsilon_e = 0.112\%$ selected for the reference curve proposed in NUREG/CR-6909, Figure 103.

The sharp bend in the ϵ - N curve towards infinite lives and a reinforced endurance limit was explained by pronounced secondary hardening which begins well before 100 000 cycles and gradually reduces the plastic strain amplitude, Figure 104. In addition, cyclic hardening mitigates strain localization, which often precedes crack initiation. Secondary cyclic hardening was later observed also when slow rate straining was applied at elevated temperature, both in air and in PWR water environment. This kind of hardening is affected by thermally activated time dependent processes when sufficient time is available. Furthermore, it seems that hardening is more pronounced in PWR water environment, Figure 105.

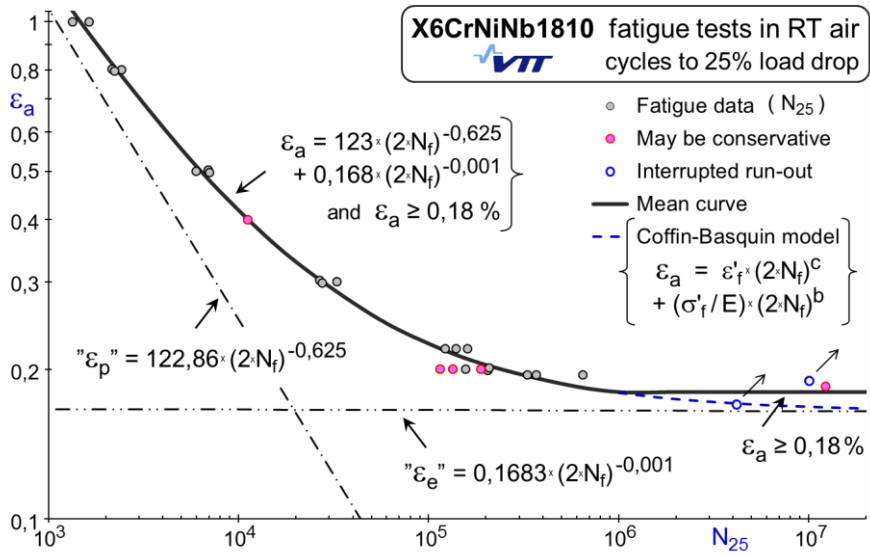


Figure 103. Strain life data and experimental reference curve. Solin et al. (2009), later edited.

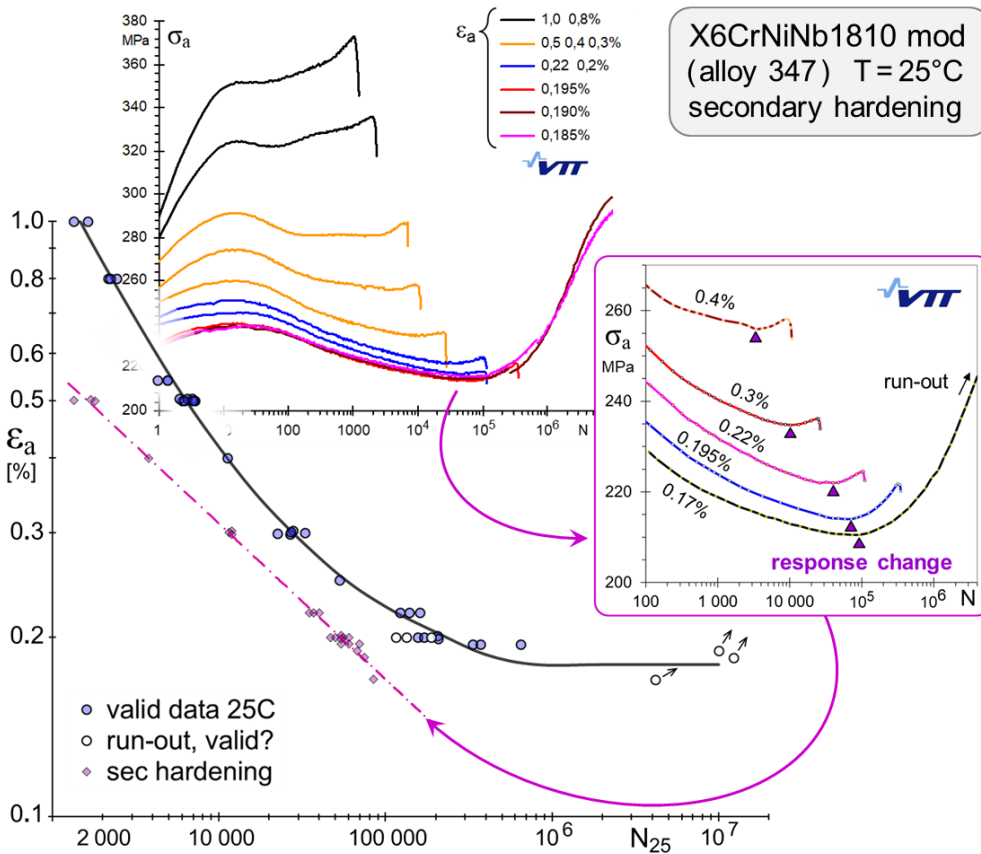


Figure 104. Stress responses at room temperature and cycles to begin of secondary hardening shown in comparison with the $\epsilon - N$ curve. Solin et al. (2009), later composed and edited.

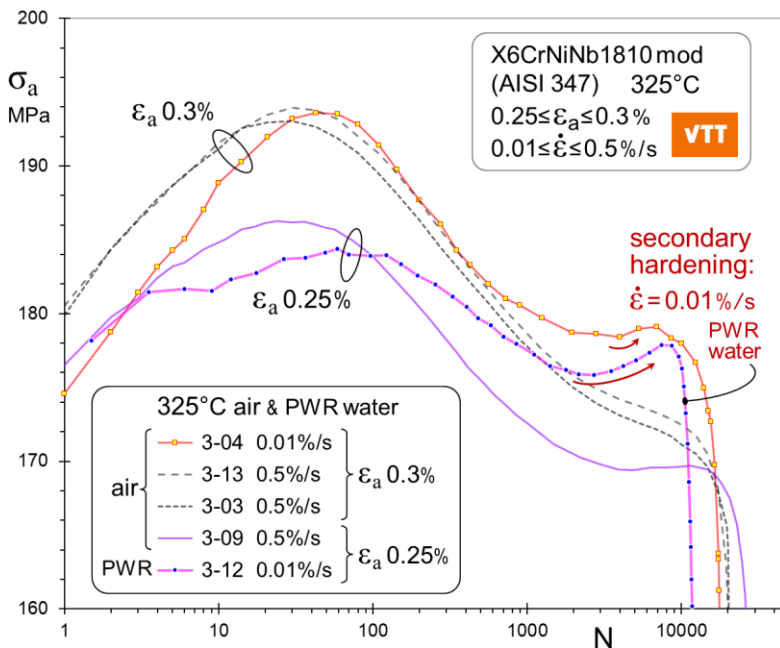


Figure 105. Stress responses for alloy 347 at 325°C. Reduced strain rate promotes secondary hardening both in air and in simulated PWR coolant water. Edited from Solin et al. (2013).

Effect of temperature

Fundamentals of metal fatigue analysis applied in automotive industries and many other fields assume that softer steels usually perform better in LCF regime and harder steels in HCF. The strain-life fatigue curve for a quenched and tempered QT steel determined over the LCF/HCF transition range tends to rotate round a fixed rotation point when hardness of the steel is modified by altering the tempering temperature after quenching (Bannantine et al., 1989). Similar effects can be expected also when material strength is altered through changes in test temperature. But if fatigue endurance are compared close to the rotation point, temperature effects will vanish. This may partially explain, why it was concluded that the effects of temperature can be ignored (O. K. Chopra & Shack, 2007), also ignoring the critical remarks by Louis F. Coffin (1978), who criticized extension of the LCF curve beyond million cycles and noted that the fatigue limits are affected by the temperature.

Temperature effects on the fatigue mean curve for this AISI 347 type piping material were studied through a test campaign covering altogether six temperatures in air. The data shown in Figure 106 did not justify regression analysis for separate reference curves at each temperature, but the results demonstrated indisputable temperature effects in air, just as predicted:

- The “ ϵ -N curve rotation model” describes well the temperature effects in a finite life region up to about 100 000 cycles with a rotation point at $\epsilon_a \approx 0.5\%$ and $N_{25} \approx 6000$ cycles, but
- all ϵ -N curves seem to bend towards temperature dependent endurance limits within the range of $10^5 < N_{25} < 10^6$ cycles, and
- an inverse correlation between temperature and endurance limit was demonstrated.

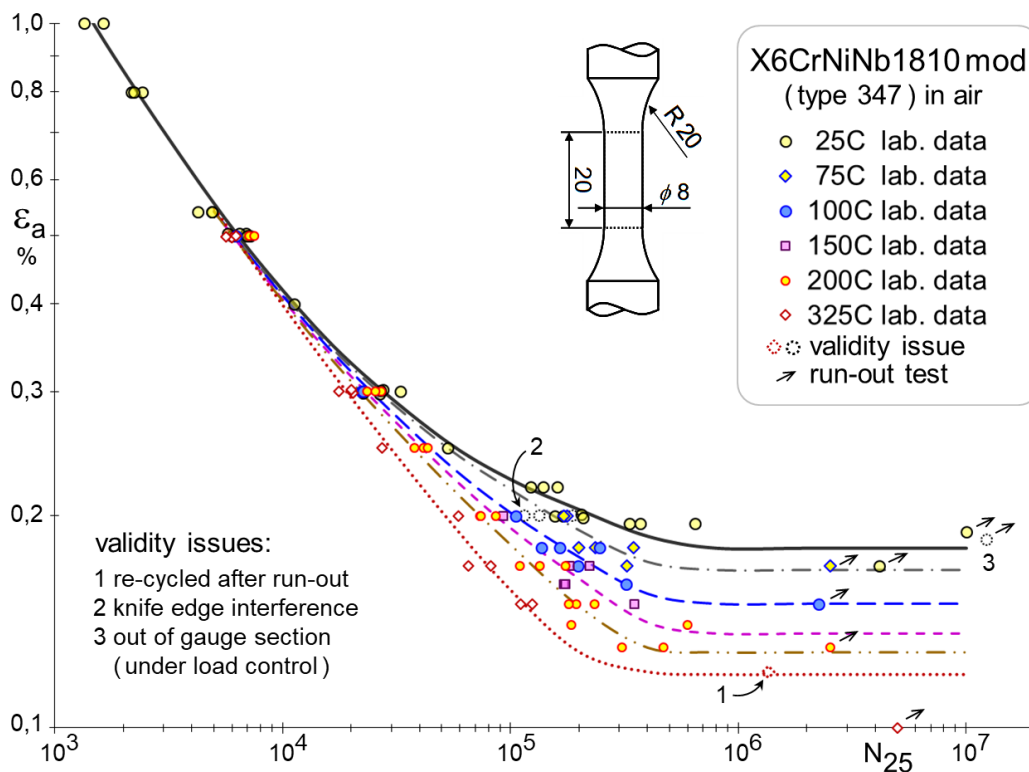


Figure 106. Strain life data for the niobium stabilized stainless steel. The trend curves at elevated temperatures are “hand drawn” assuming consistent temperature dependency of the fatigue limit. Edited from Solin et al. (2013).

Effect of environment

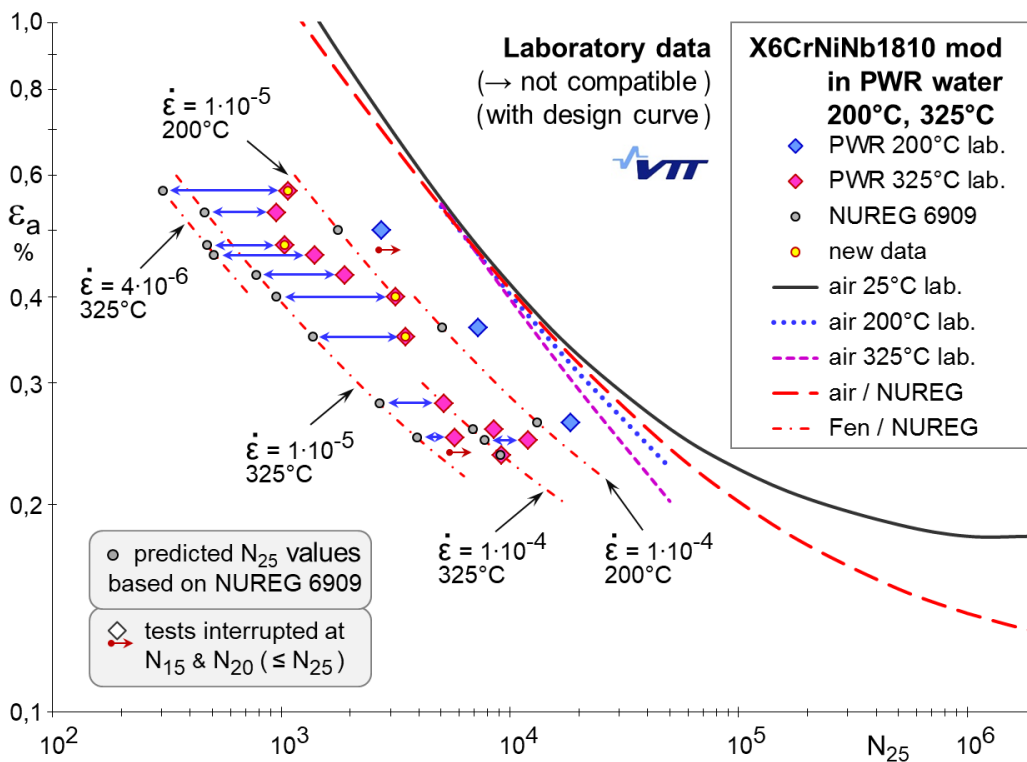
The VTT results in simulated PWR water deviated notably from the fatigue lives predicted according to the NUREG/CR-6909, reports. The tests focused on the conservative edge of experimental parameters; very low strain rates applied at 325°C. The aim was not to measure environmental penalty factors relevant for real transients in PWR plants, but to estimate conservativeness in the proposed F_{en} models, understand mechanisms responsible for reduction of fatigue lives in environment and ultimately to develop mechanism informed EAF models. The experiments confirmed measurable environmental effects but were unable to reach as high F_{en} factors as calculated according to the report NUREG/CR-6909 (O. K. Chopra & Shack, 2007) and the code JSME S NF1-2009 (JSME, 2009).

The tests were performed in simulated PWR water chemistry according to VGB recommendation (VGB, 2006). Dissolved oxygen was reduced from the water by hydrogen bubbling before feeding to the pressurized hot circulation loop. Presoaking was continued for minimum a week until the oxide growth on specimen surface was completed, and corrosion potential stabilized before beginning of cyclic straining. The EAF test parameters are listed in Table 22. The results are presented in Figure 107 as raw data in comparison with F_{en} factors calculated for each applied temperature and strain rate according to NUREG/CR-6909 (O. K. Chopra & Shack, 2007). All but one test at the lowest strain amplitude ($\epsilon_a = 0.24\%$; $\dot{\epsilon} = 0.01\%/s$) endured clearly longer than predicted.

Table 22. Test parameters and obtained fatigue lives for the AISI 347 type German piping material.

environment	T_{fatigue} °C	strain signal	strain rate %/s	strain ampl. %	fatigue life N_{25}	notes
PWR	325	triangle	0,0004	0,48	1 040	
PWR	325	triangle	0,0004	0,46	1 400	
PWR	325	triangle	0,0004	0,57	1 070	
PWR	325	triangle	0,001	0,25	5 765	#
PWR	325	triangle	0,001	0,28	5 145	
PWR	325	triangle	0,001	0,53	955	
PWR	325	triangle	0,001	0,43	1 900	
PWR	325	triangle	0,001	0,35	3 510	
PWR	325	triangle	0,001	0,40	3 170	
PWR	325	triangle	0,01	0,24	9 200	
PWR	325	triangle	0,01	0,26	8 500	
PWR	325	triangle	0,01	0,25	12 000	
PWR	200	triangle	0,001	0,50	2 736	#
PWR	200	triangle	0,01	0,26	18 500	
PWR	200	triangle	0,01	0,36	7 280	

N_{25} is conservative, because test was interrupted before N_{25} criterion is met
 # N_{15} criterion was met at time of interruption


 Figure 107. The EAF results shown as raw data in comparison with F_{en} factors calculated for each applied temperature and strain rate according to NUREG/CR-6909, rev.0. (J. Solin et al., 2016)

4.5.3 Material response – effect of strain rate and environment

Several interesting and important findings on material response to cyclic straining at elevated temperature and in PWR water environment are summarized in Figure 108 and further clarified in Figure 109. The findings are introduced here using the data obtained with the niobium stabilized alloy 347, but as shown in Figure 110, similar changes and trends in stress responses were measured also with non-stabilized alloy 304L.

The first striking observation is the inverse correlation between strain rate and stress response. It is typically observed that an increase of displacement rate during a tensile test increases the flow stress, and this happens also with this material, but a reverse effect in cyclic response is seen in Figure 108. The lowest black curve represents a normal LCF test in air conducted at strain rate of 0.5%/s ($\dot{\epsilon}=5\cdot 10^{-3}$). A decrease of the strain rate by 1/50 to $\dot{\epsilon}=1\cdot 10^{-4}$ increases the cycle-based initial hardening and the following softening rates. This suggests that thermally activated time and temperature dependent processes – such as diffusion – contribute to the cyclic hardening and softening.

Secondly, further (1/10 or 1/100) decreases of the strain rate do not change the response in air. This means that the contribution of time dependent thermally activated processes is saturated already when $\dot{\epsilon}=1\cdot 10^{-4}$. However, the saturation is removed, and time dependent processes affect the cyclic hardening and softening responses significantly more effectively in PWR water environment. The maximum stress amplitude obtained by the lowest strain rate ($\dot{\epsilon}=4\cdot 10^{-6}$) is 17% higher than in air. This reveals new kind of environmental effects in bulk of the specimen.

The effects of environment prior to the formation of growing crack(s) have typically been discussed in terms related to the interfaces between the metal, oxide film and water environment, how cyclic deformation breaks the oxide film, enabling the environment to affect crack initiation. However, the different stress responses in air and water cannot be explained solely by load carrying capacity of the oxide film. It is a 'bulk effect', which requires time dependent thermally activated diffusion between the water interface and bulk of the specimen.

So far, no direct evidence on the mechanisms is available and dedicated research would be needed to explain if and how the changed stress strain response affects fatigue usage in laboratory specimens and in reactor components. One plausible hypothesis is that the correlation between the strain rate and stress response depends on the content of soluble hydrogen in the steel matrix. In PWR water environment the content of hydrogen increases by intake of the hydrogen released due to oxide growth during the pre-soaking period, eventually also during the test.

If intake and diffusion of hydrogen play roles in the laboratory tests, this hypothesis opens new questions related to transferability of EAF laboratory test results to reactor components in plant operation. The laboratory results were conducted using 8 mm round bars immersed in PWR water. If the bulk material response is affected by hydrogen or vacancies migrating from the specimen surface, the situation might be much different in a thick-walled component. For example, hydrogen absorbed during oxide growth on the inner surface of a pipe might slowly diffuse and escape from the outer side during long times at operation temperature. On the other hand, if the pre-soaking period plays a major role in hydrogen intake, the material performance and even fatigue life in an EAF test might be affected by the pre-soaking procedure, or exclusion of it. At VTT, the target duration of pre-soaking has been a week, except in a collaborative project, where immediate test start was applied for interlaboratory procedure harmonization.

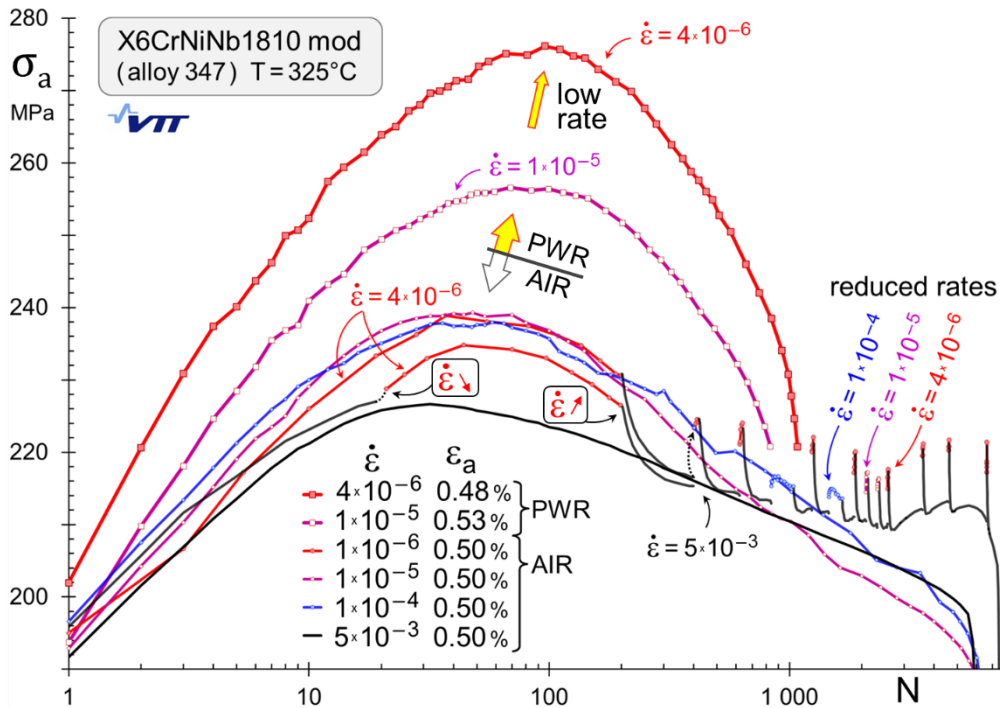


Figure 108. Stress responses during LCF tests at 325°C in air and in simulated PWR water. Systematic effects of strain rate were demonstrated in both environments. PWR water cancels the low-rate saturation and amplifies the change of response. (J. Solin et al., 2018) [note: repeated and confirming test data is omitted for clarity]

Material response – effect on remote or direct strain control

Even though the results are reported as function of strain amplitude, majority of EAF tests have not been performed under strain control. The controlled displacements may be measured outside of the autoclave (e.g. ANL, Figure 46) or at the specimen shoulders inside the autoclave (e.g. Areva, Figure 92), rather than within the smooth gauge section of the specimen. Because the strains within and out of the gauge section are not linearly related, a change in stress response affects the applied strain. Thus, the stress responses can be correctly measured only when direct strain control is applied, which probably explains why the ‘bulk effects’ in EAF tests have long remained hidden.

One certain consequence of the rate dependent responses is that in air at higher strain rates performed strain versus displacement calibrations are not correct for EAF testing in PWR water under remote strain control. Selected responses shown in Figure 108 are repeated in Figure 109 on a linear cycle scale together with a schematic comparison between different test control modes. Assuming that the desired strain amplitude is obtained by start of the cyclic softening phase, it seems that direct strain control results to longest fatigue life in environment. Softening would result to continuous increase and localisation of strains during a load-controlled test. During a strain-controlled test, softening is compensated by reduction of load amplitude. Conducting EAF tests under displacement control provides a broad range of mixed modes as the controlled displacement contains also increasing diameter parts of the specimen and the local ratios of elastic and plastic strains are functions of time and location.

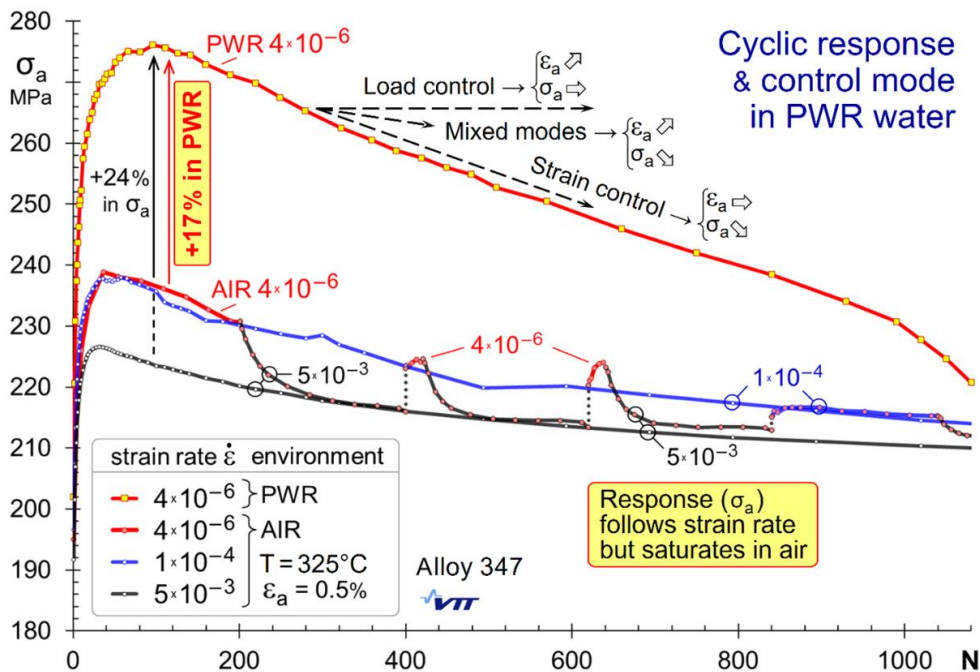


Figure 109. Selected stress responses shown in Figure 108 on linear cycle scale. A schematic comparison between different test control modes is included (J. Solin et al., 2018).

Material response – instantaneous response to rate changes

Instantaneously changing stress responses shown in Figure 108 and in Figure 109 revealed a particularly interesting repeatability. Reduction of strain rate increases the stress response within duration of one cycle, but an increase of strain rate leads to gradual relaxation of stress response, and this can be repeated by astonishing repeatability as many times as desired. Drawing of one specimen response in Figure 108 was discontinued for clarity at 400 cycles, because the follow-up responses would be overlapped with the response of another specimen. VTT experiments using variable strain rates were limited to tests in air, but we cannot see reasons why similar effects would not occur also in PWR water.

Material response – heat specific or more generic behaviour

The above presented effect of environment on material response is not limited to the niobium stabilized alloy 347. A similar difference between stress responses in air and PWR water was measured with a non-stabilized alloy 304L, as shown in Figure 110. Furthermore, these responses were measured during simulation of SIS transients aimed to resemble EAF relevant fatigue transients in PWR plants better than the standard laboratory tests. The cycles consisted of double-rate linear rate ramps. (Seppänen et al., 2019)

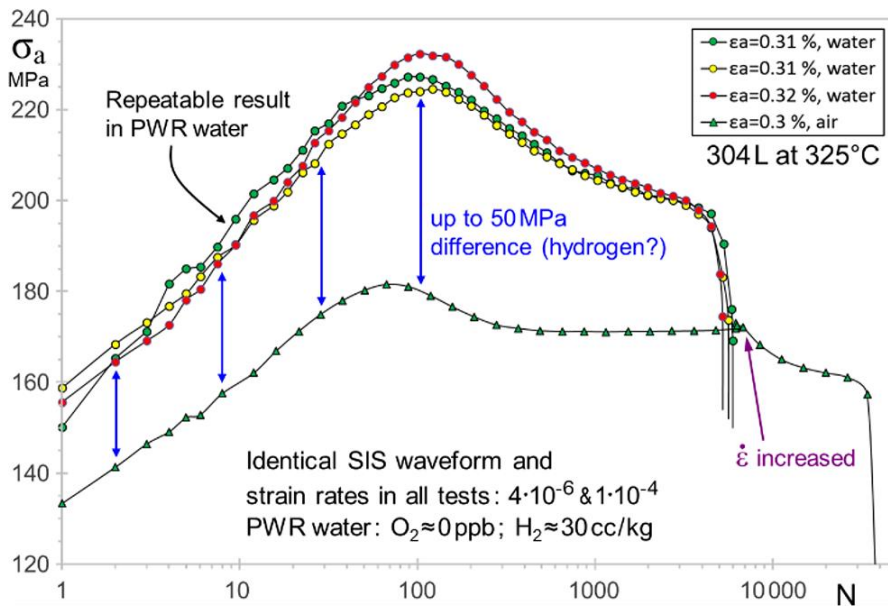


Figure 110. Stress responses of non-stabilized alloy 304L during simplified simulations of SIS transients at 325°C in air and in simulated PWR water. (Seppänen et al., 2019) (figure from presentation slides)

4.5.4 Alloy 304L and simulation on transients in plant

Another batch of 347 alloy specimens were used for simplified “SIS waveform” experiments in PWR water in comparison of alloy 304L (Seppänen et al., 2017). These double-rate experiments for both alloys together will be explained after introduction of the experimental details with alloy 304L.

The test material was non-stabilized AISI 304L stainless steel extracted in the longitudinal direction from a 30 mm thick rolled plate. The specimens were turned and polished to dimensions shown in Figure 102. Chemical composition is given in Table 23. Room temperature yield and tensile strengths were 220 and 555 MPa, modulus of elasticity was 196 GPa.

Table 23. Composition of the AISI 304L test material; wt. %.

C	N	Si	Mn	Cr	Ni	Mo	Cu	P	S
0.029	0.056	0.37	1.86	18	10	0.04	0.02	0.029	0.004

Best-fit curves for the 304L material batch were defined at three temperatures. All three curves deviate from the reference curve underlying the present stainless steel “mandatory design curve” in ASME III and fit in a model suggesting rotation of the finite life curves at elevated temperatures, Figure 111.

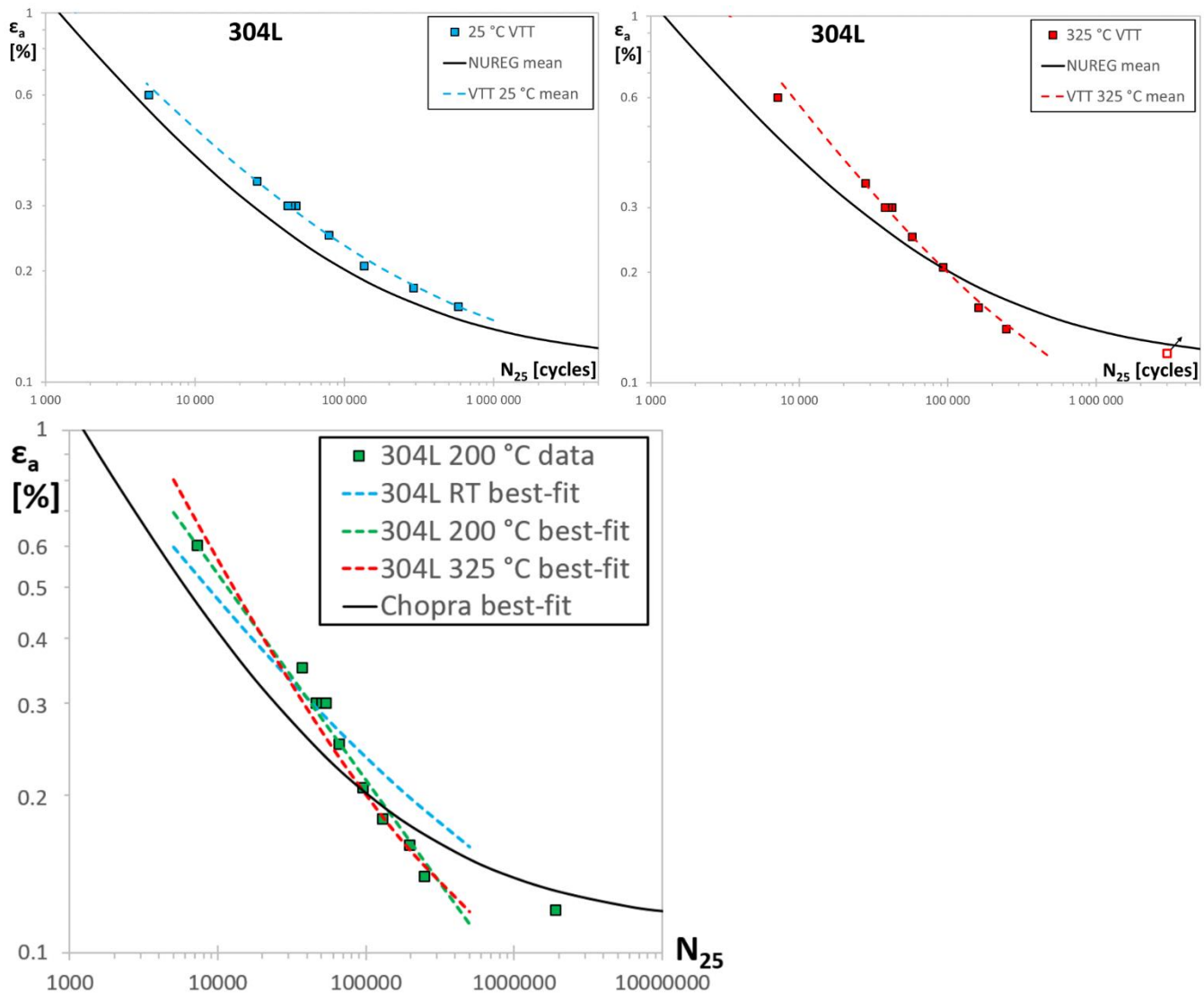


Figure 111. Fatigue results for alloy 304L in air; a) at room temperature, b) 325 °C, c) 200 °C.

Fatigue assessment for a reactor component is based on the design fatigue curve applicable for the material, e.g., the “mandatory design curve” for stainless steel given in the ASME III. The related ‘reference curve’ – not given in the ASME Code but obviously inherited from the NUREG/CR-6909 report and shown in Figure 111 – plays an important role in the F_{en} approach because the F_{en} factors are determined from the measured differences between endurance values in environment and reference values in air. Transferable F_{en} factors result when the reference values ($N_{25,air}$ at RT) match with the ‘reference curve’ underlying the design curve derived from the ‘reference curve’ with help of transferability margins. In other words, the design curve, reference curve and F_{en} factors shall all be compatible to build a solid and transferable F_{en} approach.

Questions arise when aiming to determine F_{en} factors applicable for the studied 304L heat.

- Are the resulting F_{en} factors applicable for the 304L heat, if the results in environment are compared with the NUREG reference curve?
- The compared fatigue lives in air and environment are naturally best determined with the same material, but are the resulting F_{en} factors compatible with the design curve in ASME III, if the best-fit curve does not match with the NUREG reference curve?

Seppänen et al. (2021) performed example fatigue usage calculations including environmental effects to compare the effect of using material and temperature dependent reference curves in place of the reference curve behind ASME III. Using five different criteria and the modified rate approach, it was demonstrated that in many instances the predicted CUF_{en} can be reduced with simple measures. Calculations suggest that further reduction is attainable by applying threshold conditions to strain and probably by applying more scientific mechanism-based F_{en} models as well. The effect on fatigue usage is often not significant for short term but becomes increasingly critical for long-term operation to 80 years or beyond. Relief in fatigue usage by factors in excess of $80/60=1.33$ (for a lifetime extension by 20 years) were demonstrated to be possible by the approaches studied.

Reconsideration of the wording “mandatory design curves” in design codes and/or guidance for plant life management is recommended. Alloy type or plant-specific experimental data should be allowed (or recommended), when available. Wording of original EAF guidance in Finland (STUK, 2002) questioned the use of ASME III design curves for EAF and requested that “fatigue assessment shall be based on S-N -curves applicable to each material”. This may be understood supporting our recommendation. Furthermore, the 2013 revision of the German KTA Standard was constructed such that the design curve for stabilized stainless steels is based on new German and VTT data and ASME III design curve is applied for non-stabilized stainless steels. It is also assumed that inclusion of proposed design curves in the 1963 edition of ASME III was rather aimed to help the designer than limiting the designer’s choices in “design by analysis”. This view is supported by notes on designer responsibilities on accounting, e.g., for effects of corrosive environment and radiation.

4.5.5 Transferability of F_{en} factors for fatigue transients in plant

A schematic of thermal transients caused by reversed abrupt changes of water temperature was shown in Figure 35. Such fatigue transients occur, e.g., in the surge line when flow direction between the pressurizer and hot leg changes in PWR reactors. Similar ‘SIS transients’ with larger temperature differences occur in the safety injection system, when cooler water is temporarily injected to the primary loop. SIS transients played a central role in the AREVA experimental EAF program and fatigue concept for Olkiluoto 3 EPR project in Finland as explained by Le Duff et al. (2008, 2009, 2010) and Hytönen (2011).

An example waveform for simulating the increasing strain ramps of SIS transients (compressive path shortened for test acceleration) was shown in Figure 27 and repeated in Figure 112. The rising ramp begins from compression after entry of hot water, gradually slows down during evening of the thermal gradient in depth and is fast completed by start of cold flow. The instantaneous F_{en} factors calculated in a detailed analysis are affected by changes in strain rate (from minimum to mean) and cooler temperature (from mean to maximum).

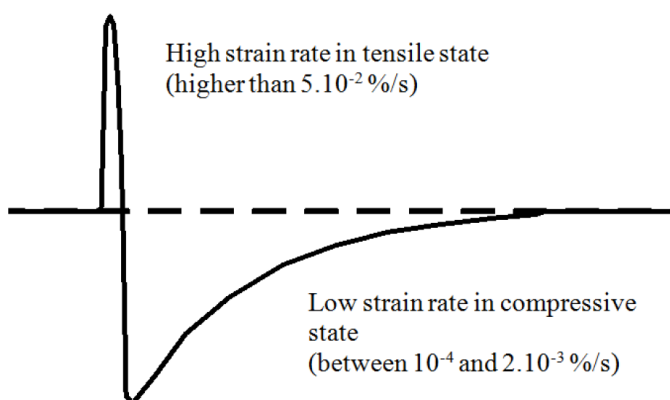


Figure 112. Schematic of simulated SIS transient. (Métais et al., 2015)

Simulation of nonlinear strain transients (at constant temperature) would have been possible in the VTT ‘FaBello’ facility, but detail analysis of results for scientific modelling would become complex and require large numbers of repeated tests. Therefore, the sequence was simplified to three constant rate parts, two rates during pulling and just one compressing rate which is claimed ineffective and ignored in the current F_{en} models. Comparison between two applied strain sequences is shown in Figure 113.

The experiments were performed at 325 °C in simulated PWR water with strain amplitude of 0.30% and strain rates of 0.01 %/s and 0.0004 %/s ($1 \cdot 10^{-4} \text{ s}^{-1}$ & $4 \cdot 10^{-6} \text{ s}^{-1}$) changed at $\epsilon = -0.15\%$ during the tensile ramp. The order of applied rates (slow-fast or fast-slow) affected the length of slow ramp and predicted F_{en} factor. As expected, the results indicated that the environmental effect is pronounced when the slow strain rate is placed at the end of tensile ramp where a larger share of strain is plastic. The NUREG/CR-6909 prediction of F_{en} factor was reasonably good for the fast-slow tests, but clearly conservative for the slow-fast sequence which is better representative for the SIS transients in the plant. The results also support our hypothesis for an improved F_{en} model suggesting that elastic strain may have negligible effects also in LWR coolant and rate of plastic strain affects more than rate of elastic strain.

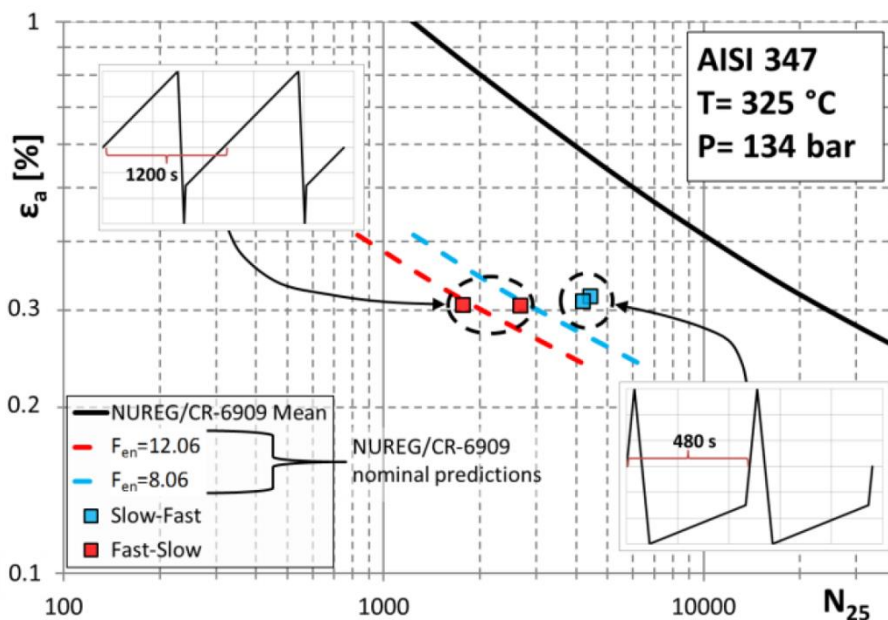


Figure 113. Linearised and modified SIS transients for experimental research and development of mechanism informed EAF model. (Seppänen et al., 2017)

A scientific model based on plastic strain rate may be unattractive to apply in design calculations. In practice, a total strain rate model based on mechanistic understanding from $F_{en} = f(\dot{\epsilon}_{pl})$ may be a tempting alternative. This is actually comparable to the way strain-life curves were constructed: LCF was explained as function of plastic strain – $N_f = f(\epsilon_{a,pl})$ (Coffin, 1953, 1954; Manson, 1953, 1954), but the design curve itself was based on total strain amplitude, which is simpler to apply in the design by analysis procedure. A constant strain amplitude was inserted to the ϵ - N curve (Langer, 1962). It was named as ‘endurance limit’, but one might call it also as an “insensitive” strain because from mechanism and model point of view it is an add-on strain amplitude which does not contribute to fatigue.

As introduced in chapter 3.3.3, Seppänen et al. (2018) developed a model based on the assumption that F_{en} is a function of temperature, water chemistry and plastic strain rate, but using total strain rate as the parameter in calculation. This was realized by introducing an “insensitive strain range” to improve the correlation between the resulting F_{en} factors and plastic components of strain. The portion of “insensitive strain range” is approximated as linear function of the strain amplitude: $\Delta\epsilon_{in}/2\epsilon_a = -0.44 \cdot \epsilon_a + 0.65$. The insensitive portion of strain is 60% when $\epsilon_a = 0.11\%$, which is close approaching the endurance limits of the studied material batches (304L and 347) at the operation temperature, decreases to 52% when $\epsilon_a = 0.3\%$ and to 39% when $\epsilon_a = 0.6\%$, which is often the largest amplitude considered for EAF.

At the time available experimental EAF results measured at VTT for two alloys of stainless steel (304L and 347) were used for developing and testing the tentative VTT F_{en} model. Altogether 16 specimens were strained at 325 °C in simulated PWR coolant water using simplified SIS transient sequences as listed in Table 24. The water chemistry parameters are shown in Table 25. The F_{en} factors ‘predicted’² using the tentative VTT F_{en} model were compared with the experimental results and F_{en} factors calculated according to the NUREG/CR-6909, rev1 (2018). Results of the comparison are shown in Figure 114.

Table 24. Test matrix for double-rate simulations of SIS transients.

alloy type	test type	rising ramp rate		change at $\epsilon =$ %	strain amplitude ϵ_a %		reference PVP paper
		ϵ_1 %/s	ϵ_2 %/s		nominal	measured	
304L	SIS slow-fast	0.0004	0.01	-0.15%	0.3	0.32 ; 0.32	PVP2018 -84197
304L	SIS fast-slow	0.01	0.0004	-0.15%	0.3	0.31 ; 0.31	
304L	SIS slow-fast	0.0004	0.01	$\pm 0\%$	0.3	0.31 ; 0.31 ; 0.32	PVP2010 -93279
304L	constant	0.0069	0.0069	none	0.21	0.21	
347	SIS slow-fast	0.0004	0.01	$\pm 0\%$	0.35	0.30 ; 0.33	PVP2016 -63294
347	SIS fast-slow	0.01	0.0004	$\pm 0\%$	0.35	0.30 ; 0.39	
347	SIS slow-fast	0.0004	0.01	-0.15%	0.3	0.32 ; 0.32	PVP2017 -65374
347	SIS fast-slow	0.01	0.0004	-0.15%	0.3	0.31 ; 0.31	

Table 25. PWR water chemistry parameters for double-rate simulations of SIS transients.

Description	Value
Temperature	325 °C
Pressure	134 bar
Water pH at RT	≈ 6.1
Water conductivity	17–20 $\mu\text{S}/\text{cm}$
Dissolved O ₂	≈ 0 ppb
Dissolved H ₂	30 cc/kg
Boric acid	1200 ppm
Lithium	2 ppm

² The term ‘predicted’ is not used in strict scientific meaning. Significant part of the data was collected before calculation.

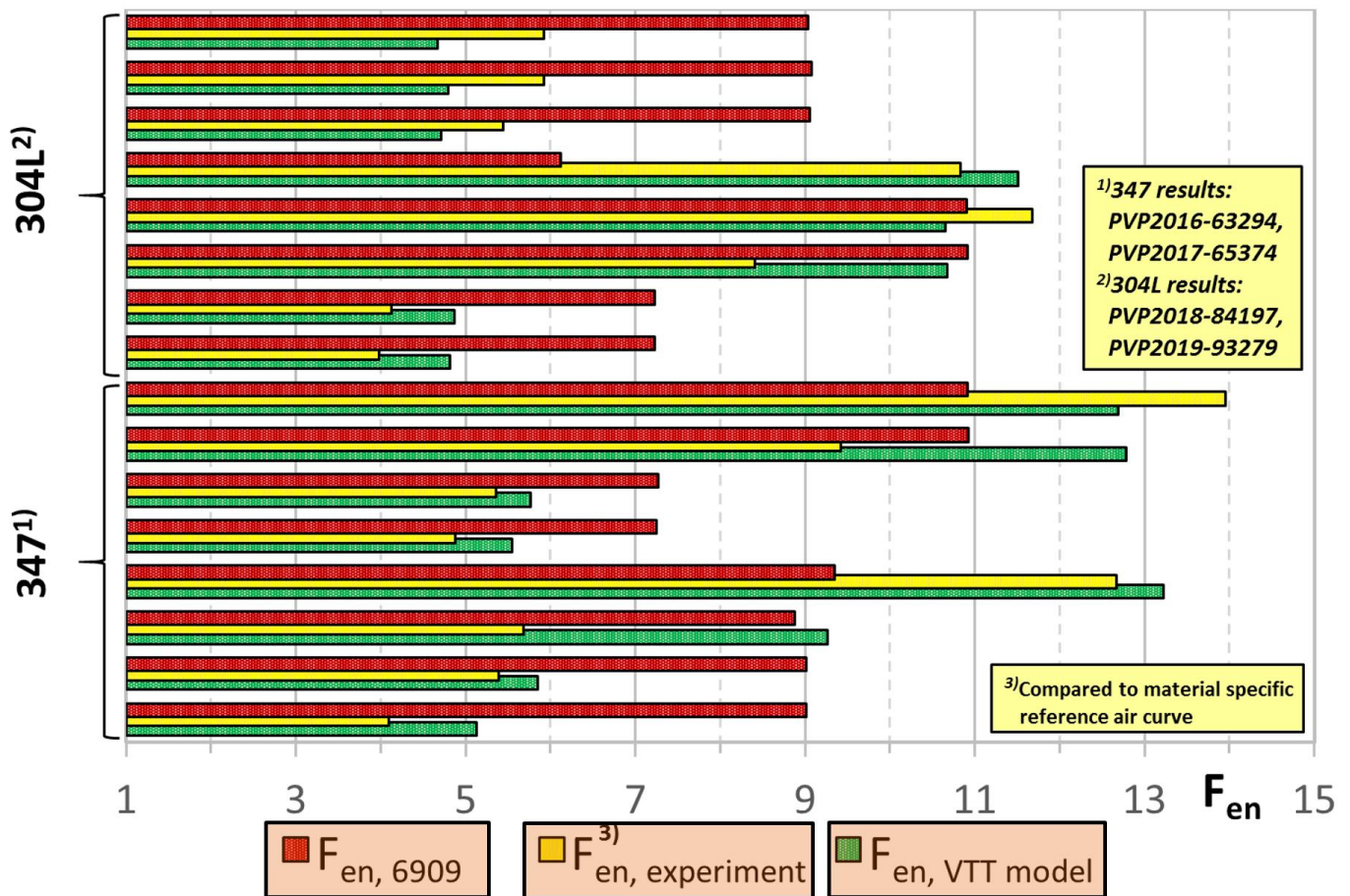


Figure 114. F_{en} factors calculated according to NUREG/CR-6909, Rev. 1 (O. K. Chopra & Stevens, 2018), predicted using a tentative VTT model and determined from experimental results in simulated PWR coolant water.

The status of VTT model verification was summarized in Figure 36 and is repeated in Figure 115. A clear F_{en} model improvement was achieved when compared to the NUREG/CR-6909, rev1 (2018). Both models resulted to predictions on the conservative side in average. The experimental fatigue lives were bounded by scatter bands of $0.8 \cdot N_{25, VTTmodel} \leq N_{25} \leq 1.6 \cdot N_{25, VTTmodel}$, and $0.8 \cdot N_{25, NUREG} \leq N_{25} \leq 3.2 \cdot N_{25, NUREG}$, i.e., within a factor of 2 (max/min) when using the VTT model and within a factor of 4 using the NUREG model. A particular improvement was achieved in modelling of the simplified simulations of SIS transient. The environmental effects measured for the more relevant slow-fast SIS simulations were overestimated using the F_{en} methodology presented in NUREG/CR-6909 Rev.1, which worked better for the unrealistic fast-slow transients. The proposed VTT model was able to differentiate between the slow-fast and fast-slow transient simulations. The model is subject to further development and tuning by help of continued research and application to design compatible experimental data. However, the analysis in Figure 115 is encouraging. The $F_{en} = f(\dot{\epsilon}_{pl})$ hypothesis may finally provide a mechanism based approach to fill some of the many identified EAF knowledge gaps.

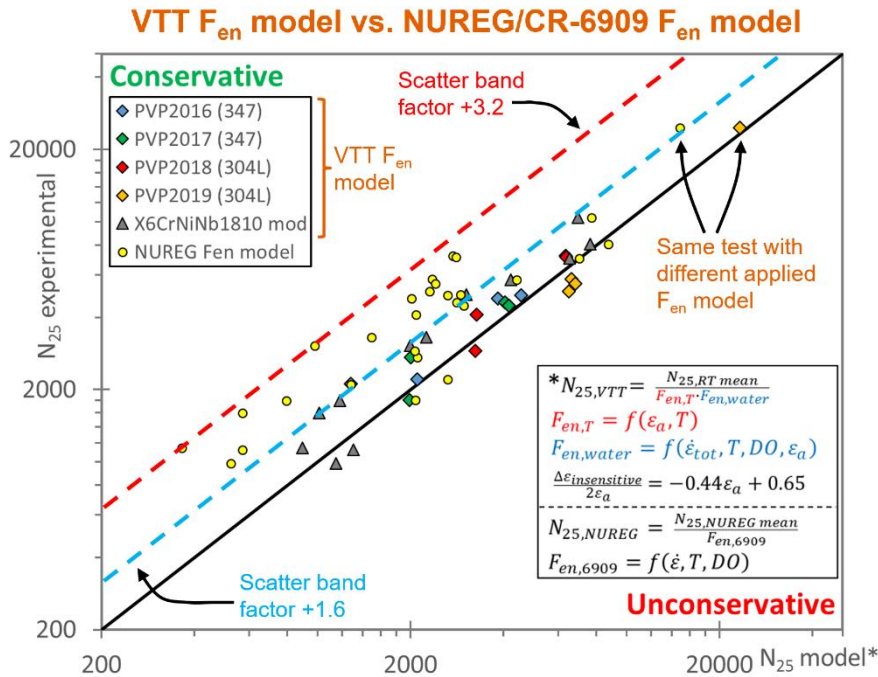


Figure 115. VTT experimental data from EAF research campaigns with stabilized and non-stabilized stainless steel batches and linearized representations of SIS transients in PWR water at 325 °C. (Seppänen et al., 2019) [a copy of Figure 36]

4.5.6 Alloy 316 L – an EPR relevant Z2 CND1812 N2 pipe

Nearly 7 m of seamless 12" Schedule 140 ($\phi 324\text{ mm} \times 28.6\text{ mm}$) stainless steel pipe was received in the solution annealed and quenched condition to be used in research of EAF and other material studies. The pipe, shown in Figure 116, fulfils the RCC-M Class 1 requirements for Z2 CND1812N2 which is roughly equivalent to AISI 316 L.

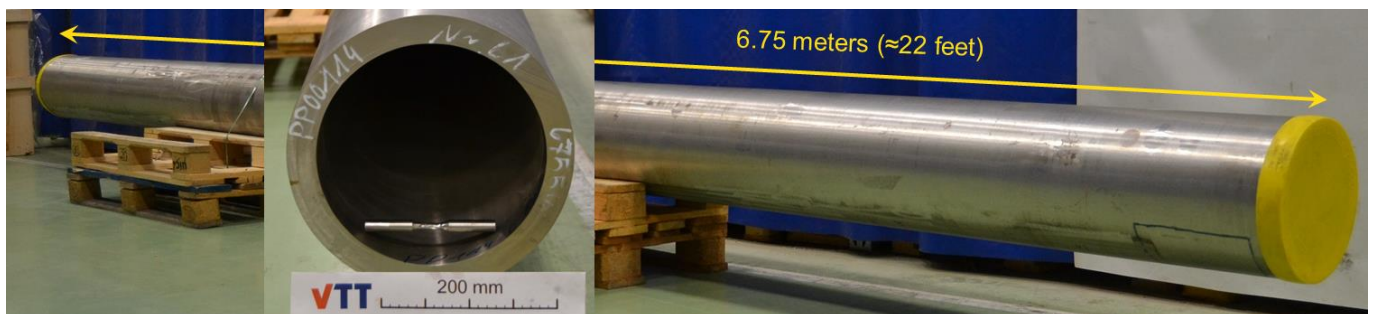


Figure 116. A Seamless 12" Schedule 140 pipe of Z2 CND1812 N2 ($\approx 316\text{ L}$) stainless steel.

Sampling and basic material characterisation

A longitudinal and rotational coordinate system was applied for sampling and careful characterization of mechanical, metallographical and other properties of the pipe material. Tensile and fatigue specimens (Figure 102) were sampled longitudinally from 200 mm long rings extracted and sectioned to 36 sector samples as close to the inner surface as feasible. The centre axis of LCF or tensile specimen is at $\approx 9\text{ mm}$ and closest gauge surface at $\approx 5\text{ mm}$ depth from the pipe inner surface.

Chemical composition from product analysis in the material report is given in Table 26. The microstructure consists of a range of grain sizes with numerous twins and an average grain size $G=6$. Room temperature tensile test were performed from both edged (rings A and ZZ) and in middle (ring P) from 4 rotation angle directions in 90° intervals. The averaged results are shown in Table 27. The yield and tensile strengths at the edge ZZ are lowest measured from the pipe, and in line with the material report. The tests performed at very slow rates resulted to higher tensile strength and elongation – as expected. The tensile curves were determined in engineering and true stress strain units, Figure 117 (a).

Table 26. Composition of the Z2 CND1812 N2 ($\approx 316L$) stainless steel; wt. %.

C	N	Si	Mn	Cr	Ni	Mo	Cu	P	S
0.028	0.08	0.39	1.81	17.1	12.03	2.27	0.56	0.022	0.002

Table 27. Average room temperature tensile test result from different parts of the pipe.

Z2 CND1812 N2 Sample source & strain rate 2 ($\epsilon > 2\%$)	Location in pipe length				room temp.
	edge "A" 0,25%/s	middle "P" 0,25%/s	middle "P" 0,0025%/s	edge "ZZ" 0,25%/s	Material report
E [GPa]	197	196	196	197	–
R_{p0.2} [MPa]	278	287	276	270	267
R_m [MPa]	586	585	592	571	574
A₅ [%]	53	55	68	56	54
Z [%]	75	77	77	79	81

Fatigue performance and LCF reference for EAF

The EAF test campaigns in simulated PWR coolant environments are about to be started soon after the delayed revitalisation maintenance and upgrade of VTT EAF facility. Meanwhile, the LCF performance in air at room temperature and 300°C has been studied to collect appropriate reference data for EAF testing and F_{en} model development. The LCF test campaign has been broad with multiple carefully sampled tests to obtain confident reference curves and to document the variation of cyclic responses and endurance within the pipe.

Cyclic stress strain curves (CSSC) at early hardened ($N \approx 150$) and at half-life stages were determined using the spectrum straining method at room temperature, Figure 117 (b). A quasi random 50 cycle block where $\epsilon_a \leq 0.6\%$ (or scaled to $\epsilon_a \leq 0.3\%$) was repeated until a drop of 25% in load carrying capacity of the specimen was measured. Comparisons with the monotonic tensile curves and CSSC determined from constant amplitude LCF data reveal differences between the three types of stress responses. The cyclic softening is illustrated by shift of the CSSC down from the hardened stage to half-life.

Strain-life reference curves were determined by strain-controlled constant amplitude fatigue tests at room temperature and 300°C . The resulting curves and shown and compared with the reference curves connected to the ASME III stainless steel Design Fatigue Curves before and after the revision in 2010, Figure 118. Like alloys 347 and 304L (Figure 106 and Figure 111), the curves seem to rotate as function of temperature and cross at the border zone between LCF and HCF regimes.

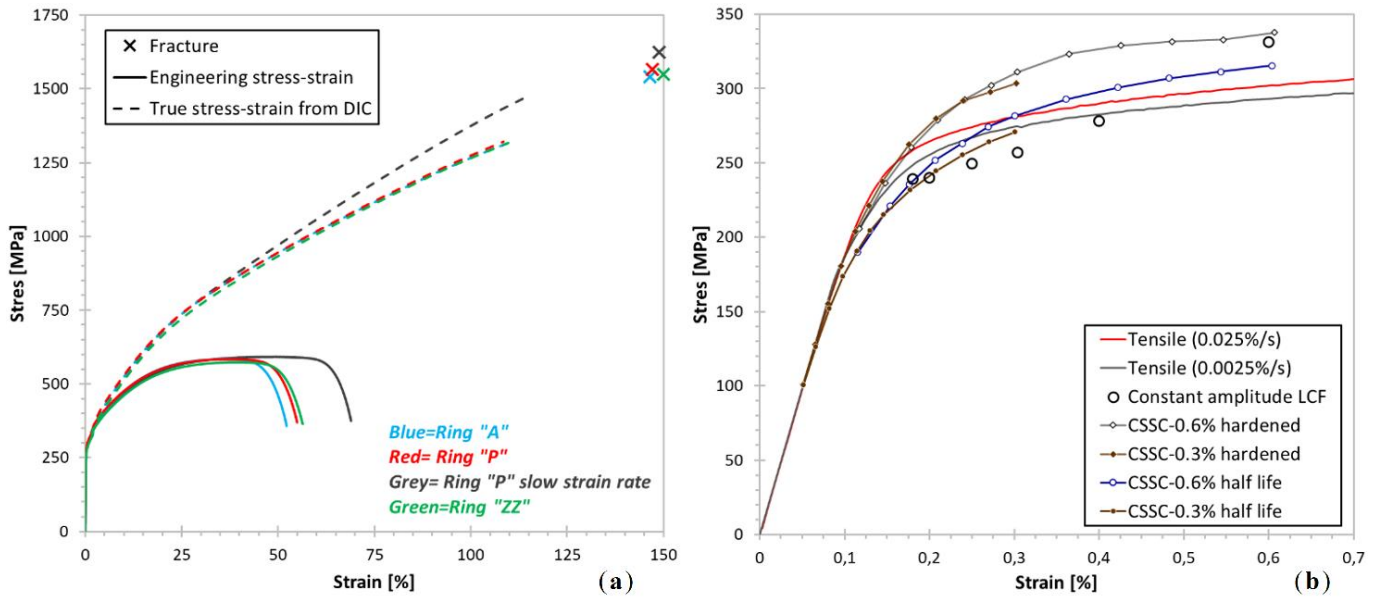


Figure 117. A selection of monotonic tensile curves (a) and cyclic stress strain curves (b) at RT.

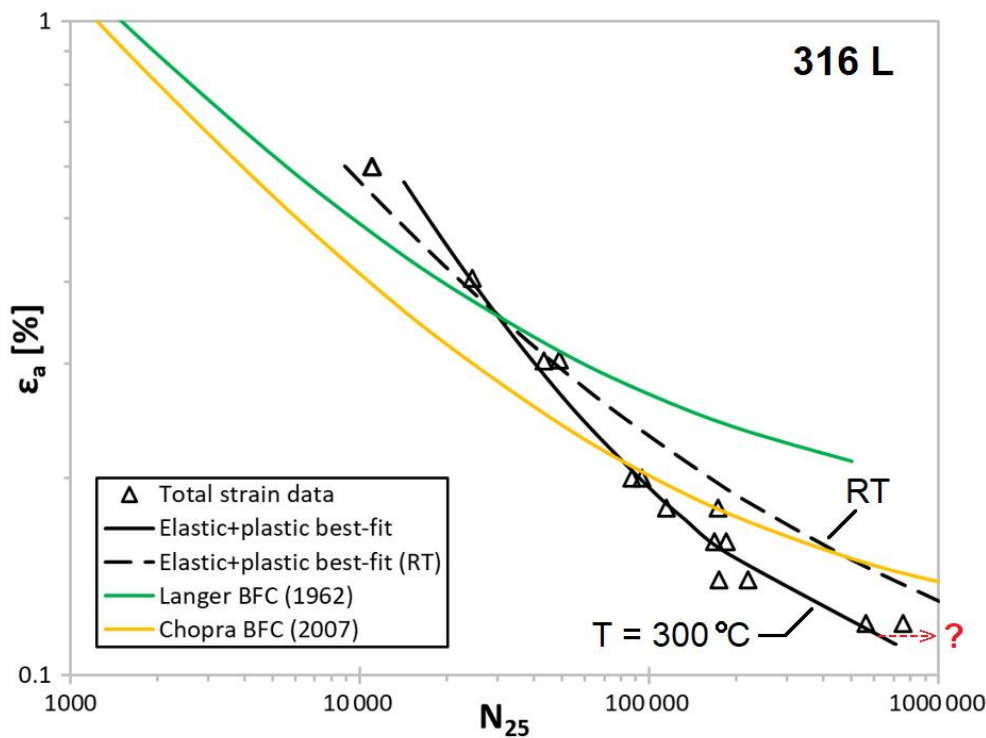


Figure 118. ϵ - N reference curves at room temperature and 300°C compared to the reference curves connected to the ASME III stainless steel DFC before and after 2010.

Cyclic hardening – effects of alloy, temperature, environment and strain rate

The “LCF” testing was extended to low strain amplitudes resulting to endurance approaching million cycles at 300°C. Straightforward extrapolation of the regression mean curve for ϵ - N data at 300°C would suggest a low endurance limit value. However, the measured stress responses in HCF regime at 300°C reveal that 99.9% of cycles were consistently spent during secondary hardening, Figure 119. During the tests at $\epsilon_{a,tot}=0.12\%$ the plastic strain amplitude decreases from $\epsilon_{a,pl}=0.028\%$ to 0.018%, probably even

more during tests at $\epsilon_{a,tot} < 0.12\%$. This gives a reason to assume that further testing could reveal a trend change and an endurance limit. However, multiple long duration (1-3 months) test would be required for confirming the endurance limit hypothesis.

The measured cyclic stress responses at different temperatures and comparison with other grades of stainless steels deserve attention. Two first stages are common for all annealed steel batches: initial cyclic hardening, typically for 10 to 100 cycles, followed by cyclic softening. The softening phase may continue until loss of load capacity due to crack growth, or a trend change to 'secondary hardening'. Figure 120 demonstrates how the responses of this 316L heat are separated depending on temperature. Secondary hardening is observed at 300 °C, but not at room temperature. In contrast, Figure 104 showed pronounced secondary hardening of niobium stabilized 347 alloy at room temperature, but absent, when normal strain rate was applied at 325 °C. However, secondary hardening was promoted by reduced strain rate at 325 °C in air, and even more in simulated PWR coolant water, Figure 105. Results for a French alloy 304L in air and PWR water at GE further complement the picture. Examples of the hardening and softening stress response in air and PWR water were shown in Figure 82 and Figure 83 at 300 °C and 150 °C, respectively. The strain-controlled tests at GE clearly demonstrated that in otherwise identical experiments the stress response is not the same in air and PWR water, (Solomon, Amzallag, DeLair, et al., 2005a).

The responses in PWR water are compiled together in Figure 121. Against a common assumption, but in line with VTT results for 347 and 304L, the initial hardening is faster and continues longer at 300 °C than at 150 °C when $\epsilon_a = 0.5\%$ and $\epsilon_a \approx 0.25\%$. As expected, the fatigue endurance (N_{25}) is shorter at 300 °C, except for the lowest amplitudes for which pronounced secondary hardening and longer fatigue endurance is measured at 300 °C. An unconfirmed mechanism is responsible for different effects of temperature, environment, and strain rate on initial and secondary cyclic hardening of the studied alloys. However, the results shown in Figure 121, Figure 120, Figure 110, and Figure 108 leave no doubt about contribution of thermally activated time dependent processes.

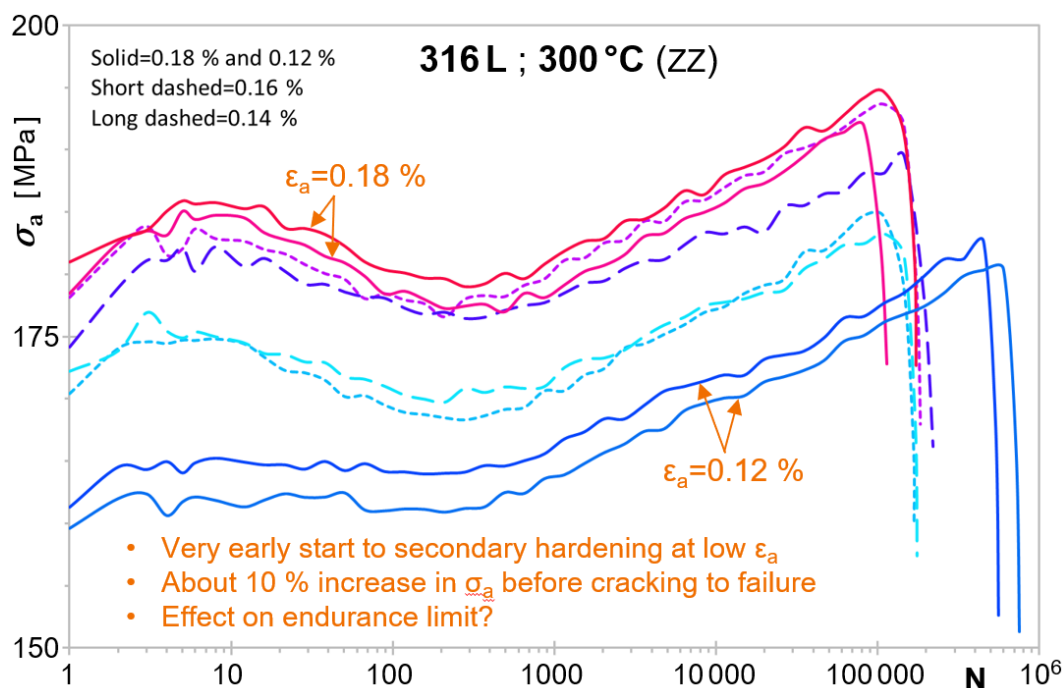


Figure 119. Stress responses during low strain amplitude tests at 300 °C.

Phase transformation from meta-stable austenite to martensite during cyclic straining has been generally assumed responsible or at least a major contributor causing secondary hardening. This would suggest that shift to more stable austenite, e.g., from 304, 321 or 347 to 316, or increase of the temperature should effectively mitigate secondary hardening. However, the strain controlled EAF results for alloy 304L at GE (Solomon, Amzallag, DeLair, et al., 2005a) and for alloys 304L, 316L and 347 at VTT contradict this idea.

Based on the composition, austenite should be more stable in alloy 316L and not easily transform to martensite at 300°C. Why would formation of martensite induce more hardening at a higher temperature, and more pronouncedly just in an alloy of stable austenite?

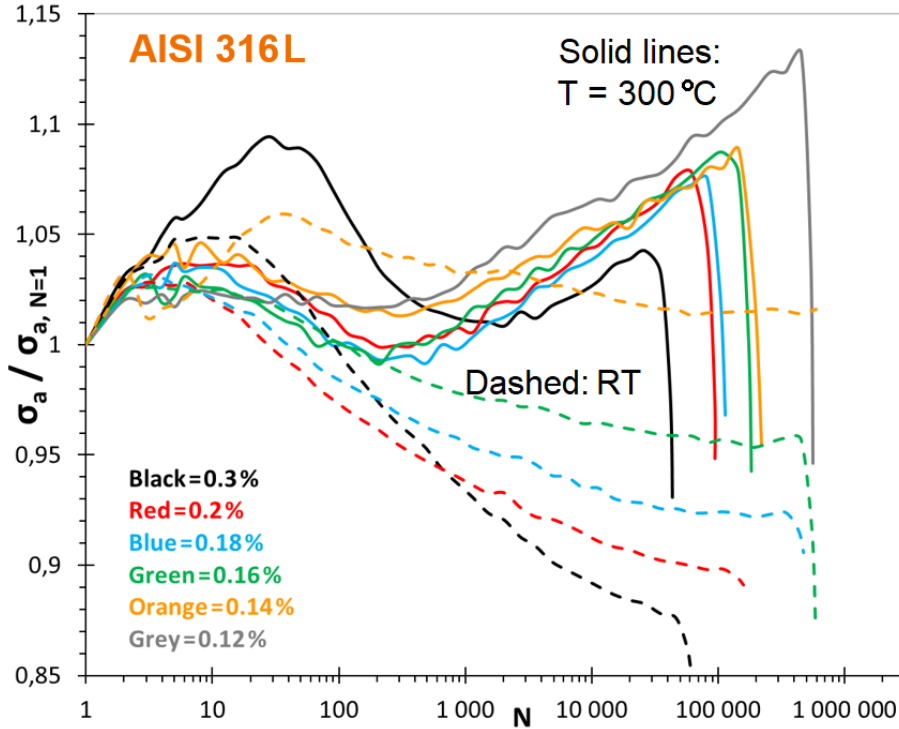


Figure 120. Stress responses during strain-controlled fatigue tests at room temperature and 300°C.

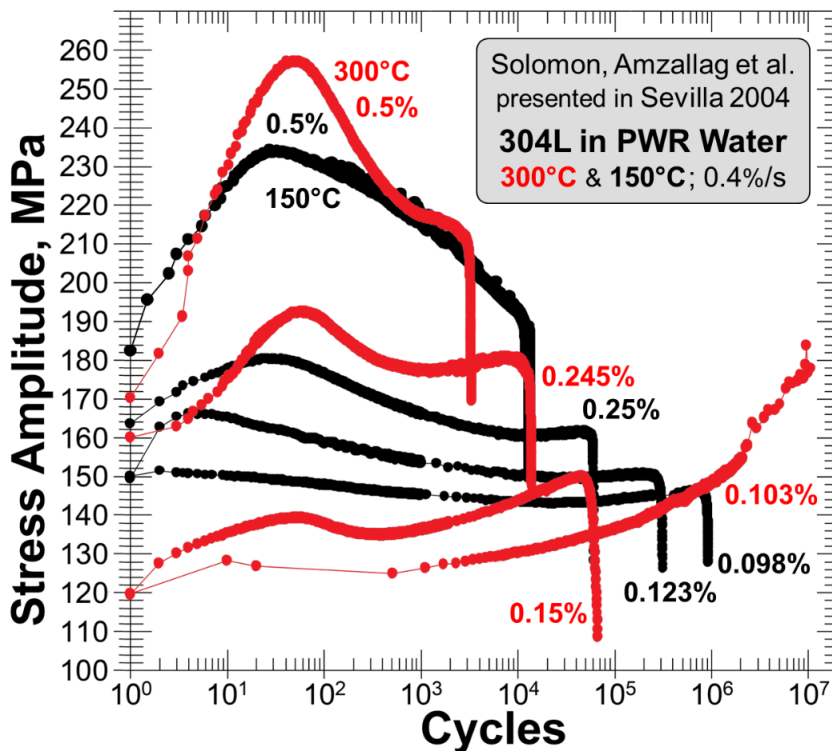


Figure 121. Stress responses in PWR water at 150°C and 300°C. Combined and edited from presentation slides of Solomon et al. (2005a).

4.5.7 Discussion on transferability of EAF data

Transferability of EAF laboratory results to components in operation has been discussed a lot, also earlier in this report. Parts of the still ongoing discussion may be considered “Laboratory evidence from Finland” and will be summarized in the following.

Effect of temperature in environment

The EAF results for alloy 347 shown in Figure 107 were less conservative than the predictions, but we considered that they still exaggerated the effects of water environment. The issue originates from the assumption in NUREG/CR-6909 (O. K. Chopra & Shack, 2007) stating that the temperature would play a role only when the surface of specimen (or component) is in contact with water environment. This assumption was embedded in definition of F_{en} factor according to equation (37):

$$F_{en} = \left(\frac{N_{f(air,RT)}}{N_{f(water,T)}} \right) \quad (37) \text{ (reprinted)}$$

As shown in Figure 106, Figure 111, Figure 118, fatigue endurance of stainless steels – also low alloy steels – is not independent of temperature in air. According to Figure 106 temperature begins to play roles when $\varepsilon_a < 0.5\%$ (when $S_a < 1000$ MPa or $N_f < 500$ for design) and the effect of temperature can become even more significant than the effect of water environment in HCF regime. Figure 106 suggests that for very long lives the effect of temperature might be best modelled in terms of strain or stress intensity, rather than endurance, but for finite lives it was found simpler to split F_{en} in two parts:

$$F_{en} = F_{en,T} \times F_{en,water} = \left(\frac{N_{f(air,RT)}}{N_{f(air,T)}} \right) \times \left(\frac{N_{f(air,T)}}{N_{f(water,T)}} \right) \quad (71)$$

This model was applied for analysing the EAF data presented in Figure 107. The amplitude dependent temperature effects ($F_{en,T}$) were calculated based on VTT air data at 25°C, 200°C and 325°C and the residuals of environmental effects were addressed as $F_{en,water}$. The resulting partial factors $F_{en,T}$ and $F_{en,water}$ were compared with the F_{en} factors calculated according to NUREG/CR-6909 (O. K. Chopra & Shack, 2007) in Figure 124. The effects of temperature remain negligible for tests run at the largest strain amplitudes and slow rates, but for low strain amplitude tests run at strain rate 10^{-4} (0.01%/s) the factors for temperature effects are close to the factors for water environment, Figure 124.

F_{en} factors paired with design fatigue curves

A consensus within the relevant expert groups³ states that F_{en} factors calculated according to the NUREG/CR-6909, rev.1 (O. K. Chopra & Stevens, 2018) should be applied with the Design Curves provided in the 2010 edition of ASME III (ASME, 2010). In other words, a change in the Code Curve, application of another Design Code or experimentally determined design curves would require re-assessment of the F_{en} factor models. Application of the design-by-experiments method with F_{en} is, naturally, not an alternative for EAF through design-by-analysis.

A new ‘Pandora’s box’ will be opened if accounting for temperature effects “in air” is amended into the codified fatigue assessment and any F_{en} factors defined according to equation (37) are to be used. A good example was given in the 2013 revision of the German KTA 3201.2 (KTA, 2013) which addressed the trend shown in Figure 106 by introducing a separate design curve for elevated temperatures.

³ in the Working Group Environmental Fatigue Evaluation Methods (SG-DM)(BPV III) and Working Group On Fatigue Strength (SG-DM)(BPV III) under the ASME Subgroup On Design Methods (SC-D)(BPV III)

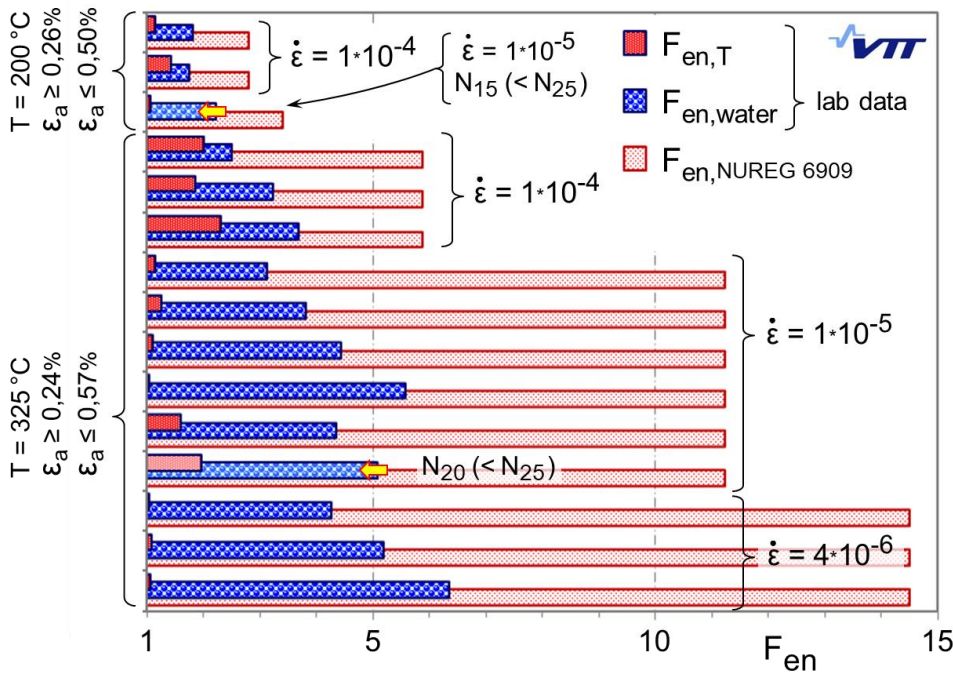


Figure 124. The EAF results from Figure 107 presented as separated effects of temperature and water environment according to equation (71) in comparison with the calculation according to NUREG/CR-6909, rev.0. (J. Solin et al., 2016)

A comparison of the resulting penalties in allowable cycles and F_{en} factors according to NUREG/CR-6909, rev.1 (O. K. Chopra & Stevens, 2018) was shown in Figure 30. The penalties due to temperature in air (by KTA) and for PWR water (by NUREG/CR-6909) are equal (3.01) when $T = 300\text{ }^{\circ}\text{C}$, $S_a = 300\text{ MPa}$ and $\dot{\epsilon} = 6.1 \cdot 10^{-4}$. For lower temperatures, lower stress intensity amplitudes or higher strain rates, the penalties in air would exceed the F_{en} and $N_{f(air,T)} < N_{f(water,T)}$, because F_{en} factors according to equation (37) need to be applied for fatigue assessment based on the design curve for room temperature.

Amplitude-dependent temperature effects could be determined relatively easily for calculation of $F_{en,T}$. Derivation of compatible $F_{en,water}$ factors just by data regression is more complex, starting from justification for applying equation (71), i.e., assumption that logarithms of $F_{en,T}$ and $F_{en,water}$ can be cumulatively used, and followed by careful experimental research to collect a sufficient amount of coherent EAF data. An example outcome of such research was illustrated in Figure 124, which summarised experimental results in form of partial penalty factors $F_{en,T}$ and $F_{en,water}$ for a specific material batch.

However, the results in Figure 124 are not suitable for creating generic solutions and factors averaged for universal EAF application. Instead, they were aimed to enhance accuracy and confidence in fatigue assessment of a dedicated material representative for the surge lines in German PWR reactors. A new scientific model founded on EAF mechanisms, probably including equation (71), is needed for broader applicability. The plastic strain based F_{en} approach proposed by Seppänen et al. (2018) is a step in that direction. Equation (71) was also adopted in the model which was introduced in chapter 3.3.3.

5. Practical application in stress analysis

Fatigue design curves adjusted to reflect the material behaviour in the specific environmental conditions, e.g., in NUREG/CR-5999 (Majumdar et al., 1993) were favoured in the U.S. NRC EACLWR program until the late 1990's. This concept was introduced to ASME III in the Code Case N-761 (ASME, 2013a). Some members of the ASME III Subgroup Fatigue Strength preferred this approach in a 'design code', because the EAF design curves could be applied for water-touching components in the same way as air fatigue curves are used without detail knowledge or prediction of the environmental parameters during operation. On the other hand, it was argued that the approach with a parametrized F_{en} is more relevant to operating reactors. The operational conditions and parameters used for calculating F_{en} factors are better known during operation, and when needed, additional efforts used in assessment can be rewarded through closer defined F_{en} factors. In following, we introduce and discuss only the approach with F_{en} factors, which dominates the current state of the art both in design and operation of reactors.

The state-of-the-art EAF approaches, e.g., in NUREG/CR-6909 (O. K. Chopra & Stevens, 2018) and JSME S NF1-2009 (JSME, 2009) assume that the codified stress and fatigue analyses are completed before F_{en} factors are applied as "add on penalty factors" to modify the ready determined Usage Factors, 'UF'. It is worth of noting that in JSME S NF1-2009 the fatigue usage factor is abbreviated shortly as 'U' and after EAF adjustment as ' U_{en} ' for 'usage factor in environment'. And abbreviation 'CUF' is used for 'Cumulative UF' in NUREG/CR-6909.

The allowable total amount of fatigue cycles (n) can be defined as the last cycle not exceeding the allowed fatigue usage factor ($U_{allowed}$), which is typically set to 1, as in equation:

$$U = \sum_{i=1}^n (U_i) \leq U_{allowed} = 1, \quad (72)$$

where U is the cumulative fatigue usage factor and U_i is a partial usage factor of a cycle.

The cumulative fatigue usage factor including environmental effects (U_{en}) is easy obtained as follows:

$$U_{en} = \sum_{i=1}^n (F_{en,i} \times U_i) \leq 1 \quad (73)$$

In other words, the allowable fatigue usage factor ($U_{allowed}$) would be reduced by an effective F_{en} value. If a common F_{en} factor is applied for all cycles, $U_{allowed} = 1/F_{en}$.

In practice, the fatigue cycles are usually counted in groups sorted according to a transient budget. In assessment of EAF, further grouping according to the environmental parameters or expected F_{en} factors is probably desired. As will be shown below, the by regulators endorsed state-of-the-art EAF approaches, (O. K. Chopra & Stevens, 2018) and (JSME, 2009) allow versatile grouping options to focus the precise calculation efforts for transients associated with largest contributions to U_{en} .

5.1 Alternative procedures for determining F_{en}

The general principles and alternative methods for F_{en} assessment are quite similar in NUREG/CR-6909, rev.1 (O. K. Chopra & Stevens, 2018) and JSME S NF1-2009 (JSME, 2009), but the language in JSME S NF1-2009 is better readable and coherent written to be used as a code for design or fatigue assessment. The NUREG/CR-6909 reports contain detailed presentation and discussion on experimental results and may be considered as research reports rather than guides for fatigue assessment. Reading the JSME code helps in understanding what NUREG/CR-6909 is aiming for.

As explained below in subchapters, the current authors have recognized that the NUREG/CR-6909 models for F_{en} application are not 100% compatible with the ASME III design procedures. However, it is generally considered that the equations for calculating F_{en} factors according to NUREG/CR-6909, rev.1 are paired with the design fatigue curves in the same report and later adopted also in the ASME III for stainless steels

(ASME, 2010). Therefore, the F_{en} factors are not assumed directly applicable to be used together with other design codes. Indeed, care is recommended when comparing or mixing EAF assessments based on different codes and F_{en} models.

Despite the above, we consider the alternative, simpler or more detailed procedures for F_{en} assessment are comparable and even interchangeable so that the procedures explained in the JSME S NF1-2009 could be followed, even when using the NUREG/CR-6909 equations for calculating F_{en} factors. In such case it is essential to specify, which reference and set of equations has been used for calculation of F_{en} .

NUREG/CR-6909 reports describe two alternative approaches that can be used for determining the F_{en} for a selected cycle: the '*Average Strain Rate Approach*' and a '*Modified Rate Approach*'. The JSME S NF1-2009 provides instructions for three alternative analysis methods: '*Factor Multiplication Method*', '*Simplified Method*' and '*Detailed Method*'. The first of these is a simplest possible approach requiring minimal effort. The two latter methods encompass the approaches suggested in the NUREG/CR-6909 reports. As the Japanese code is more comprehensive and coherently written, it will be used as the primary reference in the following.

5.2 Three levels of detail for determining F_{en}

Conservative selection of the environmental parameters (water chemistry, temperature and strain rate) for the considered fatigue transient or term of operation applied in equation (45) results to conservative F_{en} factors at a reasonable effort. The NUREG/CR-6909 '*Modified Rate Approach*' and '*Detailed Method*' of JSME S NF1-2009 allow incremental calculation of F_{en} under conditions where temperatures and/or strain rates are varied during increasing strain part of a fatigue cycle.

- The '*Factor Multiplication Method*' is the fastest and most conservative method to start with. In case of not satisfying the allowable fatigue usage factor (U), load set pairs of high partial usage values ($U_{en} = U \times F_{en}$) can be reanalyzed using another more refined method.
- The '*Simplified Method*' accounts for each load set pair separately. Conservative maximum or average parameters are used for each load set pair.
- The '*Detailed Method*' divides the analyzed strain ranges into small intervals. F_{en} is calculated for each interval and weighted by the corresponding strain range. Weighted values are then summed and averaged for each load set pair.

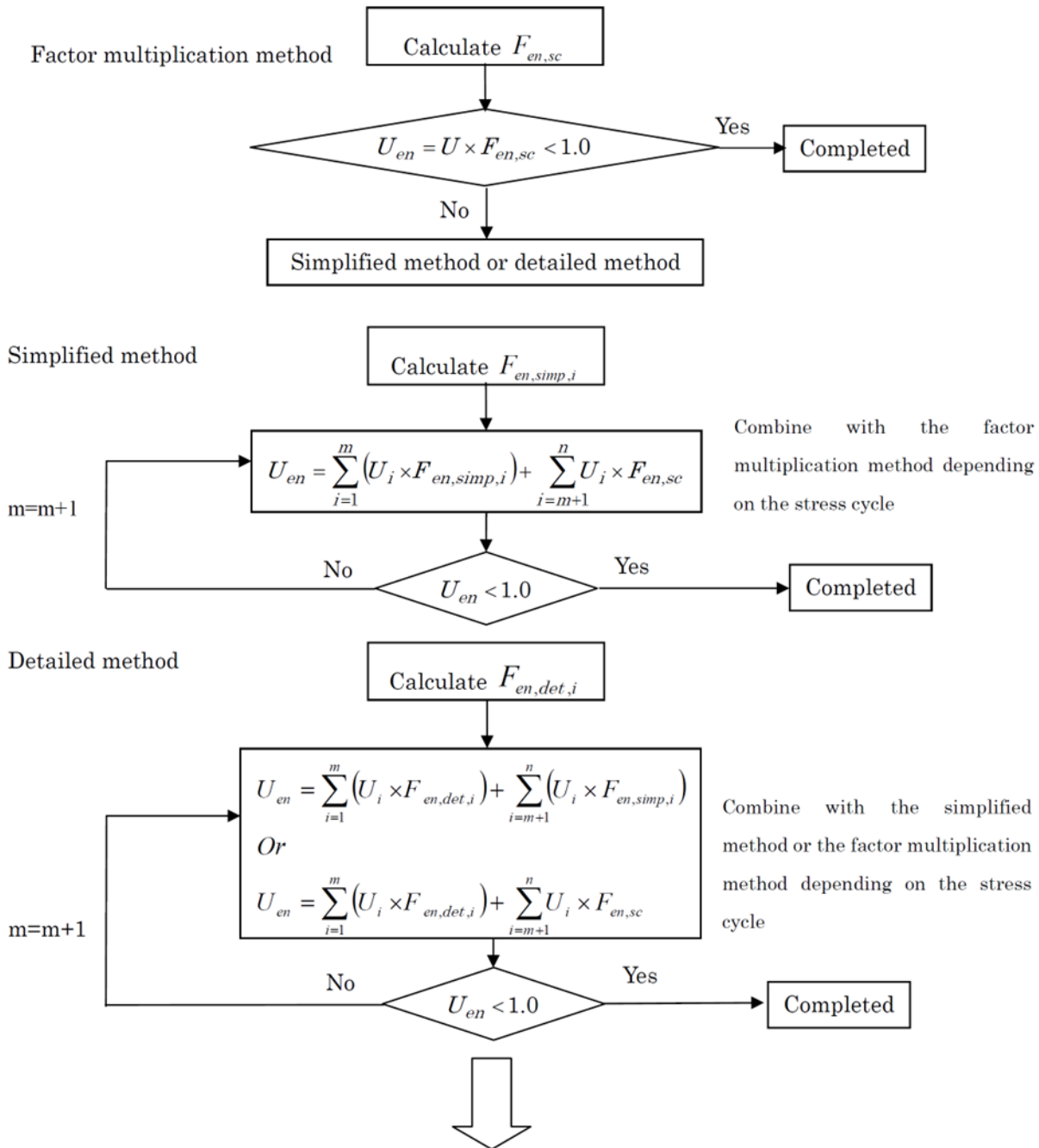
The JSME S NF1-2009 code provides options to combine any of the three methods for fatigue assessment of a component. Usage for a fatigue cycle can be multiplied by a F_{en} factor calculated using any of the three methods, and the total usage (U_{en}) is obtained by summing up partial usages: $U_{en,i} = \sum (U_i \times F_{en,i})$. This introduces a new version of the cumulative fatigue damage principle applicable for EAF.

In case of not satisfying the allowable usage value, a cycle with high usage contribution ($U_i \times F_{en,i}$) can be reanalyzed using more refined methods as outlined in Figure 125.

5.2.1 The Factor Multiplication Method

An $F_{en,sc}$ factor is easily and very conservatively calculated with this '*Factor Multiplication Method*'. The cumulative fatigue usage without environmental effects at a studied location is multiplied by the maximum $F_{en,sc}$ for that location. The environmental parameters are selected as follows:

- Temperature: The maximum value during the transient, or higher.
- DO concentration: An applicable value resulting to the maximum F_{en} factor.
- Strain rate: Constant 0.0004%/sec (the saturated conservative value).



Consider possible application of other techniques if $U_{en} < 1.0$ is not achieved.

Figure 125. Flow chart of environmental fatigue evaluation adopting Factor Multiplication Method, Simplified Method and Detailed Method Successively to reduce excess conservatism. (JSME, 2009)

5.2.2 The Simplified Method

An $F_{en,simp}$ factor is obtained for each load set pair, and it is used to multiply the usage of each load set pair in air. The environmental parameters are selected as follows:

- Temperature: The maximum value for each load set pair.
- DO concentration: The momentary value resulting to the maximum F_{en} factor.
- Strain rate: Average tensile strain rate for each load set pair.

Over-conservativeness due to saturated strain rate value in the 'Factor Multiplication Method' is reduced when F_{en} is calculated with this method. However, use of a mean strain rate is often more conservative than letting the strain rate vary with time. For the purpose of explanation, two transients (A and B) were used in JSME S NF1-2006 (JSME, 2006) to demonstrate the simplified and detailed methods in Figure 126 and Figure 127. These methods shall be applied until all fatigue cycles have been included in the evaluation. To perform an evaluation using the 'Simplified Method', $F_{en,simp,A}$ and $F_{en,simp,B}$ shall be calculated respectively for two transients (A and B), which constitute the stress cycle used in the calculation of a fatigue usage factor, Figure 126.

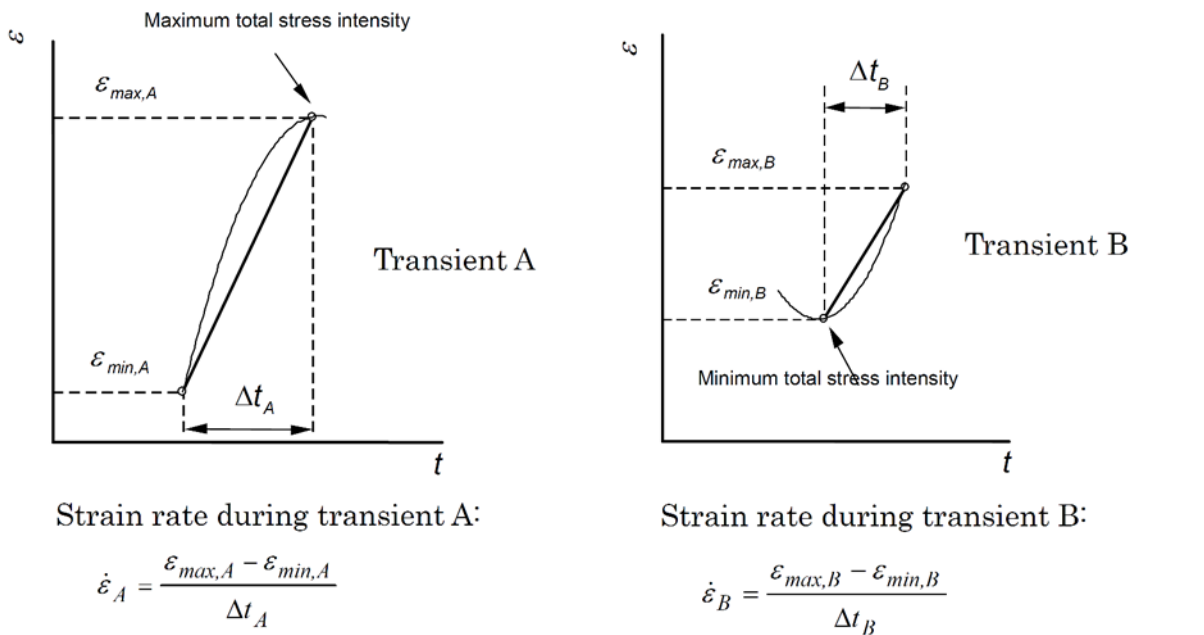


Figure 126. Calculation of the strain rate using the 'Simplified Method'. (JSME, 2009)

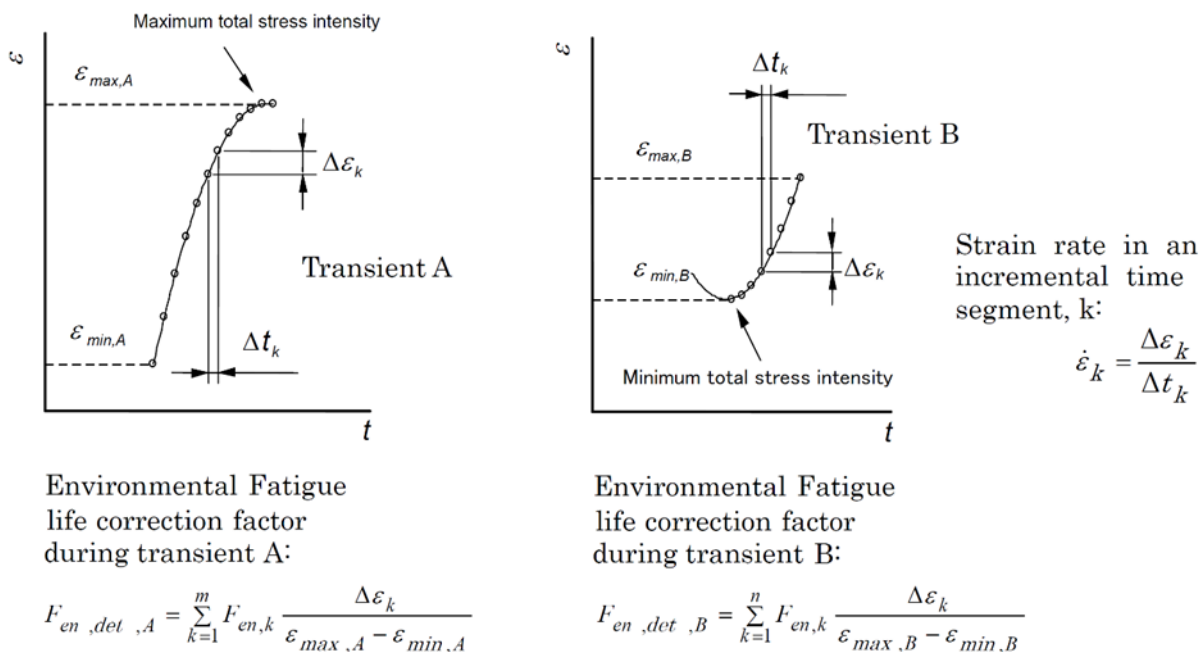


Figure 127. Calculation of the strain rate using the 'Detailed Method'. (JSME, 2009)

5.2.3 The Detailed Method

As shown in Figure 127, the range (ε_{\min} to ε_{\max}) where strains continuously increase is divided into 'm' or 'n' time segments to be evaluated. Then, momentary values of the strain rate, temperature and dissolved oxygen concentration are defined for each time segment 'k'. The segment specific $F_{en,k}$ values shall be calculated using the appropriate equations common for all three methods. The $F_{en,det}$ for each transient (e.g. A and B in Figure 127) shall be calculated using equation 74. $F_{en,det}$ for the stress cycle consisting of transients A and B is combined using equation 75:

$$F_{en,det, A \text{ or } B} = \sum_{k=1}^n F_{en,k} \frac{\Delta \varepsilon_k}{\varepsilon_{max} - \varepsilon_{min}} \quad (74)$$

$$F_{en,det} = \frac{F_{en,det,A} \times (\varepsilon_{max,A} - \varepsilon_{min,A}) + F_{en,det,B} \times (\varepsilon_{max,B} - \varepsilon_{min,B})}{(\varepsilon_{max,A} - \varepsilon_{min,A}) + (\varepsilon_{max,B} - \varepsilon_{min,B})} \quad (75)$$

5.2.4 Usage factor for environmental fatigue

As illustrated in Figure 125, the JSME S NF1-2009 code allows different combinations of the three methods for the EAF assessment. In practice, this could mean e.g., that

- insignificant fatigue cycles are simply multiplied by the maximum F_{en} value obtained by the '*Factor Multiplication Method*',
- some cycles are analyzed using the '*Simplified Method*', and
- the cycles contributing the largest shares of EAF usage are subjected to assessment using the '*Detailed Method*'.

The cumulative EAF usage factor U_{en} would then be calculated using equation 76:

$$U_{en} = \sum_{i=1}^m U_i \times F_{en,det,i} + \sum_{i=m+1}^n U_i \times F_{en,simp,i} + \sum_{i=n+1}^o U_i \times F_{en,sc,i} \quad (76)$$

where U_i is the partial usage for a cycle, $F_{en,det,i}$ is a penalty factor analyzed by the '*Detailed Method*', $F_{en,simp,i}$ is calculated by the '*Simplified Method*' and $F_{en,sc,i}$ is a conservative factor applicable for remaining cycles, for which parametric F_{en} factors are not separately calculated, i.e., the '*Factor Multiplication Method*' is used. The resulting cumulative fatigue usage factor U_{en} represents the standard fatigue usage multiplied by an average environmental factor weighed by calculated fatigue usages and levels of analysis detail.

5.3 Threshold strain for determining F_{en}

The F_{en} factor is defined as a ratio of cycles in RT air and in hot environment. Because finite numbers of cycles exist only above the endurance limit, the endurance limit at room temperature sets a theoretical limit for the experimental determination of F_{en} . Respecting this, the JSME S NF1-2009 code provides the endurance limit value for the air reference curve as a threshold amplitude value for calculation of F_{en} values. For carbon and low-alloy steels this threshold is 0.042% and 0.11% for austenitic stainless steels and Ni-Cr-Fe alloys. Thus, $F_{en} = 1$, if $\varepsilon_a \leq 0.11\%$ and the factor is calculated for a whole cycle.

This threshold allows exclusion of strain rate calculation for vibration and other minor load cycles when the ‘Factor Multiplication Method’ or the ‘Simplified Method’ is used, but it is not applicable for the ‘Detailed Method’, in which the rising strain ramp is split in parts (JSME, 2009).

In NUREG/CR-6717 (O. K. Chopra & Shack, 2001) and other Argonne reports, rupture strain of the surface oxide film has been suggested as a potential (non-confirmed) justification for a threshold of environmental effects. Breaking of the oxide film is assumed as a prerequisite for environmental effects. For stainless steels, this threshold has been 0.1% or 195 MPa in all versions of NUREG/CR-6909 report. The threshold values match with the strain amplitudes at 100 000 cycles according to the respective design curves and are below the endurance limit of the reference curve in air.

In other words, the threshold strain ϵ_{th} required for $F_{en} > 1$ was introduced in two alternative meanings (O. K. Chopra & Stevens, 2018):

- ϵ_{th} is a strain amplitude threshold justifying ignoring environmental effects, or
- ϵ_{th} is a strain range that can be excluded from the F_{en} calculation.

The latter meaning of ϵ_{th} is applied in the instruction provided on page 4-74 of NUREG/CR-6909 Rev.1 (O. K. Chopra & Stevens, 2018):

“In application of the modified rate approach when a threshold strain, ϵ_{th} , is considered, the following equation” (77) “can be used to calculate F_{en} for the total strain transient:”

$$F_{en} = \sum_{k=1}^n F_{en,k}(\dot{\epsilon}_k, T_k) \frac{\Delta\epsilon_k}{(\epsilon_{max} - \epsilon_{min}) - \epsilon_{th}}, \quad (77)$$

where ϵ_{max} and ϵ_{min} define the peak and valley strains of the transient.

According to equation (77), calculation of the incremental F_{en} values begins at $\epsilon_{min} + \epsilon_{th}$. However, the threshold does not affect the ready calculated fatigue usage. It just changes the range of data used for calculation of F_{en} .

The reduced range of F_{en} calculation may lead to smaller or larger F_{en} , depending on the transient type. Application of the strain range threshold ϵ_{th} for F_{en} factor calculation as in equation (77), is prohibited elsewhere in the same report. A statement on page 4-43 (O. K. Chopra & Stevens, 2018) instructs:

“this threshold strain amplitude should not be considered when the modified rate approach is used to determine F_{en} .”

This latter statement is compatible with JSME S NF1-2009, which does not allow use of the threshold strain ϵ_{th} in the ‘Detailed Method’.

5.4 Calculation example

To illustrate the calculation of F_{en} factor (with or without a threshold strain), a typical cycle caused by abrupt changes of water temperature was analyzed. This happens e.g., in a PWR surge line where water flows back and forth between the circulation loop and pressurizer. The cycle consists of four transients 1-4 as shown in Figure 128:

1. In surge of cooler water causes tensile strain and stress on the inner surface.
2. The stress on surface relaxes when thermal gradient over thickness relaxes.
3. Out surge of warmer water causes a reverse gradient and surface stress.

4. The rising ramp of the cycle begins by relaxation of the compressive gradient.

The rising strain transients 4 and 1 need to be analysed for obtaining a F_{en} factor for the cycle. Not surprisingly, higher instantaneous environmental factors $F_{en,k}$ are calculated during the slow transient 4 and the $F_{en,k}$ factors even saturate for strain rates $\dot{\epsilon} \leq 0.0004\%/s$ before half way of the ramp, Figure 129. In addition, the surface temperature at water interface is higher than during the transient 1. The change of surface temperature is assumed completed during the first calculation increment. This can be seen in the $F_{en,k}$ factor trend in begin of transient 1, which starts with a temperature drop from 325°C to 275°C.

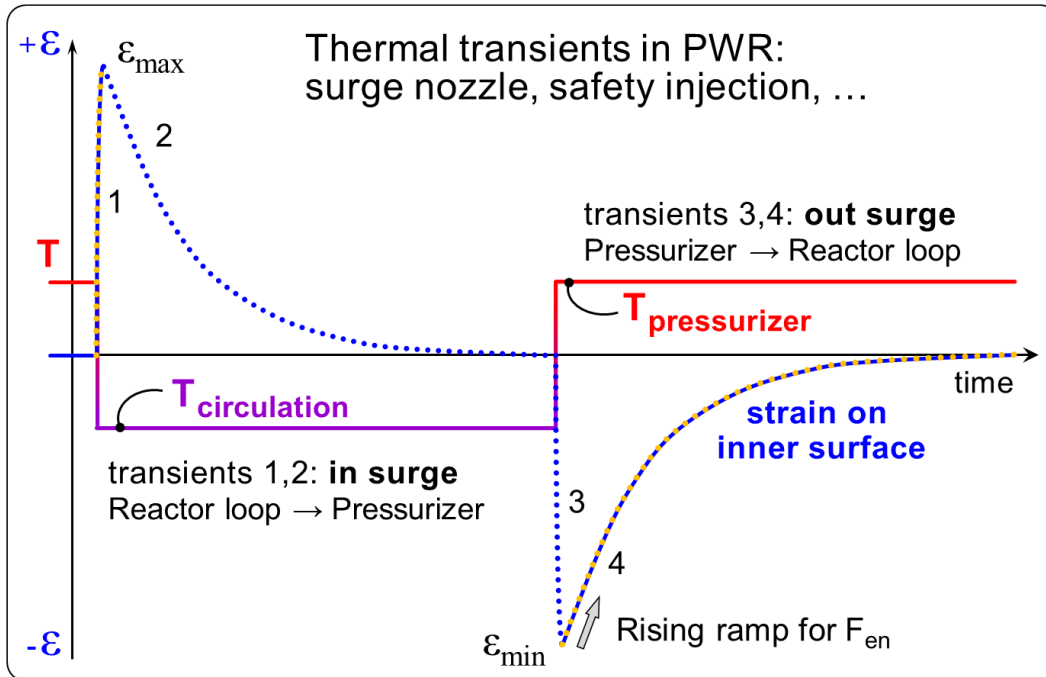


Figure 128. Thermal transients during PWR pressurizer in surge and out surge events.

The F_{en} factors obtained by different methods are shown in Table 28. The first three rows report the partial F_{en} factors for the transients and the two last rows for the complete cycle. The results on the second last row would be applicable for fatigue assessment. The Factor Multiplication Method simplifies the rising ramp as a linear ramp from -0.4% to +0.4% during 600 seconds, which gives $\dot{\epsilon} = 0.00133\%/s$ and $F_{en,sc} = 9.35$, when $T_{max} = 325^\circ C$, Figure 129.

Table 28. Environmental effects as F_{en} factors for transients shown in Figure 129, Figure 130, Figure 131 and Figure 132. The F_{en} factors are calculated using the factor multiplication ($F_{en,sc}$), simplified ($F_{en,simp}$) and detailed ($F_{en,det}$) methods.

Transient or cycle	Point range	ϵ_i %	$\Delta\epsilon$ %	Average ϵ rate %/s	Effective T_{surge}	$F_{en,sc}$	$F_{en,simp}$	$F_{en,det}$			
SIS.4 out surge	10	-0,4	0,40	6,77E-4	325						
	62	0									
SIS.1 in surge	64	0	0,40	4,44E-2	275					11,16	9,32
	116	0,4								3,75	2,69
SIS.4,th $\epsilon_{th} \approx 0.1\%$	22	-0,304	0,304	5,47E-4	325					11,80	9,82
	62	0									
SIS.4+1 out & in	10	-0,4	0,80	1,33E-3	325						
	116	0,4			275						
SIS,th $\epsilon_{th} \approx 0.1\%$	22	-0,304	0,704	1,25E-3	325				9,35	7,45	5,55
	116	0,4			275				9,52	7,22	5,77
Method of F_{en} calculation									eq. in JSME		
$F_{en,sc,a}$	Single F_{en} factor for all fatigue usage; $U_{en} = U \times F_{en,sc,a}$								EF-8a		
$F_{en,sc,b}$	Separate F_{en} factor for each cycle; $U_{en,i} = U_i \times F_{en,sc,i}$					EF-8b					
$F_{en,simp}$	F_{en} factor for a cycle split in rising transients					EF-15					

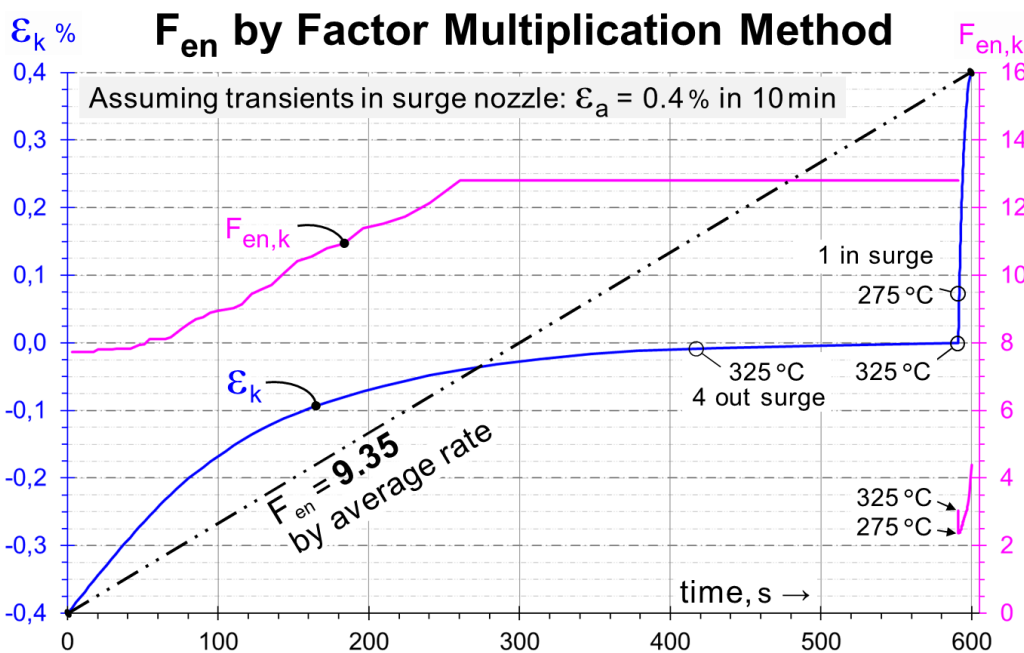


Figure 129. Rising strain ramps and instantaneous $F_{en,k}$ factors during the transients 4 and 1 shown in Figure 128. Determination of F_{en} by the Factor Multiplication Method is illustrated. The rising ramp consisting of two transients is considered as a whole.

The simplified and detailed method calculations (two last columns in Table 28) make a difference between the transients. The Simplified Method applies the average strain rates for each transient in calculation of the F_{en} factor and results to ($F_{en,simp} = 7.45$) after averaging the factors for the transients weighted by the range of strain increase within the transient, Figure 130.

The Detailed Method, which separates the cycle in 100 increments in strain ($\Delta\varepsilon_k=0.008$), gives the lowest F_{en} factor ($F_{en,det}=5.55$), Figure 131.

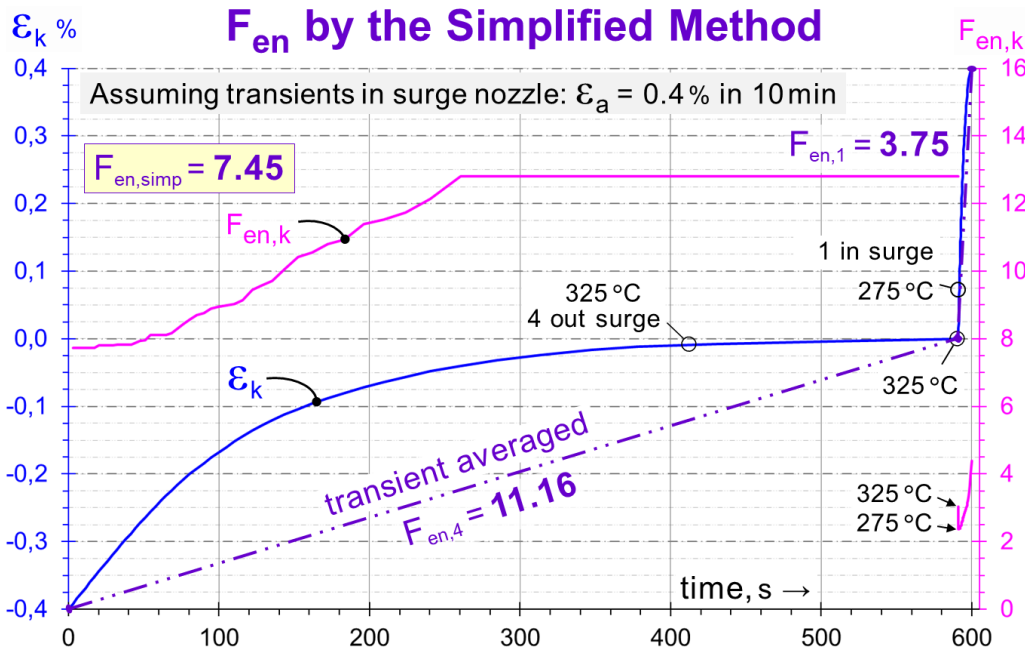


Figure 130. Rising strain ramps and instantaneous $F_{en,k}$ factors during the transients 4 and 1 shown in Figure 128. Determination of F_{en} by the Simplified Method is illustrated. Calculation of the two separated transients results to a weighted average F_{en} factor, as detailed in Table 28.

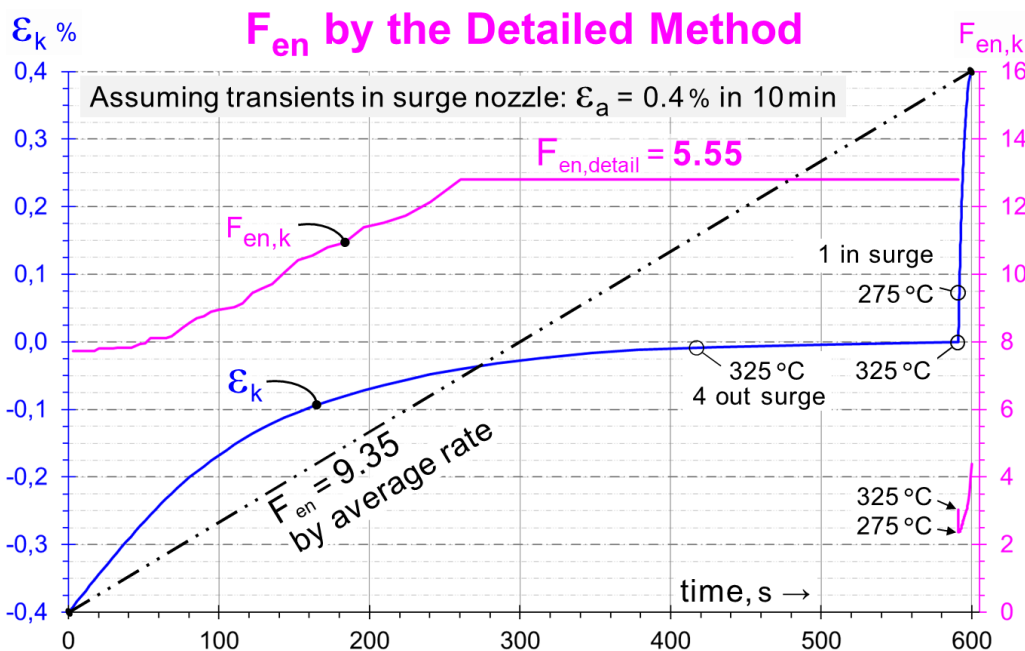


Figure 131. Rising strain ramps and instantaneous $F_{en,k}$ factors during the transients 4 and 1 shown in Figure 128. Determination of F_{en} by the Detailed Method is illustrated.

If we assume a strain threshold according to equation (77) and exclude the first 0.1 % of the ramp, the Factor Multiplication Method results to an increased F_{en} factor ($F_{en,sc}=9.52$, if $\varepsilon_{th}=0.1\%$), Figure 132. This is due to a lower average rate $\dot{\varepsilon}=0.00125\%/s$ (from -0.3% to $+0.4\%$ during 565 seconds). A diagonal over the two transients from -0.4% to $+0.4\%$ in Figure 129 crosses the blue (ε_k) line at about halfway of

transient 4, at $\epsilon_k = -0.05\%$ after 240 seconds. This reveals that any threshold value lower than 0.35% would increase the environmental penalty factor ($F_{en,sc} \geq 9.35$) obtained by the simplest Factor Multiplication method – for this particular case study.

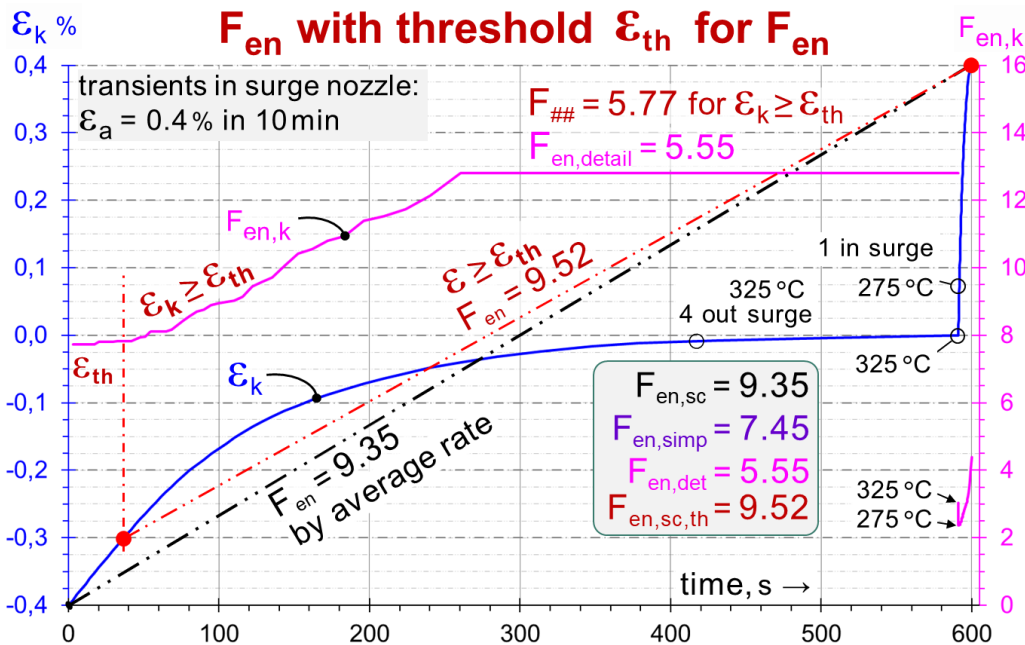


Figure 132. Rising strain ramps and instantaneous $F_{en,k}$ factors during the transients 4 and 1 shown in Figure 128. Application of the strain threshold for F_{en} by the Factor Multiplication Method is illustrated. Note that the threshold is not applicable for the Detailed Method (marked as $F_{\#}$).

The Simplified Method would provide a slightly lower $F_{en,simp}$ factor with the threshold. The partial $F_{en,simp}$ factor for the transient 4 increases, but the remaining transient 4 has a smaller range and weight factor ($\Delta\epsilon = 0.304\%$) when the $F_{en,simp}$ factor is combined for the whole cycle. Therefore, the penalty factor becomes smaller in this case if the threshold concept is applied.

If we – against the instructions given in both procedures (O. K. Chopra & Stevens, 2018; JSME, 2009) – assume a strain threshold according to equation (77) and exclude the first 0.1% of the ramp when using the Detailed Method, the resulting F_{en} factor would increase from $F_{en,det} = 5.55$ to $F_{\#} = 5.77$ because the weight given for the more severe transient 4 would be reduced in combining the transients. We use here the notation $F_{\#}$ to avoid misunderstanding and remind that the threshold concept is not recommended with the Detailed Method.

The JSME Code (JSME, 2009) is unambiguous and leaves no room for use of a strain threshold together with the Detailed Method. The NUREG/CR-6909 report (O. K. Chopra & Stevens, 2018) is confusingly

- providing an equation (77 in the current report) for adopting a strain threshold together with the modified rate approach,
- stating a prohibition against use of the threshold together with the modified rate approach, and
- effectively hiding instructions to define a value for the threshold.

Furthermore, the threshold concept is questionably differentiating the data used for the fatigue assessment and for calculating the environmental penalty factor. Adoption of the threshold concept could unpredictably increase or decrease conservatism of the EAF assessment.

From the mechanisms point of view, a strain threshold for environmental effects is a reasonable concept, but we recommend adopting rather a new mechanism informed model, or to refrain from using the concept in framework of the current modified rate approaches (Van Der Sluys & Nickell, 2003).

The threshold amplitude for environmental effects can still be used for excluding the smallest cycles from calculation of the F_{en} factor.

6. Summary

Fatigue as such or as “environmentally assisted” (EAF) is one of the degradation mechanisms of nuclear power plant materials. The original 1963 Code (ASME III, Article 4 – Design, footnote on page 18) stated: “... the designer shall evaluate separately any effects on fatigue life which might result from unusually corrosive environment”. In addition, a transferability margin (20 in life or 2 in stress intensity) aimed to represent the difference between material performance in a laboratory test and component durability in reactor operation. However, only a minor unquantified portion of this margin was usable as provision for possible environmental effects.

Laboratory experiments with primary circuit materials have later demonstrated reduced fatigue crack initiation lifetimes in simulated reactor coolant environments. A penalty factor F_{en} for environmental effects based on comparison between EAF data ($N_{HT,water}$) and the reference ϵ -N fatigue curve ($N_{RT,air}$) and defined as ($F_{en} = N_{RT,air}/N_{HT,water}$) was endorsed by the U.S. NRC in 2007 and become a global reference approach. Correlations between test parameters and resulting EAF lives have been obtained by regression analyses and used for parametric calculation of F_{en} factors while success in scientific research, understanding and modelling of material performance in EAF has been limited. The current F_{en} models are often claimed as unrealistic, notably for actual plant transients. The database behind the development of the NUREG/CR-6909 F_{en} model includes questionable reference data in air and even more questions raise about the environment data. The sum of uncertainties prevents reliable assessment of individual effects quantitatively.

Transferability of laboratory results to fatigue assessment of reactor components has been questioned referring in particular to claimed inconsistency between laboratory data and plant operating experience. Efforts to improve and verify the transferability of the EAF research results to practical applications, consistent with operating experience, are needed. In addition, imperfect calibrations and verifications of non-standard laboratory procedures applied in hot pressurized water environment together with broad scattered reference air data leave room and need for improved experimental methods and transferability. Thermodynamic parameters related to temperature, time and rate, which are key parameters in calculation of F_{en} factors sometimes play roles and affect material performance also in air, but still get ignored in the definition of F_{en} factors.

Severe difficulties and variability in solutions for performing laboratory experiments in simulated reactor coolant make it challenging to verify and quantify complex environmental (and associated) effects. A large fraction of laboratory data does not meet standard requirements for design code compatible strain-controlled testing in one or more ways. This prevents making an accurate assessment of the uncertainties and bias associated with the experimental results. Furthermore, quantifying parametrised operational experience is extremely challenging, and it may be the only way to verify transferability of the small-scale data to plant components. Until the basic mechanisms of EAF are known and scientifically justified assessment and transferability models are developed, engineering judgement and tolerance for unknowns will be needed.

The scope of EAF extends beyond the correction factors, which are inseparable from specific fatigue curves. The Design Fatigue Curve and F_{en} factors to be applied for EAF assessment shall have common roots (reference ϵ -N fatigue curve used in the laboratory) and traceable evolution history to ensure compatibility. Otherwise, transferability of the lab data to component assessment is compromised. Therefore, a consensus exists on the wording in the U.S. NRC Reg Guide 1.207 rev.1: “Specifically, these methods include calculating the CUF in air using ASME Code, Section III analysis procedures, and then employing the environmental fatigue correction factor (F_{en}), as described in NUREG/CR-6909, Revision 1”. In other words, the F_{en} factors according to NUREG/CR-6909 should be used together with the current Design Fatigue Curve in ASME III. The F_{en} factors according to NUREG/CR-6909 are not directly compatible, for example, with the current KTA design curve determined for stabilized stainless steels.

This report provides an extensive and detailed summary on the evolution of Codes and Standards from the perspective of fatigue and EAF. A particular emphasis is placed on the ASME Code and comparisons with the RCC-M and other Codes. Analysis of the fundamental principles originally adopted and along the

years supplemented to the ASME Code, Section III serves as background information on roots also for the other codes. Publicly available historical and current data is collected to summarise the technical basis behind the existing or proposed methods, some of which may or may not yet have regulatory approval.

To maintain consistency, it is essential to understand why and how, for example, the former and current RCC-M Code approaches differ from the combination of ASME Code, Section III paired with the NUREG/CR-6909. The Design Fatigue Curves for stainless steels were initially similar in the ASME III and RCC-M, then diverged, and as proposed in the Probationary Phase Rule (RPP) No. 2 for RCC-M, would again refer to a common reference fatigue curve, though with different transferability margins, and an endurance limit for the RCC-M. Another Probationary Phase Rule (RPP) No. 3 introduces a new approach for transferability of EAF laboratory data and calculation of F_{en} factors. If RPP's 2 and 3 are both endorsed and applied, the claimed conservatism in the combination of ASME III + NUREG/CR-6909 can be avoided in EAF assessment according to RCC-M Code.

The recently approved EAF & fatigue relevant Code Cases in ASME Section III are described together with emerging approaches and ongoing activities on agendas of the most relevant ASME BPV III / Subgroup on Design Methods / Working Groups in 2023 are introduced. The WG Fatigue Strength (WGFS) has a long history in developing advanced fatigue design criteria and analysis methods. In parallel and co-operation for recent ten years, the WG Environmental Fatigue Evaluation Methods (WGEFEM) has been evaluating methods of assessing cyclic life of components subjected to wetted environments, including evaluations of fatigue usage and crack growth.

A wealth of experimental evidence exists to support arguments for or against a particular methodology. A selection of international research and laboratory evidence of environmental effects was introduced and discussed. An overview of experimental research at VTT under the current and previous research programmes was presented, including an improved EAF approach developed. The VTT F_{en} model is based on the assumption that F_{en} is a function of temperature, water chemistry and plastic strain rate (plastic instead of total strain). The model provided notable improvements in modelling EAF for simplified variants of safety injection system transient simulations but is subject for further verification and eventual tuning in the current project. In general, there remains ample room for further research and development to achieve the aims of understanding and quantifying the environmental and thermodynamical effects in fatigue of safety class 1 components in reactor cooling circuits.

References

- AFCEN. (2014). *Criteria RCC-M Prevention of Damages in Mechanical Components* (J. M. Grandemange, Ed.). Association française pour les règles de conception, de construction et de surveillance en exploitation des matériels des chaudières électro-nucléaires.
- AFCEN. (2016). *RCC-M 2016 Règles de conception et de construction des matériels mécaniques des îlots nucléaires REP (in French)*. Association française pour les règles de conception, de construction et de surveillance en exploitation des matériels des chaudières électro-nucléaires.
- Amzallag, C. (2003). High-Cycle Fatigue Behavior of Austenitic Stainless Steels. *Materials Reliability Program: Second International Conference on Fatigue of Reactor Components (MRP-84)* (1003536), 392–428.
- Asada, S. (2021). Proposal of Total Fatigue Life Approach in Considering #15-352. *36th WG EFEM Meeting, Online, Virtual, July 26, 2021*.
- Asada, S. (2022). Total Fatigue Life Approach. *39th WG EFEM Meeting, Online, Virtual, April 25, 2022*.
- Asada, S., Hirano, A., Itatani, M., Yasuda, M., Sera, T., & Kobayashi, H. (2013). Plan and Status of Development of Design Fatigue Curves (Phase 1). *Proceedings of the ASME 2013 Pressure Vessels and Piping Conference*. <https://doi.org/10.1115/PVP2013-97767>
- Asada, S., Hirano, A., Saito, T., Takada, Y., & Kobayashi, H. (2018). Development of New Design Fatigue Curves in Japan: Proposal of a New Fatigue Evaluation Method. *Proceedings of the ASME 2018 Pressure Vessels and Piping Conference*. <https://doi.org/10.1115/PVP2018-84432>
- Asada, S., Hirano, A., Wang, Y., Itatani, M., Takanashi, M., Nomura, Y., Ochi, F., & Ogawa, T. (2022). Investigation of Surface Finish Effect on Fatigue Strength of Carbon and Low Alloy Steels. *Proceedings of the ASME 2022 Pressure Vessels & Piping Conference*. <https://doi.org/10.1115/PVP2022-84695>
- Asada, S., Hirano, T., & Sera, T. (2015). Study On A New Design Fatigue Evaluation Method. *Proceedings of the ASME 2015 Pressure Vessels and Piping Conference*. <https://doi.org/10.1115/PVP2015-45089>
- Asada, S., Nakamura, T., Kamaya, M., & Takahashi, Y. (2023). Technical Revisions of JSME Environmental Fatigue Evaluation Method. *Proceedings of the ASME 2023 Pressure Vessels and Piping Conference*.
- Asada, S., & Nomura, Y. (2021). Development of New Design Fatigue Curves in Japan – Treatment of Variable Loading Amplitude Effect. *Proceedings of the ASME 2021 Pressure Vessels & Piping Conference*. <https://doi.org/10.1115/PVP2021-60418>
- Asada, S., Ogawa, T., Higuchi, M., Kanasaki, H., & Takada, Y. (2016). Study on Mean Stress Effects for Design Fatigue Curves. *Proceedings of the ASME 2016 Pressure Vessels and Piping Conference*. <https://doi.org/10.1115/PVP2016-63796>
- Asada, S., Tsutsumi, K., Fukuta, Y., & Kanasaki, H. (2017). Applicability of Hollow Cylindrical Specimens to Environmental Assisted Fatigue Tests. *Proceedings of the ASME 2017 Pressure Vessels and Piping Conference*. <https://doi.org/10.1115/PVP2017-65514>
- Asada, S., Zhang, S., Takanashi, M., & Nomura, Y. (2019). Study on Incorporation of a New Design Fatigue Curve Into the JSME Environmental Fatigue Evaluation Method. *Proceedings of the ASME 2019 Pressure Vessels and Piping Conference*. <https://doi.org/10.1115/PVP2019-93273>
- Asada, S., Zhang, S., Takanashi, M., & Nomura, Y. (2020). Study on Incorporation of New Design Fatigue Curves and a New Environmental Fatigue Correction Factor for PWR Environment Into the JSME Environmental Fatigue Evaluation Method. *Proceedings of the ASME 2020 Pressure Vessels & Piping Conference*. <https://doi.org/10.1115/PVP2020-21078>
- Asada, Y. (1993). Rate Approach for Fatigue Life Reduction Factors in LWR Water Environment. *Welding Research Council Progress Report, XLVIII(9/10)*.
- ASME. (1963). *ASME Boiler and Pressure Vessel Code, Section III, Nuclear Vessels*. American Society of Mechanical Engineers.
- ASME. (1969). Criteria of the ASME Boiler and Pressure Vessel Code for Design by Analysis in Sections III and VIII, Division 2. In *Pressure Vessels and Piping: Design and Analysis, Volume 1* (pp. 61–83). American Society of Mechanical Engineers.

- ASME. (2010). *ASME Boiler and Pressure Vessel Code, Section III - Rules for Construction of Nuclear Facility Components*. American Society of Mechanical Engineers.
- ASME. (2012). *Code Comparison Report for Class 1 Nuclear Power Plant Components (STP-NU-051-1)*. American Society of Mechanical Engineers.
- ASME. (2013a). Case N-761: Fatigue Design Curves for Light Water Reactor (LWR) Environments Section III, Division 1. In *BPVC Code Cases: Nuclear Components*. American Society of Mechanical Engineers.
- ASME. (2013b). Case N-792-1: Fatigue Evaluations Including Environmental Effects Section III, Division 1. In *BPVC Code Cases: Nuclear Components*. American Society of Mechanical Engineers.
- ASME. (2017). *ASME Boiler and Pressure Vessel Code, Section III, Rules for Construction of Nuclear Facility Components, Division I*. American Society of Mechanical Engineers.
- ASME. (2019). Case N-884: Procedure to Determine Strain Rate for Use With the Environmental Fatigue Design Curve Method and the Environmental Fatigue Correction Factor, Fen, Method as Part of an Environmental Fatigue Evaluation for Components Analyzed per the NB-3200 Rules Section III, Division 1. In *BPVC Code Cases: Nuclear Components*. American Society of Mechanical Engineers.
- ASME. (2021a). Case N-902: Thickness and Gradient Factors for Piping Fatigue Analyses Section III, Division 1. In *BPVC Code Cases: Nuclear Components*. American Society of Mechanical Engineers.
- ASME. (2021b). Case N-904: Alternative Rules for Simplified Elastic-Plastic Analysis Section III, Division I. In *BPVC Code Cases: Nuclear Components*. American Society of Mechanical Engineers.
- ASME. (2021c). Case N-905: Alternate Design Fatigue Curves to Those Given in For Section III Appendices, Mandatory Appendix I, Figures I-9.1 and I-9.1M Section III, Division 1. In *BPVC Code Cases: Nuclear Components*. American Society of Mechanical Engineers.
- ASME. (2023a). Case N-919: Alternative Fatigue Evaluation Method to Consider Environmental Effects on Class 1 Components Section III, Division 1. In *BPVC Code Cases: Nuclear Components*. American Society of Mechanical Engineers.
- ASME. (2023b). Case N-920: Alternative Fatigue Design Curves for Ferritic Steels With Ultimate Tensile Strengths (UTS) ≤ 80 ksi (552 MPa) and Austenitic Steels Section III, Division 1. In *BPVC Code Cases: Nuclear Components*. American Society of Mechanical Engineers.
- ASTM. (2021). *ASTM E606/E606M-21 Standard Test Method for Strain-Controlled Fatigue Testing*. American Society for Testing and Materials.
- Baldwin, E. E., Sokol, G. J., & Coffin, L. F. (1957). Cyclic Strain Fatigue Studies on AISI Type 347 Stainless Steel. *ASTM Proceedings 1957*, 57, 567–586.
- Balkey, K. R. (2006). Letter, Kenneth R. Balkey (ASME) to NRC Rules and Directives Branch, “ASME Comments on Draft Regulatory Guide DG-1144: “Guidelines for Evaluating Fatigue Analyses Incorporating the Life Reduction of Metal Components Due to the Effects of the Light-Water Re. American Society of Mechanical Engineers.
- Bannantine, J. A., Comer, J. J., & Handrock, J. L. (1989). *Fundamentals of Metal Fatigue Analysis*. Prentice Hall.
- Barrachin, B., Garnier, C., Kowalczyk, G., & Podeur, J. (1981). Low Cycle Fatigue in Hot Water. In J. Rastoin (Ed.), *Transactions of the 6th International Conference on Structural Mechanics in Reactor Technology (SMiRT 6)*. North-Holland Publishing Company.
- Batten, J., Currie, C., Mann, J., & Morley, A. (2020). Proposal for a Total Fatigue Life Assessment Methodology That Predicts Fatigue Life From Defect Initiation to Through Wall Leak. *Proceedings of the ASME 2020 Pressure Vessels and Piping Conference*. <https://doi.org/10.1115/PVP2020-21706>
- Batten, J., Currie, C., Mann, J., & Wright, K. (2019). Scaling of SN Curves for Varying ‘Initiation’ Crack Definitions From Striation Counted Environmental Fatigue Specimens: A 250 Micron Austenitic Stainless Steel SN Curve and Associated Fen Factors. *Proceedings of the ASME 2019 Pressure Vessels and Piping Conference*. <https://doi.org/10.1115/PVP2019-93847>
- Beckjord, E. S. (1992). Memorandum, Eric S. Beckjord (NRC) to Warren Minners (NRC), “Generic Issue No. 78, ‘Monitoring of Fatigue Transient Limits for Reactor Coolant System’”, July 10, 1992. U.S. Nuclear Regulatory Commission.

- Bienussa, K., & Schulz, H. (1986). Protection Against Fatigue Damage with Respect to the Environmental Influence of LWR Operating Conditions. *Nuclear Engineering and Design*, 94(3), 317–324. [https://doi.org/https://doi.org/10.1016/0029-5493\(86\)90014-2](https://doi.org/https://doi.org/10.1016/0029-5493(86)90014-2)
- Blatman, G., Le Roux, J., Wallin, K., Solin, J., Métais, T., Karabaki, E., & Mayinger, W. (2016). Statistical Methods and Database Splitting for HCF Data Analysis. *Proceedings of the ASME 2016 Pressure Vessels and Piping Conference*. <https://doi.org/https://doi.org/10.1115/PVP2016-63141>
- Blatman, G., Métais, T., Le Roux, J., & Cambier, S. (2014). Statistical Analyses of High Cycle Fatigue French Data for Austenitic SS. *Proceedings of the ASME 2014 Pressure Vessels and Piping Conference*. <https://doi.org/https://doi.org/10.1115/PVP2014-28409>
- Bodai, M., Fukuta, Y., Asada, S., & Hayashi, K. (2018). Development of New Design Fatigue Curves in Japan: Discussion of Best Fit Curves Based on Fatigue Test Data With Large Scale Piping. *Proceedings of the ASME 2018 Pressure Vessels and Piping Conference*. <https://doi.org/https://doi.org/10.1115/PVP2019-93272>
- Bodai, M., Fukuta, Y., Asada, S., & Hayashi, K. (2019). Development of New Design Fatigue Curves in Japan: Discussion of Fatigue Crack Growth Based on Fatigue Test Data With Large Scale Piping. *Proceedings of the ASME 2019 Pressure Vessels and Piping Conference*. <https://doi.org/https://doi.org/10.1115/PVP2019-93272>
- Braden, D., & Stancavage, P. (1994). *BWR Primary Coolant Pressure Boundary License Renewal Industry Report (TR-103843, Revision 1)*. Electric Power Research Institute, U.S. Department of Energy and Nuclear Energy Institute.
- Buckthorpe, D., Tashkinov, A., Brynda, J., Davies, L. M., Cuote-Felgeueroso, C., Detroux, P., Beiniussa, K., & Guinovart, J. (2003). Review and Comparison of WWER and LWR Codes and Standards. In S. Vejvoda (Ed.), *Transactions of the 17th International Conference on Structural Mechanics in Reactor Technology (SMiRT 17), Part F*.
- CEN. (2009). *EN 13445-3:2009 Unfired Pressure Vessels-Part 3: Design*. European Committee for Standardization.
- Chopra, O., Alexandreanu, B., & Shack, W. J. (2005). *Effect of Material Heat Treatment on Fatigue Crack Initiation in Austenitic Stainless Steels in LWR Environments (NUREG/CR-6878, ANL-03/35)*. U.S. Nuclear Regulatory Commission.
- Chopra, O. K. (1994). *Letter to C.Hrabel (NRC) "Monthly Business Letter Report for program GI-78, Statistical Analysis of Fatigue Data" October 19*.
- Chopra, O. K. (1999). *Effects of LWR Coolant Environments on Fatigue Design Curves of Austenitic Stainless Steels (NUREG/CR-5704, ANL-98/31)*. U.S. Nuclear Regulatory Commission.
- Chopra, O. K. (2001). Environmental Effects on Fatigue Crack Initiation in Piping and Pressure Vessel Steels. *Proceedings of the 2000 International Conference on Fatigue of Reactor Components (MRP- 46): PWR Materials Reliability Program (PWRMRP) (1006070)*, 467–479.
- Chopra, O. K. (2002). *Mechanism and Estimation of Fatigue Crack Initiation in Austenitic Stainless Steels in LWR Environments (NUREG/CR-6787, ANL-01/25)*. U.S. Nuclear Regulatory Commission.
- Chopra, O. K., & Gavenda, D. J. (1997). Effects of LWR Coolant Environments on Fatigue Lives of Austenitic Stainless Steels. In D. P. Jones, B. R. Newton, W. J. O'Donnell, R. Vecchio, G. A. Amtaki, D. Bhavani, N. G. Cofie, & G. L. Hollinger (Eds.), *Pressure Vessel and Piping Codes and Standards, PVP Vol. 353* (pp. 87–97). American Society of Mechanical Engineers.
- Chopra, O. K., Gavenda, D. J., & Shack, W. J. (1995a). Fatigue of Ferritic Steels. In *Environmentally Assisted Cracking in Light Water Reactors Semiannual Report October 1994–March 1995 (NUREG/CR-4667 Vol. 20, ANL-95/41)* (pp. 1–19). U.S. Nuclear Regulatory Commission.
- Chopra, O. K., Gavenda, D. J., & Shack, W. J. (1995b). Fatigue of Ferritic Steels. In *Environmentally Assisted Cracking in Light Water Reactors Semiannual Report April–September 1994 (NUREG/CR-4667 Vol. 19, ANL-95/2)* (pp. 1–17). U.S. Nuclear Regulatory Commission.
- Chopra, O. K., Michaud, W. F., & Shack, W. J. (1993). Technical Progress. In *Environmentally Assisted Cracking in Light Water Reactors Semiannual Report October 1992–March 1993 (NUREG/CR-4667 Vol. 16, ANL-93/27)* (pp. 5–19). U.S. Nuclear Regulatory Commission.

- Chopra, O. K., Michaud, W. F., & Shack, W. J. (1995). Fatigue of Ferritic Steels. In *Environmentally Assisted Cracking in Light Water Reactors Semiannual Report October 1993–March 1994* (NUREG/CR-4667 Vol. 18, ANL-95/2) (pp. 1–10). U.S. Nuclear Regulatory Commission.
- Chopra, O. K., & Shack, W. J. (1995). Effects of LWR Environments on Fatigue Life of Carbon and Low Alloy Steels. In S. Yukawa, D. P. Jones, & H. S. Mehta (Eds.), *Fatigue and Crack Growth: Environmental Effects, Modeling Studies, and Design Considerations*, PVP-Vol. 306 (pp. 95–109). American Society of Mechanical Engineers.
- Chopra, O. K., & Shack, W. J. (1998a). *Effects of LWR Coolant Environments on Fatigue Design Curves of Carbon and Low-Alloy Steels* (NUREG/CR-6583, ANL-97/18). U.S. Nuclear Regulatory Commission.
- Chopra, O. K., & Shack, W. J. (1998b). Environmental Effects on Fatigue Strain-versus-Life (S-N) Behavior of Primary Pressure Boundary Materials. Carbon and Low-Alloy Steels. In *Environmentally Assisted Cracking in Light Water Reactors Semiannual Report January 1997–June 1997* (NUREG/CR-4667 Vol. 24, ANL-98/6) (pp. 5–31). U.S. Nuclear Regulatory Commission.
- Chopra, O. K., & Shack, W. J. (1999). Methods for Incorporating Effects of LWR Coolant Environments into ASME Code Fatigue Evaluations. In S. Rahman (Ed.), *Probabilistic and Environmental Aspects of Fracture*, PVP-Vol.386 (pp. 171–181). American Society of Mechanical Engineers.
- Chopra, O. K., & Shack, W. J. (2001). *Environmental Effects on Fatigue Crack Initiation in Piping and Pressure Vessel Steels* (NUREG/CR-6717, ANL-00/27). U.S. Nuclear Regulatory Commission.
- Chopra, O. K., & Shack, W. J. (2003a). Methods for Incorporating the Effects of LWR Coolant Environments in Pressure Vessel and Piping Fatigue Evaluations. *Materials Reliability Program: Second International Conference on Fatigue of Reactor Components (MRP-84) (1003536)*, 674–691.
- Chopra, O. K., & Shack, W. J. (2003b). *Review of the Margins for ASME Code Fatigue Design Curve - Effects of Surface Roughness and Material Variability* (NUREG/CR-6815, ANL-02/39). U.S. Nuclear Regulatory Commission.
- Chopra, O. K., & Shack, W. J. (2007). *Effect of LWR Coolant Environments on the Fatigue Life of Reactor Materials* (NUREG/CR-6909 Rev. 0, ANL-06/08). U.S. Nuclear Regulatory Commission.
- Chopra, O. K., & Smith, J. L. (1998). Estimation of Fatigue Strain–Life Curves for Austenitic Stainless Steels in Light Water Reactor Environments. In H. S. Mehta, R. W. Swindeman, J. A. Todd, S. Yukawa, M. Zako, W. H. Bamford, M. Higuchi, E. Jones, H. Nickel, & S. Rahman (Eds.), *Fatigue, Environmental Factors and New Materials*, PVP-Vol. 374 (pp. 249–259). American Society of Mechanical Engineers.
- Chopra, O. K., Smith, J. L., & Shack, W. J. (1998). Environmental Effects on Fatigue Strain-versus-Life (S-N) Behavior of Austenitic Stainless Steels. In *Environmentally Assisted Cracking in Light Water Reactors Semiannual Report July 1997–September 1997* (NUREG/CR-4667 Vol. 25, ANL-98/18) (pp. 2–25). U.S. Nuclear Regulatory Commission.
- Chopra, O. K., & Stevens, G. L. (2014). *Effect of LWR Coolant Environments on the Fatigue Life of Reactor Materials* (NUREG/CR-6909 Rev. 1, ANL-12/60) (Draft). U.S. Nuclear Regulatory Commission.
- Chopra, O. K., & Stevens, G. L. (2018). *Effect of LWR Coolant Environments on the Fatigue Life of Reactor Materials* (NUREG/CR-6909 Rev. 1, ANL-12/60). U.S. Nuclear Regulatory Commission.
- Coffin, L. F. (1953). *A Study of the Effects of Cyclic Thermal Stresses on a Ductile Metal* (KAPL-853). General Electric Company.
- Coffin, L. F. (1954). A Study of the Effects of Cyclic Thermal Stresses on a Ductile Metal. *Transactions of ASME*, 76, 931–950.
- Coffin, L. F. (1978). Discussion of Fatigue Design Criteria for Pressure Vessel Alloys by Jaske & O'Donnell (1977). *Journal of Pressure Vessel Technology*, 100(2), 238–242. <https://doi.org/https://doi.org/10.1115/1.3454459>
- Coffin, L. F. (1979). Fatigue in machines and structures-Power generation. In M. Meshii (Ed.), *Fatigue and Microstructure* (pp. 1–27). American Society for Metals.
- Cole, J. R., & Minichiello, J. C. (2010). Status Report on ASME Section III Subgroup on Design Plan for Code Changes to Implement Environmental Fatigue Evaluation Methods. *Proceedings of the ASME*

- 2010 Pressure Vessels and Piping Conference Pressure Vessels and Piping Conference. <https://doi.org/https://doi.org/10.1115/PVP2010-25677>
- Colin, J. (2009). *Deformation History and Load Sequence Effects on Cumulative Fatigue Damage and Life Predictions*. (PhD thesis), University of Toledo.
- Cooper, W. E. (1992). The Initial Scope and Intent of the Section III Fatigue Design Procedure. *PVRC Workshop on Environmental Effects on Fatigue Performance*.
- Courtin, S., Lefrançois, A., Le Duff, J. A., & Le Pécheur, A. (2012). Environmentally Assisted Fatigue Assessment Considering an Alternative Method to the ASME Code Case N-792. *Proceedings of the ASME 2012 Pressure Vessels & Piping Conference*. <https://doi.org/10.1115/PVP2012-78088>
- Courtin, S., Métais, T., Triay, M., Meister, E., & Marie, S. (2016). Modifications of the 2016 Edition of the RCC-M Code to Account for Environmentally Assisted Fatigue. *Proceedings of the ASME 2016 Pressure Vessels and Piping Conference*. <https://doi.org/10.1115/PVP2016-63127>
- Craig, J. W. (1991). Letter, John W. Craig (NRC) to Edward Griffing (NUMARC), "Fatigue Evaluation in NUMARC License Renewal Industry Reports", July 2, 1991. U.S. Nuclear Regulatory Commission.
- Craig, J. W. (1992). Summary of Meeting with NUMARC on Fatigue Evaluation with Respect to Industry Reports for License Renewal Applications, March 12, 1992. U.S. Nuclear Regulatory Commission.
- Craig, J. W. (1999). Letter, John W. Craig (NRC) to John H. Ferguson (ASME BNCS), December 1, 1999. U.S. Nuclear Regulatory Commission.
- Currie, C., Morley, A., Leary, D., Platts, N., Twite, M., & Wright, K. (2018). Further Validation of the Strain-Life Weighted (SNW) Fen Method for Plant Realistic Strain and Temperature Waveforms. *Proceedings of the ASME 2018 Pressure Vessels and Piping Conference*. <https://doi.org/10.1115/PVP2018-84879>
- Currie, C., Morley, A., Platts, N., Twite, M., & Wright, K. (2017). Models for Calculating the Effect of Environment on Fatigue Life (Fen) for Complex Waveforms and/or Non-Isothermal Conditions. *Proceedings of the ASME 2017 Pressure Vessels and Piping Conference*. <https://doi.org/10.1115/PVP2017-66030>
- Cuvilliez, S., McLennan, A., Mottershead, K., Mann, J., & Bruchhausen, M. (2020). INCEFA-PLUS Project: Lessons Learned From the Project Data and Impact on Existing Fatigue Assessment Procedures. *Proceedings of the ASME 2020 Pressure Vessels and Piping Conference*. <https://doi.org/10.1115/PVP2020-21106>
- De Baglion, L. (2011). *Comportement et endommagement en fatigue oligocyclique d'un acier inoxydable austénitique 304L en fonction de l'environnement (vide, air, eau primaire REP) à 300°C (PhD thesis)*. ISAE-ENSMA Ecole Nationale Supérieure de Mécanique et d'Aérotechnique - Poitiers.
- De Baglion, L., Cedat, D., Ould, P., & Chitty, W. J. (2014). Low Cycle Fatigue Behavior in Air and in PWR Water of a Type 304L Austenitic Stainless Steel Manufactured by Hot Isostatic Pressing Process. *Proceedings of the ASME 2014 Pressure Vessels & Piping Conference*. <https://doi.org/10.1115/PVP2014-28329>
- De Baglion, L., & Mendez, J. (2010). Low cycle fatigue behavior of a type 304L austenitic stainless steel in air or in vacuum, at 20 °C or at 300 °C: Relative effect of strain rate and environment. *Procedia Engineering*, 2(1), 2171–2179. <https://doi.org/10.1016/j.proeng.2010.03.233>
- De Baglion, L., Mendez, J., Le Duff, J.-A., & Lefrancois, A. (2012). Influence of PWR Primary Water on LCF Behavior of Type 304L Austenitic Stainless Steel at 300°C: Comparison With Results Obtained in Vacuum or in Air. *Proceedings of the ASME 2012 Pressure Vessels & Piping Conference*. <https://doi.org/10.1115/PVP2012-78767>
- Deardorff, A. F., Dedhia, D., Rosinski, S. T., & Harris, D. O. (2003). Probabilistic Analysis of 60-Year Environmental Fatigue Effects for Reactor Components. *Proceedings of the ASME 2003 Pressure Vessels and Piping Conference*. <https://doi.org/10.1115/PVP2003-1779>
- Deardorff, A. F., & Smith, J. K. (1994). *Evaluation of Conservatisms and Environmental Effects in ASME Code, Section III, Class 1 Fatigue Analysis (SAND94-0187)*. Sandia National Laboratories.
- Diercks, D. R. (1979). Development of Fatigue Design Curves for Pressure Vessel Alloys Using a Modified Langer Equation. *Journal of Pressure Vessel Technology*, 101(4), 292–297. <https://doi.org/https://doi.org/10.1115/1.3454636>
- EFD Committee. (1995). Progress report on experimental research on fatigue life in LWR environment May, 1993 to September, 1995. In *PVRC Fall Meeting, Columbus, Ohio, October 9–11, 1995*.

- Emslie, J., Cruchley, S., Currie, C., & Wright, K. (2017). Further Validation of the Weighted Stress Intensity Factor Rate (WKR) Method for Stainless Steel Pressurised Water Reactor Fatigue Crack Growth Calculations. *Proceedings of the ASME 2017 Pressure Vessels and Piping Conference*. <https://doi.org/https://doi.org/10.1115/PVP2017-65645>
- Emslie, J., Gill, C., & Wright, K. (2016). Assessment Method to Account for the Rise Time of Complex Waveforms in Stainless Steel Environmental Fatigue Crack Growth Calculations. *Proceedings of the ASME 2016 Pressure Vessels and Piping Conference*. <https://doi.org/https://doi.org/10.1115/PVP2016-63497>
- Endo, T., Fujiwara, M., & Kanasaki, H. (1985). Low-Cycle Fatigue Strength and Fracture Mode of 304 Stainless Steel in High Temperature Water. *Journal of the Society of Materials Science*, 34(381), 715–720. <https://doi.org/https://doi.org/10.2472/jsms.34.715>
- Energoatomizdat. (1989). *PNAE G-7-002-86 Regulations of Strength Analysis of Equipment and Piping of Nuclear Power Facilities*. Energoatomizdat.
- EPRI. (1992). *Metal Fatigue in Operating Nuclear Power Plants (TR-100252)*. Electric Power Research Institute.
- EPRI. (1998a). *Environmental Fatigue Evaluations of Representative BWR Components (TR-107943)*. Electric Power Research Institute, BWROG and GE Nuclear Energy.
- EPRI. (1998b). *Evaluation of Environmental Fatigue Effects for a Westinghouse Nuclear Power Plant (TR-110043)*. Electric Power Research Institute.
- EPRI. (2001a). *Materials Reliability Program: Guidelines for Addressing Fatigue Environmental Effects in a License Renewal Application (MRP-47) (1003083)*. Electric Power Research Institute.
- EPRI. (2001b). *Materials Reliability Program (MRP) Evaluation of Fatigue Data Including Reactor Water Environmental Effects (MRP-49) (1003079)*. Electric Power Research Institute, U.S. Department of Energy.
- EPRI. (2002). *Materials Reliability Program: Re-Evaluation of Results in NUREG/CR-6674 for Carbon and Low-Alloy Steel Components (MRP-74) (1003667)*. Electric Power Research Institute.
- EPRI. (2003). *Draft Interim Staff Guidance-13 "Environmental Assisted Fatigue for Carbon/Low-Alloy Steel."* Electr.
- EPRI. (2005a). *Materials Reliability Program: Guidelines for Addressing Fatigue Environmental Effects in a License Renewal Application (MRP-47, Rev.1) (1012017)*. Electric Power Research Institute.
- EPRI. (2005b). *Materials Reliability Program: Reevaluation of Stainless Steel Components in NUREG/CR-6674 (MRP-172) (1012896)*. Electric Power Research Institute.
- EPRI. (2012). *Guidelines for Addressing Environmental Effects in Fatigue Usage Calculations (1025823)*. Electric Power Research Institute.
- EPRI. (2018a). *Development of an Alternative Approach to ASME Code Simplified Elastic-Plastic Analysis (3002014122)*. Electric Power Research Institute.
- EPRI. (2018b). *Development of Fatigue Usage Life and Gradient Factors (3002014121)*. Electric Power Research Institute.
- EPRI. (2018c). *Environmentally Assisted Fatigue (EAF) Knowledge Gap Analysis: Update and Revision of the EAF Knowledge Gaps (3002013214)*. Electric Power Research Institute.
- EPRI. (2019). *BWRVIP-322: BWR Vessel and Internals Project Revised Allowable High-Cycle Fatigue Curves for Austenitic and Ferritic Steels (3002014859)*. Electric Power Research Institute.
- Faidy, C. (2008). Status of French Fatigue Analysis Procedure. *Proceedings of the ASME 2008 Pressure Vessels and Piping Conference*. <https://doi.org/https://doi.org/10.1115/PVP2008-61911>
- Faidy, C. (2012). Status of French Road Map to Improve Environmental Fatigue Rules. *Proceedings of the ASME 2012 Pressure Vessels and Piping Conference*. <https://doi.org/https://doi.org/10.1115/PVP2012-78805>
- Faidy, C. (2014). Fatigue Design Rules in Pressure Vessel Codes Uncertainties and Remaining Open Points. *Proceedings of the 22nd International Conference on Nuclear Engineering*. <https://doi.org/10.1115/ICONE22-30715>
- Filatov, V. M., & Zelensky, A. V. (1990). Low Cycle Fatigue of Structural Materials in Water Operating Environments. In W. H. Cullen (Ed.), *Proceedings of the Third International Atomic Energy Agency Specialists' Meeting on Subcritical Crack Growth (NUREG/CP-0112, ANL-90/22 Vol.1)* (pp. 215–222). U.S. Nuclear Regulatory Commission.

- Filatov, V. M., & Zelensky, A. V. (2003). Long-Term Low-Cycle Corrosion Fatigue of Steel 08Kh18N10T and its Welded Joints in Water of High Parameters. *Transactions of the 17th International Conference on Structural Mechanics in Reactor Technology (SMiRT 17), Part W*.
- Frost, N. E., Marsh, K. J., & Pook, L. P. (1974). *Metal Fatigue*. Clarendon Press.
- Fujiwara, M., Endo, T., & Kanasaki, H. (1986). Strain Rate Effects on the Low Cycle Fatigue Strength of 304 Stainless Steel in High Temperature Water Environment. In V. S. Goel (Ed.), *Fatigue life: Analysis and Prediction: Proc. of the Fatigue Program and Related Papers Presented at the Intl. Conference and Exposition on Fatigue, Corrosion Cracking, Fracture Mechanics and Failure Analysis, 2-6 December, 1985, Salt Lake City, Utah, USA* (pp. 309–313). American Society for Metals.
- Fukuta, Y., Kanasaki, H., Asada, S., & Sera, T. (2014). Proposal of Surface Finish Factor on Fatigue Strength in Design Fatigue Curve. *Proceedings of the ASME 2014 Pressure Vessels and Piping Conference*. <https://doi.org/https://doi.org/10.1115/PVP2014-28601>
- Fukuta, Y., Nomura, Y., Saruwatari, T., & Asada, S. (2013). High Strain Rate Effects on Environment Assisted Fatigue for Austenitic Stainless Steels in PWR Environment. *Proceedings of the ASME 2013 Pressure Vessels and Piping Conference*. <https://doi.org/10.1115/PVP2013-97158>
- Garnier, C., Barrachin, B., & Roche, R. (1975). Low Cycle Fatigue of Austenitic Alloys in Hot Water. In T. A. Jaeger (Ed.), *Transactions of the 3rd International Conference on Structural Mechanics in Reactor Technology (SMiRT 3), Part L*. North-Holland Publishing Company.
- Garnier, C., Kowalczyk, G., Roche, R. L., & Barrachin, B. (1979). Low Cycle Fatigue of Steels for Nuclear Pressure Vessels in Hot Water. In T. A. Jaeger & B. A. Boley (Eds.), *Transactions of the 5th International Conference on Structural Mechanics in Reactor Technology (SMiRT 5)*. North-Holland Publishing Company.
- Gavenda, D. J., & Chopra, O. K. (1996). Austenitic Stainless Steels. In *Environmentally Assisted Cracking in Light Water Reactors Semiannual Report January-June 1996 (NUREG/CR-4667 Vol.22, ANL-97/9)* (pp. 30–39). U.S. Nuclear Regulatory Commission.
- Gerber, D. A., & Stevens, G. L. (1997). *Evaluation of Thermal Fatigue Effects on Systems Requiring Aging Management Review for License Renewal for the Calvert Cliffs Nuclear Power Plant (TR-107515)*. Electric Power Research Institute.
- Gill, P., Brown, P., Tice, D., Platts, N., & Currie, C. (2019). Fatigue Initiation of 304L Stainless Steel Subject to Thermal Shock Loading in a PWR Environment. *Proceedings of the ASME 2019 Pressure Vessels and Piping Conference*. <https://doi.org/10.1115/PVP2019-93923>
- Gill, P., James, P., Currie, C., Madew, C., & Morley, A. (2017). An Investigation Into the Lifetimes of Solid and Hollow Fatigue Endurance Specimens Using Cyclic Hardening Material Models in Finite Element Analysis. *Proceedings of the ASME 2017 Pressure Vessels and Piping Conference*. <https://doi.org/10.1115/PVP2017-65975>
- Gill, P., Madew, C., James, P., Platts, N., & Twite, M. (2017). Thermomechanical Fatigue of Hollow Specimens in a Light Water Reactor Environment - Latest Test Results and Analysis. *Transactions of the 24th International Conference on Structural Mechanics in Reactor Technology (SMiRT 24)*.
- Gill, P., Onwuarolu, P., Smith, R., Coult, B., Kirkham, M., Sutcliffe, M., Cooper, K., Schofield, T., Madew, C., McLennan, A., & Currie, C. (2021). A Method for Investigating Multi-Axial Fatigue in a PWR Environment. *Proceedings of the ASME 2021 Pressure Vessels and Piping Conference*. <https://doi.org/10.1115/PVP2021-62429>
- Gill, P., Platts, N., Currie, C., & Grieveson, E. (2018). A Thermomechanical PWR Test Facility to Investigate Thermal Shock Loading on a Small Scale Tubular Specimen. *Proceedings of the ASME 2018 Pressure Vessels and Piping Conference*. <https://doi.org/10.1115/PVP2018-84923>
- Gonzalez, H. J., & Chopra, O. K. (2006). Resolution to Public Comments on DG-1144 and Draft NUREG/CR-6909. *ACRS Subcommittee Meeting on Materials, Metallurgy and Reactor Fuels December 6, 2006*.
- Grandemange, J. M., & Faidy, C. (2000). Démarche générale de prévention du risque d'endommagement par fatigue des matériels des chaudières nucléaires: de la conception au suivi en exploitation. *Endommagement Par Fatigue Des Installations Nucleaires*, 19–36.
- Griffing, E. P. (1991a). *Letter, Edward P. Griffing (NUMARC) to John Craig (NRC), July 19, 1991*. Nuclear Management and Resources Council.

- Griffing, E. P. (1991b). *Letter, Edward P. Griffing (NUMARC) to John W. Craig (NRC), May 29, 1991*. Nuclear Management and Resources Council.
- Griffiths, A., Gill, P., Coult, B., Beswick, J., Platts, N., Mann, J., Currie, C., & Airey, J. (2021). Negative R Fatigue Short Crack Growth Rate Testing on Austenitic Stainless Steels. *Proceedings of the ASME 2021 Pressure Vessels and Piping Conference*. <https://doi.org/https://doi.org/10.1115/PVP2021-62909>
- Grimes, C. I. (1998). *Letter, Christopher I. Grimes (NRC) to Douglas J. Walters (NEI), "Request for Additional Information on the Industry's Evaluation of Fatigue Effects for License Renewal", November 2, 1998*. U.S. Nuclear Regulatory Commission.
- Grimes, C. I. (1999). *Letter, Christopher I. Grimes (NRC) to Douglas J. Walters (NEI), "Request for Additional Information on the Industry's Evaluation of Fatigue Effects for License Renewal", August 6, 1999*. U.S. Nuclear Regulatory Commission.
- Grimes, C. I. (2000). *Summary of Meeting with the Nuclear Energy Institute (NEI) to Discuss Fatigue of Metal Components for 60-year Plant Life July 18, 2000*. U.S. Nuclear Regulatory Commission.
- Hale, D. A., Wilson, S. A., Kass, J. W., & Kiss, E. (1981). Low Cycle Fatigue of Commercial Piping Steels in a BWR Primary Water Environment. *Journal of Engineering Materials and Technology*, 103(1), 15–25. <https://doi.org/10.1115/1.3224967>
- Hale, D. A., Wilson, S. A., Kiss, E., & Giannuzzi, A. J. (1977). *Low Cycle Fatigue Evaluation of Primary Piping Materials in a BWR Environment (GEAP-20244)*. General Electric Company.
- Hechmer, J. (1998). Evaluation Methods for Fatigue—A PVRC Project. In H. S. Mehta, R. W. Swindeman, J. A. Todd, S. Yukawa, M. Zako, W. H. Bamford, M. Higuchi, E. Jones, H. Nickel, & S. Rahman (Eds.), *Fatigue, Environmental Factors and New Materials, PVP-Vol. 374* (pp. 191–199). American Society of Mechanical Engineers.
- Hechmer, J., & Hollinger, G. L. (2006). Subsection NB — Class 1 Components. In K. R. Rao (Ed.), *Companion Guide to the ASME Boiler & Pressure Vessel Code Volume 1* (2nd ed., pp. 193–232). American Society of Mechanical Engineers.
- Hicks, P. D., & Shack, W. J. (1992). Fatigue of Ferritic Steels. In *Environmentally Assisted Cracking in Light Water Reactors Semiannual Report April–September 1991 (NUREG/CR-4667 Vol. 13, ANL-92/6)* (pp. 3–8). U.S. Nuclear Regulatory Commission.
- Higuchi, M. (2001). An Updated Method to Evaluate Reactor Water Effects on Fatigue Life for Carbon and Low Alloy Steels. *Proceedings of the 2000 International Conference on Fatigue of Reactor Components (MRP- 46): PWR Materials Reliability Program (PWRMRP) (1006070)*, 651–676.
- Higuchi, M. (2005). Japanese Program Overview. *Materials Reliability Program: Third International Conference on Fatigue in Reactor Components (MRP-151) (1011958)*.
- Higuchi, M., Hirano, T., & Sakaguchi, K. (2004). Evaluation of Fatigue Damage on Operating Plant Components in LWR Water. *Proceedings of the ASME 2004 Pressure Vessels and Piping Conference*, 129–138. <https://doi.org/10.1115/PVP2004-2682>
- Higuchi, M., & Iida, K. (1989). An Investigation of Fatigue Strength Correction Factor for Oxygenated High Temperature Water Environment. In L. Cengdian & R. W. Nichols (Eds.), *Pressure Vessel Technology. Proceedings of the Sixth International Conference held in Beijing, People's Republic of China, 11-15 September 1988. Volume 2: Materials & Fabrication* (pp. 1157–1164). Pergamon Press.
- Higuchi, M., & Iida, K. (1991). Fatigue strength correction factors for carbon and low-alloy steels in oxygen-containing high-temperature water. *Nuclear Engineering and Design*, 129(3), 293–306. [https://doi.org/10.1016/0029-5493\(91\)90138-8](https://doi.org/10.1016/0029-5493(91)90138-8)
- Higuchi, M., Iida, K., & Asada, Y. (1995). Effects of Strain Rate Change on Fatigue Life of Carbon Steels in High-Temperature Water. In S. Yukawa, D. P. Jones, & H. S. Mehta (Eds.), *Fatigue and Crack Growth: Environmental Effects, Modeling Studies, and Design Considerations, PVP-Vol. 306* (pp. 111–116). American Society of Mechanical Engineers.
- Higuchi, M., Iida, K., & Asada, Y. (1997). Effects of Strain Rate Change on Fatigue Life of Carbon Steel in High- Temperature Water. In W. A. Van Der Sluys, R. S. Piascik, & R. Zawierucha (Eds.), *Effects of the Environment on the Initiation of Crack Growth (ASTM STP1298)* (pp. 216–231). American Society for Testing and Materials. <https://doi.org/10.1520/STP19963S>

- Higuchi, M., Iida, K., Hirano, A., Tsutsumi, K., & Sakaguchi, K. (2002). A Proposal of Fatigue Life Correction Factor F_{en} for Austenitic Stainless Steels in LWR Water Environments. *Proceedings of the ASME 2002 Pressure Vessels and Piping Conference*.
- Higuchi, M., Iida, K., Tsutsumi, K., Hirano, A., & Sakaguchi, K. (2003). Revised Proposal of Fatigue Life Correction Factor F_{en} for Austenitic Stainless Steels in LWR Water. *Materials Reliability Program: Second International Conference on Fatigue of Reactor Components (MRP-84) (1003536)*, 657–673.
- Higuchi, M., Nakamura, T., & Sugie, Y. (2009). Updated Knowledge Implemented to the Revision of Environmental Fatigue Evaluation Method for Nuclear Power Plant in JSME Code. *Proceedings of the ASME 2008 Pressure Vessels and Piping Conference*, 123–132. <https://doi.org/10.1115/PVP2009-77077>
- Higuchi, M., & Sakaguchi, K. (2005). Review and Consideration of Unsettled Problems on Evaluation of Fatigue Damage in LWR Water. *Proceedings of the ASME 2005 Pressure Vessels and Piping Conference*, 99–108. <https://doi.org/10.1115/PVP2005-71306>
- Higuchi, M., Sakaguchi, K., & Nomura, Y. (2007). Effects of Strain Holding and Continuously Changing Strain Rate on Fatigue Life Reduction of Structural Materials in Simulated LWR Water. *Proceedings of the ASME 2007 Pressure Vessels and Piping Conference*, 123–131. <https://doi.org/10.1115/PVP2007-26101>
- Higuchi, M., Sakaguchi, K., Nomura, Y., & Hirano, A. (2007). Final Proposal of Environmental Fatigue Life Correction Factor (F_{en}) for Structural Materials in LWR Water Environment. *Proceedings of the ASME 2007 Pressure Vessels and Piping Conference*. <https://doi.org/10.1115/PVP2007-26100>
- Higuchi, M., & Sakamoto, H. (1985). Low Cycle Fatigue of Carbon Steel in High Temperature Pure Water Environment. *Tetsu-to-Hagane*, 71(8), 1025–1031. https://doi.org/https://doi.org/10.2355/tetsutohagane1955.71.8_1025
- Higuchi, M., Tsutsumi, K., Hirano, A., & Sakaguchi, K. (2003). A Proposal of Fatigue Life Correction Factor F_{en} for Austenitic Stainless Steels in LWR Water Environments. *Journal of Pressure Vessel Technology*, 125(4), 403–410. <https://doi.org/10.1115/1.1613945>
- Hirano, A. (2023). Status on Code Case Proposal “Strain Rate for Piping and Valves.” *44th WG EFEM Meeting, Online, Virtual, August 7, 2023*.
- Hirano, A., Nakane, M., Asada, S., & Sera, T. (2014). Study on Consideration of Size Effects on Design Fatigue Curve. *Proceedings of the ASME 2014 Pressure Vessels and Piping Conference*. <https://doi.org/https://doi.org/10.1115/PVP2014-28573>
- Hirano, A., & Sakaguchi, K. (2006). Modified Rate Approach Method to Evaluate Fatigue Life of Carbon Steel Under Simulated Synchronously Changing BWR Conditions. *Proceedings of the ASME 2006 Pressure Vessels and Piping Conference*. <https://doi.org/10.1115/PVP2006-ICPVT-11-94066>
- Hirano, A., Yamamoto, M., Sakaguchi, K., & Shoji, T. (2004). Effects of Water Flow Rate on Fatigue Life of Carbon and Stainless Steels in Simulated LWR Environment. *Proceedings of the ASME 2004 Pressure Vessels and Piping Conference*. <https://doi.org/10.1115/PVP2004-2680>
- Hirano, A., Yamamoto, M., Sakaguchi, K., Shoji, T., & Iida, K. (2002). Effects of Water Flow Rate on Fatigue Life of Ferritic and Austenitic Steels in Simulated LWR Environment. *Proceedings of the ASME 2002 Pressure Vessels and Piping Conference*. <https://doi.org/https://doi.org/10.1115/PVP2002-1231>
- Hou, S. (2000). *Memorandum, Shou-nien Hou (NRC) to Edmund J. Sullivan (NRC), “Trip Report- PVRC Committee Meetings”, February 25, 2000*. U.S. Nuclear Regulatory Commission.
- Hytönen, Y. (2011). Environmental effects in Fatigue of Olkiluoto 3 stainless steel components A short overview of Finnish Nuclear Safety Authority. *ICG-EAC Annual Meeting*.
- Iida, K. (1989). Fatigue Problems in Nuclear and Offshore Structures. In *Proceedings of the International Conference on Evaluation of Materials Performance in Severe Environments: toward the development of materials for marine and other uses, EVALMAT89, Vol.1* (pp. 19–34). Iron & Steel Institute of Japan.
- Iida, K. (1992). A review of fatigue failures in LWR plants in Japan. *Nuclear Engineering and Design*, 138(3), 297–312. [https://doi.org/https://doi.org/10.1016/0029-5493\(92\)90068-7](https://doi.org/https://doi.org/10.1016/0029-5493(92)90068-7)

- Iida, K. (2001). Comparison of Japanese MITI Guideline and other Methods for Evaluation of Environmental Fatigue Life Reduction. In M. Rana (Ed.), *Pressure Vessel and Piping Codes and Standards, PVP Vol. 419* (pp. 73–81). American Society of Mechanical Engineers.
- Iida, K., Fukakura, J., Higuchi, M., Kobayashi, H., Miyazono, S., & Nakao, M. (1988). Survey of Fatigue Strength Data of Nuclear Structural Materials in Japan (Abstract of DBA Committee Report, 1988). *ASME Subgroup on Fatigue Strength, New York, December 5, 1988*.
- Iida, K., Kobayashi, H., & Higuchi, M. (1986). Predictive Method of Low Cycle Fatigue Life of Carbon and Low-Alloy Steels in High Temperature Water Environments. In W. H. Cullen (Ed.), *Proceedings of the Second International Atomic Energy Agency Specialists' Meeting on Subcritical Crack Growth (NUREG/CP-0067, MEA-2090, Vol. 2)* (pp. 385–409). U.S. Nuclear Regulatory Commission.
- Iwasaki, M., Takada, Y., & Nakamura, T. (2005). Evaluation of Environmental Fatigue in PWR PLM Activities. *Proceedings of the ASME 2005 Pressure Vessels and Piping Conference*, 183–191. <https://doi.org/10.1115/PVP2005-71509>
- JAERI. (1992). *Low cycle fatigue data collection of nuclear structural materials (JAERI-M-91-224)*. Japan Atomic Energy Research Institute.
- Jaske, C. E., & O'Donnell, W. J. (1977). Fatigue Design Criteria for Pressure Vessel Alloys. *Journal of Pressure Vessel Technology*, 99(4), 584–592. <https://doi.org/10.1115/1.3454577>
- JNES. (2007). *Environmental Fatigue Evaluation Method for Nuclear Power Generation Facilities (JNES-SS-0701)*. Japan Nuclear Safety Organization.
- JSME. (2001). *Standards for Nuclear Power Generation Facilities- Design and Construction Standards, JSME S NC1-2001*. Japan Society of Mechanical Engineers.
- JSME. (2006). *Codes for Nuclear Power Generation Facilities- Environmental Fatigue Evaluation Method for Nuclear Power Plants, JSME S NF1-2006*. Japan Society of Mechanical Engineers.
- JSME. (2009). *Codes for Nuclear Power Generation Facilities- Environmental Fatigue Evaluation Method for Nuclear Power Plants, JSME S NF1-2009*. Japan Society of Mechanical Engineers.
- JWES. (2023). *Fatigue Knowledge Platform*. https://www-it.jwes.or.jp/fatigue_knowledge/fatigue_committee.jsp#
- Kalinousky, D., & Muscara, J. (2001). Fatigue of Reactor Components: NRC Activities. *Proceedings of the 2000 International Conference on Fatigue of Reactor Components (MRP- 46): PWR Materials Reliability Program (PWRMRP) (1006070)*, 112–147.
- Kanasaki, H., Hayashi, M., Iida, K., & Asada, Y. (1995). Effects of Temperature Change on Fatigue Life of Carbon Steel in High Temperature Water. In S. Yukawa, D. P. Jones, & H. S. Mehta (Eds.), *Fatigue and Crack Growth: Environmental Effects, Modeling Studies, and Design Considerations, PVP-Vol. 306* (pp. 117–122). American Society of Mechanical Engineers.
- Kanasaki, H., Higuchi, M., Asada, S., Yasuda, M., & Sera, T. (2013). Proposal of Fatigue Life Equations for Carbon and Low-Alloy Steels and Austenitic Stainless Steels as a Function of Tensile Strength. *Proceedings of the ASME 2013 Pressure Vessels and Piping Conference*. <https://doi.org/https://doi.org/10.1115/PVP2013-97770>
- Kanasaki, H., Hirano, A., Iida, K., & Asada, Y. (1997). Corrosion Fatigue Behavior and Life Prediction Method under Changing Temperature Conditions. In W. A. Van Der Sluys, R. S. Piascik, & R. Zawierucha (Eds.), *Effects of the Environment on the Initiation of Crack Growth (ASTM STP1298)* (pp. 267–281). American Society for Testing and Materials. <https://doi.org/https://doi.org/10.1520/STP19966S>
- Kanasaki, H., Umehara, R., Mizuta, H., & Suyama, T. (1997a). Effects of Strain Rate and Temperature Change on the Fatigue Life of Stainless Steel in PWR Primary Water. In M. Livolant (Ed.), *Transactions of the 14th International Conference on Structural Mechanics in Reactor Technology (SMiRT 14), Part D* (pp. 485–493). CEA, EDF, Framatome, INSA.
- Kanasaki, H., Umehara, R., Mizuta, H., & Suyama, T. (1997b). Fatigue Lives of Stainless Steels in PWR Primary Water. In M. Livolant (Ed.), *Transactions of the 14th International Conference on Structural Mechanics in Reactor Technology (SMiRT 14), Part D* (pp. 473–484). CEA, EDF, Framatome, INSA.
- Karcher, G. G. (1999). Minutes of the PVRC (Combined Division) and Executive Committee Meeting, June 16, 1999. In *WRC Progress Reports Volume 54, No. 5/6 1999* (pp. 1–28). Welding Research Council.

- Keisler, J., & Chopra, O. K. (1995). Statistical Analysis of Fatigue Strain-Life Data for Carbon and Low-Alloy Steels. In E. D. Jones & F. L. Cho (Eds.), *Risk and Safety Assessments: Where is the Balance?*, PVP-Vol.296 (pp. 355–366). American Society of Mechanical Engineers.
- Keisler, J., Chopra, O. K., & Shack, W. J. (1994). *Statistical Analysis of Fatigue Strain-Life Data for Carbon and Low-Alloy Steels (NUREG/CR-6237, ANL-94/21)*. U.S. Nuclear Regulatory Commission.
- Keisler, J., Chopra, O. K., & Shack, W. J. (1995). *Fatigue Strain-Life Behavior of Carbon and Low-Alloy Steels, Austenitic Stainless Steels, and Alloy 600 in LWR Environments (NUREG/CR-6335, ANL-95/15)*. U.S. Nuclear Regulatory Commission.
- Keisler, J. M., Chopra, O. K., & Shack, W. J. (1996). Statistical models for estimating fatigue strain-life behavior of pressure boundary materials in light water reactor environments. *Nuclear Engineering and Design*, 167(2), 129–154. [https://doi.org/10.1016/S0029-5493\(96\)01293-9](https://doi.org/10.1016/S0029-5493(96)01293-9)
- Khaleel, M. A., Simonen, F. A., Phan, H. K., Harris, D. O., & Dedhia, D. (2000). *Fatigue Analysis of Components for 60-Year Plant Life (NUREG/CR-6674, PNNL-13227)*. U.S. Nuclear Regulatory Commission.
- KHK. (2010). *KHKS-0220 Standard for Pressure Equipment Containing Ultrahigh Pressure Gas*. High Pressure Gas Safety Institute of Japan.
- Kilsby Jr., E. R. (1964). *A Survey of Water Reactor Primary System Conditions Pertinent to the Study of Pipe Rupture (GEAP-4445)*. General Electric Company.
- Kishida, K. (1997). Advances in Environmental Fatigue Evaluation for Light Water Reactor Components. In W. A. Van Der Sluys, R. S. Piascik, & R. Zawierucha (Eds.), *Effects of the Environment on the Initiation of Crack Growth (ASTM STP1298)* (pp. 282–297). American Society for Testing and Materials. <https://doi.org/10.1520/STP19967S>
- Kishida, K., Suzuki, S., & Asada, Y. (1995). Evaluation of Environmental Fatigue Life for Light Water Reactor Components. In S. Yukawa, D. P. Jones, & H. S. Mehta (Eds.), *Fatigue and Crack Growth: Environmental Effects, Modeling Studies, and Design Considerations, PVP-Vol. 306* (pp. 139–147). American Society of Mechanical Engineers.
- Klepfer, H. H. (1965). *Experimental and Analytical Program Recommendations (GEAP-4474)*. General Electric Company.
- Kress, T. S. (1996). *Letter, Thomas S. Kress (ACRS) to James M. Taylor (NRC), "Resolution of Generic Safety Issue 78, "Monitoring of Fatigue Transient Limits for the Reactor Coolant System"", March 14, 1996*. U.S. Nuclear Regulatory Commission.
- KTA. (2013). *KTA 3201.2 Komponenten des Primärkreises von Leichtwasserreaktoren Teil 2: Auslegung, Konstruktion und Berechnung*. Kerntechnischer Ausschuss.
- Kuo, P. T. (1991). *Summary of Meeting with NUMARC on Fatigue Evaluation with Respect to Industry Reports for License Renewal Application, August 8, 1991*. U.S. Nuclear Regulatory Commission.
- Kuo, P. T. (2002). *Letter, Pao-Tsin Kuo (NRC) to Alan P. Nelson (NEI), "Request for Additional Information Regarding EPRI Technical Report, "Guidelines for Addressing Fatigue Environmental Effects in a License Renewal Application (MRP-47)", June 26, 2002*. U.S. Nuclear Regulatory Commission.
- Kuo, P. T. (2003). *Letter, Pao-Tsin Kuo (NRC) to Fred A. Emerson (NEI), "Request for Additional Information for Proposed Interim Staff Guidance (ISG)-11: Recommendations for Fatigue Environmental Effects in a License Renewal Application", June 30, 2003*. U.S. Nuclear Regulatory Commission.
- Kuo, P. T. (2004). *Letter, Pao-Tsin Kuo (NRC) to Fred A. Emerson (NEI), "Evaluation of Proposed Interim Staff Guidance (ISG)-11: Recommendations for Fatigue Environmental Effects in a License Renewal Application", January 21, 2004*. U.S. Nuclear Regulatory Commission.
- Langer, B. F. (1962). Design of Pressure Vessels for Low-Cycle Fatigue. *Journal of Basic Engineering*, 84(3), 389–399. <https://doi.org/10.1115/1.3657332>
- Larkins, J. T. (2006). *Memorandum, John T. Larkins (ACRS) to Luis A. Reyes (NRC), "Draft Regulatory Guide DG-1144", May 5, 2006*. U.S. Nuclear Regulatory Commission.
- Le Duff, J. A., Lefrançois, A., & Vernet, J. P. (2008). Effects of Surface Finish and Loading Conditions on the Low Cycle Fatigue Behavior of Austenitic Stainless Steel in PWR Environment: Comparison of

- LCF Test Results With NUREG/CR-6909 Life Estimations. *Proceedings of the ASME 2008 Pressure Vessels and Piping Division Conference*. <https://doi.org/10.1115/PVP2008-61894>
- Le Duff, J. A., Lefrançois, A., & Vernot, J. P. (2009). Effects of Surface Finish and Loading Conditions on the Low Cycle Fatigue Behavior of Austenitic Stainless Steel in PWR Environment for Various Strain Amplitude Levels. *Proceedings of the ASME 2009 Pressure Vessels and Piping Division Conference*. <https://doi.org/10.1115/PVP2009-78129>
- Le Duff, J. A., Lefrançois, A., Vernot, J. P., & Bossu, D. (2010). Effect of Loading Signal Shape and of Surface Finish on the Low Cycle Fatigue Behavior of 304L Stainless Steel in PWR Environment. *Proceedings of the ASME 2010 Pressure Vessels and Piping Conference*. <https://doi.org/10.1115/PVP2010-26027>
- Le Pécheur, A. (2009). *Fatigue thermique d'un acier inoxydable austénitique: influence de l'état de surface par une approche multi-échelles*. (PhD thesis), Ecole Centrale Paris.
- Lee, S. (1990). *Summary of the Meeting with NUMARC on Fatigue Evaluation with Respect to the Industry Reports Which Address the Subject of License Renewal, November 16, 1990*. U.S. Nuclear Regulatory Commission.
- Majumdar, S., Chopra, O. K., & Shack, W. J. (1993). *Interim Fatigue Design Curves for Carbon, Low-Alloy, and Austenitic Stainless Steels in LWR Environments (NUREG/CR-5999, ANL-93/3)*. U.S. Nuclear Regulatory Commission.
- Manjoine, M. J., & Tome, R. E. (1983). Proposed Design Criteria for High Cycle Fatigue of Stainless Steels. In D. A. Woodford & J. R. Whitehead (Eds.), *The Materials Conference: Proc. ASME International Conference on Advances in Life Prediction Methods, April 18–20, 1983, Albany, New York* (pp. 51–57). American Society of Mechanical Engineers.
- Manson, S. S. (1953). *Behavior of Materials Under Conditions of Thermal Stress (NACA TN 2933)*. National Advisory Committee for Aeronautics.
- Manson, S. S. (1954). *Behavior of Materials Under Conditions of Thermal Stress (NACA-TR-1170)*. National Advisory Committee for Aeronautics.
- Manson, S. S., & Halford, G. R. (1967). *A Method of Estimating High-Temperature Low-Cycle Fatigue Behavior of Materials (NASA TM X-52270)*. National Aeronautics and Space Administration.
- Marion, A. (2003). *Letter, Alexander Marion (NEI) to Pao-Tsin Kuo (NRC), "Revision 1 to Interim Staff Guidance (ISG)-11: "Environmental Assisted Fatigue for Carbon Low-Alloy Steel"", October 3, 2003*. Nuclear Energy Institute.
- McCree, V. M. (2017). *Letter, Victor M. McCree (NRC) to Dennis Bley (ACRS), "Revision of Regulatory Guidance for Evaluating Effects of Light-Water Reactor Water Environments in Fatigue Analyses of Metal Components", March 24, 2017*. U.S. Nuclear Regulatory Commission.
- McKillop, S., Donavin, P., & Keating, R. (2021). ASME Section III Standards Committee Fatigue Action Plan. *Proceedings of the ASME 2021 Pressure Vessels and Piping Conference*. <https://doi.org/10.1115/PVP2021-61295>
- McLennan, A., Cicero, R., Mottershead, K., Courtin, S., Que, Z., & Cicero, S. (2022). INCEFA-SCALE (Increasing Safety in NPPs by Covering Gaps in Environmental Fatigue Assessment - Focusing on Gaps Between Laboratory Data and Component-Scale). *Proceedings of the ASME 2022 Pressure Vessels and Piping Conference*. <https://doi.org/10.1115/PVP2022-84625>
- McLennan, A., Morley, A., & Cuvilliez, S. (2020). Further Evidence of Margin for Environmental Effects, Termed Fen-Threshold, in the ASME Section III Design Fatigue Curve for Austenitic Stainless Steels Through the Interaction Between the PWR Environment and Surface Finish. *Proceedings of the ASME 2020 Pressure Vessels and Piping Conference*. <https://doi.org/10.1115/PVP2020-21262>
- McLennan, A., Tweddle, A., Meldrum, J., Holden, J., McVey, L., Austin, C., Platts, N., & Twite, M. (2017). Effect of Shoulder Extension Control on Fatigue Endurance Testing of Stainless Steels. *Fatigue of Nuclear Reactor Components, Proceedings of the OECD/NEA CSNI WGIAGE Fourth International Conference*.
- Mehta, H., & Nickell, R. (1999). Impact of Current Data. In *Industry /NRC Meeting on Fatigue Reactor Water Environmental Effects, April 27, 1999*.
- Mehta, H. S. (1998). Application of EPRI GE Environmental Factor Approach to Representative BWR Pressure Vessel and Piping Fatigue Evaluations. In B. T. Lubin, T. Tahara, P. O'Regan, N. G.

- Cofie, K. R. Rao, & Y. Hari (Eds.), *Pressure Vessel and Piping Codes and Standards, PVP Vol. 360* (pp. 413–425). American Society of Mechanical Engineers.
- Mehta, H. S. (1999). An Update on the EPRI GE Environmental Fatigue Evaluation Methodology and its Applications. In S. Rahman (Ed.), *Probabilistic and Environmental Aspects of Fracture, PVP-Vol.386* (pp. 183–193). American Society of Mechanical Engineers.
- Mehta, H. S. (2000). An Update on the Consideration of Reactor Water Effects in Code Fatigue Initiation Evaluations for Pressure Vessels and Piping. In R. Mohan (Ed.), *Assessment Methodologies for Preventing Failures-II: Service Experience and Environmental Considerations, PVP-Vol.410-2* (pp. 45–51). American Society for Testing and Materials.
- Mehta, H. S. (2001). An Update on the Consideration of Reactor Water Effects in Code Fatigue Initiation Evaluations for Pressure Vessels and Piping. *Proceedings of the 2000 International Conference on Fatigue of Reactor Components (MRP- 46): PWR Materials Reliability Program (PWRMRP) (1006070)*, 749–757.
- Mehta, H. S., & Gosselin, S. R. (1995). *An Environmental Factor Approach to Account for Reactor Water Effects in Light Water Reactor Pressure Vessel and Piping Fatigue Evaluations (TR-105759)*. Electric Power Research Institute.
- Mehta, H. S., & Gosselin, S. R. (1996). An Environmental Factor Approach to Account for Reactor Water Effects In Light Water Reactor Pressure Vessels and Piping Fatigue Evaluations. In H. S. Mehta (Ed.), *Fatigue and Fracture Volume I, PVP-Vol.323* (pp. 171–185). American Society of Mechanical Engineers.
- Mehta, H. S., & Gosselin, S. R. (1998). Environmental Factor Approach to Account for Water Effects In Pressure Vessel and Piping Fatigue Evaluations. *Nuclear Engineering and Design*, 181(1–3), 175–197. [https://doi.org/https://doi.org/10.1016/S0029-5493\(97\)00344-0](https://doi.org/https://doi.org/10.1016/S0029-5493(97)00344-0)
- Mehta, H. S., Ranganath, S., & Weinstein, D. (1986). *Application of Environmental Fatigue Stress Rules to Carbon Steel Reactor Piping (NP-4644M)*. Electric Power Research Institute.
- Meldrum, J., Gill, P., Mann, J., McLennan, A., Platts, N., & Toal, M. (2023). Shoulder Control for Fatigue Endurance Tests Carried Out Under Variable Amplitude Loading Conditions . *Proceedings of the ASME 2023 Pressure Vessels and Piping Conference*.
- Métais, T., Courtin, S., De Baglion, L., Gourdin, C., & Le Roux, J.-C. (2017). ASME Code-Case Proposal to Explicitly Quantify the Interaction Between the PWR Environment and Component Surface Finish. *Proceedings of the ASME 2017 Pressure Vessels and Piping Conference*. <https://doi.org/10.1115/PVP2017-65367>
- Métais, T., Courtin, S., Genette, P., De Baglion, L., Gourdin, C., & Le Roux, J. (2014). Status of the French Methodology Proposal for Environmentally Assisted Fatigue Assessment. *Proceedings of the ASME 2014 Pressure Vessels and Piping Conference*. <https://doi.org/https://doi.org/10.1115/PVP2014-28408>
- Métais, T., Courtin, S., Genette, P., De Baglion, L., Gourdin, C., & Le Roux, J. (2015). Overview Of French Proposal Of Updated Austenitic SS Fatigue Curves And Of A Methodology To Account For EAF. *Proceedings of the ASME 2015 Pressure Vessels and Piping Conference*. <https://doi.org/https://doi.org/10.1115/PVP2015-45158>
- Métais, T., Courtin, S., Genette, P., Lefrancois, A., Massoud, J., & De Baglion, L. (2013). French Methodology Proposal for Environmentally Assisted Fatigue Assessment. *Proceedings of the ASME 2013 Pressure Vessels and Piping Conference*. <https://doi.org/https://doi.org/10.1115/PVP2013-97203>
- Métais, T., Morley, A., de Baglion, L., Tice, D., Stevens, G. L., & Cuvilliez, S. (2018). Explicit Quantification of the Interaction Between the PWR Environment and Component Surface Finish in Environmental Fatigue Evaluation Methods for Austenitic Stainless Steels. *Proceedings of the ASME 2018 Pressure Vessels and Piping Conference*. <https://doi.org/10.1115/PVP2018-84240>
- Miner, M. A. (1945). Cumulative Damage in Fatigue. *Journal of Applied Mechanics*, 12(3), 159–164.
- MITI. (2000). *MITI Guideline for Evaluating Fatigue Initiation Life Reduction in LWR Environment (in Japanese)*. Ministry of International Trade and Industry.
- Mohanty, S., Soppet, W. K., Majumdar, S., & Natesan, K. (2015). Pressurized Water Reactor Environment Effect on 316 Stainless Steel Stress Hardening/Softening: An Experimental Study.

- Proceedings of the ASME 2015 Pressure Vessels and Piping Conference*.
<https://doi.org/10.1115/PVP2015-45694>
- Mohanty, S., Soppet, W. K., Majumdar, S., & Natesan, K. (2016). In-air and pressurized water reactor environment fatigue experiments of 316 stainless steel to study the effect of environment on cyclic hardening. *Journal of Nuclear Materials*, 473, 290–299.
<https://doi.org/10.1016/j.jnucmat.2016.01.034>
- Morley, A., & McLennan, A. (2022). Statistical Analyses of Austenitic Stainless Steel High Cycle Fatigue Data to Support a Revised Design Factor for Design Fatigue Curve Development. *Proceedings of the ASME 2022 Pressure Vessels and Piping Conference*. <https://doi.org/10.1115/PVP2022-84249>
- Morley, A., Twite, M., Platts, N., McLennan, A., & Currie, C. (2018). Effect of Surface Condition on the Fatigue Life of Austenitic Stainless Steels in High Temperature Water Environments. *Proceedings of the ASME 2018 Pressure Vessels and Piping Conference*. <https://doi.org/10.1115/PVP2018-84251>
- Morrison, D. (1997). *Memorandum, David Morrison (NRC) to Hugh L. Thompson Jr. (NRC), "Closeout of Generic Safety Issue 78, "Monitoring of Fatigue Transient Limits for Reactor Coolant System (RCS)" and Generic Safety Issue 166, 'Adequacy of Fatigue Life of Metal Components", F. U.S. Nuclear Regulatory Commission.*
- Mottershead, K., Bruchhausen, M., Cicero, S., & Cuvilliez, S. (2020). INCEFA-PLUS: Increasing Safety in NPPs by Covering Gaps in Environmental Fatigue Assessment. *Proceedings of the ASME 2020 Pressure Vessels and Piping Conference*. <https://doi.org/10.1115/PVP2020-21220>
- Murley, T. E., & Beckjord, E. S. (1993). *Memorandum, Thomas E. Murley and Eric S. Beckjord (NRC) to James H. Sniezek (NRC), "Resolution of Fatigue and Environmental Qualification Issues Related to License Renewal", April 1, 1993. U.S. Nuclear Regulatory Commission.*
- Nagata, N., Sato, S., & Katada, Y. (1989). Low Cycle Fatigue Behaviour of Low Alloy Steels in High Temperature Pressurized Water. In A. H. Hadjian (Ed.), *Transactions of the 10th International Conference on Structural Mechanics in Reactor Technology (SMiRT 10), Part F* (pp. 209–214). American Association for Structural Mechanics in Reactor Technology.
- Nagata, N., Sato, S., & Katada, Y. (1991). Low Cycle Fatigue Behavior of Pressure Vessel Steels in High Temperature Pressurized Water. *ISIJ International*, 31(1), 106–114.
<https://doi.org/https://doi.org/10.2355/isijinternational.31.106>
- Nakamura, T., Higuchi, M., Kusunoki, T., & Sugie, Y. (2006). JSME Codes on Environmental Fatigue Evaluation. *Proceedings of the ASME 2006 Pressure Vessels and Piping Conference*.
<https://doi.org/10.1115/PVP2006-ICPVT-11-93305>
- Nakamura, T., & Madarame, H. (2005). Current Status of Development on Codes for Fatigue Evaluation in JSME. *Materials Reliability Program: Third International Conference on Fatigue in Reactor Components (MRP-151) (1011958)*.
- Nakamura, T., Saito, I., & Asada, Y. (2003). Guidelines on Environmental Fatigue Evaluation for LWR Component. *Proceedings of the ASME 2003 Pressure Vessels and Piping Conference*, 161–171.
<https://doi.org/10.1115/PVP2003-1780>
- Nakamura, T., & Sugie, Y. (2011). Establishment of Voluntary Consensus Codes and the Role of Code Engineers—Example of Creating the Environmental Fatigue Evaluation Method for Light Water Reactors—. *Journal of Nuclear Science and Technology*, 48(7), 970–983.
<https://doi.org/10.1080/18811248.2011.9711784>
- Nakane, M., Wang, Y., Hato, H., Yamamoto, M., Hirano, A., & Hayashi, K. (2019). Development of New Design Fatigue Curves in Japan: Discussion of Effect of Surface Finish on Fatigue Strength of Nuclear Component Materials. *Proceedings of the ASME 2019 Pressure Vessels and Piping Conference*. <https://doi.org/https://doi.org/10.1115/PVP2019-93167>
- Nelson, A. P. (2003). *Letter, Alan P. Nelson (NEI) to Pao-Tsin Kuo (NRC), "Interim Staff Guidance (ISG): Recommendations for Fatigue Environmental Effects in a License Renewal Application", January 17, 2003. Nuclear Energy Institute.*
- Nickell, R. E., Gerber, D. A., & Stevens, G. L. (2001). An Approach for Evaluating the Effects of Reactor Water Environments on Fatigue Life. *Proceedings of the 2000 International Conference on Fatigue of Reactor Components (MRP- 46): PWR Materials Reliability Program (PWRMRP) (1006070)*, 567–616.

- Nishimura, M., Nakamura, T., & Asada, Y. (2003). TENPES Guidelines for Environmental Fatigue Evaluation in LWR Nuclear Power Plants in Japan. *Materials Reliability Program: Second International Conference on Fatigue of Reactor Components (MRP-84) (1003536)*, 611–655.
- Nomura, Y., Asada, S., Nakamura, T., & Tanaka, M. (2010). Effects of continuous strain rate changing on environmental fatigue for stainless steels in PWR environment. *American Society of Mechanical Engineers, Pressure Vessels and Piping Division (Publication) PVP*, 1, 209–214. <https://doi.org/10.1115/PVP2010-25194>
- Nomura, Y., Higuchi, M., Asada, Y., & Sakaguchi, K. (2004). The Modified Rate Approach Method to Evaluate Fatigue Life Under Synchronously Changing Temperature and Strain Rate in Elevated Temperature Water in Austenitic Stainless Steel. *Proceedings of the ASME 2004 Pressure Vessels and Piping Conference*, 101–108. <https://doi.org/10.1115/PVP2004-2679>
- Nomura, Y., Tsutsumi, K., Inoue, T., Asada, S., & Nakamura, T. (2009). Optimization of Environmental Fatigue Evaluation (Step 2). *Proceedings of the ASME 2009 Pressure Vessels and Piping Conference*. <https://doi.org/https://doi.org/10.1115/PVP2009-77115>
- O'Donnell, W. J. (2014). The ASME Approach for the Nuclear Industry. *FESI Bulletin*, 8(1), 9–26.
- O'Donnell, W. J., & O'Donnell, W. J. (2008). Temperature Dependence of Reactor Water Environmental Fatigue Effects on Carbon, Low Alloy and Austenitic Stainless Steels. *Proceedings of the ASME 2008 Pressure Vessels and Piping Conference*. <https://doi.org/https://doi.org/10.1115/PVP2008-61917>
- O'Donnell, W. J., O'Donnell, W. J., & O'Donnell, T. P. (2005a). Proposed New Fatigue Design Curves for Austenitic Stainless Steels, Alloy 600 and Alloy 800. *Proceedings of the ASME 2005 Pressure Vessels and Piping Conference Pressure Vessels and Piping Conference*. <https://doi.org/https://doi.org/10.1115/PVP2005-71409>
- O'Donnell, W. J., O'Donnell, W. J., & O'Donnell, T. P. (2005b). Proposed New Fatigue Design Curves for Carbon and Low Alloy Steels in High Temperature Water. *Proceedings of the ASME 2005 Pressure Vessels and Piping Conference Pressure Vessels and Piping Conference*. <https://doi.org/https://doi.org/10.1115/PVP2005-71410>
- O'Donnell, W. J., Porowski, J. S., Hampton, E. J., Badlani, M. L., Weidenhamer, G. H., Jones, D. P., Abel, J. S., & Tomkins, B. (1989). Aging and Reactor Water Effects on Fatigue Life. In A. Beranek (Ed.), *Proceedings of the International Nuclear Power Plant Aging Symposium held in Bethesda, Maryland August 30–September 1, 1988 (NUREG/CP-0100)* (pp. 100–113). U.S. Nuclear Regulatory Commission.
- Ohata, H. (2001). Environmental Fatigue Evaluation on Japanese Nuclear Power Plants. *Proceedings of the 2000 International Conference on Fatigue of Reactor Components (MRP- 46): PWR Materials Reliability Program (PWRMRP) (1006070)*, 497–513.
- Olshan, L. N. (2001). *Memorandum, Leonard N. Olshan (NRC) to Stuart A. Richards (NRC), "Summary of January 31, 2001 Meeting with Electric Power Research Institute to Discuss Fatigue Evaluation Guidelines", January 31, 2001*. U.S. Nuclear Regulatory Commission.
- Palmgren, A. G. (1924). Die Lebensdauer von Kugellagern. *Zeitschrift Des Vereines Deutscher Ingenieure*, 68(14), 339–341.
- Pellereau, B. (2021). Unlocking Total Life: Summary of Key Topics. *37th WG EFEM Meeting, Online, Virtual, November 1, 2021*.
- Platts, N., Brown, P., Gill, P. J., Smith, R. D., & Stairmand, J. W. (2016). Development of a New Thermo-Mechanical Environmental Fatigue Testing Facility to Investigate the Impact of Thermal Strain Gradients on Fatigue Initiation. *Proceedings of the ASME 2016 Pressure Vessels and Piping Conference*. <https://doi.org/10.1115/PVP2016-63161>
- Platts, N., Tice, D. R., & Nicholls, J. (2015). Study of Fatigue Initiation of Austenitic Stainless Steel in a High Temperature Water Environment and in Air Using Blunt Notch Compact Tension Specimens. *Proceedings of the ASME 2015 Pressure Vessels and Piping Conference*. <https://doi.org/10.1115/PVP2015-45844>
- Platts, N., Tice, D., Stairmand, J., Mottershead, K., Zhang, W., Meldrum, J., & McLennan, A. (2015). Effect of Surface Condition on the Fatigue Life of Austenitic Stainless Steels in High Temperature Water Environments. *Proceedings of the ASME 2015 Pressure Vessels and Piping Conference*. <https://doi.org/10.1115/PVP2015-45029>

- Pleune, T. T., & Chopra, O. K. (1997). Artificial Neural Networks and Effects of Loading Conditions on Fatigue Life of Carbon and Low-Alloy Steels. In S. Rahman, K. K. Yoon, S. Bhandari, R. Warke, & J. M. Bloom (Eds.), *Fatigue and Fracture Volume 1, PVP-Vol.350* (pp. 413–423). American Society of Mechanical Engineers.
- Pleune, T. T., & Chopra, O. K. (2000). Using artificial neural networks to predict the fatigue life of carbon and low-alloy steels. *Nuclear Engineering and Design*, 197(1–2), 1–12. [https://doi.org/https://doi.org/10.1016/S0029-5493\(99\)00252-6](https://doi.org/https://doi.org/10.1016/S0029-5493(99)00252-6)
- Pook, L. P. (2007). *Metal Fatigue What It Is, Why It Matters*. Springer.
- Poulain, T., de Baglion, L., Mendez, J., & Hénaff, G. (2019). Influence of Strain Rate and Waveshape on Environmentally-Assisted Cracking during Low-Cycle Fatigue of a 304L Austenitic Stainless Steel in a PWR Water Environment. *Metals*, 9(2), 197. <https://doi.org/10.3390/met9020197>
- Powers, D. A. (1999). Letter, Dana A. Powers (NRC) to William D. Travers (NRC), “Proposed Resolution of Generic Safety Issue-190, “Fatigue Evaluation of Metal Components for 60-year Plant Life””, December 10, 1999. U.S. Nuclear Regulatory Commission.
- Ranganath, S., Kass, J. N., & Heald, J. D. (1982a). *BWR Environmental Cracking Margins for Carbon Steel Piping (NP-2406, Appendix 3)*. Electric Power Research Institute.
- Ranganath, S., Kass, J. N., & Heald, J. D. (1982b). Fatigue Behavior of Carbon Steel Components in High-Temperature Water Environments. In C. Amzallag, B. Leis, & P. Rabbe (Eds.), *Low-Cycle Fatigue and Life Prediction (ASTM STP 770)* (pp. 436–459). American Society for Testing and Materials. <https://doi.org/https://doi.org/10.1520/STP32440S>
- Reedy, R. F. (2006). A Commentary for Understanding and Applying the Principles of the ASME Boiler and Pressure Vessel Code. In K. R. Rao (Ed.), *Companion Guide to the ASME Boiler & Pressure Vessel Code Volume 1* (2nd ed., pp. 147–160). American Society of Mechanical Engineers.
- Robinson, G. (1994). *PWR Reactor Coolant System License Renewal Industry Report (TR-103844, Revision 1)*. Electric Power Research Institute, U.S. Department of Energy and Nuclear Energy Institute.
- Robinson, M. R. (2002). Aging Management of Environmental Fatigue for Carbon/Low-Alloy Steels. *Presented at the NRC-NEI Meeting, Washington, D.C., September 18, 2002*.
- Robinson, M., & Rosinski, S. (2003). US Utility Program for Fatigue Management. *Materials Reliability Program: Second International Conference on Fatigue of Reactor Components (MRP-84) (1003536)*, 26–43.
- Sakaguchi, K., Nomura, Y., Suzuki, S., & Kanasaki, H. (2006). Applicability of the Modified Rate Approach Method Under Various Conditions Simulating Actual Plant Conditions. *Proceedings of the ASME 2006 Pressure Vessels and Piping Conference*. <https://doi.org/10.1115/PVP2006-ICPVT-11-93220>
- Sakaguchi, K., Nomura, Y., Suzuki, S., Tsutsumi, K., Kanasaki, H., & Higuchi, M. (2006). Effect of Factors on Fatigue Life in PWR Water Environment. *Proceedings of the ASME 2006 Pressure Vessels and Piping Conference*. <https://doi.org/10.1115/PVP2006-ICPVT-11-93217>
- Sato, S., Nagata, N., & Katada, Y. (1989). Low Cycle Fatigue Behaviour of Pressure Vessel Steels in High Temperature Pressurized Water. *Tetsu-to-Hagane*, 75(10), 1928–1935. https://doi.org/https://doi.org/10.2355/tetsutohagane1955.75.10_1928
- Sayano, A., Higuchi, M., Hirano, A., Tsutsumi, K., Yamamoto, Y., Sakaguchi, K., & Iida, K. (2002). Development of a Fatigue Strength Database for LWR Water Environment. *Proceedings of the ASME 2002 Pressure Vessels and Piping Conference*, 199–208. <https://doi.org/10.1115/PVP2002-1236>
- Schuler, X., Herter, K., & Rudolph, J. (2013). Derivation of Design Fatigue Curves for Austenitic Stainless Steel Grades 1.4541 and 1.4550 Within the German Nuclear Safety Standard KTA 3201.2. *Proceedings of the ASME 2013 Pressure Vessels and Piping Conference*. <https://doi.org/https://doi.org/10.1115/PVP2013-97138>
- Seppänen, T., Alhainen, J., Arilahti, E., & Solin, J. (2017). Strain waveform effects for low cycle fatigue in simulated PWR water. *Proceedings of the ASME 2017 Pressure Vessels and Piping Conference*. <https://doi.org/10.1115/PVP2017-65374>

- Seppänen, T., Alhainen, J., Arilahti, E., & Solin, J. (2018). Low cycle fatigue (EAF) of AISI 304L and 347 in PWR water. *Proceedings of the ASME 2018 Pressure Vessels and Piping Conference*. <https://doi.org/10.1115/PVP201884197>
- Seppänen, T., Alhainen, J., Arilahti, E., & Solin, J. (2019). Strain-Controlled Low Cycle Fatigue of Stainless Steel in PWR Water. *Proceedings of the ASME 2019 Pressure Vessels and Piping Conference*. <https://doi.org/10.1115/PVP2019-93279>
- Seppänen, T., Alhainen, J., Arilahti, E., & Solin, J. (2021). Material and Temperature Effects in Low and High Cycle EAF of Austenitic Stainless Steels. *Proceedings of the ASME 2021 Pressure Vessels and Piping Conference*. <https://doi.org/10.1115/PVP2021-61507>
- Seppänen, T., Alhainen, J., Arilahti, E., Solin, J., & Vanninen, R. (2023). EPR Piping Material Study: Effects of Sampling Location and Temperature on Low Cycle Fatigue in Air. *Proceedings of the ASME 2023 Pressure Vessels and Piping Conference*. <https://doi.org/10.1115/PVP2023-106439>
- Shack, W. J., & Burke, W. F. (1988). Fatigue of Type 316NG Stainless Steel. In *Environmentally Assisted Cracking in Light Water Reactors Semiannual Report April 1987–September 1987 (NUREG/CR-4667 Vol. V, ANL-88-32)* (pp. 17–22). U.S. Nuclear Regulatory Commission.
- Shack, W. J., & Burke, W. F. (1990). Fatigue of Type 316NG SS. In *Environmentally Assisted Cracking in Light Water Reactors Semiannual Report April 1988–September 1988 (NUREG/CR-4667 Vol. 7, ANL-89/40)* (pp. 15–17). U.S. Nuclear Regulatory Commission.
- Shack, W. J., & Burke, W. F. (1991). Fatigue Life of Type 316NG SS. In *Environmentally Assisted Cracking in Light Water Reactors Semiannual Report October 1989–March 1990 (NUREG/CR-4667 Vol. 10, ANL-91/5)* (pp. 2–6). U.S. Nuclear Regulatory Commission.
- Shack, W. J., Kassner, T. F., Maiya, P. S., Park, J. Y., & Ruther, W. E. (1986). *Environmentally Assisted Cracking in Light Water Reactors Semiannual Report April-September 1985 (NUREG CR-4667 Vol. 1, ANL-86-31)*. U.S. Nuclear Regulatory Commission.
- Solin, J., Alhainen, J., Arilahti, E., Väinölä, J., Marjavaara, P., Järvinen, E., Halonen, M., Patalainen, M., Kaunisto, K., & Moilanen, P. (2011). Fatigue of Primary Circuit Components (FATE). In E. K. Puska & V. Suolanen (Eds.), *SAFIR2010, The Finnish Research Programme on Nuclear Power Plant Safety 2007-2010 Final Report (VTT Research Notes 2571)* (pp. 368–380). VTT.
- Solin, J., Alhainen, J., Karabaki, E., & Mayinger, W. (2016). Effects of Hot Water and Holds on Fatigue of Stainless Steel. *Proceedings of the ASME 2016 Pressure Vessels and Piping Conference*. <https://doi.org/10.1115/PVP2016-63291>
- Solin, J., Karjalainen-Roikonen, P., Arilahti, E., & Moilanen, P. (2005). Low cycle fatigue behaviour of 316NG alloy in PWR environment. *Materials Reliability Program: Third International Conference on Fatigue in Reactor Components (MRP-151) (1011958)*.
- Solin, J., Karjalainen-Roikonen, P., & Moilanen, P. (2003). Fatigue Testing in Reactor Environments for Quantitative Plant Life Management. *Materials Reliability Program: Second International Conference on Fatigue of Reactor Components (MRP-84) (1003536)*, 479–495.
- Solin, J., Nagel, G., & Mayinger, W. (2009). Cyclic Behavior and Fatigue of Stainless Surge Line Material. *Proceedings of the ASME 2009 Pressure Vessels and Piping Conference*, 611–619. <https://doi.org/10.1115/PVP2009-78138>
- Solin, J. P. (2006). Fatigue of Stabilized SS and 316 NG Alloy in PWR Environment. *Proceedings of the ASME 2006 Pressure Vessels and Piping Conference*. <https://doi.org/10.1115/PVP2006-ICPVT-11-93833>
- Solin, J., Reese, S., Karabaki, H. E., & Mayinger, W. (2013). Environmental Fatigue Factors (NUREG/CR-6909) and Strain Controlled Data for Stabilized Austenitic Stainless Steel. *Proceedings of the ASME 2013 Pressure Vessels and Piping Conference*. <https://doi.org/10.1115/PVP2013-97500>
- Solin, J., Reese, S., & Mayinger, W. (2011). Discussion on Fatigue Design Curves for Stainless Steels. *Proceedings of the ASME 2011 Pressure Vessels and Piping Conference*. <https://doi.org/10.1115/PVP2011-57943>
- Solin, J., Seppänen, T., & Mayinger, W. (2020). Fatigue Performance of Austenitic Stainless Steel: Enforced Endurance Limit and Questionable Design Curve. *Proceedings of the ASME 2020 Pressure Vessels and Piping Conference*. <https://doi.org/10.1115/PVP2020-21050>

- Solin, J., Seppänen, T., Mayinger, W., & Karabaki, H. E. (2018). Hidden Roles of Time and Temperature in Cyclic Behavior of Stainless Nuclear Piping. *Proceedings of the ASME 2018 Pressure Vessels and Piping Conference*. <https://doi.org/https://doi.org/10.1115/PVP2018-84936>
- Solomon, H. D., & Amzallag, C. (2005). Statistical analysis of the LCF behavior of type 304L SS tested at 150°C and 300°C in air and PWR water. In T. R. Allen, P. J. King, & L. Nelson (Eds.), *Proceedings of the 12th International Conference on Environmental Degradation of Materials in Nuclear Power Systems – Water Reactors –* (pp. 1091–1098). The Minerals, Metals & Materials Society.
- Solomon, H. D., Amzallag, C., DeLair, R. D., & Vallee, A. J. (2005a). Strain Controlled Fatigue of Type 304L SS in Air and PWR Water. *Materials Reliability Program: Third International Conference on Fatigue in Reactor Components (MRP-151) (1011958)*.
- Solomon, H. D., Amzallag, C., DeLair, R. E., & Vallee, A. J. (2005b). Comparison of the fatigue life of type 304L SS as measured in load and strain controlled tests. In T. R. Allen, P. J. King, & L. Nelson (Eds.), *Proceedings of the 12th International Conference on Environmental Degradation of Materials in Nuclear Power Systems – Water Reactors –* (pp. 1101–1109). The Minerals, Metals & Materials Society.
- Solomon, H. D., Amzallag, C., Vallee, A. J., & DeLair, R. E. (2005a). 10^7 cycle fatigue limit of type 304L SS in air and PWR water, at 150°C and 300°C. In T. R. Allen, P. J. King, & L. Nelson (Eds.), *Proceedings of the 12th International Conference on Environmental Degradation of Materials in Nuclear Power Systems – Water Reactors –* (pp. 1083–1089). The Minerals, Metals & Materials Society.
- Solomon, H. D., Amzallag, C., Vallee, A. J., & DeLair, R. E. (2005b). Influence of Mean Stress on the Fatigue Behavior of 304L SS in Air and PWR Water. *Proceedings of the ASME 2005 Pressure Vessels and Piping Conference*. <https://doi.org/10.1115/PVP2005-71064>
- Speis, T. P. (1996). *Memorandum, Themis P. Speis (NRC) to Ashok C. Thadani (NRC), “Generic Safety Issue (GSI)-166, ‘Adequacy of Fatigue Life of Metal Components’”, August 26, 1996*. U.S. Nuclear Regulatory Commission.
- Steinger, D., Wright, K., Twite, M., Morley, A., Métails, T., Léopold, G., & Le Roux, J. C. (2017). Component Testing Proposal to Quantify Margins in Existing Environmentally Assisted Fatigue (EAF) Requirements. *Proceedings of the ASME 2017 Pressure Vessels and Piping Conference*. <https://doi.org/https://doi.org/10.1115/PVP2017-65995>
- Stevens, G. L. (1998). *Evaluation of Environmental Thermal Fatigue Effects on Selected Components in a BWR Plant (TR-110356)*. Electric Power Research Institute.
- STUK. (2002). *YVL 3.5 Ensuring the Firmness of Pressure Vessels of a NPP*. Säteilyturvakeskus.
- Tagart Jr., S. W. (1964). *Mechanical Design Considerations in Primary Nuclear Piping (GEAP-4578)*. General Electric Company.
- Takahashi, Y., & Nakamura, T. (2003). Statistical Analyses of In-Air and In-Water Fatigue Test Data of Austenitic Stainless Steels and Ferritic Steels. *Proceedings of the ASME 2003 Pressure Vessels and Piping Conference*, 113–122. <https://doi.org/10.1115/PVP2003-1775>
- Takanashi, M., Ueda, H., Saito, T., Ogawa, T., & Hayashi, K. (2019). Development of New Design Fatigue Curves in Japan: Discussion of Crack Growth Behavior in Large-Scale Fatigue Tests of Carbon and Low-Alloy Steel Plates. *Proceedings of the ASME 2019 Pressure Vessels and Piping Conference*. <https://doi.org/10.1115/PVP2019-93393>
- Taylor, J. M. (1993). *Implementation of 10 CFR Part 54’ “Requirements for Renewal of Operating Licences for Nuclear Power Plants” (SECY-93-049)*. U.S. Nuclear Regulatory Commission.
- Taylor, J. M. (1994). *Fatigue Design of Metal Components (SECY-94-191)*. U.S. Nuclear Regulatory Commission.
- Taylor, J. M. (1995). *Completion of the Fatigue Action Plan (SECY-95-245)*. U.S. Nuclear Regulatory Commission.
- TENPES. (2002). *TENPES Guidelines for Environmental Fatigue Evaluation for LWR Component (in Japanese)*. Thermal and Nuclear Power Engineering Society.
- Thadani, A. C. (1999). *Memorandum, Ashok C. Thadani (NRC) to William D. Travers (NRC), “Closeout of Generic Safety Issue 190, “Fatigue Evaluation of Metal Components for 60-year Plant Life””, December 26, 1999*. U.S. Nuclear Regulatory Commission.

- Tice, D. R. (1985). A review of the U.K. collaborative programme to test the effects of mechanical and environmental variables on environmentally assisted crack growth of PWR pressure vessel steels. *Corrosion Science*, 25(8–9), 705–743. [https://doi.org/10.1016/0010-938X\(85\)90007-1](https://doi.org/10.1016/0010-938X(85)90007-1)
- Trownson, G., Gill, P., Brayshaw, W., Watson, J., & Mann, J. (2022). Thermomechanical Fatigue Initiation in Nuclear Grades of Austenitic Stainless Steel Using Plant Realistic Loading. *Proceedings of the ASME 2022 Pressure Vessels and Piping Conference*. <https://doi.org/10.1115/PVP2022-84760>
- Tsutsumi, K., Dodo, T., Kanasaki, H., Nomoto, S., Minami, Y., & Nakamura, T. (2001). Fatigue Behavior of Stainless Steel Under Conditions of Changing Strain Rate in PWR Primary Water. In M. D. Rana (Ed.), *Pressure Vessel and Piping Codes and Standards, PVP Vol. 419* (pp. 135–141). American Society of Mechanical Engineers.
- Tsutsumi, K., Higuchi, M., Iida, K., & Yamamoto, Y. (2002). The Modified Rate Approach Method to Evaluate Fatigue Life Under Synchronously Changing Temperature and Strain Rate in Elevated Temperature Water. *Proceedings of the ASME 2002 Pressure Vessels and Piping Conference*. <https://doi.org/10.1115/PVP2002-1227>
- Tsutsumi, K., Higuchi, M., Iida, K., & Yamamoto, Y. (2003). The Modified Rate Approach Method to Evaluate Fatigue Life under Synchronously Changing Temperature and Strain Rate in Elevated Temperature Water. *Materials Reliability Program: Second International Conference on Fatigue of Reactor Components (MRP-84) (1003536)*, 1025–1043.
- Tsutsumi, K., Kanasaki, H., Umakoshi, T., Nakamura, T., Urata, S., Mizuta, H., & Nomoto, S. (2000). Fatigue Life Reduction in PWR Water Environment for Stainless Steels. In R. Mohan (Ed.), *Assessment Methodologies for Predicting Failure: Service Experience and Environmental Considerations, PVP Vol. 410-2* (pp. 23–34). American Society of Mechanical Engineers.
- Tsutsumi, K., Kanasaki, H., Umakoshi, T., Nakamura, T., Urata, S., Mizuta, H., & Nomoto, S. (2001). Fatigue Life Reduction in PWR Water Environment for Stainless Steels. *Proceedings of the 2000 International Conference on Fatigue of Reactor Components (MRP- 46): PWR Materials Reliability Program (PWRMRP) (1006070)*, 553–564.
- Twite, M., Platts, N., McLennan, A., Meldrum, J., & McMinn, A. (2016). Variations in Measured Fatigue Life in LWR Coolant Environments Due to Different Small Specimen Geometries. *Proceedings of the ASME 2016 Pressure Vessels and Piping Conference*. <https://doi.org/10.1115/PVP2016-63584>
- U.S. DoC. (1958). *Tentative Structural Design Basis for Reactor Pressure Vessels and Directly Associated Components (PB 151987)*. U.S. Department of Commerce, Office of Technical Service.
- U.S. NRC. (1979). *Cracking in Feedwater System Piping (IE Bulletin No. 79-13 Rev.2)*. U.S. Nuclear Regulatory Commission.
- U.S. NRC. (1988a). *Pressurizer Surge Line Thermal Stratification (NRC Bulletin No. 88-11)*. U.S. Nuclear Regulatory Commission.
- U.S. NRC. (1988b). *Rapidly Propagating Fatigue Cracks in Steam Generator Tubes (NRC Bulletin No. 88-02)*. U.S. Nuclear Regulatory Commission.
- U.S. NRC. (1988c). *Thermal Stresses in Piping Connected to Reactor Coolant Systems (NRC Bulletin No. 88-08)*. U.S. Nuclear Regulatory Commission.
- U.S. NRC. (1991). *Fatigue Evaluation Procedures (Branch Technical Position PDLR D-1)*. U.S. Nuclear Regulatory Commission.
- U.S. NRC. (2001a). *Generic Aging Lessons Learned (GALL) Report Summary (NUREG-1801, Vol. 1)*. U.S. Nuclear Regulatory Commission.
- U.S. NRC. (2001b). *Generic Aging Lessons Learned (GALL) Report Tabulation of Results (NUREG-1801, Vol. 2)*. U.S. Nuclear Regulatory Commission.
- U.S. NRC. (2001c). *Standard Review Plan for Review of License Renewal Applications for Nuclear Power Plants (NUREG-1800)*. U.S. Nuclear Regulatory Commission.
- U.S. NRC. (2005a). *Generic Aging Lessons Learned (GALL) Report Tabulation of Results (NUREG-1801, Vol. 2 Rev. 1)*. U.S. Nuclear Regulatory Commission.
- U.S. NRC. (2005b). *Standard Review Plan for Review of License Renewal Applications for Nuclear Power Plants (NUREG-1800 Rev. 1)*. U.S. Nuclear Regulatory Commission.
- U.S. NRC. (2006a). *Advisory Committee on Reactor Safeguards 538th Meeting December 7, 2006*. U.S. Nuclear Regulatory Commission.

- U.S. NRC. (2006b). *Advisory Committee on Reactor Safeguards Subcommittee on Materials, Metallurgy and Reactor Fuels December 6, 2006*. U.S. Nuclear Regulatory Commission.
- U.S. NRC. (2006c). *Draft Regulatory Guide DG-1144 Guidelines for Evaluating Fatigue Analyses Incorporating the Life Reduction of Metal Components Due to the Effects of the Light-Water Reactor Environment for New Reactors*. U.S. Nuclear Regulatory Commission.
- U.S. NRC. (2006d). *Minutes of the 538th ACRS Meeting December 7–9, 2006*. U.S. Nuclear Regulatory Commission.
- U.S. NRC. (2007a). *Regulatory Guide 1.207 Rev.0, “Guidelines for Evaluating Fatigue Analyses Incorporating the Life Reduction of Metal Components Due to the Effects of the Light-Water Reactor Environment for New Reactors.”* U.S. Nuclear Regulatory Commission.
- U.S. NRC. (2007b). *Staff Responses to Public Comments on Draft Regulatory Guide DG-1144 (proposed new Regulatory Guide 1.207), “Guidelines for Evaluating Fatigue Analyses Incorporating the Life Reduction of Metal Components Due to the Effects of the Light-Water Reactor Envi.* U.S. Nuclear Regulatory Commission.
- U.S. NRC. (2011a). Issue 78: Monitoring of Fatigue Transient Limits for Reactor Coolant System (Rev. 3). In *Resolution of Generic Safety Issues (NUREG-0933, Main Report with Supplements 1–34)*. U.S. Nuclear Regulatory Commission.
- U.S. NRC. (2011b). Issue 166: Adequacy of Fatigue Life of Metal Components (Rev. 2). In *Resolution of Generic Safety Issues (NUREG-0933, Main Report with Supplements 1–34)*. U.S. Nuclear Regulatory Commission.
- U.S. NRC. (2011c). Issue 190: Fatigue Evaluation of Metal Components for 60-Year Plant Life (Rev. 2). In *Resolution of Generic Safety Issues (NUREG-0933, Main Report with Supplements 1–34)*. U.S. Nuclear Regulatory Commission.
- U.S. NRC. (2017). *Regulatory Guide 1.193 Rev. 5, “ASME Code Cases Not Approved for Use.”* U.S. Nuclear Regulatory Commission.
- U.S. NRC. (2019). *Regulatory Guide 1.193 Rev. 6, “ASME Code Cases Not Approved for Use.”* U.S. Nuclear Regulatory Commission.
- U.S. NRC. (2023a). *Draft Regulatory Guide DG-1405 Proposed Revision 40 to Regulatory Guide RG1.84*. U.S. Nuclear Regulatory Commission.
- U.S. NRC. (2023b). *Draft Regulatory Guide DG-1408 Proposed Revision 8 to Regulatory Guide 1.193*. U.S. Nuclear Regulatory Commission.
- Van Der Sluys, W. A. (1993). Evaluation of the Available Data on the Effect of the Environment on the Low Cycle Fatigue Properties in Light Water Reactor Environments. In R. Gold & E. P. Simonen (Eds.), *Proceedings of the Sixth International Symposium on Environmental Degradation of Materials in Nuclear Power Systems-Water Reactors, San Diego, California, August 1–5, 1993* (pp. 1–9). The Minerals, Metals & Materials Society.
- Van Der Sluys, W. A. (2003a). *WRC Bulletin 487 PVRC’s Position on Environmental Effects on Fatigue Life in LWR Applications*. Welding Research Council.
- Van Der Sluys, W. A. (2003b). Review of Margins Needed to Develop Fatigue Design Curves from Laboratory Test Data. *Proceedings of the ASME 2003 Pressure Vessels and Piping Conference Pressure Vessels and Piping Conference*. <https://doi.org/https://doi.org/10.1115/PVP2003-1781>
- Van Der Sluys, W. A., & Nickell, R. (2003). Evaluation of Proposed Revisions to ASME Code Fatigue Analysis to Account for Environmental Effects on Carbon and Low-Alloy Steels Using Structural Fatigue Test Results. *Materials Reliability Program: Second International Conference on Fatigue of Reactor Components (MRP-84) (1003536)*, 709–718.
- Van Der Sluys, W. A., & Yukawa, S. (1998). S-N Fatigue Properties of Pressure Boundary Materials in LWR Coolant Environments. In H. S. Mehta, R. W. Swindeman, J. A. Todd, S. Yukawa, M. Zako, W. H. Bamford, M. Higuchi, E. Jones, H. Nickel, & S. Rahman (Eds.), *Fatigue, Environmental Factors and New Materials, PVP-Vol. 374* (pp. 269–276). American Society of Mechanical Engineers.
- Vankeerberghen, M., Mclennan, A., Simonovski, I., Barrera, G., Arrieta Gomez, S., Ernestova, M., Platts, N., Scibetta, M., & Twite, M. (2020). Strain Control Correction for Fatigue Testing in LWR Environments. *Proceedings of the ASME 2020 Pressure Vessels and Piping Conference*. <https://doi.org/10.1115/PVP2020-21373>

- VGB. (2006). *VGB-R 401 J. Richtlinie für das Wasser in Kernkraftwerken mit Leichtwasserreaktoren. Dritte Ausgabe 2006 (in German)*. VGB PowerTech e.V.
- Vincent, L., Le Roux, J. C., & Taheri, S. (2012). On the high cycle fatigue behavior of a type 304L stainless steel at room temperature. *International Journal of Fatigue*, 38, 84–91. <https://doi.org/10.1016/j.ijfatigue.2011.11.010>
- Wallis, G. B. (2006a). *Letter, Graham B. Wallis (ACRS) to Luis A. Reyes (NRC), "Draft Final Regulatory Guide 1.207 (DG-1144)", December 18, 2006*. U.S. Nuclear Regulatory Commission.
- Wallis, G. B. (2006b). *Letter, Graham B. Wallis (ACRS) to Luis A. Reyes (NRC), "Draft Final Regulatory Guide 1.207 (DG-1144), "Guidelines for Evaluating Fatigue Analyses Incorporating the Life Reduction of Metal Components Due to the Effects of the Light-Water Reactor Environme. U.S. Nuclear Regulatory Commission*.
- Walters, D. J. (2001). *Letter, Douglas J. Walters (NEI) to Eugene V. Imbro (NRC), "Industry Guidance for Addressing Fatigue Environmental Effects in a License Renewal Application ", July 31, 2001*. Nuclear Energy Institute.
- Wang, K. (2023). Code Case N-792 Update - status of Ballot 22-2243. *44th WG EFEM Meeting, Online, Virtual, August 7, 2023*.
- Wang, Y., Hatoh, H., Yamamoto, M., Nakane, M., Hirano, A., & Hayashi, K. (2018). Development of New Design Fatigue Curves in Japan: Discussion of Best-Fit Curves Based on Fatigue Test Data With Small-Scale Test Specimen. *Proceedings of the ASME 2018 Pressure Vessels and Piping Conference*. <https://doi.org/https://doi.org/10.1115/PVP2018-84052>
- Ward, D., & Shewmon, P. (1992). *Summary/Minutes of the Joint Meeting of the ACRS Subcommittees on Plant License Renewal/Materials and Metallurgy, July 7, 1992*. U.S. Nuclear Regulatory Commission.
- Ware, A. G., Morton, D. K., & Nitzel, M. E. (1995). *Application of NUREG/CR-5999 interim fatigue curves to selected nuclear power plant components (NUREG/CR-6260, INEL-95/0045)*. U.S. Nuclear Regulatory Commission.
- Wirsching, P. H. (1995). Probabilistic Fatigue Analysis. In *Probabilistic Structural Mechanics Handbook* (pp. 146–165). Springer. https://doi.org/10.1007/978-1-4615-1771-9_7
- Wright, K. (2017). Developments in Environmentally Assisted Fatigue Methodologies. *Transactions of the 24th International Conference on Structural Mechanics in Reactor Technology (SMiRT 24)*.
- Yukawa, S. (1998). Steering Committee on Cyclic Life and Environmental Effects in Nuclear Applications October 13, 1998. In *WRC Progress Reports Volume 53, No. 9/10 1998* (pp. 18–31). Welding Research Council.
- Yukawa, S. (1999). Minutes of the PVRC Steering Committe on Cyclic Life and Environmental Effects in Nuclear Applications, June 16, 1999. In *WRC Progress Reports Volume 54, No. 5/6 1999* (pp. 33–36). Welding Research Council.
- Yukawa, S., & Van Der Sluys, W. A. (1995). Status of PVRC Evaluation of LWR Coolant Environmental Effects on the S-N Fatigue Properties of Pressure Boundary Materials. In S. Yukawa, D. P. Jones, & H. S. Mehta (Eds.), *Fatigue and Crack Growth: Environmental Effects, Modeling Studies, and Design Considerations, PVP-Vol. 306* (pp. 47–58). American Society of Mechanical Engineers.

7. Appendices

7.1 Evolution of F_{en} models in NUREG reports for US NRC

Parametric evolution of F_{en} as a function of temperature, strain rate and dissolved oxygen in NUREG/CR reports for the EACLWR project will be explained and discussed in the following. The EAF model introduced in the NUREG/CR-5704 report deviated so notably from the previous and follow-up NUREG reports that this version will be separately explained in a chapter of its own. Another separate chapter is devoted to the three versions of NUREG/CR-6909 report (original in 2007, draft revision in 2014, and revision 1 in 2018).

7.1.1 F_{en} models before NUREG/CR-6909

The model for environmental F_{en} factors for stainless steels in NUREG/CR-6335 introduced a parametric dependency on strain rate applied during pulling of the laboratory specimen and this was applied in all water chemistries and temperatures. The report NUREG/CR-5704 differentiated between the low and high oxygen water chemistries (PWR or BWR) and introduced a threshold for temperature. The threshold temperature was broadened to a range of gradual change since NUREG/CR-6717.

The stainless alloy grades 304 & 316 versus 316NG were modelled separately both in terms of the best-fit curve in RT air and in terms of sensitivity to environmental effects, until the grades were grouped together in NUREG/CR-6909. The parametrised effects of alloy grade, temperature, strain rate and water chemistry are summarized in Table 29 and Table 30.

Table 29. Early F_{en} models presented by ANL in the EACLWR program.

NUREG/CR-6335	NUREG/CR-6717	NUREG/CR-6787, 6815 & 6878
$\ln(N_{water}) = \ln(N_{RT}) + T_1^* \dot{\epsilon}^* O^*$ $F_{en} = \exp(X - T_1^* \dot{\epsilon}^* O^*)$	$\ln(N_{water}) = \ln(N_{RT}) + T_1^* \dot{\epsilon}^* O^*$ $F_{en} = \exp(X - T_1^* \dot{\epsilon}^* O^*)$	$\ln(N_{water}) = \ln(N_{RT}) + T_1^* \dot{\epsilon}^* O^*$ $F_{en} = \exp(X - T_1^* \dot{\epsilon}^* O^*)$
$X = 0.359$ if stainless note: different air curves for 316 NG until CR-6878	$X = 0.935$ if 304 & 316 $X = 0.359$ if 316NG	$X = 1.028$ if 304 & 316 $X = 0.311$ if 316NG
$T_1^* = 1$ if stainless	$T_2^* = 0$ if $T < 180^\circ\text{C}$ $T_1^* = 1$ if $T > 220^\circ\text{C}$ $T_1^* = (T - 180)/40$ if $180 \leq T \leq 220^\circ\text{C}$	$T_2^* = 0$ if $T < 150^\circ\text{C}$ $T_1^* = 1$ if $T > 325^\circ\text{C}$ $T_1^* = (T - 150)/175$ if $150 \leq T \leq 325^\circ\text{C}$
$\dot{\epsilon}^* = 0$ if $\dot{\epsilon} > 1\%/s$ $\dot{\epsilon}^* = 0.134 \cdot \ln(0.001)$ if $\dot{\epsilon} \leq 0.001\%/s$ $\dot{\epsilon}^* = 0.134 \cdot \ln(\dot{\epsilon})$ if $0.001 \leq \dot{\epsilon} \leq 1\%/s$	$\dot{\epsilon}^* = 0$ if $\dot{\epsilon} > 0.4\%/s$ $\dot{\epsilon}^* = \ln(\dot{\epsilon}/0.4)$ if $0.0004 \leq \dot{\epsilon} \leq 0.4\%/s$ $\dot{\epsilon}^* = \ln(0.0004/0.4)$ if $\dot{\epsilon} \leq 0.0004\%/s$	$\dot{\epsilon}^* = 0$ if $\dot{\epsilon} > 0.4\%/s$ $\dot{\epsilon}^* = \ln(\dot{\epsilon}/0.4)$ if $0.0004 \leq \dot{\epsilon} \leq 0.4\%/s$ $\dot{\epsilon}^* = \ln(0.0004/0.4)$ if $\dot{\epsilon} \leq 0.0004\%/s$
$O^* = 1$ if in water $O^* = 0$ if in air	$O^* = 0.260$ if DO < 0.05 ppm $O^* = 0$ if DO ≥ 0.05 ppm	$O^* = 0.281$ if DO < 0.05 ppm $O^* = 0.281$ if DO ≥ 0.05 ppm

The EAF model introduced in the NUREG/CR-6335 report suggested fatigue life reduction factors between 1.43 and 3.61 depending only on the strain rate in water, Figure 133. This followed a model, where strain rate was about as effective in air at 335°C , but notably more effective in LWR waters (NUREG/CR-5704; see below). The current type of F_{en} models was outlined in the report NUREG/CR-6717, where effects of temperature and strain rate are negligible in air environment, but the parametric definition of term $\dot{\epsilon}^*$ representing the effect of strain rate was restored for PWR water environment, Figure 133.

According to NUREG/CR-5704, the effect of temperature on F_{en} was simply divided in two: whether $T \geq 200^\circ\text{C}$, or not. In NUREG/CR-6717, this binary threshold was broadened to 40°C , ($180 \leq T \leq 220^\circ\text{C}$) for PWR water, but F_{en} was fixed to moderate constant values independent of temperature or strain rate in BWR water. Low carbon 316NG was assumed less sensitive in both water types, Figure 133.

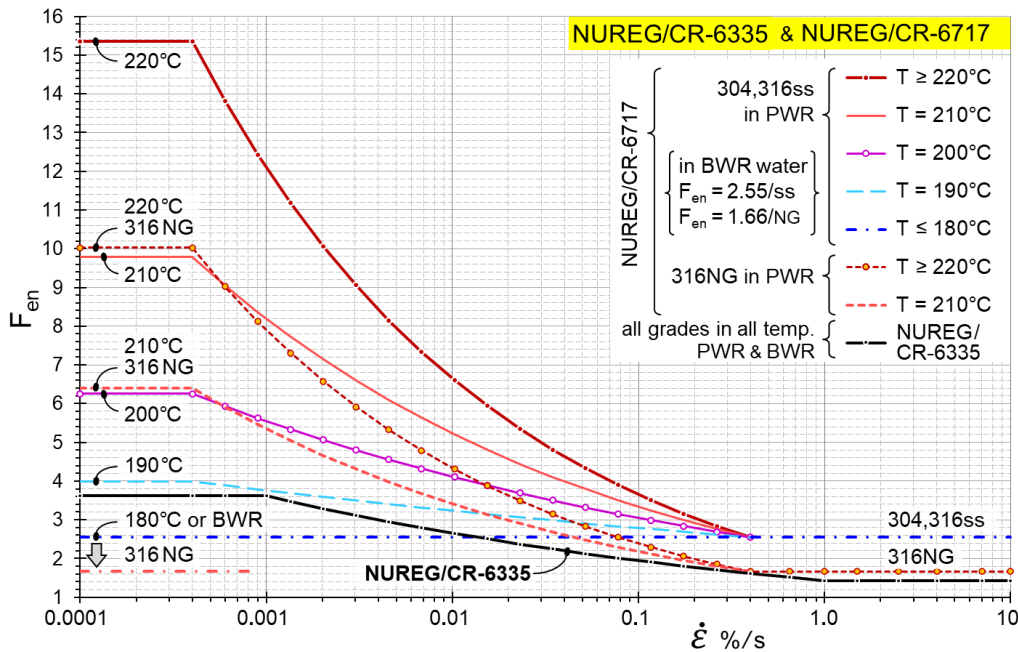


Figure 133. F_{en} factors according to NUREG/CR-6335 and NUREG/CR-6717 as function of strain rate in low oxygen PWR water. F_{en} according to NUREG/CR-6717 depends on temperature at $180^{\circ}\text{C} \leq T \leq 220^{\circ}\text{C}$, is reduced for 316NG and settles down to the lower bound in BWR water.

The F_{en} model was next revised in NUREG/CR-6787, where the range of temperatures effective on F_{en} was further broadened to 175°C , ($150 \leq T \leq 325^{\circ}\text{C}$) for LWR waters. Low carbon 316NG was again assumed less sensitive in both water types, but no difference between the low oxygen PWR and higher oxygen BWR waters were considered, Figure 134.

The difference between EAF performance of the conventional stainless steels (304 and 316) and low carbon nuclear grade 316NG was assumed as combination of different air curves and different effects of water environment on fatigue curves. Actually, the reports NUREG/CR-6717, CR-6787, CR-6815 and CR-6878 provide common F_{en} factors “for austenitic stainless steels”, which match the values derived for 304 and 316 ss, but the presented “statistical models” result to lower F_{en} factors for the nuclear grade 316NG. The F_{en} factors presented in Figure 133 and Figure 134 represent the “statistical models”.

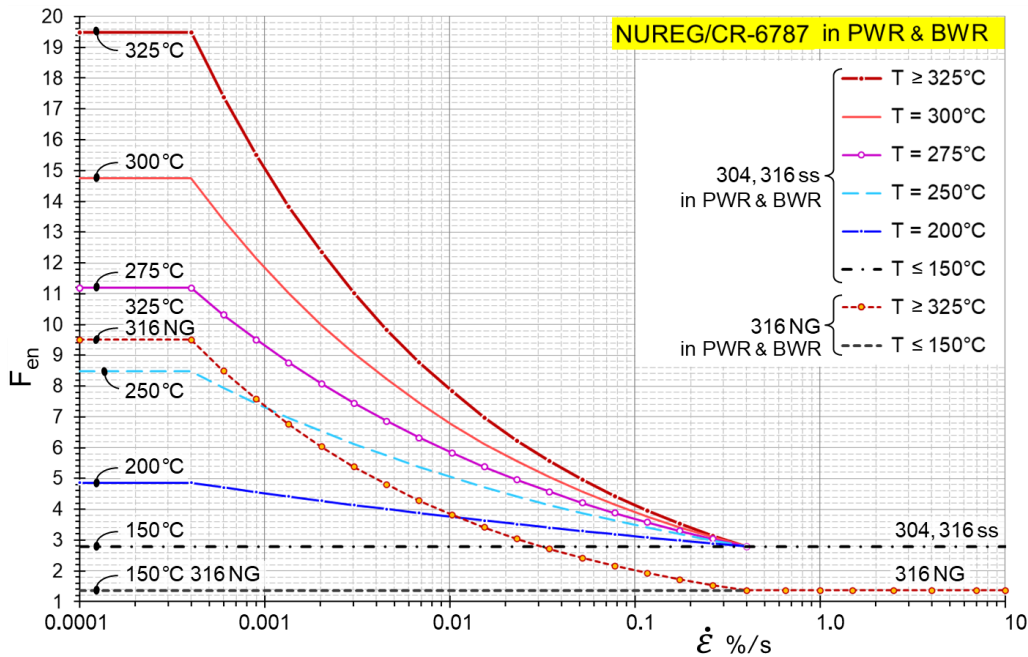


Figure 134. F_{en} factors according to NUREG/CR-6787 as function of strain rate at temperatures between $150^{\circ}\text{C} \leq T \leq 325^{\circ}\text{C}$. F_{en} is lower for 316NG, but independent of oxygen content in water. The same model was applied also in NUREG/CR-6815 and NUREG/CR-6878.

7.1.2 F_{en} model in NUREG/CR-5704 (stainless steels)

NUREG/CR-5704 report made an exception within the EAF related NUREG reports by introducing a temperature and strain rate dependent model for reduced fatigue endurance “in air”. The model was not introduced in the report as a penalty factor, but the parametric presentation resembled that of the F_{en} model. The relative effect of strain rate was claimed identical in both environments, in air and water. The effect of temperature was assumed gradually growing in air, but independent of temperature in water environment, when exceeding the respective threshold temperatures ($T_{\text{air}} \geq 250^{\circ}\text{C}$ and $T_{\text{water}} \geq 200^{\circ}\text{C}$), Table 30.

The stainless alloy grades 304 & 316 versus 316NG were modelled separately. The best-fit curve in RT air was higher for 316NG in LCF ($N_{25} \leq 47500$; $\epsilon_a \geq 0.261\%$) and 316NG was assumed less sensitive for environmental effects in hot water.

Table 30. F_{en} model presented by ANL in the NUREG/CR-5704 report. Notations $F_{en,air}$ and $F_{en,water}$ were not used in NUREG/CR-5704, they are introduced here for comparison.

<i>Temperature and strain rate effect in air:</i>		<i>Environmental effect in water:</i>	
$\ln(N_T) = \ln(N_{RT}) + T_1^* \dot{\epsilon}^*$		$\ln(N_{water}) = \ln(N_{RT}) + T_2^* \dot{\epsilon}^* O^*$	
$F_{en,air} = \exp(X - T_1^* \dot{\epsilon}^*)$		$F_{en} = \exp(X - T_2^* \dot{\epsilon}^* O^*)$	
$X = 0$	<i>if</i> 304 & 316	$X = 0.935$	<i>if</i> 304 & 316
$X = 0$	<i>if</i> 316NG	$X = 0.509$	<i>if</i> 316NG
$T_1^* = 0$	<i>if</i> $T < 250^\circ\text{C}$	$T_2^* = 0$	<i>if</i> $T < 200^\circ\text{C}$
$T_1^* = [(T-250)/525]^{0.84}$	<i>if</i> $250 \leq T < 400^\circ\text{C}$	$T_2^* = 1$	<i>if</i> $T \geq 200^\circ\text{C}$
$\dot{\epsilon}^* = 0$	<i>if</i> $\dot{\epsilon} > 0.4\%/s$	$O^* = 0.260$	<i>if</i> $\text{DO} < 0.05\text{ppm}$
$\dot{\epsilon}^* = \ln(\dot{\epsilon}/0.4)$	<i>if</i> $0.0004 \leq \dot{\epsilon} \leq 0.4\%/s$	$O^* = 0.172$	<i>if</i> $\text{DO} \geq 0.05\text{ppm}$
$\dot{\epsilon}^* = \ln(0.0004/0.4)$	<i>if</i> $\dot{\epsilon} \leq 0.0004\%/s$	$-6,9077 \leq \dot{\epsilon}^* \leq 0$	<i>as in air</i>

We use notation ' $F_{en,air}$ ', because the model for effects of temperature and strain rate in air is much similar to the model for F_{en} in water environment, as seen Table 30. The resulting $F_{en,air}$ factors are shown in Figure 135. Because the endurance at room temperature is used as reference for definition of F_{en} , the factor $F_{en,air}$ vanishes and is replaced by F_{en} in water environment, Figure 136.

Comparison of the alternative factors $F_{en,air}$ and F_{en} derived from the statistical model in NUREG/CR-5704 reveals that an effect of water environment would decrease when $T > 250^\circ\text{C}$. An effect separated for water environment at a selected temperature ' $F_{water} = N_{T,air}/N_{T,water}$ ' can be extracted as $F_{water} = F_{en}/F_{en,air}$. The resulting effects of low (PWR) and higher oxygen (BWR) water environments are shown in Figure 137 to Figure 140. The effect of a low oxygen (PWR) water is assumed more severe than a higher oxygen (BWR) water and the low carbon alloy 316NG was assumed less sensitive for environmental effects.

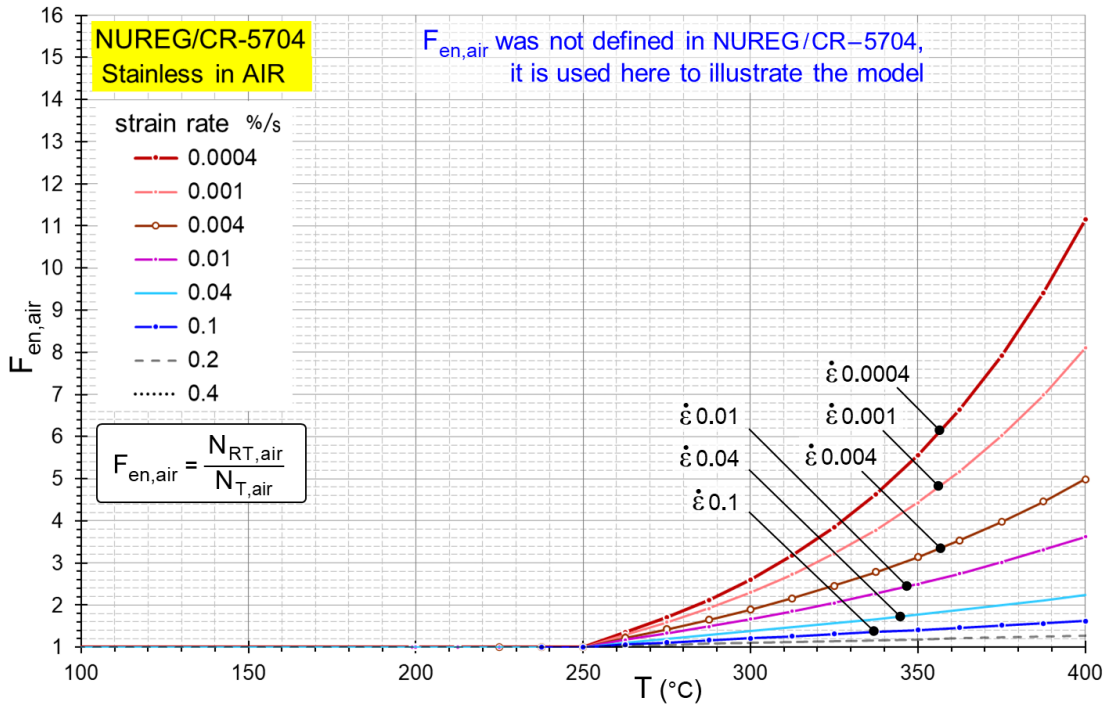


Figure 135. Fatigue life reduction factor 'F_{en,air}' derived from statistical model in NUREG/CR-5704.

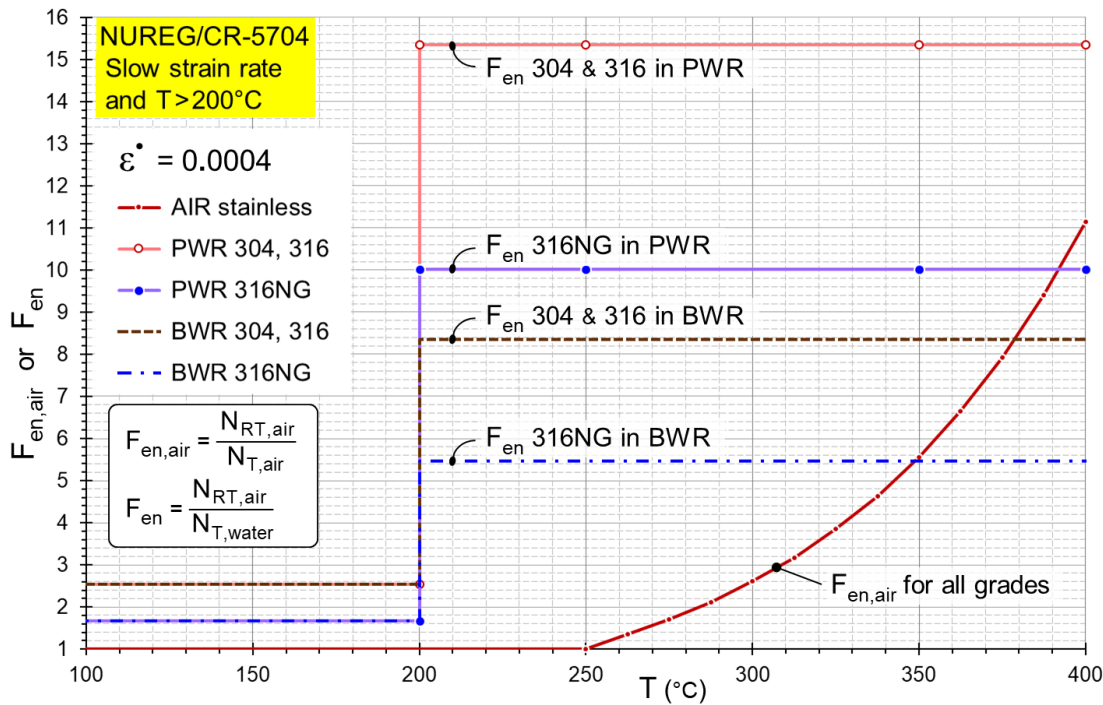


Figure 136. Saturated fatigue life reduction factors 'F_{en,air}' and F_{en} derived from the statistical model in NUREG/CR-5704. Drawn as function of temperature for $\dot{\epsilon} = 0.0004$ %/s.

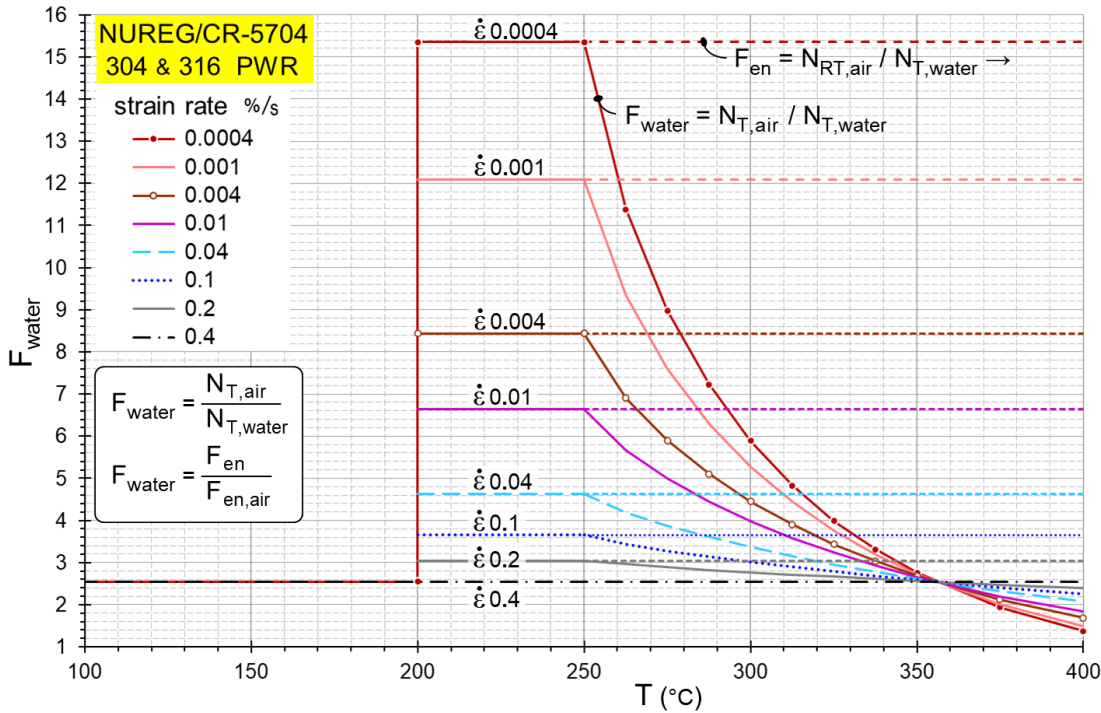


Figure 137. Fatigue life reduction factors 'F_{water}' (equal to F_{en} when T ≤ 250°C) for 304 and 316ss in PWR water as function of temperature for selected strain rates according to NUREG/CR-5704.

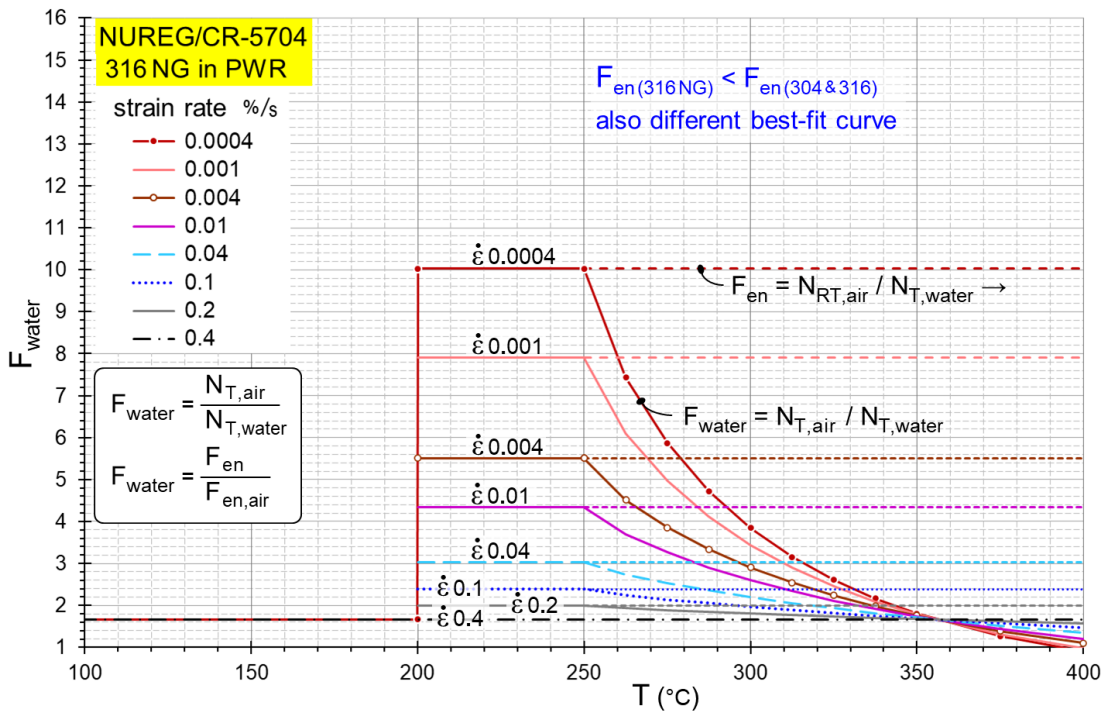


Figure 138. Fatigue life reduction factors 'F_{water}' (equal to F_{en} when T ≤ 250°C) for 316NG in PWR water as function of temperature for selected strain rates according to NUREG/CR-5704.

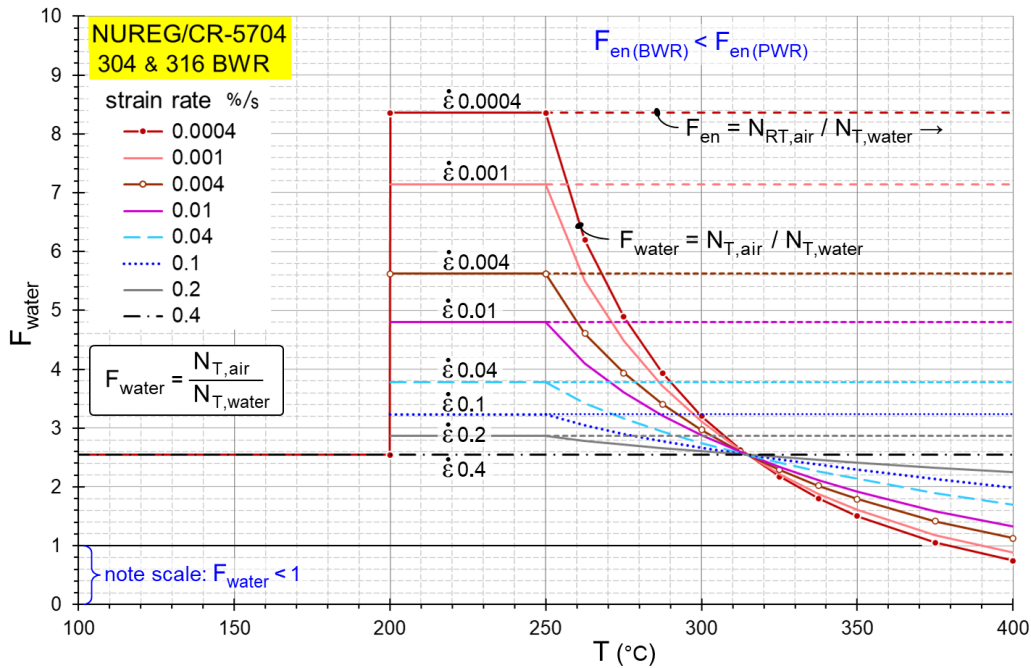


Figure 139. Fatigue life reduction factors 'F_{water}' (equal to F_{en} when T ≤ 250°C) for 304 and 316ss in BWR water as function of temperature for selected strain rates according to NUREG/CR-5704.

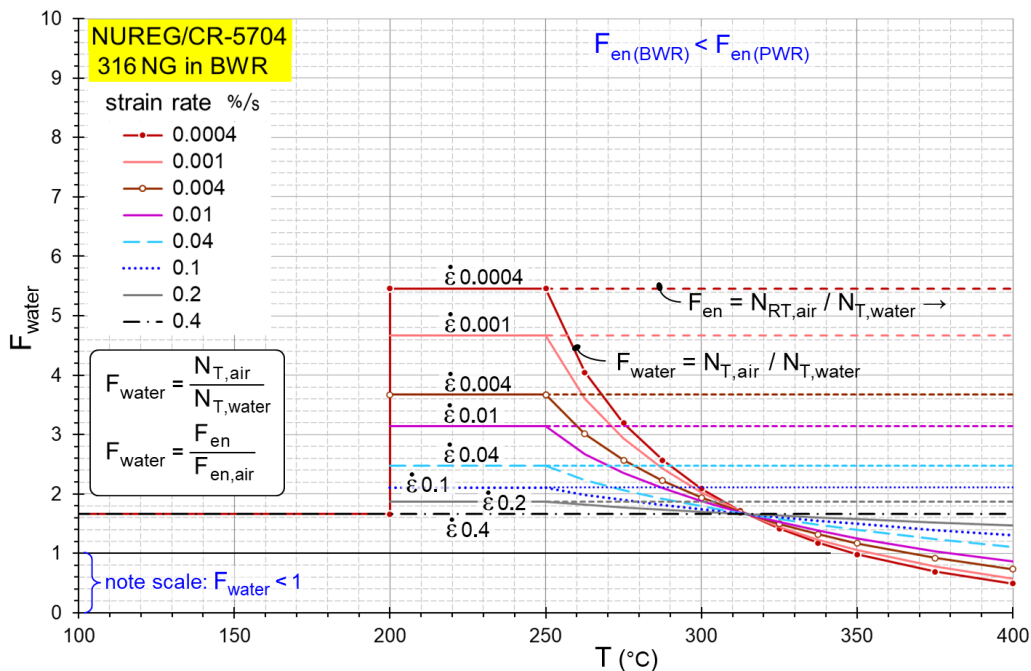
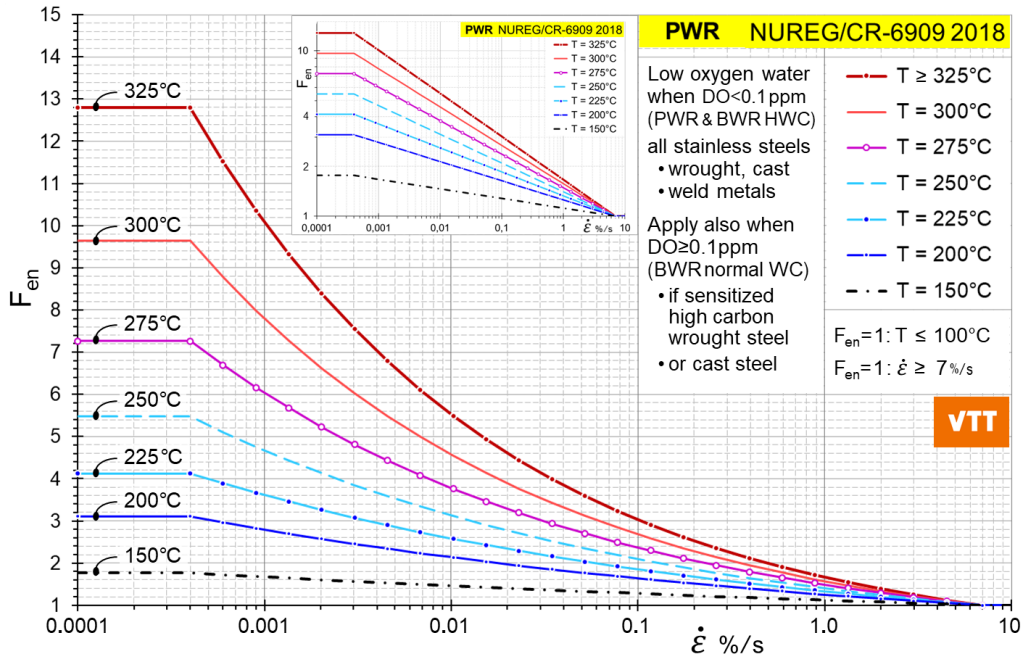


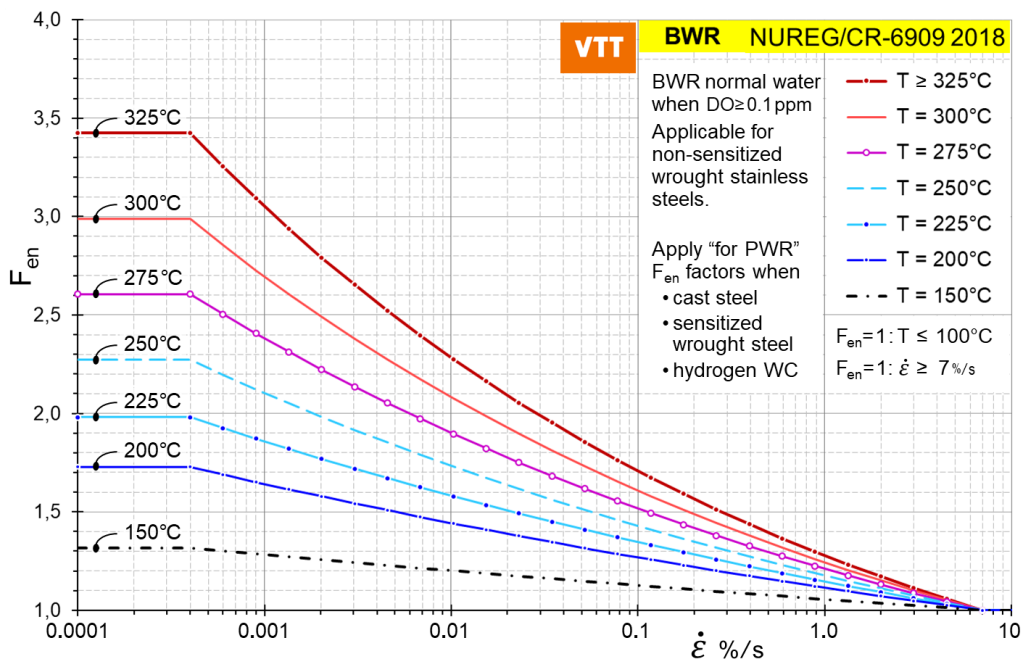
Figure 140. Fatigue life reduction factors 'F_{water}' (equal to F_{en} when T ≤ 250°C) for 316NG in BWR water as function of temperature for selected strain rates according to NUREG/CR-5704.

7.1.3 F_{en} models in NUREG/CR-6909

The F_{en} factors calculated according to the latest 2018 revision 1 of the NUREG/CR-6909 report are presented as function of strain rate at selected temperatures in Figure 141 and as function of temperature at selected strain rates in Figure 142.

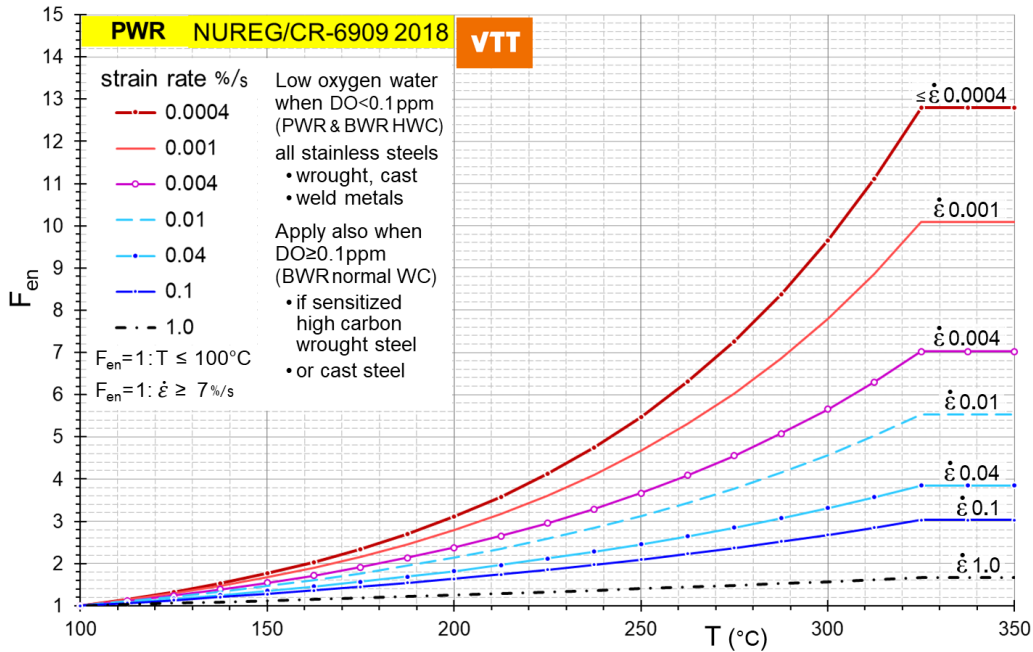


(a)

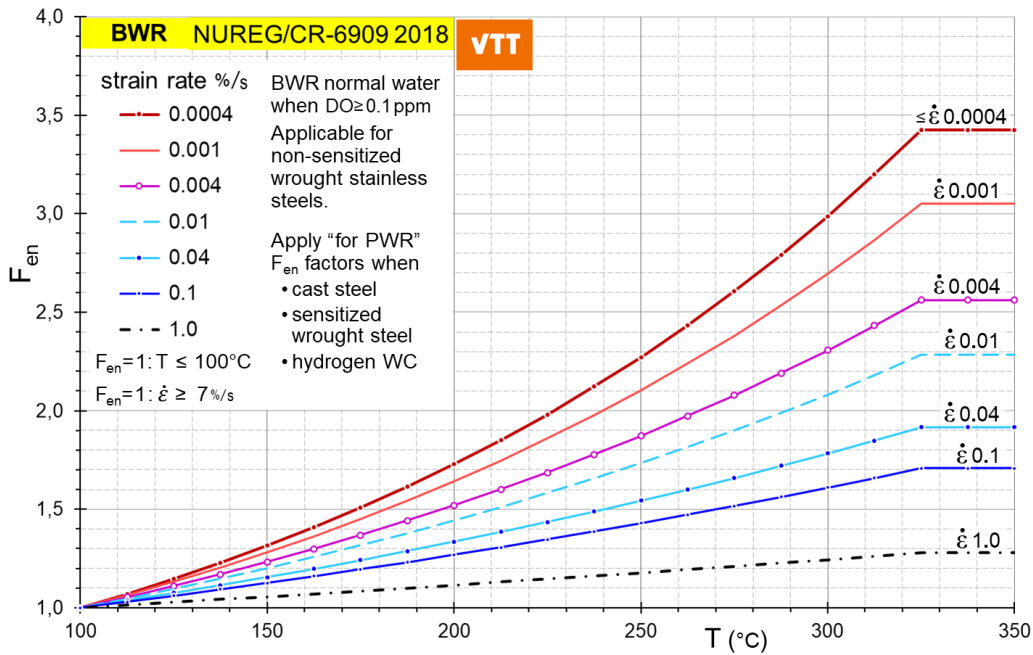


(b)

Figure 141. F_{en} factors according to NUREG/CR-6909 revision 1 (2018) as function of strain rate at temperatures between $150^{\circ}\text{C} \leq T \leq 325^{\circ}\text{C}$. (a): Enhanced F_{en} factors are assumed in low oxygen PWR water or in hydrogen water chemistry for BWR. (b): Notably lower F_{en} factors are assumed for wrought non-sensitized stainless steels in normal BWR water chemistry.



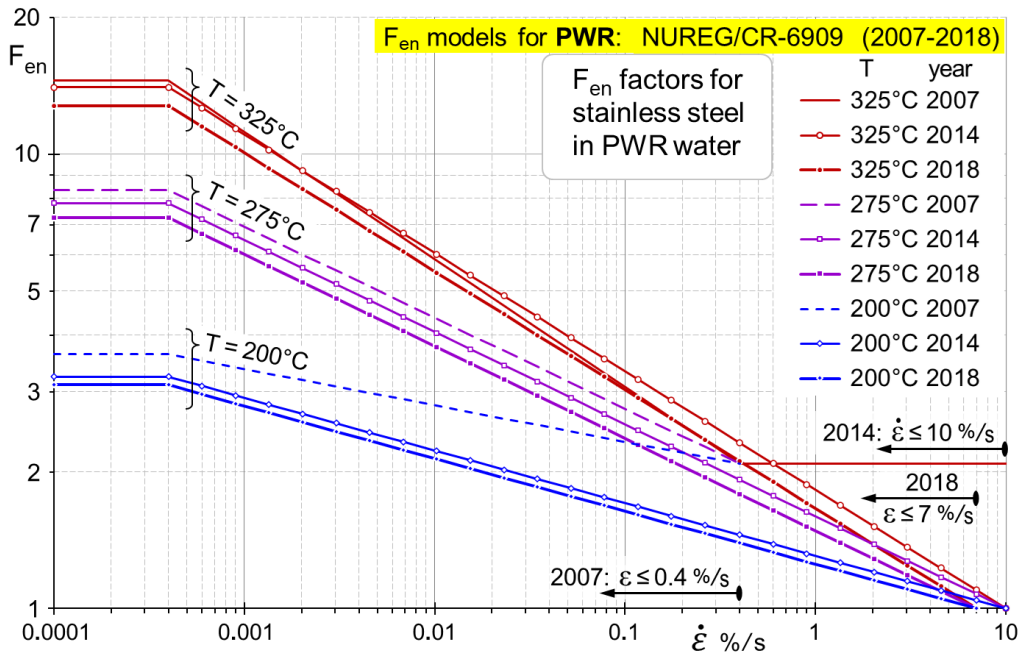
(a)



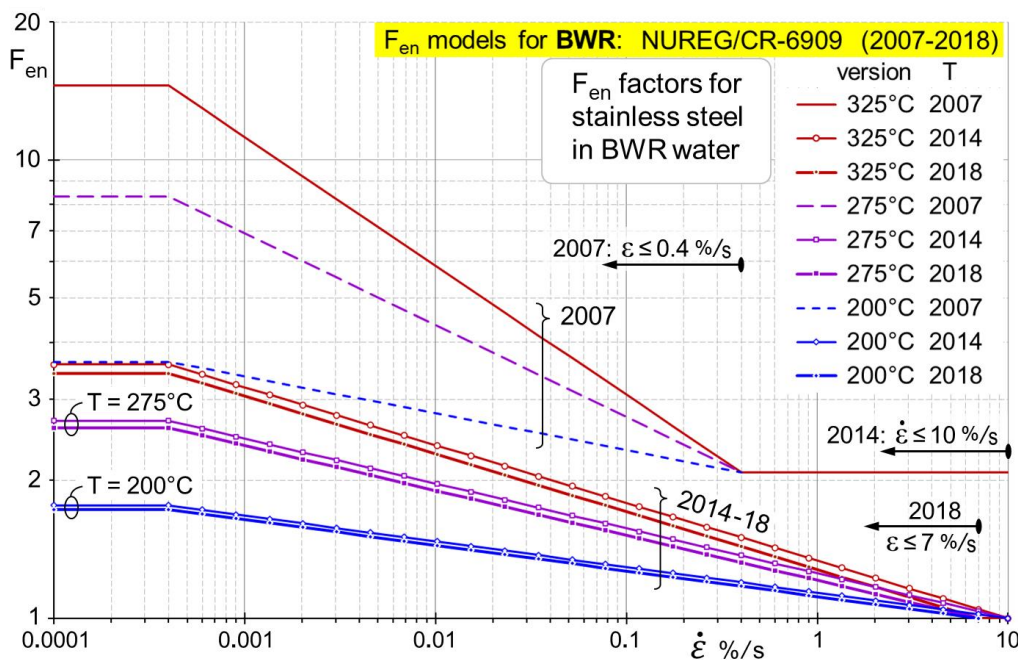
(b)

Figure 142. F_{en} factors according to NUREG/CR-6909 revision 1 (2018) as function of temperature at selected strain rates. (a): Enhanced F_{en} factors are assumed in low oxygen PWR water or in hydrogen water chemistry for BWR. (b): Notably lower F_{en} factors are assumed for wrought non-sensitized stainless steels in normal BWR water chemistry.

A general trend towards lower saturated F_{en} factors in the 2014 draft revision and in the 2018 revision 1 can be seen in Figure 143. However, this trend is not uniform at higher strain rates, because a minimum factor $F_{en}=2.08$ was initially applied in 2007 and the highest strain rates to be considered have been modified each time. The first 2007 report did not differentiate between water chemistries, but remarkable reductions of F_{en} factors for normal BWR water chemistry were proposed in 2014 and again in 2018, as shown in Figure 143b. The correlations between F_{en} and strain rate are linear on the log-log scales, which are used for comparisons, Figure 143.



(a)



(b)

Figure 143. Evolution of F_{en} factors according to revisions of NUREG/CR-6909. (a): PWR or BWR hydrogen water chemistry, (b): normal BWR water chemistry.

7.2 Japanese F_{en} models in JSME S NF1-2009

The Japanese authorities and industry codified F_{en} models for accounting on environmental effects during operation of NPP's already before the US NRC endorsed the approach of NUREG/CR-6909 in the Regulatory Guide 1.207 (U.S. NRC, 2007a). The Japan Society of Mechanical Engineers, JSME addressed its Environmental Fatigue Evaluation Method for NPP's as "Codes for Nuclear Power Generation Facilities" (JSME, 2006, 2009), i.e., for operation of the plants rather than as a Design Code.

The Japanese and American EAF evaluation methods and models are based on parallel and shared laboratory data but result in different F_{en} factors. The Japanese evaluation methods were discussed in the main report. The resulting F_{en} factors are introduced and compared with the NUREG models in the following.

7.2.1 F_{en} models in JSME S NF1-2006 and JSME S NF1-2009

The Japanese F_{en} models apply two different limits for strain rate effects, which are assumed saturated when $\dot{\epsilon} \leq 4 \cdot 10^{-6}/s$ for wrought stainless steels in low oxygen PWR water. This limit is similar to that in NUREG/CR-6909 reports, but the saturation is postponed by one order of magnitude to $\dot{\epsilon} \leq 4 \cdot 10^{-7}/s$ for cast stainless steels in PWR water and for all stainless steels in BWR water. According to JSME S NF1-2009 resulting F_{en} factors in PWR water are introduced in Figure 144. F_{en} factors for stainless steels in PWR water chemistry as function of strain rate at selected temperatures according to JSME S NF1-2009. The maximum F_{en} factors are higher for cast steels because an order of magnitude lower strain rates is considered for them, as illustrated in the small log-log graph. Figure 144.

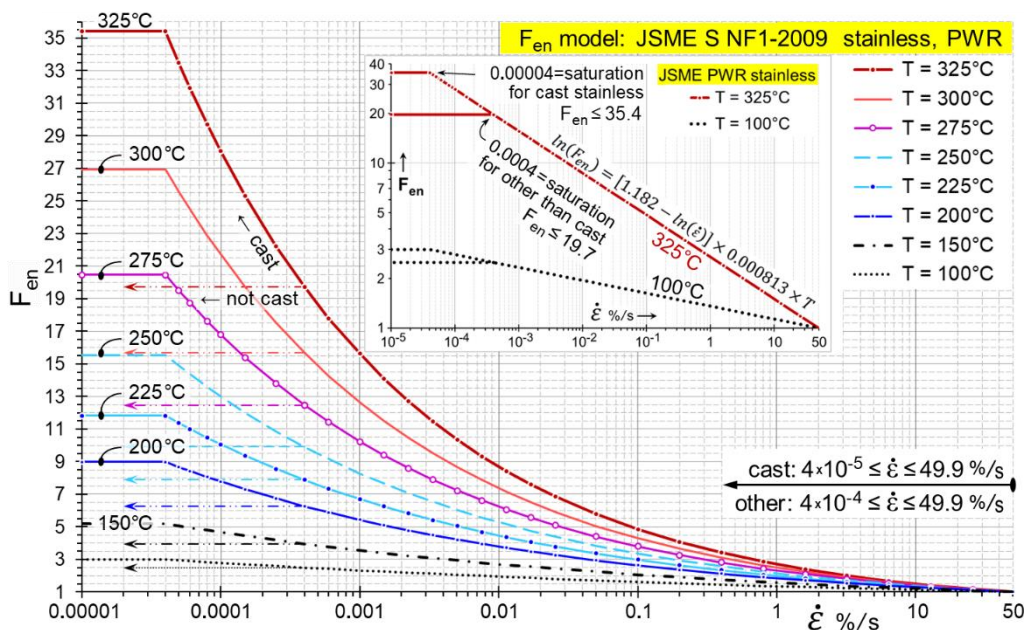


Figure 144. F_{en} factors for stainless steels in PWR water chemistry as function of strain rate at selected temperatures according to JSME S NF1-2009. The maximum F_{en} factors are higher for cast steels because an order of magnitude lower strain rates is considered for them, as illustrated in the small log-log graph.

The F_{en} model of JSME S NF1-2009 does not differentiate between low carbon non-sensitized and sensitized stainless steels in BWR water chemistry. Therefore, the saturation limit of strain rates is conservatively set to $\dot{\epsilon} \leq 4 \cdot 10^{-7}/s$ for all stainless steels in BWR water, Figure 145. F_{en} factors

for stainless steels in PWR water chemistry as function of strain rate at selected temperatures according to JSME S NF1-2009. The maximum F_{en} factors are higher for cast steels because an order of magnitude lower strain rates is considered for them, as illustrated in the small log-log graph.. On the other hand, environmental effects can be ignored for strain rates larger than 0.0269 in BWR water, while this omission limit s 0.5 in PWR water.

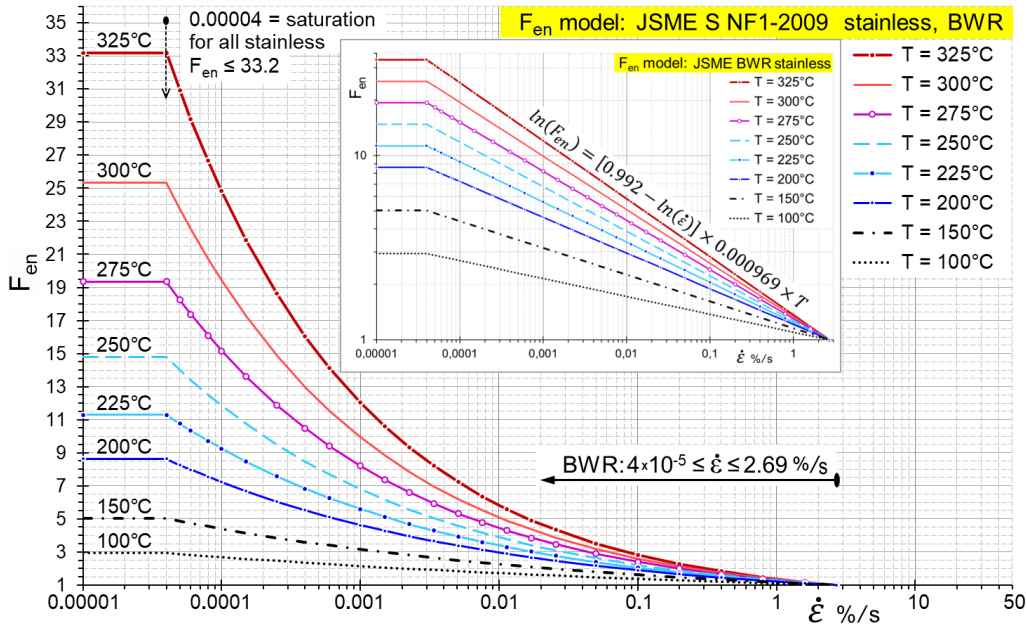


Figure 145. F_{en} factors for stainless steels in BWR water chemistry as function of strain rate at selected temperatures according to JSME S NF1-2009. The F_{en} factor are slightly lower than those in PWR at moderate strain rates, but lowest rates are considered also for wrought steels.

The F_{en} models set for stainless steels in PWR water in the JSME S NF1-2006 remained identical in the JSME S NF1-2009 update, but the models for stainless steels in BWR water were updated. The saturated F_{en} factors were increased and the advantage of wrought stainless steels in BWR water was removed, as shown in Figure 146.

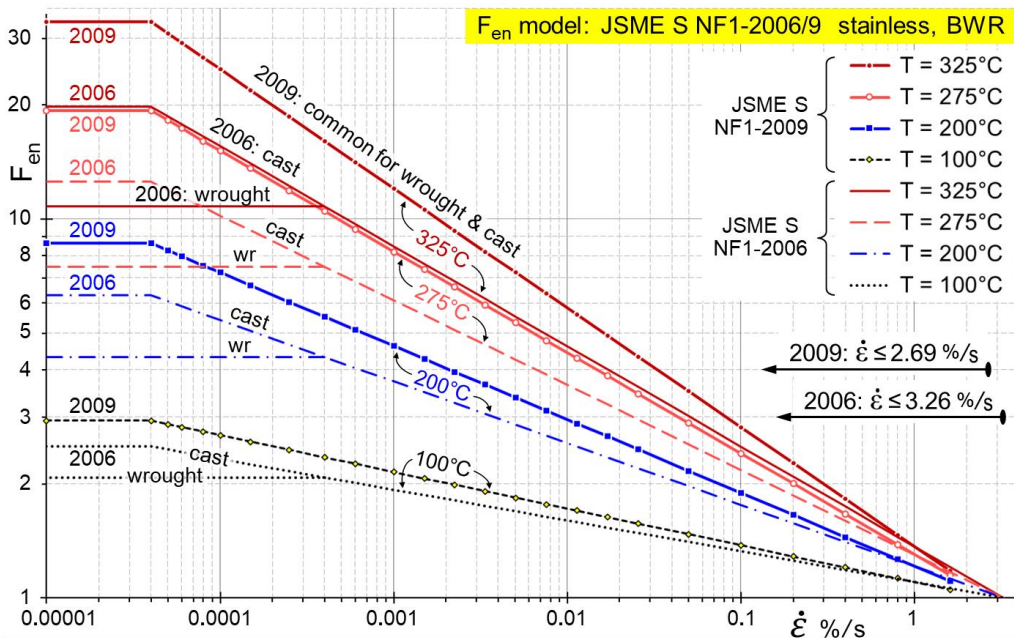


Figure 146. F_{en} factors according to the 2006 and 2009 versions of the JSME S NF1-200{x} Code. The JSME S NF1-2009 assumed higher saturated F_{en} factors and removed the advantage of wrought stainless steels in BWR water, but all F_{en} factors in PWR water remained identical.

7.2.2 Comparison of F_{en} models in JSME S NF1-2009 and NUREG/CR-6909

The Japanese F_{en} models provide notably higher F_{en} factors for certain conditions. The lower strain rate saturation limit applied for wrought stainless steels in PWR water is common with the NUREG/CR-6909 reports, but an order of magnitude lower saturation limit ($\dot{\epsilon} \leq 4 \cdot 10^{-7}/s$) is set for cast stainless steels in PWR water and for all stainless steels in BWR water. This results to very high F_{en} factor values at strain rates applied also in slow strain rate tests (SSRT) for studying material susceptibility to stress corrosion cracking, SCC. It seems that the Japanese F_{en} models have aimed to unite concerns on EAF at extremely low strain rates and time dependent crack growth by mechanisms like SCC.

The F_{en} models in JSME S NF1-2009 (JSME, 2009) and NUREG/CR-6909 rev.1 and the resulting F_{en} factors at 300°C temperature are compared in Figure 147. A particular difference is observed in the F_{en} factors predicted for not sensitized stainless steel in BWR normal water chemistry.

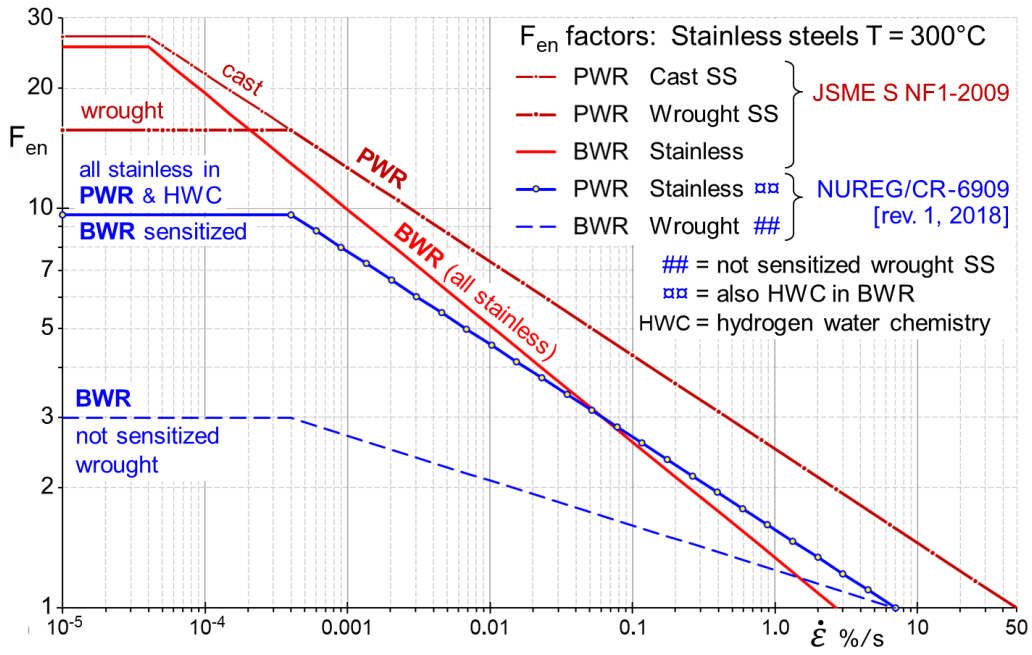


Figure 147. Comparison of F_{en} factors at 300°C in PWR or BWR water chemistries according to JSME S NF1-2009 and NUREG/CR-6909 rev.1.